DETERMINING A ROLE FOR THE CALCIUM-SENSING RECEPTOR (CaR) IN PULMONARY DEVELOPMENT

A thesis submitted to Cardiff University for the degree of PhD

2008

Brenda A. Finney

Cardiff School of Biosciences
Cardiff University

ProQuest LLC
789 East Eisenhower Parkway
P.O. Box 1346
Ann Arbor, MI 48106-1346

Summary of Thesis

In the adult, changes in free ionized plasma calcium concentration ($[Ca^{2+}]_o$) are monitored by the G-protein-coupled, extracellular calcium-sensing receptor, CaR, but whether CaR plays a role in lung development is unknown. CaR has the potential to be a key regulator of Ca^{2+} dependent cell fate during development. It is hypothesized that extracellular calcium is an important extrinsic factor that modulates the intrinsic lung developmental programme, through activation of the CaR. CaR is expressed in the developing mouse lung in the pseudoglandular phase, from embryonic day 10.5 (E10.5), with a peak of expression at E12.5 and a subsequent decrease by E18, after which the receptor is absent. Lung branching morphogenesis *in vitro* is sensitive to $[Ca^{2+}]_o$, being negatively modulated by the higher, fetal (*i.e.*, 1.7 mM) $[Ca^{2+}]_o$ yet optimal at physiological adult $[Ca^{2+}]_o$ (*i.e.*, 1.05-1.2 mM). Administration of the specific CaR positive allosteric modulator, the calcimimetic R-568, mimics the suppressive effects of high Ca^{2+}_o on branching morphogenesis while both phospholipase C and PI_3 kinase inhibition reverse these effects. CaR activation suppresses cell proliferation while it enhances lung distension, fluid secretion and intracellular calcium signalling. Conditions which are restrictive to branching and fluid secretion can be rescued by manipulating $[Ca^{2+}]_o$ in the culture medium. Lung explant cultures from the current mouse model of CaR inactivation respond in a similar manner to $[Ca^{2+}]_o$ and the calcimimetic R-568. These results indicate the presence of expression of a functional CaR splice variant, which is detected at E11.5, 12.5 and 15.5 in CaR knockout lungs. The observations presented here support a novel role for the CaR in preventing hyperplastic lung disease *in utero* and present two potential models for its mode of action within this system.

Acknowledgements

I would like to thank both Paul Kemp and Daniela Riccardi for their supervision and guidance (and the loan of their spare-room!) throughout the past four years.

I would also like to thank David Warburton and Pierre DelMoral for their generosity in collaboration. As well as for teaching me the lung explant culture technique and their discussion about the phenomena witnessed throughout the course of this project.

Thank you to the rest of the Kemp/Riccardi lab; Captain Brazier, Bill, Seb, Catrina, Bourke, Lydia, Jane and all "my students" for the support, both experimental and social of the past four years.

To my parents, there are not words to express my gratitude for supporting every decision that I have made, bringing me to this point in my life. Love to you both.

Lastly, to Matthew, my reason for being where I am in the world today, I love you and cannot tell you how much the encouragement and dinners on the table have helped me plug on through. Thank you so much, for everything.

Table of Contents

List of Figures and Tables

Abbreviations

α-SMA	Alpha-smooth muscle actin
AA	Aminoacid
AbDF	Antibody dilution fluid
AC	Adenylate cyclase
ADH	Autosomal dominant hypocalcaemia
AGA	Aminoglycoside antibiotics
ASM	Airway smooth muscle
ATII	Alveolar Type II cells
Bmp4	Bone morphogenic protein 4
BoPCaR1	Bovine parathyroid calcium-sensing receptor
BSA	Bovine serum albumin
$[Ca^{2+}]_i$	Intracellular calcium concentration
$[Ca^{2+}]_o$	Extracellular calcium concentration
CaR	Extracellular calcium-sensing receptor
CDH	Congenital diaphragmatic hernia
CHO	Chinese hamster ovary cells
DAB	Diaminobenzadine
DKK1	Dikkopf 1
ECD	Extracellular domain
EGF	Epidermal growth factor
ERK1/2	Extracellular signal regulated kinase – 1/2
FCS	Fetal calf serum
FGF	Fibroblast growth factor
Fgfr2	Fibroblast growth factor receptor 2
FHH	Familial hypocalciuric hypercalcaemia
Flk-1	Fetal liver kinase-1
FN	Fibronectin
FRC	Fetal rat calvarial cells
GABA	γ-aminobutyric acid
Gcm2	Glial cell missing 2
GIRK	G-protein activated inwardly rectifying K^+
GPC	Growth plate chondrocytes
GPCR	G-protein coupled receptor
GSK3β	Glycogen synthase kinase – 3β
HEK293	Human embryonic kidney 293 cells
IP_3	Inositol 1,4,5-trisphosphate
ISH	*In situ* hybridisation

JNK	c-Jun terminal kinase
MAP	Mitogen activated protein
MDCK	Madin-Darby canine kidney cells
MEK	Mitogen-activated protein kinase kinase
mGluR	Metabotropic glutamate receptor
NEO	Neomycin resistance cassette
NSHPT	Neonatal severe hyperparathyroidism
O_2	Oxygen
ODN	Oligodeoxynucleotide
OK	Opossum kidney
OSE	Ovarian surface epithelial cells
PFA	Paraformaldehyde
PI_3K	Phosphatidylinositol – 3 kinase
PLC	Phospholipase C
PLD	Phospholipase D
PKC	Protein kinase C
Po_2	Oxygen tension
PtdIns	Phosphatidylinositol
PTH	Parathyroid hormone
PTHrP	Parathyroid hormone related-peptide
RaKCaR	Rat kidney calcium-sensing receptor
SCG	Superior cervical ganglia
s.d.	Standard deviation
s.e.m.	Standard error of the mean
Shh	Sonic Hedgehog
SP-A, C	Surfactant protein- A and C
Spry2	Sprouty 2
SPV	Splice variant
TGF-β	Transforming growth factor - β
TMD	Transmembrane domain
TPD	Transepithelial potential difference
VEGF	Vascular Endothelial Growth Factor
VSOR	Volume-sensitive outwardly rectifying
WT	Wildtype

CHAPTER 1:
GENERAL INTRODUCTION

1.1 Ionic Calcium

The observation by Sidney Ringer in 1883 showing that calcium (Ca^{2+}) was necessary to maintain the contractions in isolated rat hearts (Ringer, 1883) moved Ca^{2+} from the realm of inert structural element to that of an active signalling molecule. Over time Ca^{2+} has been studied for its activity in muscle contraction (Weber *et al.*, 1964), eventually being recognised for its role throughout the body and cellular life. Several proteins were characterised for their ability to bind Ca^{2+} and modulate its activity within the cell; including EF hand proteins which change conformation upon binding to Ca^{2+}, as well as Ca^{2+} channels which do not directly process the Ca^{2+} signal, but can be targets of Ca^{2+} regulation (Carafoli, 2002).

Ca^{2+} waves that spread from a point within the cell throughout its cytoplasm were first observed in fertilized oocytes (Ridgway *et al.*, 1977) followed by repetitive oscillations, initially seen in hepatocytes (Woods *et al.*, 1987). Ca^{2+} wave oscillations of several different kinds have now been observed in almost every cell type tested. The variation in the type and shape of the oscillations is a way in which the Ca^{2+} signal can be deciphered. Ca^{2+} can act as a first messenger, initiating increases in intracellular Ca^{2+} concentration ($[Ca^{2+}]_i$) and as a second messenger within a signalling pathway (Carafoli, 2002). For instance, Ca^{2+} can both protect cells from, or promote cells into, undergoing apoptosis, either of which require a different signalling pattern (Orrenius *et al.*, 2003). For example, human tracheal epithelial cells have increased proliferation in high calcium conditions, whereas they differentiate with little proliferation in low calcium conditions (Chopra *et al.*, 1990). However, sustained increases or decreases in Ca^{2+} levels can interfere with Ca^{2+} signalling and are detrimental to cellular health and functioning. Therefore the

concentration of extracellular Ca^{2+} ($[Ca^{2+}]_o$) must be globally and locally controlled within the body.

1.2 Evidence for a Membrane-bound Calcium Sensing Receptor

In the systemic context, Ca^{2+}_o levels regulate the secretion of parathyroid hormone (PTH) from the parathyroid glands. Initial studies found that in dissociated bovine parathyroid tissue, increasing $[Ca^{2+}]_o$ from 0.5 mM up to 2 mM increased $[Ca^{2+}]_i$ concentrations while inhibiting PTH secretion, where PTH secretion was measured by radioimmunoassay (Shoback *et al.*, 1983). This suppression of PTH secretion was considered unusual in the context of other secretory systems where increases in $[Ca^{2+}]_i$ normally promote secretion (Douglas, 1978). Further investigation into this phenomenon showed that the suppression of PTH secretion was accompanied by increases in $[Ca^{2+}]_i$, which could also be induced by the divalent cation ionophore ionomycin in the presence of 1 mM Ca^{2+}_o. This response was similar to changes produced with 1.5 mM Ca^{2+}_o alone. The results of this study increased the evidence for parathyroid cells having an inverse relationship between $[Ca^{2+}]_i$ and PTH release, leading to the hypothesis that the parathyroid cell contained a mechanism to detect small changes in $[Ca^{2+}]_o$ that could induce large changes in $[Ca^{2+}]_i$ (Shoback *et al.*, 1984).

As stated in the previous section, Ca^{2+}_o can initiate different types of $[Ca^{2+}]_i$ responses which determine the type of cellular response (Carafoli, 2002). Nemeth and Scarpa (1987) detailed that there were two different types of $[Ca^{2+}]_i$ response to Ca^{2+}_o in bovine parathyroid cells. These responses were: 1. An increase in the steady state level of $[Ca^{2+}]_i$, and 2. A transient increase in $[Ca^{2+}]_i$. Each of these two responses occurs via a different mechanism for releasing Ca^{2+} into the cytoplasm, as

evidenced by their differential sensitivity. In bovine parathyroid cells, La^{3+} (10 μM) and high concentrations of Mg^{2+} (8 mM, above the concentration that evokes transient increases in $[Ca^{2+}]_i$) block transmembrane influx of extracellular Ca^{2+} from raising the steady-state $[Ca^{2+}]_i$. The dynamics of the responses to La^{3+} and high concentrations of Mg^{2+} were not sensitive to nifedipine and were only partially sensitive to verapamil which indicated the presence of membrane-bound ion channels. The transient $[Ca^{2+}]_i$ increases were elicited by various divalent cations, including Ca^{2+}_o, but could also be produced by certain membrane-impermeant cations in the absence of Ca^{2+}_o, indicating that the transient increases in $[Ca^{2+}]_i$ were the result of Ca^{2+}_i release from within the cell itself. Therefore these do not necessarily enter the cell but react at the membrane, presumably at a receptor which is sensitive to physiological millimolar concentrations of cations (Nemeth & Scarpa, 1987). Evidence that the interaction of cations, particularly Ca^{2+} and Mg^{2+}, occur at a membrane-bound receptor came from studies again using dispersed bovine parathyroid cells. It was shown that Ca^{2+} and Mg^{2+} quickly instigate an increase in inositol 1,4,5-trisphosphate (IP_3), with Ca^{2+} being more potent than Mg^{2+}in producing a response. This change in IP_3 was consistent with phospholipase C (PLC) activation, known in other cells to be coupled to G-protein activation (Brown *et al.*, 1987).

1.3 Cloning of the Extracellular Calcium-Sensing Receptor

The receptor responsible for these responses was cloned by Brown et al. in 1993 from mRNA isolated from calf parathyroid glands and was named bovine parathyroid calcium-sensing receptor (BoPCaR1). Hydropathy plots provided the potential structure of this receptor; 1085 total amino acids with 613 of these making

a large extracellular amino-terminus, 250 amino acids making up seven transmembrane domains and 222 amino acids constituting a cytoplasmic carboxy-terminus. This structure is characteristic of the G-protein-coupled receptor (GPCR) superfamily; specifically the Group C GPCRs which include γ-aminobutyric acid (GABA) receptors, odorant and pheromone receptors as well as taste receptors (Chang & Shoback, 2004). BoPCaR1 was found to have conserved regions similar to other Group C GPCRs, namely the metabotropic glutamate receptors (mGluRs), mGluR1 and mGluR5. Transcripts of this receptor were also detected in bovine kidney, thyroid and some brain regions by Northern blot analysis (Brown *et al.*, 1993).

X. laevis oocytes injected with BoPCaR1 cRNA were used for functional characterisation of this receptor because, when phosphatidylinositol (PtdIns) coupled receptors are expressed in this cell type, endogenous inward currents from Ca^{2+}-activated Cl^- channels are activated in response to agonists. These responses were instigated by release of Ca^{2+}_i from intracellular stores via activation of PLC (Brown *et al.*, 1993). Oocytes expressing BoPCaR1 responded with large inward currents in a dose dependent manner to application of Ca^{2+}, Mg^{2+}, Gd^{3+} and neomycin. The EC_{50} values in this system for Ca^{2+}= 3 mM, Mg^{2+} = 10mM, Gd^{3+} = 20 μM and neomycin = 60 μM were nearly identical to values previously determined on isolated bovine parathyroid cells (Brown *et al.*, 1993). Similar structural and functional results were also obtained from a homologous rat extracellular calcium-sensing receptor (RaKCaR) cloned shortly after BoPCaR1 from a rat kidney cDNA library (Riccardi *et al.*, 1995).

Receptors with significant homology to BoPCaR1 have since been cloned from human parathyroid (Garrett *et al.*, 1995a) and kidney (Aida *et al.*, 1995), rat thyroid (Garrett *et al.*, 1995b) and brain (Ruat *et al.*, 1995), rabbit kidney (Butters *et al.*, 1997), human and mouse bone marrow cells (House *et al.*, 1997). Other homologous receptors have been cloned from non-mammalian species, including chicken (Diaz *et al.*, 1997) and fish (Loretz *et al.*, 2004), suggesting an evolutionarily conserved role for this receptor as a part of the Ca^{2+}_o homeostatic system. As it has widespread species and tissue distribution, this receptor is generally referred to as the extracellular calcium-sensing-receptor (CaR).

Immunoblotting of endosomal proteins from rat kidney with CaR-specific antisera revealed multiple CaR species with molecular weights of 121, 138-169 and 240-310 kDa. When these proteins were solubilised and subjected to density gradient ultracentrifugation, CaR immunoreactivity detected a species of approximately 220 kDa that was not associated with any complex-bound G-proteins, but consisted of a dimeric CaR that was only partially dissociated by standard denaturing and reducing conditions. Upon addition of Ca^{2+} or Gd^{3+} to solubilised CaR, detection of the monomeric (121, 138-169 kDa) CaR species decreased while detection of the dimeric (240-310 kDa) species increased; suggesting that the binding of di- and tri-valent cations to the CaR stabilises dimerization of the receptor (Ward *et al.*, 1998).

Further studies using immunoprecipitation of Flag-tagged human CaR expressed in human embryonic kidney 293 (HEK293) cells showed that monomeric CaR protein was detected in the cell membrane. When non-reducing conditions were used (sample buffer lacking DTT) immunoprecipitation revealed that detection of the monomeric species was replaced with detection of the dimeric species. Cross-linking studies along with the detection of the dimeric CaR in non-reducing conditions

further confirmed that the CaR resides at the cell membrane as di-sulfide bonded homodimers (Bai *et al.*, 1998).

The Ca^{2+} homeostatic activity of the CaR in the parathyroid is then mediated by homodimers of CaR in the cell membrane that detect small changes in $[Ca^{2+}]_o$. Activation or inactivation of the CaR controls the secretion of PTH, that in conjunction with its effectors controls the excretion and absorption of Ca^{2+} throughout the body (Fig. 1.1). In the kidney, for example, reduction of PTH secretion during hypercalcemia allows for urinary excretion of excess Ca^{2+} thus contributing to the restoration of normal Ca^{2+} levels in the body (Ward & Riccardi, 2002).

1.4 Differential Expression with Differential Activity

To date the CaR has been found to be expressed in at least 14 different tissue types, for a comprehensive review see Brown and MacLeod, 2001. Obviously, not all of these are involved with Ca^{2+} homeostasis and therefore, the fact that the CaR can perform different functions depending upon the type of tissue in which it is expressed should come as no surprise. A summary of some of the localities where the CaR is expressed and its biological responses to agonists in those areas is presented in Table 1.1. As the activity of the receptor in the parathyroid gland has already been detailed in Section 1.2 and 1.3, other tissues which may be relevant to the results of this study are detailed below.

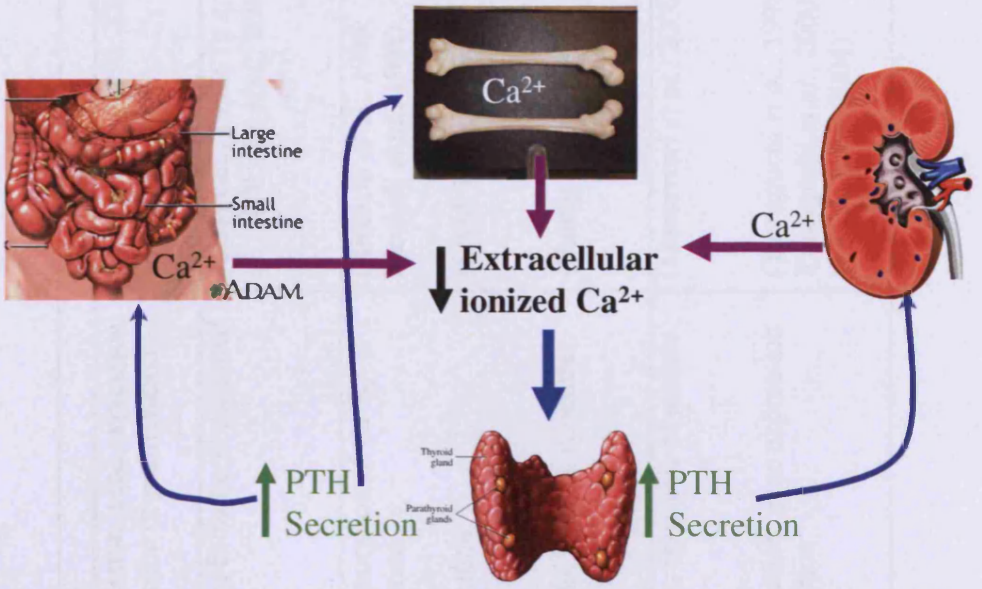

Figure 1.1: Schematic representation of Ca^{2+}_o homeostasis. The CaR initiates its G-protein mediated signalling pathways when extracellular ionized Ca^{2+} ($[Ca^{2+}]_o$) levels are within physiological ranges (1.2 mM in adults). When there is a drop in $[Ca^{2+}]_o$ CaR becomes inactive allowing for secretion of parathyroid hormone (**PTH**) from the parathyroid glands. This hormone **affects** the kidney, intestine and bone and causes them to **reabsorb Ca^{2+}_o** feeding it back into circulation to raise **extracellular ionized Ca^{2+} levels**, reactivating the CaR and suppressing **PTH** secretion.

Table 1.1: Localities of CaR expression and responses to CaR agonists.

Cell / Tissue	Signalling Initiated	Biological Responses	Reference
Parathyroid gland	PLC activation, increased $[Ca^{2+}]_i$, ERK1/2 activation	Inhibition of PTH secretion, gene expression changes, tonic suppression of proliferation	(Brown *et al.*, 1993; Kifor *et al.*, 2001)
Keratinocytes	Production of inositol triphosphate (IP_3), interaction with PLCγ, increased $[Ca^{2+}]_i$,	Cellular differentiation, E-cadherin mediated cell adhesion	(Oda *et al.*, 1998; Tu *et al.*, 2001; Tu *et al.*, 2008)
Kidney	Production of IP_3, inhibition of adenylate cyclase	Urinary excretion/reabsorption of Ca^{2+}_o, decreased Cl^- reabsorption	(Riccardi *et al.*, 1995; Riccardi *et al.*, 1998)
-Glomerular Mesangial cells	PLC activation, biphasic increase in $[Ca^{2+}]_i$	Stimulation of proliferation	(Kwak *et al.*, 2005)
-Madin-Darby canine kidney cells	Rho activation, PLD activation	Possible implications for cellular structure	(Huang *et al.*, 2004)
Bone –Osteoclasts	PLC activation, IP_3 production. activation of NFκB	Cellular differentiation, apoptosis of mature osteoclasts	(Mentaverri *et al.*, 2006)
Osteoblasts	ERK 1/2 activation, Akt stimulation, phosphorylation of GSK3β	Stimulation of proliferation, gene expression changes, nodule formation	(Yamaguchi *et al.*, 1998; Yamaguchi *et al.*, 2000; Dvorak *et al.*, 2004)

-Bone Marrow, hematopoetic stem cells	To be determined	Adherence to collagen 1, binding to extracellular matrix	(Adams *et al.*, 2006)
Chondrocytes	Inositol phosphate (IP) production, decrease cAMP	Gene expression changes, modulation of differentiation	(Chang *et al.*, 1999b; Rodriguez *et al.*, 2005)
Intestine	Production of IP_3, increase in $[Ca^{2+}]_i$, inhibition of PLA mediated production of arachidonic acid, cAMP accumulation	Modulation of fluid secretion, gene expression changes, inhibition of cell proliferation	(Kallay *et al.*, 1997; Kallay *et al.*, 2003; Cheng *et al.*, 2004)
Pancreas	Increase in $[Ca^{2+}]_i$	Secretion of fluid and HCO_3^-	(Bruce *et al.*, 1999)
Neonatal Ventricular Cardiomyocytes	Production of IP, ERK1/2 activation	Decrease in proliferation	(Tfelt-Hansen *et al.*, 2006)
Adult Ventricular Cardiomyocytes	PLC activation, increase in $[Ca^{2+}]_i$, production of IPs	Control of apoptosis in response to injury	(Wang *et al.*, 2003; Zhang *et al.*, 2006)
Mammary gland	To be determined	Decrease in PTHrP secretion, Ca^{2+}transport into milk, gene expression changes	(VanHouten *et al.*, 2004; VanHouten *et al.*, 2007)
Placenta	Biphasic increase in $[Ca^{2+}]_i$	Control of fetal Ca^{2+}-homeostasis, PTHrP secretion	(Bradbury *et al.*, 1998; Kovacs *et al.*, 1998)

Lens epithelial cells	To be determined	Regulation of activation of Ca^{2+}-activated K^+ channel	(Chattopadhyay *et al.*, 1997)
Pituitary Gland	Increase in $[Ca^{2+}]_i$, cAMP accumulation	Unknown	(Shorte & Schofield, 1996; Romoli *et al.*, 1999)
Astrocytoma cells	p38 activation	Regulation of activation of Ca^{2+}-activated K^+ channel	(Ye *et al.*, 2004)
Embryonic Superior cervical ganglion	To be determined	Increased axonal growth and arborisation	(Vizard *et al.*, 2008)

1.4.1 Control of Proliferation, Differentiation and Apoptosis

Patients with non-functioning CaR and mice who lack expression of CaR both have hyperplastic parathyroid glands (Ho *et al.*, 1995). The interpretation of these findings is that the CaR tonically suppresses proliferation in the parathyroid glands (Ho *et al.*, 1995). This role as a suppressor of cellular proliferation has also been noted in intestinal colonocytes where decreasing $[Ca^{2+}]_o$ increased proliferation due to inactivation of the CaR (Kallay *et al.*, 2000). Keratinocytes, from both humans and mice, respond to increasing $[Ca^{2+}]_o$ with an increase in $[Ca^{2+}]_i$ and an increase in IP_3 production, similar to that seen in parathyroid cells (Bikle & Pillai, 1993). CaR activity in keratinocytes from skin has a dual role because $Ca^{2+}{}_o$-mediated CaR activity both halts proliferation and drives differentiation. As the keratinocytes proliferate and reach confluency in the culture system, the $Ca^{2+}{}_i$ responses diminish along with expression of CaR (Oda *et al.*, 1998; Oda *et al.*, 2000). These results indicate that CaR drives differentiation, but is not required for the maintenance of terminally differentiated keratinocytes.

CaR activation has been shown to be a regulator of proliferation in a positive fashion as well. In organ cultures of rat metatarsal bones, CaR activation using both Ca^{2+} and the CaR specific allosteric agonist NPS-R-568 increased metatarsal length by inducing proliferation and hypertrophy of chondrocytes (Wu *et al.*, 2003). This positive effect is also seen in ovarian surface epithelial cells (OSEs). These cells respond to increasing $[Ca^{2+}]$ with an increase in $[Ca^{2+}]_i$, and the phosphorylation of extracellular signal related kinases 1/2 (ERK1/2) causing proliferation (Hobson *et al.*, 2000). Proliferation is also induced by 1.8-2.5 mM $Ca^{2+}{}_o$ in fetal rat calvarial (FRC) cells, a model for osteoblasts, possibly occurring via CaR activation of ERK1/2 (Dvorak *et al.*, 2004).

Complicating matters are results that demonstrate that both proliferative and pro-apoptotic signals are induced by CaR activation in opossum kidney (OK) cells. Proliferative signals are induced by acute treatment with the aminoglycoside antibiotic, gentamicin (an activator of the CaR, see section 1.5.2). However if applied chronically, gentamicin induces apoptosis in OK and HEK293 cells stably expressing the CaR (Ward *et al.*, 2005)

1.4.2 Control of Secretion and Gene Expression

The role of the CaR in controlling the secretion of PTH is well-known; however it has also been shown to regulate secretion in tissues such as the intestine and the pancreas. In the pancreas, where the composition of pancreatic juice containing bicarbonate and free-ionised Ca^{2+}_o is balanced to prevent the formation of calcium carbonate stones, the CaR was localised with immunohistochemistry in the ducts, acini and certain cells in the islets of Langerhans (Bruce *et al.*, 1999). Measurements of ductal secretion showed that Gd^{3+} application caused secretion of fluid and HCO_3^- similar to a known secretion stimulator, forskolin. Based on both the localisation and functional observations, Bruce and colleagues hypothesised that in the pancreas the CaR is involved in controlling fluid secretion ensuring that luminal $[Ca^{2+}]$ remains too low for pancreatic stones to precipitate in the high concentrations of bicarbonate within pancreatic juice.

The CaR has been detected along the length of the gastrointestinal tract from the stomach (Cheng *et al.*, 1999) through the small and large intestine, mostly in epithelial cells (Chattopadhyay *et al.*, 1998). Isolated colonic epithelial crypt cells express the CaR on both apical and basolateral membranes. Experimentation using these crypts show that CaR modulates fluid secretion in response to Ca^{2+} (Cheng *et al.*, 2002) by enhancing the destruction of cyclic nucleotides, inhibiting a sodium and

chloride co-transporter and activating of fluid absorption (Geibel *et al.*, 2006) thus preventing secretory diarrhoea.

Additionally in the intestine, dietary Ca^{2+} has been shown to be a chemoprotective agent against colon cancer formation (Peterlik & Cross, 2005) through mechanisms that could be mediated by Ca^{2+} -dependent activation of the CaR. CaR activation can inhibit defective canonical Wnt signalling in APC truncated-adenocarcinoma cells by inducing secretion of Wnt5a, a non-canonical inhibitor of canonical Wnt signalling, which has also been associated with longer survival in Dukes B colon cancer patients (MacLeod *et al.*, 2007). In colon carcinoma cells activation of the CaR promotes the expression of E-cadherin, a glycoprotein responsible for calcium-dependent, cell-to-cell adhesion that also interacts with β-catenin, a canonical Wnt-signalling pathway component. In the same study, CaR activation suppressed the ability of β-catenin to bind to its target transcription factors. Thus, the malignant behaviour of these cells was prevented by CaR-mediated inhibition of gene transcription and activation, as well as CaR-mediated inhibition of anchorage-independent growth (Chakrabarty *et al.*, 2003).

E-cadherin mediated cellular adhesion is vital for maintaining the structural integrity of the skin and correct differentiation of epidermal keratinocytes (Xie & Bikle, 2007). It has been previously discussed in Section 1.4.1 that CaR activation is also vital for the differentiation of epidermal keratinocytes (Oda *et al.*, 2000). Recently it has been determined that there is a link between CaR activation and E-cadherin in epidermal keratinocytes (Tu *et al.*, 2008). Using CaR anti-sense cDNA which blocked expression of the native CaR, this group showed that not only does CaR activation play a role in calcium signalling, cell survival and differentiation, but also in E-cadherin-mediated cell adhesion and signalling. Reduction of CaR

expression also blocks the activation and association of phosphatidylinositol 3-kinase (PI_3K) with E-cadherin via a mechanism involving *Src*-family tyrosine kinase signalling (Tu *et al.*, 2008).

CaR activation mediates gene expression in several tissues including chondrocytes (Chang *et al.*, 1999a), osteoblasts (Dvorak *et al.*, 2004) and the parathyroid gland (Yamamoto *et al.*, 1989). Chondrocytes are cells which form cartilage and the putative skeleton. A cell line commonly used as a chondrocyte model, C5.18 respond to increasing $[Ca^{2+}]_o$ with CaR activation which in turn suppresses nodule formation and expression of the genes encoding aggrecan, type II collagen and type X collagen (Chang *et al.*, 1999a). In osteoblasts, CaR activation increases the mRNA for type 1 collagen, core binding factor 1, osteocalcin and osteopontin possibly in order to regulate the mineralisation process (Dvorak *et al.*, 2004). In the parathyroid glands, sustained exposure to high $Ca^{2+}_{o,}$ not only inhibits PTH secretion, but also the gene expression for PTH (Yamamoto *et al.*, 1989).

1.5 Ligands for the CaR

The above detailed effects of CaR activation can be instigated by a variety of ligands. The CaR is distinctive amongst GPCRs in its ability to bind inorganic molecules, Ca^{2+} and Mg^{2+} being just two of these. Although the CaR takes its name from its primary physiological ligand, Ca^{2+}, this receptor also responds to other polyvalent cations such as Gd^{3+}, as well as polyvalent peptides (*i.e.* amyloid-β peptides and glutathione), polyamines such as spermine, aminoglycoside antibiotics and amino acids (Steddon & Cunningham, 2005). Ligands are divided into two categories, Type I or Type II calcimimetics. Type I calcimimetics are conventional receptor agonists (like Ca^{2+} and Gd^{3+}) while Type II calcimimetics are positive allosteric modulators of the CaR. Positive allosteric modulators bind to the receptor

at a site separate to endogenous receptor agonists and require the presence of an endogenous agonist in order to modulate receptor activity (Schwartz & Holst, 2006). Both types of ligands are discussed in detail in the following sections.

1.5.1 Type I Calcimimetics

Ca^{2+}_o binding occurs in the extracellular domain (ECD) of the CaR involving residues Ser-170 and, to a lesser extent, Ser-147 (Brauner-Osborne *et al.*, 1999) shown by producing chimeric receptors containing the ECD of the CaR with the transmembrane domain (TMD) and C- terminal tail of mGluR1. The Hill coefficient (indicates cooperativity in ligand-protein interaction) for the CaR with Ca^{2+} is approximately 3 (Bai *et al.*, 1996), which implies that there are several additional Ca^{2+}_o binding sites within the CaR (Brown & MacLeod, 2001). The EC_{50} for Ca^{2+}_o varies depending upon the cell type and system in which the CaR is expressed; however it is generally in the low millimolar range. The following list contains examples of different cell types and their respective EC_{50}:

Colonic epithelial cells – $EC_{50} = 0.759 \pm 0.1$ mM (Cheng *et al.*, 2004);

Parafollicular cells of thyroid gland – $EC_{50} = 1.2 - 2.4$ mM (McGehee *et al.*, 1997) ;

Oligodendrocytes – $EC_{50} = 1.4$ mM (Ferry *et al.*, 2000);

AT-3 prostate carcinoma cells – $EC_{50} = 6.1$ mM (Lin *et al.*, 1998).

While the primary physiological ligand for the CaR is Ca^{2+}, this receptor also responds to other inorganic cations. Their potency depends on the charge and radius of the cation. Therefore Gd^{3+} and La^{3+}, are stronger agonists than Ca^{2+} and Ba^{2+}, which are stronger than Mg^{2+} and Na^{+} (Chang & Shoback, 2004). In a similar fashion the CaR responds, at concentrations which are present in some tissues like the brain, to polyamines (spermine and spermidine) based on the net positive charge of the molecules at physiological pH (Quinn *et al.*, 1997).

1.5.2 Type II Calcimimetics

Amino acids are positive modulators of the CaR, meaning they are ineffective at promoting signalling activities in the absence of Ca^{2+}_o. The modulation of the CaR by amino acids is stereoselective with L-amino acids more potent than D-amino acids (Conigrave *et al.*, 2000). It is thought that amino acid sensing by the CaR contributes to physiological Ca^{2+}-homeostasis because at physiological $[Ca^{2+}]_o$ (1.1 mM), application of several L-amino acids at the physiological concentration of 1 mM suppressed PTH secretion to levels normally seen in the presence of 1.2 mM Ca^{2+}_o (Conigrave *et al.*, 2004). The amino acid sensitivity of the CaR could also have effects in the intestine where the CaR is expressed in epithelial cells and amino acids are released from food (Chang & Shoback, 2004).

Several pharmacological compounds have been produced to modulate the CaR, including the clinically available Cinacalcet (AMG-073). Two earlier calcimimetic compounds are NPS-R-467 and Amgen R-568. All of these compounds are small, organic, phenylalkylamine compounds without polycationic structure (Fig.1.2A) that have been structurally modified from fendiline, a calcium channel blocker (Nemeth *et al.*, 1998). These calcimimetics are also stereoselective, which means that a stereoisomer of the compound is less active than its counterpart (Ferry et al., 2000; Quarles et al., 2003); these are generally used as negative controls for the activity of the calcimimetics. R-568 (3 μM) shifted the EC_{50} for the $[Ca^{2+}]_o$ response of oocytes (Fig.1.2B) from 7.6±1.7 mM to 3.4±0.7 mM (Hammerland *et al.*, 1998). Both NPS-R-467 and R-568 (100 nM) shifted the EC_{50} for the $[Ca^{2+}]_o$ response of bovine parathyroid cells to Ca^{2+}_o to the left, moving the EC_{50} from 1.66±0.34 mM to 0.61±0.04 mM (Nemeth *et al.*, 1998). The same study also determined that these calcimimetics only affected stimulation of the CaR when in the

presence of Ca^{2+}_o at a concentration of at least 0.5 mM and did not produce any additional stimulation when Ca^{2+}_o was raised above 1.5 mM. The range of $[Ca^{2+}]_o$ in which these calcimimetics are active is 0.1 mM – 3 mM (Nemeth, 2004). Additionally, in both HEK293 cells stably expressing human CaR and bovine parathyroid cells, R-568 was approximately twice as potent at inducing CaR activation as NPS-R-467 (Nemeth *et al.*, 1998). It should also be noted that regardless of their respective EC_{50}s, these compounds are the same, they both inhibit secretion of PTH and elicit increases in $[Ca^{2+}]_i$.

Zhang *et al.* (2002) looked at the effect of NPS-R-467 on HEK293 cells, transiently transfected with either wildtype (WT) CaR or mutated CaR. Treatment with 1 μM NPS-R-467 decreased the EC_{50} for Ca^{2+}_o of the WT receptor by 39%. This concentration also significantly decreased the EC_{50} for Ca^{2+}_o of many of the mutant receptors produced for this study. Additionally, this study looked at another allosteric modulator of the CaR, L-phenylalanine, which in some cases did not shift the EC_{50} for Ca^{2+}_o in several of the mutant CaRs. It can therefore be deduced that there are separate sites for allosteric binding in the CaR (Zhang *et al.*, 2002). NPS-R-467 also helps to potentiate secretion of insulin from cells in the pancreas via interaction of the CaR with a nonspecific cation channel (Straub *et al.*, 2000).

Studies with R-568 have shown its effectiveness at modulating the response of the CaR when applied to bovine parathyroid cells (Nemeth *et al.*, 1998) and when administered subcutaneously to adult rats. In adult rats it reduces levels of parathyroid hormone and calcium in the serum after nephrectomy, thus implying that its actions are mediated via CaR located in the parathyroid and not in the kidney (Fox *et al.*, 1999b). R-568 also reduces the parathyroid cell proliferation normally seen after this procedure (Wada *et al.*, 1997). However R-568 can also cause

hypocalcemia in normal rats by inhibiting PTH secretion and stimulating calcitonin secretion (Fox *et al.*, 1999a).

It has also been shown that R-568 not only modulates the responsiveness of the CaR, but can also influence receptor expression. Treatment of transiently transfected HEK293 cells with R-568 (10 μM) increased the expression of CaR protein after 12 h in culture (Huang & Breitwieser, 2007). Interestingly, this treatment also rescued the expression of several loss-of-function CaR mutants. HEK293 cells transiently transfected with these mutants initially showed very little cell surface expression, while after 12 h of R-568 treatment, there was an increase in the plasma membrane expression of the CaR mutants. These mutants also showed an increase in ERK1/2 phosphorylation, indicating functional signalling responses once the receptor was located in the membrane (Huang & Breitwieser, 2007). These results indicate that R-568 not only modulates the response of wildtype CaR, but can also modulate the responses of several mutant CaR configurations by increasing their movement to the plasma membrane.

A.

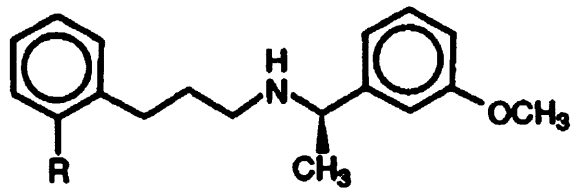

R = H: NPS 467
R = Cl: NPS 568

B.

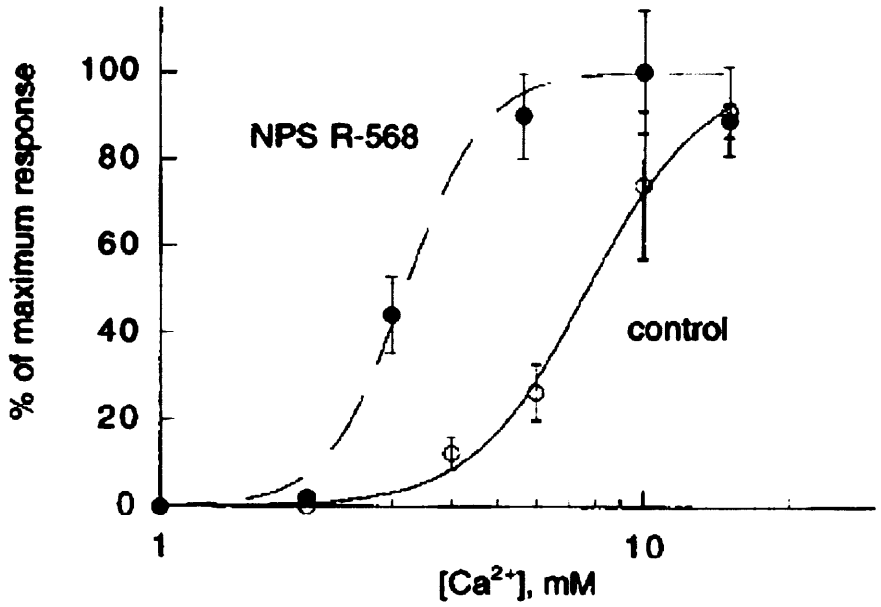

Figure 1.2: Type II calcimimetic structure and effect on $[Ca^{2+}]_o$ concentration response of oocytes. A). NPS-R-467 and R-568 are structurally similar compounds derived from the structure of the calcium channel blocker fendiline. Figure taken from Nemeth *et al.*, 1998. **B).** Application of 3 μM R-568 (closed circles) to oocytes in the presence of increasing $[Ca^{2+}]_o$ shifts the response to the left making the CaR more sensitive to lower $[Ca^{2+}]_o$. Figure taken from Hammerland *et al.*, 1998.

Aminoglycoside antibiotics such as neomycin and gentamicin are also activators of the CaR in some tissues. Neomycin has been shown to be a concentration-dependent activator of $[Ca^{2+}]_i$ increases in oocytes expressing the bovine parathyroid CaR (Brown *et al.*, 1993). In HEK293 cells stably expressing the CaR; neomycin, tobramycin and gentamicin all produced dose-dependent CaR signalling responses (McLarnon *et al.*, 2002). This activation of the CaR by these antibiotics is thought to contribute to the renal toxicity effects sometimes seen when these antibiotics are taken (McLarnon & Riccardi, 2002).

Table 1.1 demonstrates the point that the CaR has phenotypic pharmacology, that is, the pharmacological phenotype will change dependent upon the cellular locality in which CaR is expressed (Nemeth, 2004). Therefore aminoglycoside antibiotics, and indeed other CaR agonists, may not elicit responses in all tissues and cell types to which they are applied. For example, the calcimimetic AMG-073 induces relaxation of contraction in isolated rat aortas, but this is not mimicked by application of neomycin (Smajilovic *et al.*, 2007). Human aortic endothelial cells, presumably also part of the isolated aortas in the previous example, exhibit a similar lack of response to neomycin (Ziegelstein *et al.*, 2006).

1.6 CaR Signalling

Activation of the CaR is linked to a diverse range of signalling pathways. This is due to the fact that the CaR is a pleiotropic G-protein coupled receptor, meaning that upon binding by its associated ligands, it can produce diverse effects by changing its interactions with several different G-proteins or other associated proteins like filamin (Huang & Miller, 2007). G-proteins interact with GPCRs, like the CaR, and upon receptor activation release the biologically active subunits α-GTP and $\beta\gamma$ (Albert & Robillard, 2002). CaR activation can result in the stimulation of

both pertussis toxin sensitive and insensitive G-protein mediated responses (Brown & MacLeod, 2001). Different combinations of subunits designate different G-protein subfamilies and the CaR has been shown to interact with G_s G_q, G_i and $G_{12/13}$ (Ward, 2004; Mamillapalli *et al.*, 2008). Again, the cellular context of CaR expression seems to determine the predominant signalling pathway that is initiated. This has been elegantly demonstrated in experiments using breast epithelial cells. In normal mammary epithelial cells CaR activation is linked to G_i signalling. When mammary cells become malignant, the CaR switches from G_i-coupled to G_s-coupled signalling. The underlying reason for this change is currently unknown, but this process could be contributing to the malignancy of breast cancer (Mamillapalli *et al.*, 2008). This ablity to change G-protein partners is one reason for the ability of the CaR to affect so many different cellular processes. A summary of CaR ligands and signalling pathways is shown in Figure 1.3.

1.6.1 Phospholipase Activation and Interactions with Rho by CaR

In parathyroid cells, Ca^{2+}_o induces PLC mediated increases in IP_3 and attendant release of Ca^{2+}_i, which are indicative of G_q activation (Brown *et al.*, 1987). Activation of PLC via G_q in parathyroid cells and transfected HEK293 cells is pertussis toxin insensitive (Brown & MacLeod, 2001). The evidence for interaction of CaR with G_q in the parathyroid is further strengthened by the phenotype of mice lacking expression of G_q in their parathyroid glands. These mice have symptoms very similar to CaR knockout mice (see Section 1.8.1) with increased serum [Ca^{2+}] and [PTH], hyperplastic PTH glands and early post-natal lethality (Wettschureck *et al.*, 2007). CaR may influence G_q signalling elsewhere in the body, implied by Gd^{3+} stimulated activation of the CaR increasing G_q protein in Madin-Darby Canine Kidney (MDCK) cells (Arthur *et al.*, 1997). PLC activation via CaR interaction with

G_q has been identified in the majority of systems where CaR has been found to be expressed including; kidney (Riccardi *et al.*, 1995), pancreas (Bruce *et al.*, 1999), placenta (Bradbury *et al.*, 1998), intestine (Gama *et al.*, 1997), ovarian epithelial cells and fibroblasts (McNeil *et al.*, 1998a; McNeil *et al.*, 1998b).

Phospholipase D (PLD) is also activated by high Ca^{2+} in CaR transfected MDCK cells. Activation of PLD is pertussis toxin insenstitive, but can be inhibited by disruption of Rho, indicating the involvement of $G_{12/13}$ (Huang *et al.*, 2004). However, the interaction with Rho may also be dependent on CaR interaction with filamin, as well as $G_{12/13}$, due to the lack of response seen when dominant-negative Rho is applied to CaR transfected HEK293 cells (Pi *et al.*, 2002). CaR demonstrates ligand specific pharmacology, as well as differentially timed responses in HEK293 cells stably expressing the CaR. In these cells, Ca^{2+} and NPS-R-467 can initiate G_q mediated PLC signalling, initiating $Ca^{2+}{}_i$ mobilisation and ERK 1/2 activation within minutes of treatment. It can also initiate $G_{12/13}$ and Rho resulting in actin stress fiber assembly and changes in cell morphology after several hours of treatment. In these same cells, L-amino acids initiated $Ca^{2+}{}_i$ mobilisation, but no detectable activation of ERK 1/2 or changes in cell morphology (Davies *et al.*, 2006).

1.6.2 Protein Kinase Activation by CaR

Mitogen activated protein (MAP) kinases are a family of protein kinases that includes extracellular signal-regulated kinases (ERK), c-Jun N kinases (JNK) and p38. All have been shown to be activated by the CaR, although in several different systems. ERK activation is by far the most common form of MAP kinase activation by CaR reported. In CaR transfected HEK293 cells and bovine parathyroid cells ERK 1/2 activation has been induced by CaR activation, both by high $Ca^{2+}{}_o$ and calcimimetic NPS-R-467. This ERK 1/2 activation was blocked by addition of

U73122, a PLC inhibitor, and by GF109203X, a protein kinase C (PKC) inhibitor, indicating the involvement of G_q (Kifor *et al.*, 2001). Inhibition of PI_3K also inhibited ERK activation in CaR transfected HEK293 cells (Hobson *et al.*, 2003). Inactivation of PI_3K has also been used in other native CaR expressing systems to inhibit ERK activation including: ovarian surface epithelial cells (Hobson *et al.*, 2000), opossum kidney cells (Ward *et al.*, 2002) and hyperplastic human parathyroid cells (Corbetta *et al.*, 2002).

JNK is a stress activated MAP kinase family member that is phosphorylated in MDCK cells responding Gd^{3+} or high Ca^{2+} exposure (Arthur *et al.*, 2000). H-500 Leydig cancer cells are a model for humoral hypercalcemia that is associated with malignancy of cancer. They have been used to investigate CaR signalling that induces parathyroid hormone-related peptide (PTHrP) release. The release of PTHrP in these cells is abolished when JNK or PKC is inhibited and potentiated upon application of a PKC activator (Tfelt-Hansen *et al.*, 2003).

PTHrP secretion by H-500 Leydig cells is attenuated when p38 MAPK is inhibited (Tfelt-Hansen *et al.*, 2003). Further studies with these cells showed that p38 activation by the CaR was responsible for an increase in proliferation and protection from apoptosis when exposed to high Ca^{2+}_o or NPS-R-467 (Tfelt-Hansen *et al.*, 2004). Activation of p38 by the CaR is also involved in the CaR-mediated activation of a Ca^{2+}-activated K^+ channel in U87 astrocytoma cells (Ye *et al.*, 2004).

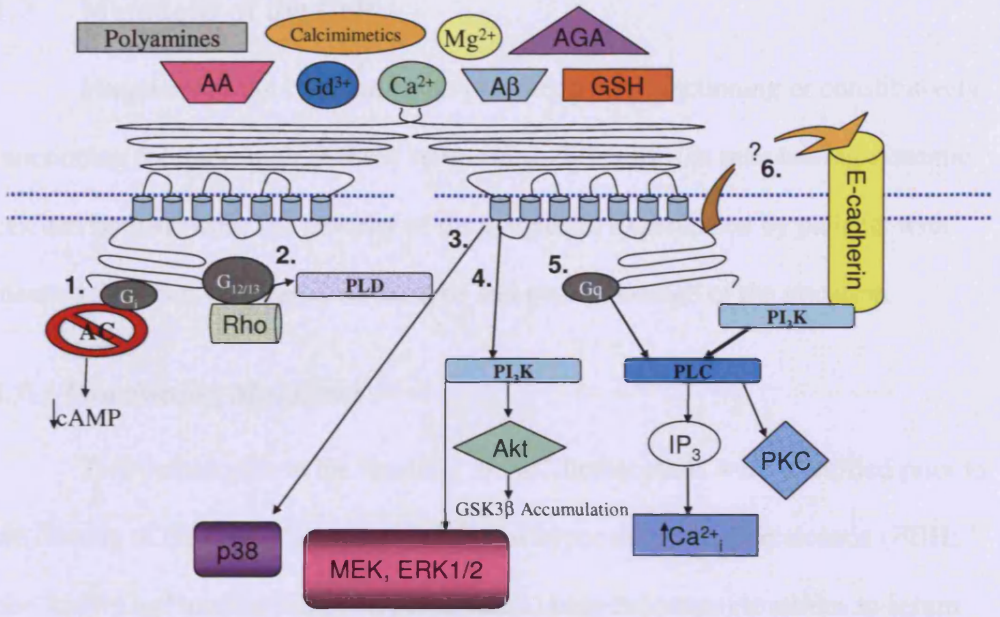

Figure 1.3: Schematic diagram of extracellular calcium-sensing receptor signalling. The CaR is present in the cell membrane as a constitutive homodimer with a large extracellular domain. This receptor can be activated not only by Ca^{2+}_o, but also by polyamines, Gd^{3+}, calcimimetic compounds, Mg^{2+}, amino acids (AA), amyloid-β peptides (Aβ), glutathione (GSH) and aminoglycoside antibiotics (AGA). Signalling cascades initiated by CaR include, but are not limited to: **1.** G_i inhibition of adenylate cyclase (AC), reducing cAMP production; **2.** $G_{12/13}$ and Rho mediated activation of phospholipase D (PLD); **3.** activation of p38; **4.** phosphatidylinositol 3-kinase (PI_3K) activation of MEK and ERK1/2 and/or activation of Akt leading to the phosphorylation of glycogen synthase kinase 3β (GSK3β); **5.** G_q mediated activation of phospholipase C (PLC), activating protein kinase C (PKC) and/or inositol trisphosphate (IP_3) leading to release of Ca^{2+} from internal stores; **6.** CaR interaction with E-cadherin (through an as yet undetermined mechanism) which recruits and associates with PI_3K leading to activation of PLC and Ca^{2+}_i increase. Figure adapted from Ward 2004, Tfelt-Hansen *et al.*, 2004 and Tu *et al.*, 2008.

1.7 Mutations of the CaR

Mutations of the CaR can result in either a non-functioning or constitutively functioning receptor; both of these states cause difficulties in maintaining systemic calcium homeostasis. The severity of the symptoms experienced by patients with mutated CaR can vary based on the type and genetic dosage of the mutation.

1.7.1 Inactivating Mutations

Two pathologies in the handling of Ca^{2+} homeostasis were identified prior to the cloning of the CaR. Patients with familial hypocalciuric hypercalcemia (FHH; also known as Familial benign hypercalcemia) have moderate elevations in serum Ca^{2+} levels and low excretion of Ca^{2+} in the urine, as the name suggests. They also have PTH levels that are not physiologically compatible with their level of serum Ca^{2+} (Attie *et al.*, 1983). As FHH is an autosomal dominant disorder, offspring of these patients are also highly likely to have FHH, generally an asymptomatic condition, or a more severe condition, neonatal severe hyperparathyroidism (NSHPT) if the mutation is homozygous. NSHPT can be lethal unless diagnosed quickly and rectified with an immediate parathyroidectomy. This lethality is due to the severity of the Ca^{2+} and PTH elevation in the serum of these patients. In patients with either FHH or NSHPT there is a pathologic response to changes in Ca^{2+}_o (Steinmann *et al.*, 1984).

After cloning of the CaR in 1993, screening was performed on patients suffering from either of these diseases. It was found that mutations in conserved regions of the CaR gene rendered the CaR of these patients less responsive to Ca^{2+}, Gd^{3+} and neomycin application thus providing the link between the CaR, FHH and NSHPT (Pollak *et al.*, 1993). NSHPT results from having two copies of FHH

causing mutations, dramatically changing the set point at which the parathyroid responds to Ca^{2+}_o (Pollak *et al.*, 1994b). Since the linkage of CaR mutations to FHH and NSHPT, many different mutations have been described which inactivate the CaR. Many of these mutations are in the extracellular and transmembrane domains, regions that are highly conserved across human, bovine and rat sequences (Pearce *et al.*, 1995; Pearce *et al.*, 1996c; Cole *et al.*, 1997; Demedts *et al.*, 2008) and are listed on the CaR mutations database found on www.casrdb.mcgill.ca. Several mutations result in defective processing and trafficking of the receptor to the cellular membrane, thus explaining the decreased ability to respond to Ca^{2+} (Pidasheva *et al.*, 2005; Pidasheva *et al.*, 2006). Other mutations may truncate the protein, producing a non-functional CaR or interfere with the ligand-binding sites within the receptor (Cole *et al.*, 1997). Another type of mutation resulting in a non-functioning CaR is the insertion of a repetitive Alu-sequence into exon 7 of the CaR gene which results in a protein without much of its intracellular carboxy terminus, impairing its trafficking and signal transduction capabilities (Janicic *et al.*, 1995; Bai *et al.*, 1997; Cole *et al.*, 1997).

1.7.2 Activating Mutations

Autosomal dominant hypocalcaemia (ADH) is caused by activating mutations in the CaR which result in inappropriate activation of the receptor. The first described mutation, Glu128Ala, resulted in an alanine substitution within exon 2 in the ECD of the CaR protein. This substitution resulted in a mutant receptor that produced significantly more IP_3 in response to both 0.5 and 5 mM Ca^{2+} than wildtype receptors. Therefore, the mutated receptor had a greater amount of activity regardless of $[Ca^{2+}]_o$ (Pollak *et al.*, 1994a).

Many other mutations have since been described which produce a CaR with an increased sensitivity to Ca^{2+} (Pearce *et al.*, 1996b; Watanabe *et al.*, 1998; Lienhardt *et al.*, 2000; Lienhardt *et al.*, 2001). One of these mutations was found to be a large deletion in the cytoplasmic tail of the receptor and this mutated receptor had a greater cell surface expression than wildtype CaR, possibly accounting for the increase in CaR activity. Interestingly, ADH seems to be independent of any gene-dosage effect, as one male from this study was homozygous for this mutation, but had similar symptoms to other heterozygous family members (Lienhardt *et al.*, 2000).

1.7.3 Splice Variants of the CaR

In the course of sequencing the CaR in normal human keratinocytes a splice variant was detected (Oda *et al.*, 1998). This splice variant lacks the 231 nucleotides which encode exon 5 of the full-length receptor, resulting in a protein reduced by 77 amino acids. In the keratinocyte cultures used for this study, the exon-5-less splice variant (SPV) does not induce an IP_3 response to Ca^{2+}-stimulation and as the keratinocytes differentiated, full-length CaR expression decreased while SPV expression remained relatively constant. When co-expressed in HEK293 cells with the full-length CaR, the SPV reduces the normal IP_3 response by about 30% (Oda *et al.*, 1998). This SPV was also detected in mouse keratinocytes and kidney from animals in which wild-type CaR expression had been disrupted (Oda *et al.*, 2000). Neither one of these studies was able to elicit normal CaR signalling responses from the SPV.

The SPV was later also detected in mouse growth plate chondrocytes (GPCs). In this instance the SPV was detected at the cell membrane of GPCs and produced normal responses to classic agonists of the CaR (Ca^{2+}, Mg^{2+}, Sr^{2+}, Mn^{2+},

and neomycin). The detection of the SPV at the membrane and signalling responses were only detected in the native GPC cell population. When expressed in heterologous systems, chinese hamster ovary (CHO) cells and HEK293 cells, SPV protein is retained intracellularly and therefore is unable to provoke normal signalling responses. These results indicate that in native tissues there is a mechanism, lacking in heterologous expression systems, that allows trafficking of the SPV to the membrane where it can then signal and at least partially compensate for the loss of the full-length CaR (Rodriguez *et al.*, 2005).

1.8 Animal models of CaR activity

1.8.1 Mutants with Inactivated CaR

The first mouse with an inactivation of the CaR was made by insertion of a neomycin resistance cassette into the then exon 4 (since re-designated exon 5) of the CaR gene (Ho *et al.*, 1995). This mouse mimicked symptoms of both FHH and NSHPT depending on the heterozygosity or homozygosity of the mutation (Fig. 1.4). Heterozygotes (HET) were viable and physically indistinguishable from their wildtype (WT) littermates. They did however, have elevated serum Ca^{2+} and elevated PTH levels with hypocalciuria, similar to human patients with FHH. Homozygotes null (NULL) for the CaR were indistinguishable from their WT littermates at birth. However they failed to develop normally and remained much smaller. These mice died between post-natal day 3 and 30 with substantially elevated serum Ca^{2+} and PTH levels, as well as enlarged parathyroid glands and skeletal abnormalities, making them a model for patients with NSHPT (Ho *et al.*, 1995).

However severe their phenotype, mice NULL for the CaR do naturally express the exon-5 less splice variant of the CaR in some tissues, including keratinocytes (Oda *et al.*, 2000), kidney (Oda *et al.*, 2000) and chondrocytes

(Rodriguez *et al.*, 2005), but not in others like the superior cervical ganglia (Vizard *et al.*, 2008). This variable expression makes them an incomplete knockout model.

Many of the symptoms seen in the NULL mouse are thought to be the effects of severe up-regulation of PTH secretion and the attendant hypercalcemia (Kos *et al.*, 2003). Due to the varied distribution of the CaR in tissues not responsible for Ca^{2+}_o homeostasis, two modifications to the original CaR knockout mouse have been made. The first modification was done by crossing the original CaR knockout with a PTH knockout resulting in CaR/PTH NULL mice that were viable. Mice which were CaR/PTH NULL still had hyperplastic parathyroid glands with a trend towards hypercalciuria and hypercalcemia. This trend was characterised by greater variability in the range of values seen for serum Ca^{2+} and urine Ca^{2+}in CaR/PTH NULL mice than in mice null for PTH alone. While this cross prevented the major effects of over secretion of PTH, it still demonstrates that CaR has a role in Ca^{2+} homeostasis without PTH and provides a model to look at the non-PTH related roles of the CaR (Kos *et al.*, 2003).

The second mouse model removed the effects of PTH excess by crossing the original CaR mice with glial cells missing 2 (Gcm2) deficient mice (Tu *et al.*, 2003). Gcm2 is the master gene responsible for development of the parathyroid gland. Therefore these mice lack a parathyroid gland and display normal skeletal development. Their serum Ca^{2+} and PTH levels are similar to their Gcm2 deficient littermates, although their hypocalciuria is maintained confirming the role of the CaR at least in renal excretion of Ca^{2+} (Tu *et al.*, 2003). However, regardless of the reduced severity of their phenotypes, these two mouse models retain the limitation of the original CaR knockout. This limitation is the result of the expression and activity

of the exon-5-less SPV in several cell types and tissues which would not be affected by cross-breeding with PTH NULL and Gcm2 mice.

Recently, a floxed CaR mouse has been described with the insertion of LoxP sites flanking exon 7 of the CaR gene (Chang *et al.*, 2008). This mouse can be used to produce tissue-specific knockouts of the CaR when bred with other transgenic mice expressing Cre-recombinase under the control of tissue-specific promoter sequences. It also means that the problem with possible SPV expression is solved, as removing exon 7 disrupts expression of both full-length and SPV CaR.

This mouse has been used to produce knockout of CaR expression in parathyroid cells, osteoblasts and chondrocytes. Regardless of the promoter sequence used, offspring presented with gene-dosage specific phenotypes, with the heterozygous phenotype being less severe than the homozygous. For brevity, only the homozygous phenotypes will be detailed below. As in the original CaR knockout (Ho *et al.*, 1995), when CaR expression is removed from parathyroid cells specifically, there is a 45% reduction in overall post-natal growth with an undermineralised skeleton. However, the hyperparathyroidism in homozygous parathyroid cell knockouts was 7.5-fold more severe than in the original CaR NULL mouse. This implies that the SPV is indeed partially compensating for the lack of full-length CaR expression in the original CaR NULL mouse (Chang *et al.*, 2008).

Two different promoter sequences were used to remove CaR expression from osteoblasts. Both promoters, which blocked CaR expression at the late, post-natal stage of osteoblast lineage and embryonic/early postnatal stage independently, blocked post-natal growth and resulted in undermineralised skeletons. Therefore, CaR modulates the growth and differentiation of osteoblasts which is an essential part of post-natal skeletal development.

When CaR expression was initially ablated from chondrocytes using a CART promoter, the phenotype was embryonically lethal, with embryos dying between E12 and E13. The use of this promoter for CaR removal inhibits early cartilage and bone mineralisation. As these embryos were non-viable, a tamoxifen-inducible CART promoter was used for CaR ablation at E16-E17. The offspring produced from this strategy had 10% decreased skeletal length as well as delayed chondrocyte maturation and terminal differentiation, due in part to reduced insulin-like growth factor 1 signalling. Therefore, there is a role for Ca^{2+} sensing by the CaR in chondrocytes. The culmination of the results from all three of these tissues show that signalling by the CaR is directly involved in the differentiation and development of the skeleton and that this involvement, in some tissues, begins in the embryo.

1.8.2 Mutants with Activated CaR

As stated earlier activating mutations of the CaR result in ADH (Pearce *et al.*, 1996a), and while mice with inactivated CaR have been characterised for some time, the mouse line which possesses an activating mutation of the CaR is relatively newly described. This mouse line was found to have a homozygous missense mutation to the fourth TMD of the CaR which results in a significant shift in the concentration response curve, with the mutant CaR responding to a lower $[Ca^{2+}]_o$ than wildtype receptors (Hough *et al.*, 2004).

This mouse line has been designated *Nuf* for the "nuclear flecks" which are present in the lens of the eye. The mutation is also autosomal dominant with the resulting heterozygous (*Nuf/+*) mouse phenotype similar to that experienced by human ADH patients who are heterozygous for CaR mutations. These symptoms include, low plasma PTH concentrations, hypocalcaemia and hyperphosphatemia. Homozygotes (*Nuf/Nuf*) and heterozygotes (*Nuf/+*) have additional pathology to that

presented by human ADH patients. *Nuf/Nuf* and *Nuf/+* have ectopic calcification in various tissues including the tongue, jaws, kidneys, heart and lungs as well as the cataracts for which they were named (Hough *et al.*, 2004).

A second mouse model was produced by directing a constitutively active CaR to the osteoblasts by using a human osteocalcin promoter (Dvorak *et al.*, 2007). These mice do not have any of the metabolic disturbances normally associated with global expression of a constitutively active CaR. They do have significantly lower amounts of cancellous bone than their wildtype littermates by 12-weeks of age regardless of gender, and this decrease becomes more pronounced as they age. Within their bones they also have increased production and activity of osteoclasts concomitant with increased RANK-L expression, a stimulator of osteoclast differentiation and activity. Therefore the phenotype of these mice indicates that CaR signalling in osteoblasts is vital for osteoclastic maintenance and turnover, locally regulating bone remodelling (Dvorak *et al.*, 2007).

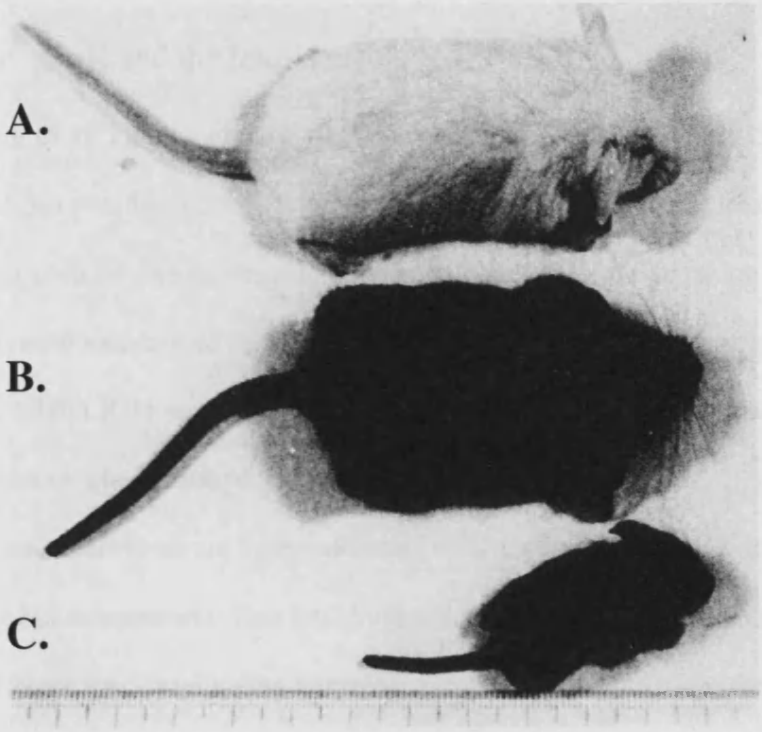

Figure 1.4: The phenotype of CaR knockout mice. CaR knockout mice were created by inserting a neomycin cassette into exon 5 of the CaR gene. This resulted in mice which have gene-dose dependent phenotypes similar to human phenotypes; the mice shown are 23 days old. **A).** Topmost white mouse is wildtype with no abnormalities. **B).** The middle black mouse is a heterozygote which has no gross abnormalities, but is a model of Familial Hypocalciuric Hypercalcemia with elevated levels of Ca^{2+} and PTH. **C).** The small black mouse is a homozygote, with obvious growth retardation, is a model for Neonatal Severe Hyperparathyroidism. Other symptoms this mouse displays are lethargy, enlarged parathyroid gland, severely elevated Ca^{2+} and PTH. Figure reproduced from Ho *et al.,* 1995.

1.9 Ca^{2+}, CaR and the fetus

Prior to the cloning of the CaR, experiments by LeBoff *et al.* (1985) determined that parathyroid cells from neonatal calves required exposure to a higher $[Ca^{2+}]_o$ than adult bovine parathyroid cells in order to inhibit the secretion of PTH. Neonatal bovine parathyroid cells required 1.27±0.11 mM $Ca^{2+}{}_o$ in order to half-maximally inhibit PTH secretion, while adult bovine parathyroid cells produced a similar response when exposed to 1.06±0.11 mM $Ca^{2+}{}_o$ (LeBoff *et al.*, 1985). Therefore neonatal calves are hypercalcaemic with a reduced sensitivity to $[Ca^{2+}]$ than their adult counterparts. This fetal hypercalcemia has been documented in several different species including humans, rodents and sheep at stages fairly early in pregnancy; 35 days in sheep and 15 weeks in humans (Kovacs & Kronenberg, 1997).

In a pivotal study for understanding the phenomenon of hypercalcemia in the fetus, Kovacs *et al.,* (1998) demonstrated that $[Ca^{2+}]_o$ in the fetus is maintained independently of the maternal $[Ca^{2+}]_o$ by the CaR. This was shown in studies using CaR knockout mice which showed that HET or NULL embryos had increased $[Ca^{2+}]_o$ levels and decreased placental $Ca^{2+}{}_o$ transport in comparison to their WT littermates regardless of the genotype and $[Ca^{2+}]_o$ of their mother. HET and NULL embryos also had significantly increased $[Ca^{2+}]_o$ in their amniotic fluid in comparison to their WT littermates indicating that renal handling of $Ca^{2+}{}_o$ is not vital to maintaining the hypercalcaemic status of the fetus. Double knockouts were produced by crossbreeding CaR knockouts to either PTHrP or PTH/PTHrP receptor knockout mice. Analysis of the embryonic $[Ca^{2+}]_o$ from these matings showed that the elevation of $[Ca^{2+}]_o$ in CaR HET and NULL embryos requires activation of the PTH/PTHrP receptor through binding of PTHrP.

In WT mice, $[Ca^{2+}]_o$ is maintained at approximately 1.7 mM in E18.5 mouse fetuses, significantly higher than the 1.2 mM maintained by their mothers. Therefore, in the developing fetus parathyroid CaR suppresses PTH secretion in response to this higher $[Ca^{2+}]_o$, and placental CaR through interactions with PTHrP influences the dynamics of placental $Ca^{2+}{}_o$ transport in order to maintain hypercalcemia (Kovacs *et al.*, 1998). At birth this hypercalcemia begins to be resolved to post-natal normocalcaemia within 24 hours (Kovacs & Kronenberg, 1997) indicating that the control of $[Ca^{2+}]_o$ by the CaR is developmentally regulated.

Developmental regulation of CaR activity and expression has also been shown in tissues besides the placenta. Rat kidney expresses CaR in a developmentally regulated manner, with protein expression detected at E18 in large tubules thought to be branching ureteric buds. Over the first week after birth expression of CaR mRNA greatly increases from pre-natal levels and reaches adult levels of expression by post-natal day 14. These increases presumably are linked with the need for increased renal function after birth excreting unnecessary Ca^{2+}in the urine (Chattopadhyay *et al.*, 1996).

Developmental regulation of the CaR has also been shown in cells not classically known for their expression of the CaR. Recently, Vizard *et al.*, (2008) reported that CaR expression in the superior cervical ganglion (SCG) of embryonic mice is developmentally regulated, with low expression levels at embryonic day (E)16 that increase to a peak at E18 and then falls back to E16 levels post-natally. In this developmental window, SCG neurons are growing and branching extensively to innervate their targets, a process that is susceptible to changes in $[Ca^{2+}]_o$, and treatment with calcimimetics. Growth of sympathetic neurons has also shown to be curtailed in CaR NULL mice indicating that the effect of CaR activation on growth

in vitro is relevant *in vivo* for normal sympathetic innervation density (Vizard *et al.*, 2008). It is possible that other tissues developmentally regulate CaR expression and activity, but have yet to be investigated.

1.10 Lung Development

In the mouse, lung development begins at E9.5 when there is an evagination of the foregut endoderm forming the primordial trachea which quickly splits into two primordial lung buds (Hogan, 1999). This process of branching occurs in five stages (Fig. 1.5), ultimately resulting in mature lungs capable of gas exchange within minutes of birth (Warburton *et al.*, 2005). Lung development begins in the embryonic phase (E9.5 – E11.5 in mice; 3-7 weeks in humans) with branching morphogenesis continues thorough the pseudoglandular stage (E11.5-E16.5 in mice; 5-17 weeks in humans) of lung development where there are robust interactions between two cell layers; epithelium/endoderm and mesenchyme/mesoderm (Whitsett *et al.*, 2004). The budding pattern at these early stages is stereotypic and reproducible, producing lungs that have dorsal-ventral and medial-lateral axes, along with identity from left to right (Hogan, 1999). Recently this pattern has been mapped to take place with three different genetically encoded modes of branching (domain branching, planar bifurcation and orthogonal bifurcation) each resulting in a different branch arrangement that ultimately results in a lung with an intricate yet stereotypical pattern of branches (Metzger *et al.*, 2008).

As stated earlier, this process of branching is genetically encoded, with the interaction of various intrinsic growth factors, transcription factors and proteins critical for the proper development of the lung. Mutations or disruptions to these intrinsic factors, as well as the influence of some extrinsic factors can alter the course of lung development resulting in hypo- or hyperplastic lungs with impaired

function (Warburton & Olver, 1997). A brief overview of the resulting phenotype from the inactivation or activation of several of the most robustly studied factors is presented in Table 1.2. Specific factors that are relevant to this study are detailed in sections 1.10.1 and 1.10.2.

1.10.1 Intrinsic Factors affecting Lung Development

Fibroblast Growth Factor (FGF) signalling has an evolutionarily conserved role in lung branching and morphogenesis; FGF homologues in *Drosophila* are critical to the development of the trachea, specifying the tracheal branching pattern and later controlling finer branching at the tips of the primary branches (Sutherland *et al.*, 1996). The mammalian counterpart to the *drosophila* FGF Branchless is FGF-10 which is of particular importance to the mammalian developing lung (Park *et al.*, 1998). Using whole mount *in situ* hybridisation, it is detected in the mesenchyme surrounding the primitive tracheal tube at E9.5. By E10.5 FGF-10 expression is restricted to the distal mesenchyme of the two main bronchi and remains in the distal mesenchyme until at least E14.5. At this point, whole mount *in situ* hybridisation is not possible, but FGF-10 RNA was detected up until E18.5 by Northern blot analysis (Bellusci *et al.*, 1997b). Knockout of FGF-10 in mice results in pups lacking lungs, with the tracheas of the embryos being terminated without any bronchi at the level of the thymus, indicating that FGF-10 is critical for the initiation of the primary bronchi (Min *et al.*, 1998).

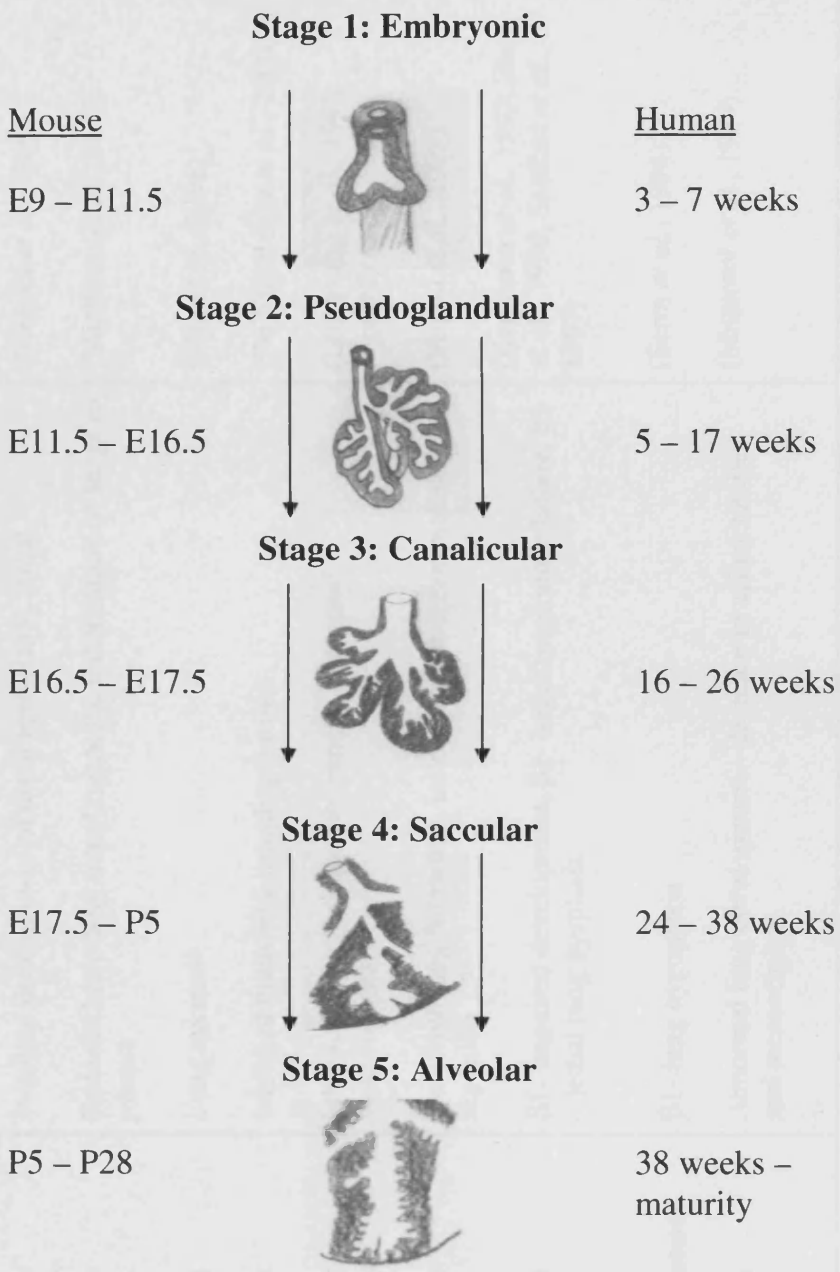

Figure 1.5: Stages of embryonic lung development. Lung morphogenesis takes place in five stages. The initial budding from the foregut endoderm is the *embryonic* phase. This is followed by the *pseudoglandular* phase, when the majority of branching morphogenesis occurs. The *canalicular* phase is next when the vascular bed begins to be organised and the pulmonary acinus forms. The peripheral airspaces are dilated and their epithelium begins to differentiate in the *saccular* phase. The final process is the *alveolar* phase when the alveoli grow and separate. Figure adapted from: Whitsett *et al.*, 2004.

Table 1.2 Overview of factors with mutations that affect lung development.

Factor	Type	Pathology	Reference
<u>Intrinsic</u>			
BMP4	Inhibition	Impaired development of distal epithelium, lethal	(Weaver *et al.*, 1999)
EGFR	Inhibition	Reduced branching morphogenesis, lethal failure of lungs to mature	(Miettinen *et al.*, 1997)
FGF-10	Inhibition	Lung agenesis	(Min *et al.*, 1998)
FGFR2b	Inhibition	Inhibited branching morphogenesis	(De Moerlooze *et al.*, 2000)
SHH	Inhibition	Inhibited branching morphogenesis, disrupted vasculogenesis	(Litingtung *et al.*, 1998; Pepicelli *et al.*, 1998)
TTF-1	Inhibition	Defective lung formation, lack of oesophageal/tracheal septation	(Minoo *et al.*, 1999)
TGFβ	Inhibition	β1- Impaired development, β2- lethal respiratory failure, β3 – lethal lung dysplasia	(Kaartinen *et al.*, 1995; Zhou *et al.*, 1996; Sanford *et al.*, 1997)
TGFβ	Overexpression	β1- lung hypoplasia	(Serra *et al.*, 1994)
VEGF	Inhibition	Abnormal lung development – decrease in acinar tubules and mesenchyme	(Miquerol *et al.*, 1999)

Wnt	Inhibition	Wnt5a – overexpansion of airways, tracheal truncation	(Li *et al.*, 2002)
Wnt	Overexpression	Wnt5a - Reduced epithelial branching, dilated distal airways	(Li *et al.*, 2005)
Extrinsic			
Diaphragmatic Hernia	Reduction of pleural space	Lung hypoplasia and inadequate lung development	(DiFiore *et al.*, 1994)
Nicotine Exposure	Receptor activation	Hyperplasia, increased branching, premature differentiation	(Wuenschell *et al.*, 1998)
Oxygen	Hyperoxia	Premature differentiation	(Acarregui *et al.*, 1993)
Tracheal Occlusion	Increased internal pressure	Increased branching morphogenesis & premature differentiation	(Quinn *et al.*, 1999)

Not only is FGF-10 vital for the primary lung buds, it serves as a chemotactic stimulus to the developing lung epithelium. When isolated epithelia are cultured in matrigel near an acrylic bead soaked in FGF-10, there is an initial outgrowth of the epithelium towards the source of FGF-10 and then branching around it (Weaver *et al.*, 2000). That the epithelium contains a receptor to detect the presence of FGF-10 can be inferred from the aforementioned results, and indeed FGF receptor 2 (*Fgfr2*) is expressed in the developing lung epithelium (Peters *et al.*, 1992). When this receptor is inactivated specifically in the lung, 2 undifferentiated epithelial tubes extend from the trachea to the diaphragm, indicating that *Fgfr2* is vital for branching and differentiation of the lung epithelium (Peters *et al.*, 1994). The specific isoform of the *Fgfr2* receptor that responds to FGF-10 is understood to be *Fgfr2b* (Fig. 1.6A). This interaction has been inferred from the similarity of mice which lack *Fgfr2b* and mice lacking FGF-10 expression. Both mice are non-viable as their lungs do not extend beyond their trachea (De Moerlooze *et al.*, 2000).

While FGF-10 is intimately involved in epithelial-mesenchymal interactions in branching morphogenesis, other FGFs also have roles within the lung. For instance, FGF-1 is present in the mesenchyme early in lung development and promotes multiple branched buds in isolated epithelial cultures, while FGF-7 is expressed from mid-gestation and induces proliferation and differentiation of isolated epithelial cultures (Cardoso *et al.*, 1997). FGF-9 is expressed in the lung epithelium and in the pleura or mesothelium covering the lung at the initiation of lung branching morphogenesis, but by E12.5 its expression is restricted to the mesothelium. Mice lacking FGF-9 show it to be responsible for lung size by controlling the proliferation of the mesenchyme (Colvin *et al.*, 2001). However, it is generally accepted that there

is a hierarchical ranking of importance in this family of growth factors, *i.e.* without FGF-10, none of the other FGFs would get a chance to be expressed.

As FGF-10 has such a marked chemotactic effect on the epithelial development of the lung, it is important to control the locality of its expression. Mice which are null for Sonic hedgehog (Shh) display a diffuse expression of FGF-10 throughout their lungs, which consist of epithelium from the two primary bronchi that are simply large cysts (Pepicelli *et al.*, 1998). Indeed Shh acts as a negative regulator of FGF-10 with its expression localised at distal epithelial tips, where it diffuses to the mesenchyme and helps regulate bud size and shape by down regulating FGF-10 expression (Bellusci *et al.*, 1997a; Lebeche *et al.*, 1999). Another factor that controls the activity of FGF-10 in the lung is sprouty 2 (Spry2; Fig. 1.6A). Spry2 expression is FGF-10 dependent and interferes with FGF-10 activity, inhibiting its signalling with *Fgfr2b* by interacting with parts of the MAP kinase signalling cascade and resulting in a net decrease in MAP kinase activation (Tefft *et al.*, 2002).

Concomitantly expressed with *Fgfr2b*, Shh and Spry2 in the distal epithelium is Bone Morphogenic Protein 4 (Bmp4), another regulator of branching morphogenesis (Bellusci *et al.*, 1996). With expression concentrated in the terminal buds at E11.5 through E15.5 and some expression in the adjacent mesenchyme, Bmp4 has been implicated in differentiation and branching morphogenesis, as demonstrated using mice in which Bmp4 is overexpressed in the epithelium using a surfactant protein – C (SP-C) promoter (Bellusci *et al.*, 1996). By E15.5 the lungs of these mice are dramatically smaller than their wildtype counterparts with fewer terminal branches that are enlarged and separated by thick mesenchyme. By E18.5 there are apparent defects in alveolarization with decreases in alveolar type II (ATII) cell number. While studies with the above mice implicate Bmp4 in later lung

developmental events, there is conflicting information about its activity earlier in lung development. Exact actions are difficult to determine due to, on one hand the late expression of SP-C in the above mouse model and on the other, the lethality of the Bmp4 null mouse, which dies before the initiation of lung formation (Winnier *et al.*, 1995). In addition, *in vitro* studies have presented conflicting results regarding its roles, which seem to depend on the method of culture (Weaver *et al.*, 2000; Bragg *et al.*, 2001). Mesenchyme-free epithelial cultures treated with exogenous Bmp4 indicate that it has a negative modulatory effect on FGF-10 signalling (Weaver *et al.*, 2000), while in whole lung explants application of physiological levels of exogenous Bmp4, enhances branching (Bragg *et al.*, 2001). The combination of these results implies that both the presence of mesenchyme, and the level of Bmp4 is expression, are vital to type of effects Bmp4 signalling has on lung branching morphogenesis (Fig. 1.6B). Gremlin is a negative modulator of Bmp4 activity during lung development. It is most highly expressed early in lung development (E11.5-14.5) where it restricts Bmp4 activity to the distal buds thereby helping to coordinate the optimal number of branching epithelia (Shi *et al.*, 2001).

Proteins from the Wnt family have been recently shown to be intrinsic factors which affect the expression of some of the above described growth factors during lung organogenesis. Members of this family fall into two different categories depending on their modes of action, canonical and non-canonical (Seto & Bellen, 2004). Canonical members stabilize β-catenin and activate target genes through its binding with TCF/LEF transcription factors (Seto & Bellen, 2004), while non-canonical Wnts are β-catenin independent and can antagonise canonical Wnt signalling (Topol *et al.*, 2003). Both canonical and non-canonical Wnts have been shown to be expressed during lung development (Cardoso & Lu, 2006).

Canonical Wnt2a, Wnt2b and Wnt7b are expressed by the lung during development. Wnt2a is expressed in the distal lung mesenchyme, and disruption of this gene results in developmental defects, but not in the lung (Monkley *et al.*, 1996). However this lack of a lung phenotype could be the result of redundancy as Wnt2b is also expressed in the mesenchyme (Katoh *et al.*, 1996). Mutants with inactivation of Wnt7b, normally expressed in the distal epithelium, have lungs which are severely hypoplastic due to proliferation and smooth muscle cell defects (Shu *et al.*, 2002).

In many cases however, the effects of canonical Wnt signalling are studied by interfering with β-catenin, rather than the Wnt proteins themselves, thereby providing an insight to the broader function of canonical Wnt signalling. Complete removal of β-catenin from the distal epithelium results in a lack of Bmp4 expression, as well as reduction of *Fgfr2b* with reduced FGF dependent ERK1/2 activity (Shu *et al.*, 2005). In addition, this study also showed that when Wnt signalling was inhibited by Dikkopf-1 (DKK1), SP-C, a marker for distal epithelial cells, was decreased in the distal epithelium while a marker for proximal epithelium, CC10, was increased (Shu *et al.*, 2005). Taken together, these results point toward canonical Wnt signalling controlling the proximal-distal patterning of the lung by controlling the expression of Bmp4 and *Fgfr2b* (Fig. 1.7). Additionally it seems that canonical Wnt signalling plays a role in the cleft formation and resultant branch formation of early lung development. This conclusion was drawn from experiments where application of DKK1 to early (E11.5) cultured lungs, which resulted in enlarged terminal buds, decreased fibronectin (FN) deposition and decreased α- smooth muscle actin (α-SMA) expression (De Langhe *et al.*, 2005).

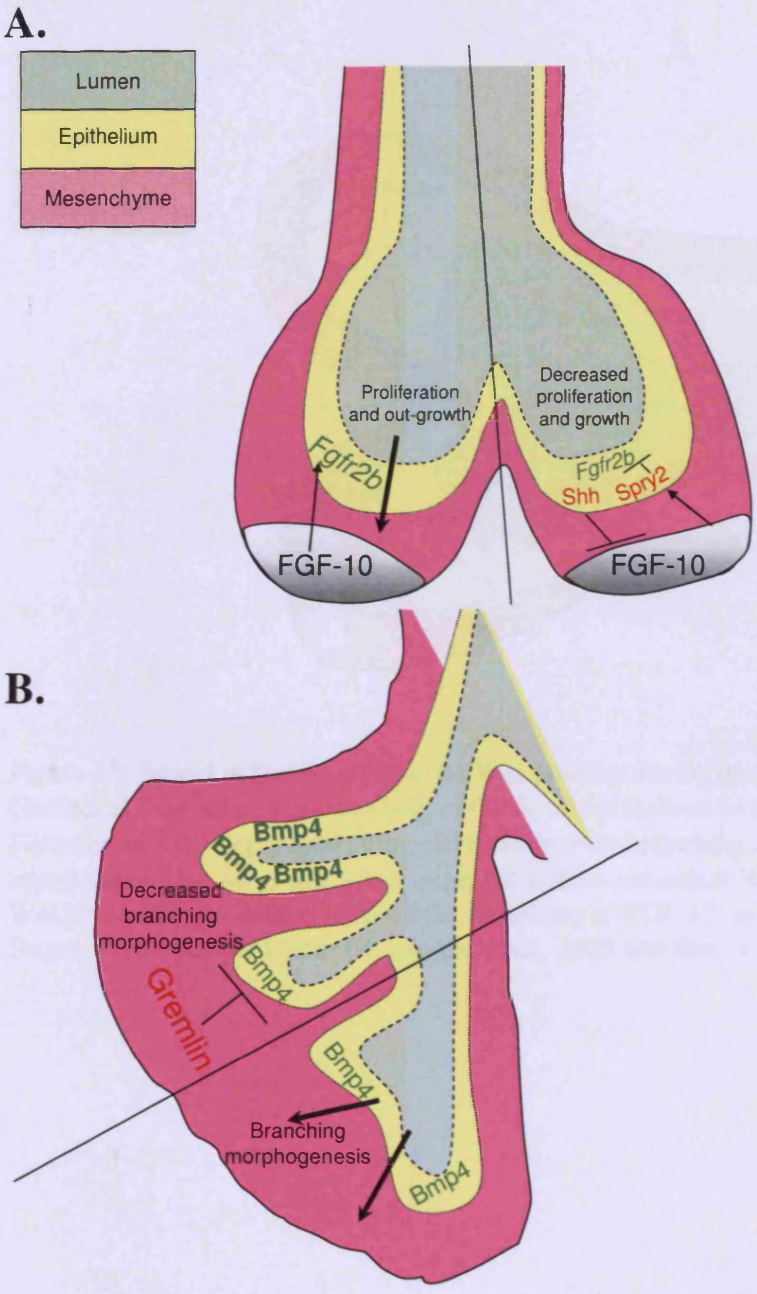

Figure 1.6: Models of FGF-10 and Bmp4 activity in lung development. A). FGF-10 is expressed in the distal mesenchyme of the developing lung exerting chemotactic effects on *Fgfr2b* expressing epithelium resulting in cellular proliferation and bud outgrowth. These effects are tempered by both Shh, which reduces the expression of FGF-10 and Spry2, which interferes with FGF-10/*Fgfr2b* signalling. **B).** Bmp4 is expressed in the distal tips of the developing lung where it enhances branching morphogenesis. Overexpression of **Bmp4** throughout the epithelium, as well as negative regulation by Gremlin, results in decreased branching morphogenesis. Figure adapted from Bellusci *et al.*,1996, 1997a and b, De Moerlooze *et al.*, 2000, Tefft *et al.*, 2002 and Shi *et al.*, 2001.

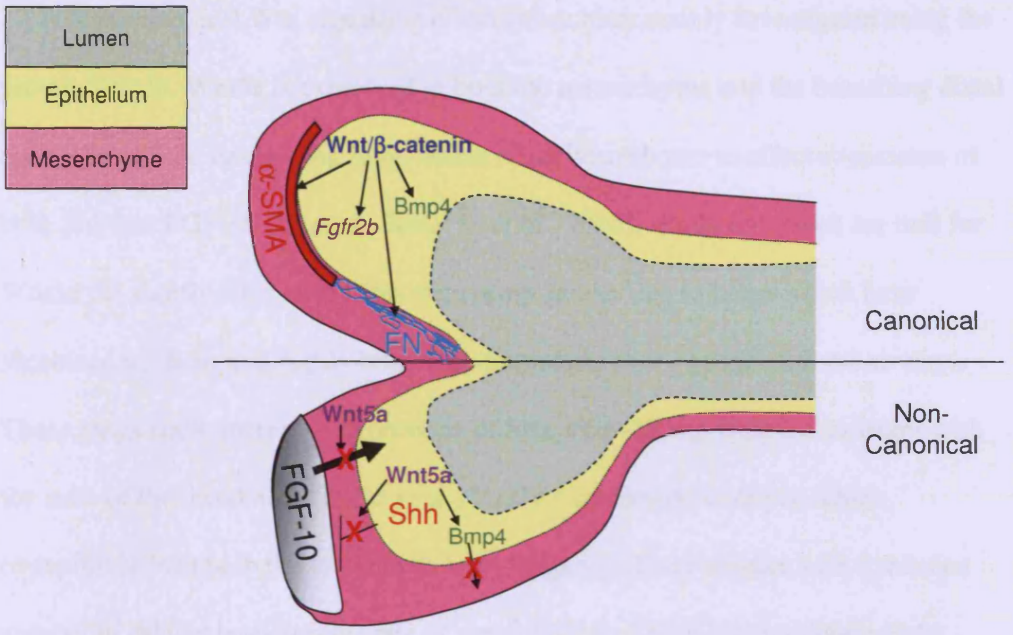

Figure 1.7: Model of factors affected by Wnt proteins during lung development. Canonical Wnt/β-catenin signalling in the distal epithelium has effects on Fibronectin (FN) deposition at the clefts formed for branching, *Fgfr2b*, α- smooth muscle actin (α-SMA) and Bmp4 expression. Non-canonical Wnt signalling by Wnt5a has antagonising effects on the signalling of FGF-10, as well as Shh and Bmp4. Figure adapted from De Langhe *et al.*, 2005 and Shu *et al.*, 2005.

Non-canonical Wnt signalling effects have been mainly investigated using the protein Wnt5a. Wnt5a is expressed in both the mesenchyme and the branching distal epithelium of the developing lung, where it has been shown to affect expression of both Shh and FGF-10 (Li *et al.*, 2002; Li *et al.*, 2005). Embryos which are null for Wnt5a die shortly after birth from respiratory failure due to lungs which have shortened tracheas and highly branched, immature, over-expanded distal airways. These lungs show increased expression of Shh, FGF-10 and Bmp4, consistent with the state of the distal airways (Li *et al.*, 2002). Conversely, embryos which overexpress Wnt5a in the epithelium have lungs which are smaller with a reduced number of dilated branches in spite of upregulation of FGF-10 expression and a decrease in Shh expression. The transgenic lungs from this study did not respond in the normal way to upregulation of FGF-10 expression, possibly due to reduced signalling between Shh and its receptor (Li *et al.*, 2005), but more likely due to an as yet undetermined effect on FGF-10 signalling itself.

In order for the lung to function properly at birth, *i.e.* perform gas exchange, the vascular network within the mesenchyme must be adequate relative to the amount of epithelial surface generated during development. The main growth factor studied for its role in vasculogenesis is vascular endothelial growth factor (VEGF), along with its cognate receptor fetal liver kinase – 1 (Flk-1). VEGF activity is critical for embryonic development in general, as mice losing one or both alleles for VEGF die early in gestation between E9.5 and E10.5 (Miquerol *et al.*, 1999) and embryos null for its receptor, Flk-1, die even earlier at E8.5-E9.5 (Shalaby *et al.*, 1995).

Expression of VEGF has been detected in the lung epithelium of human fetuses (Acarregui *et al.*, 1999) and in cultured mouse lung epithelium expression is specific to the terminal branch points (Healy *et al.*, 2000). There are several isoforms of

VEGF in the mouse. The isoform VEGF164 is the most potent mitogenic factor for endothelial cells (Keyt *et al.*, 1996), and is expressed in the epithelium and mesenchyme at E12.5 where it maintains vascular structure and endothelial cell proliferation (Akeson *et al.*, 2003). When a VEGF coated bead is placed within the cultured lung explant, a capillary bed is formed around it (Healy et al., 2000). This result suggests that VEGF is responsible for vascularisation in the developing lung. This idea is further supported by the fact that mice deficient in the VEGF receptor, Flk-1, have no blood vessel development (Shalaby *et al.*, 1995).

VEGF signalling, by application of exogenous VEGF164 to cultured lung explants, has also been shown to: a) affect proliferation of both mesenchyme (where Flk-1 is expressed) and epithelium; b) up-regulate Flk-1, SP-C and Bmp4 expression; c) down-regulate Spry2 and Spry4 expression. In contrast, it does not affect FGF-10 expression. These effects are reversed when Flk-1 expression is inhibited with antisense oligodeoxynucleotide (ODN) treatment; *i.e.* Flk-1, SP-C and Bmp4 are down-regulated while Spry2 and Spry 4 are upregulated (Del Moral *et al.*, 2006b). The combination of these two sets of results shows that the effects of VEGF164 application are mediated through its interactions with Flk-1. Therefore VEGF signalling is a vital component of epithelial – mesenchymal communication which mediates lung development.

1.10.2 Extrinsic Factors affecting Lung Development

All of the factors discussed in Section 1.9.1 are susceptible to under - and over – expression as well as inappropriate timing of expression. These faults can be caused by an inherent genetic defect, or they can be influenced by factors which come from outside the developing lung or fetus. These extrinsic factors can alter the

intrinsic programme of lung development resulting in impaired function after birth (Pinkerton & Joad, 2000).

Oxygen (O_2) is one such extrinsic factor which can affect the intrinsic lung developmental programme. Development occurs in the relative hypoxic environment of the uterus (Lee *et al.*, 2001) and the lung itself remains poorly vascularised until mid-gestation, with staining for vascular endothelial markers not appearing in the mouse lung until E12.5 (Colen *et al.*, 1999). Due to the lack of vascularisation, it is assumed that the developing lung has a lower O_2 tension (Po_2) than its adult counterpart. This has been shown in developing sheep where the pulmonary Po_2 has been shown to be 16-18 mmHg. This Po_2 indicates a hypoxic environment as the ambient external environmental Po_2 is 140-150 mmHg (Acarregui *et al.*, 1993).

A Po_2 greater than 71 mmHg causes spontaneous induction of surfactant protein – A (SP-A) expression and morphological differentiation in cultured human fetal lungs while a Po_2 of approximately 7 mmHg keeps them in a state similar to that at the beginning of culture (Acarregui *et al.*, 1993). Rat lung explants cultured at 21 mmHg display increased branching morphogenesis and proliferation as well as the correct proximal-distal differentiation for their stage. When rat lung explants are cultured at 71 mmHg, the pattern of branching morphogenesis, proliferation and proximal-distal differentiation seen in response to 21 mmHg is disrupted. Mouse lung explants in hyperoxic conditions of 250 mmHg or greater did not branch or grow (Wilborn *et al.*, 1996) setting an upper limit on the amount of O_2 that a developing lung can tolerate. As for intrinsic factors which are modulated by O_2 concentration, VEGF, Flk-1 and platelet endothelial cell adhesion molecule -1, all of which are involved in vascular development, are more highly expressed in lungs cultured at 21 mmHg than in those at 140 mmHg. Expression of FGF-10, *Fgfr2b* and

Bmp4 were unchanged between the two concentrations, however, SP-C expression increased as the lungs were maintained in culture, demonstrating an appropriate rate of epithelial differentiation in this low O_2 concentration (van Tuyl *et al.*, 2005).

Nicotine, which crosses the placental barrier and concentrates in the environment around the fetus (Luck *et al.*, 1985), is another extrinsic factor that can affect lung development. Children born to mothers who smoked throughout pregnancy have significantly decreased lung function (Cunningham *et al.*, 1994) and predisposition to episodes of wheezing (Hanrahan *et al.*, 1992). When lung explants are cultured in the presence of 1 μM nicotine, there is a 32% increase in the number of terminal airway branches when compared to culture conditions without nicotine. Following nicotine exposure there is also an increase in expression of mRNAs encoding SP-A and SP-C, which are used as markers of the lung's stage of differentiation. The increase in these surfactant proteins indicates that the lung has prematurely developed (Wuenschell *et al.*, 1998). Other studies have shown that nicotine exposure increases the proliferation of alveolar type II cells and increases surfactant protein synthesis in general (Rehan *et al.*, 2007). These changes in the terminal sacs of the airways could later impede gas exchange. While there are currently no reports linking nicotine exposure to changes in intrinsic factors such as FGF-10 or Bmp4, there have been reports of it affecting components of the extracellular matrix. These components include factors such as collagen and elastin, which are vital to forming the correct structure of the lung (Pierce & Nguyen, 2002), and defects in their expression may negatively impact the ability of the lung to expand properly.

Another extrinsic factor that can affect intrinsic lung developmental mechanisms is a mechanical impediment to lung development. One naturally

occurring mechanical change is the pathological state of congenital diaphragmatic hernia (CDH) where development of the lung is impeded by the presence of abdominal organs within the chest cavity. CDH results in lung hypoplasia with severe morbidity and mortality consequences (Stege *et al.*, 2003). In neonates suffering from this abnormality, the degree of lung hypoplasia is associated with the severity of their symptoms and survival (Smith *et al.*, 2005). At this time there is not linkage between a specific gene and the development of CDH, but it is linked with malfunctioning peristalsis in airway smooth muscle (Jesudason, 2006; Jesudason *et al.*, 2006).

One of the current treatments for CDH is tracheal occlusion, which in itself can result in defective lung development. The lung develops as a fluid-filled organ, with fluid being secreted by the developing epithelium, and tracheal occlusion greatly increases intraluminal pressure due to the inability of the secreted fluid to evacuate from the lung. Tracheal ligation may occur pathologically, as in cases of congenital tracheal agenesis (Mori *et al.*, 2001), or surgically, as in cases where it is used to treat CDH (Smith *et al.*, 2005) and it can be experimentally accomplished within *ex vivo* lung cultures. In E14 mouse lung explants tracheal ligation increased both lung growth and maturation (Blewett *et al.*, 1996), this was also true for the lungs of an infant which suffered from tracheal agenesis (Mori *et al.*, 2001).

1.11 The Lung, Calcium and the CaR

There are several studies which point to a role for Ca^{2+} in lung development. In 1995 it was reported that contractions of the developing airway smooth muscle could be abolished by the application of an L-type calcium channel blocker, nifedipine, thereby blocking the influx of Ca^{2+}_o into the lung smooth muscle cells within E11 mouse lung explants. This treatment also affected the overall growth of

the lung, producing a hypoplastic lung (Roman, 1995). Later experiments confirmed these observations and elaborated that the effect of nifedipine on lung growth could not be rescued by exogenous application of FGF-10, implicating that there was a link between FGF-10 signalling and the smooth muscle cell activity within the developing lung. Indeed, nifedipine abolished both lung smooth muscle contractions and the increases in lung growth normally mediated by FGF-10 (Jesudason *et al.*, 2005). This study also demonstrated that the contractions of airway smooth muscle were peristaltic in nature and their frequency could be modulated by application of nicotine and FGF-10.

The above studies have shown that the peristaltic movement is reliant upon Ca^{2+}_o influx, and that airway peristalsis is linked to normal development of the lung. Ca^{2+}- imaging experiments revealed that regenerative, spontaneous Ca^{2+}_i waves travel via gap junctions through the smooth muscle. Generation of these waves required Ca^{2+}_o entry and are dependent on Ca^{2+}_i release from the sarcoplasmic reticulum (Featherstone *et al.*, 2005). It is interesting that this Ca^{2+}- dependent phenomenon is developmentally regulated, related to the growth of the lung in normal conditions and yet this relationship can be broken when there is an underlying cause of lung hypoplasia, like CDH (Jesudason *et al.*, 2006). While these studies have used nominally Ca^{2+}_o-free solutions on cultured lung buds to elucidate the nature of the Ca^{2+} activity in smooth muscle, there are no studies on any effects which $[Ca^{2+}]_o$ may have on lung development.

The lack of study in to the potential effects of Ca^{2+}_o on lung development has possibly occurred because, prior to the experiments detailed in this thesis, there has been no evidence that the lung possessed a mechanism with which to respond to changes in Ca^{2+}_o. CaR transcripts have not been detected in adult lungs by Northern

blot analysis (Brown *et al.*, 1993; Riccardi *et al.*, 1995). However, there is some circumstantial evidence pointing towards the possibility that CaR activity may influence lung development.

In the vast number of reports describing different CaR mutations resulting in NSHPT, one 3-month old patient presented with hypercalcemia, hyperparathyroid bone disease and difficulty breathing. He underwent an immediate parathyroidectomy, however despite this intervention and resolution of his hypercalcemia, he died from respiratory failure (Pidasheva *et al.*, 2006). Unfortunately, there is no published information on the exact pathological status of his lungs. Another NSHPT patient was born prematurely, and was diagnosed with lung hypoplasia, respiratory distress syndrome and early pulmonary interstitial emphysema on the day of her birth. Again, despite rapid and successful interventions to mitigate severe hyperparathyroidism, this patient died from severe chronic lung disease (Fox *et al.*, 2007). Although these are two reports of lung symptoms within a larger body of published reports it is possible that other NSHPT patients have also had respiratory issues that were incidental to their other more severe symptoms. This supposition is supported by another publication which reported that in a family with a high occurrence of FHH, several children had died at the ages of 2-14 months from respiratory or gastro-intestinal disturbances or from sudden infant death (Auwerx *et al.*, 1985b).

Interstitial lung disease is one type of respiratory pathology that has been shown to have a high occurrence within FHH cohorts. It is part of a group of diseases broadly known as pulmonary fibrosis that result in respiratory deficiency due to scarring of the alveolar interstitium (Steele *et al.*, 2005). It has been published that in a familial cohort of 43 members there was a positive correlation between

inheritance of FHH and interstitial lung disease. This coexistence of pathology was regardless of patient's smoking habits and generally involved malfunctioning granulocytes (Auwerx *et al.*, 1985a; Auwerx *et al.*, 1985b). The pathologies mentioned here could be the result of defective CaR function. Even though there is no evidence to suggest that CaR is present in the lung from birth onwards to adulthood, it is entirely possibly that maladjustment to Ca^{2+}-dynamics during development due to defective CaR function results in defective lung physiology later in life.

1.12 Aims and Objectives

The division and expansion of branches in the developing lung is primarily a prenatal occurrence which occurs when the fetus is exposed to hypercalcaemic conditions compared to its adult life, with standard free ionized $[Ca^{2+}]_o$ of 1.7 mM . Given that calcium concentration has potential effects on the expression and control of vital developmental proteins in the lung; ***I hypothesize that extracellular calcium is an important extrinsic factor that modulates the intrinsic lung developmental programme.*** Furthermore, as preliminary data have shown CaR mRNA expression within the developing lung; ***I propose that the potential effects of calcium will be modulated via activation of the extracellular calcium-sensing receptor.***

Specific aims of this project include:

1. To determine the effect of changing $[Ca^{2+}]_o$ on lung branching morphogenesis;
2. To determine the detailed ontogeny and cellular distribution of CaR in lung;
3. To establish the role of CaR in lung development;
4. To determine functional consequences of CaR activation in the lung;
5. To characterize the mechanism of action of CaR-dependent regulation of

branching;

6. To characterize the lung phenotype of CaR knockout mice.

In order to accomplish these aims I will be using the established model of gas-fluid interface lung explant culture which is a robust tool due to the fact that the process of lung development is stereotypically retained when embryonic lungs are grown in culture (Jaskoll *et al.*, 1986). This culture method was chosen over other methods, *i.e.* submersion cultures (McAteer *et al.*, 1983) or Matrigel embedding, due to the desire to enable comparison of my results against other published studies using the interface culture method. Additionally, the interface method allows for uncomplicated counting of terminal branches which is the primary read-out of this study. I will also be using PCR, immunohistochemistry and transgenic mouse models to test my hypothesis.

CHAPTER 2:
EFFECT OF EXTRACELLULAR CALCIUM ON LUNG BRANCHING MORPHOGENESIS

2.1 Methods

2.1.1 Lung Explant Cultures

Embryos at day 12.5 of development (E12.5) were removed from time-mated pregnant C57/BL6 females. The morning of plug was considered E0.5 and all pregnant female mice were humanely sacrificed in accordance with UK Home Office Schedule 1 procedures or Children's Hospital Los Angeles Institutional Animal Care and Use Committee regulations by CO_2 inhalation. Embryos were removed from dead, pregnant females *in utero* to cold Hank's balanced saline solution (HBSS), gently dissected from their membranes with the aid of a stereomicroscope, decapitated and the lungs dissected from the body.

Lung explant culture experiments were based on the culture model developed by Jaskoll et al., (1986). The lungs were dissected from embryos in cold HBSS (Invitrogen, Paisley, UK) without Ca^{2+} or Mg^{2+}. For individual lobe experiments, the lungs were divided mechanically using forceps to break off each lobe. The isolated lungs or lobes were placed on Nucleopore filters (8.0 μm pore size; Whatman Intl. Ltd., Maidstone, Kent, UK) floating on the surface of 1000 μl of DMEM/F12 medium (Invitrogen, Paisley, UK) in Nunclon 4-well dishes (De Langhe *et al.*, 2005) with 1000 U/ml penicillin and 0.1 mg/ml streptomycin (Invitrogen, Paisley, UK). All explant culture experiments were performed in chemically defined, serumless conditions.

Once initial pictures were taken (t = 0 h), the cultures were placed in a cell culture incubator at 37°C, 5% CO_2/95% saturated air. Pictures were taken at 0, 24 and 48 h in culture using a Leica $MZ12_5$ stereomicroscope, digital camera and software (Leica Microsystems (UK) Ltd., Milton Keynes, Buckinghamshire, UK) at 2.5x magnification. The effect of different $[Ca^{2+}]_o$ on lung growth and branching

morphogenesis was tested by altering the $Ca^{2+}{}_o$ concentration of DMEM/F12. This medium contains a basal $[Ca^{2+}]_o$ of 1.05 mM and was adjusted by adding either 0.2 M EGTA to reduce the Ca^{2+} present in the medium, or 0.5 M $CaCl_2$ to increase the $[Ca^{2+}]_o$. $[Ca^{2+}]_o$ was measured, in 3 samples to ensure that calculated concentration and actual concentration were within a reasonable margin using a ABL 800 FLEX (Radiometer Limited, Sussex, UK) blood gas analyser. Results are presented in Table 2.1.

Branching morphogenesis was quantified by counting the number of terminal branches around the periphery of the lung explants at the time of removal, at 24 and 48 h in culture. The percent change in branching was calculated as: ($Branches_{24h \text{ or } 48h}$ – $Branches_{0h}$) / $Branches_{0h}$ x 100.

Table 2.1: Predicted and measured $[Ca^{2+}]_o$ of lung explant culture medium. Predicted $[Ca^{2+}]_o$ and measured $[Ca^{2+}]_o$ of culture medium used for lung explant cultures at 37°C , pH 7.4. 3 separate samples were measured for each $[Ca^{2+}]_o$, data presented are mean ± standard deviation.

Predicted $[Ca^{2+}]_o$	Measured $[Ca^{2+}]_o$	0.2 mM EGTA added	0.5 mM $CaCl_2$ added
0.5 mM	0.62±0.1 mM	2.75 µL	n/a
1.05 mM	0.92±0 mM	n/a	n/a
1.2 mM	1.09±0.1 mM	n/a	0.3 µL
1.7 mM	1.51±0.2 mM	n/a	1.32 µL
2.5 mM	2.49±0.1 mM	n/a	2.9 µL

2.1.2 Area Measurements of Lung Explant Cultures

Photomicrographs taken at t = 48 h were imported into Adobe Photoshop 7.0 to 100% their original size (20.43 x 27.62 cm). For all photomicrographs, brightness and contrast were increased (+43, +66) to enhance delineation between mesenchyme and lumen. Using the "lasso" tool the external edge of the lung was traced (Fig. 2.4 A*i* and *ii*), the "histogram" function was used to determine the number of pixels within the traced area, and this measurement was assumed to be the total lung area. The mean ± standard error of the mean (s.e.m.) was then calculated using Microsoft Excel producing a value for the total area of lungs cultured in the presence of 1.05 and 1.7 mM Ca^{2+}_{o}. Also using the "lasso" tool the internal lumen spaces were traced and again the "histogram" function used to determine the number of pixels contained within the traced area. This measurement was assumed to be the luminal area of the lung. The amount of mesenchyme within each lung was calculated by subtracting the luminal area from the total lung area. The percentage of lumen or mesenchyme within the total area of each lung was calculated by the following formula: (Total area – Lumen (or mesenchyme) area)/ Total area = x*100 = % lumen or % mesenchyme. The mean ± standard error of the mean (s.e.m.) was then calculated for the % lumen or % mesenchyme within lungs cultured in the presence of 1.05 and 1.7 mM Ca^{2+}_{o}.

2.1.3 Immunohistochemistry

Microdissected and cultured lungs were fixed in 4% paraformaldehyde (PFA) in phosphate buffered saline (PBS) at 4 °C for 20 min. The specimens were subsequently washed twice with PBS, then dehydrated and stored in 70% ethanol at 4°C. PFA-fixed tissue was then embedded in paraffin wax and 5 μm thick sections

were cut for histology on a standard microtome. Sections were mounted on Superfrost Plus glass slides (Fisher Scientific, UK). Tissue sections prepared for histology were de-paraffinized with Histochoice (Sigma-Aldrich, Gillingham, Dorset, UK) and rehydrated through a series of graded alcohols. After rehydration, the slides were subjected to antigen retrieval by submerging in citrate buffer (2.1g Citric Acid Monohydrate in 1 L H_2O brought to pH 6.0 with NaOH) heated to boiling in a 900 W microwave for 3 min. Once the buffer was boiling, the microwave setting was reduced to 300 W and the slides were boiled for a further 10 min. The slides were left to cool to room temperature (RT) in the citrate buffer. When the buffer was at RT, the slides were rinsed in PBS and non-specific binding of the primary antibody was prevented by incubating slides in 3% bovine serum albumin (BSA) in PBS (Sigma-Aldrich, Gillingham, Dorset, UK) containing 0.1% Triton-X100 (Sigma-Aldrich, Gillingham, Dorset, UK) for 1 h at room temperature. For proliferation studies, immunohistochemistry was performed using a rabbit polyclonal antibody against phosphorylated histone H3 (Upstate, Lake Placid, NY, USA), a marker of mitosis. The slides were incubated with this antibody at 1:200 dilution in antibody dilution fluid (AbDF; 1% BSA, 3% Seablock (EastCoast Bio, Soham, Cambridgeshire, UK) in PBS with 0.1% Triton-X100) overnight at 4°C.

The primary antibody was removed by washing in several changes of PBS. The secondary antibody (supplied in the Dako Envision Kit mentioned below) was applied for 30 min at RT, and then removed in several washes of PBS. Visualization of the detected proteins was performed using an Envision Diaminobenzidine kit (DAB; Dako, Ely, Cambridgeshire, UK) according to the manufacturer's instructions. Once the DAB was developed to an adequate level, with nuclear staining and minimal background, the slides were counterstained with Harris's

haematoxylin, dehydrated and mounted with Clarion mounting medium (Sigma-Aldrich, Gillingham, Dorset, UK). For staining of apoptotic cells in paraffin sections, an ApopTag Plus Peroxidase *In Situ* apoptosis detection kit (Chemicon/Millipore, Watford, UK) was used according to manufacturer's instructions.

For both proliferation and apoptosis quantification, three lungs were stained for each 1.05 mM and 1.7 or 2.5 mM Ca^{2+}_{o}. Once stained, 5 photomicrographs were taken at 100x magnification of two sections (5 sections apart to minimise risk of double counting cells) per lung. The number of stained cells (proliferating or apoptotic), as well as the total cell number within each photomicrograph was counted and the number of stained cells expressed as a percentage of total cell number.

2.1.4 Trans-epithelial Potential Difference

This protocol was developed, performed and kindly provided by William Wilkinson Ph.D. Lung trans-epithelial potential difference (TPD) was recorded using the current clamp technique. After 48 h in culture, individually mounted lung explants attached to filters were removed from growth medium, placed in the bottom of recording chamber and held down with a platinum ring that did not touch the lung explant. The recording chamber was then carefully filled with a solution containing (in mM); 135 NaCl, 5 KCl, 1.2 $MgCl_2$, 1 $CaCl_2$, 5 HEPES, 10 Glucose, pH 7.4 with NaOH. Borosilicate glass electrodes (World Precision Instruments, Stevenage, UK), were filled with 0.4 % trypan blue solution in 0.85% saline (Invitrogen, Paisley, UK) and had a resistance of 4-5 MΩ. Electrodes were carefully pushed into a random lumen terminal, whilst maintaining positive pressure on the electrode, when access was achieved (blue dye in lumen), positive pressure on the electrode was removed,

and equilibrium was allowed to be reached over a 5 min period before being removed. The trans-epithelial potential difference was taken as the difference between the inside and outside at the end of the 5 min. Recordings were made using an Axon Multiclamp 700A amplifier (Axon Instruments) and analysed using pClamp 9 software. Ag-AgCl reference electrode was placed in the bath approximately 5 mm from the lung explant.

2.1.5 Statistics

Graphic representations and statistics of the data were prepared with Origin 7 software. Data are presented as the mean (from multiple pooled experiments where indicated) $\pm$ s.e.m. Significance was determined using one-way ANOVA with Tukey *post-hoc* test and a p-value of ≤ 0.05 was deemed significant.

2.2 Philosophy of work

Previous studies carried out on isolated embryonic rat lung explants have indicated that altered Ca^{2+}_i dynamics influence lung growth. These studies have investigated the phenomenon of spontaneous airway contractions observed in rats, mice and humans (See section 1.11 for review), showing that $[Ca^{2+}]_o$ is involved in the generation of Ca^{2+} waves in airway smooth muscle (ASM) in the developing lung (Featherstone *et al.*, 2005). Although these studies have shown that $[Ca^{2+}]_o$ is required for the propagation of ASM Ca^{2+}-waves; the effects on branching morphogenesis of altering the $[Ca^{2+}]_o$ of the culture medium in which mouse lung explants are cultured has not been assessed. The series of experiments presented within this chapter were designed to investigate the potential effects of free-ionized Ca^{2+}_o on the branching morphogenesis programme of the lung.

2.3 Branching morphogenesis is sensitive to $[Ca^{2+}]_o$.

Using an established model of mouse lung explant cultures (Jaskoll *et al.*, 1986), E12.5 lungs were cultured for 48 h in chemically defined, serum-free medium conditions. E12.5 embryos were used for these studies because, at this point the lungs are at the beginning of the pseudoglandular stage of lung development and branching morphogenesis is easily quantifiable. A range of different $[Ca^{2+}]_o$, from 1.05 to 2.5 mM Ca^{2+}_o (Fig 2.1), was chosen to correspond with previously published lung culture studies, and to reflect physiological levels. $[Ca^{2+}]_o$ of approximately 1.2 and 1.7 mM correspond to the adult and foetal serum free ionized $[Ca^{2+}]_o$, respectively (Kovacs & Kronenberg, 1997). Additionally, we considered the range at which the CaR responds to Ca^{2+}, normally between 0.5 and 3.5 mM, as it is

responsible for maintaining physiological systemic $[Ca^{2+}]_o$ levels (Brown & MacLeod, 2001).

Lung branching morphogenesis was sensitive to Ca^{2+}_o, with differences in the amount of branching morphogenesis quantified after 48 h, depending upon the $[Ca^{2+}]_o$ to which the lung explant was exposed (Fig 2.2). Figure 2.2A shows that the most permissive conditions for branching morphogenesis occurred when the $[Ca^{2+}]_o$ was in the range of adult physiological levels of, 1.05 – 1.2 mM Ca^{2+}_o. At these concentrations, branching was increased by 123±4.5% (n=54) and 109.7±3.1% (n=88) after 48 h respectively. Lung explants cultured in the presence of $[Ca^{2+}]_o$ similar to fetal $[Ca^{2+}]_o$, 1.7 mM, were restricted in the amount of branching morphogenesis after 48 h. Branching morphogenesis in these explants was halved to 62.2±4.4% (n=45) in comparison to branching morphogenesis levels in 1.05 mM Ca^{2+}_o, and continued to be suppressed in 2mM Ca^{2+}_o (37.1±8.8%) and 2.5 mM Ca^{2+}_o (54.7±4.2%). Representative pictures of lung explants cultured in either permissive or restrictive conditions at 0, 24 and 48 h in culture can be seen in Figure 2.2B.

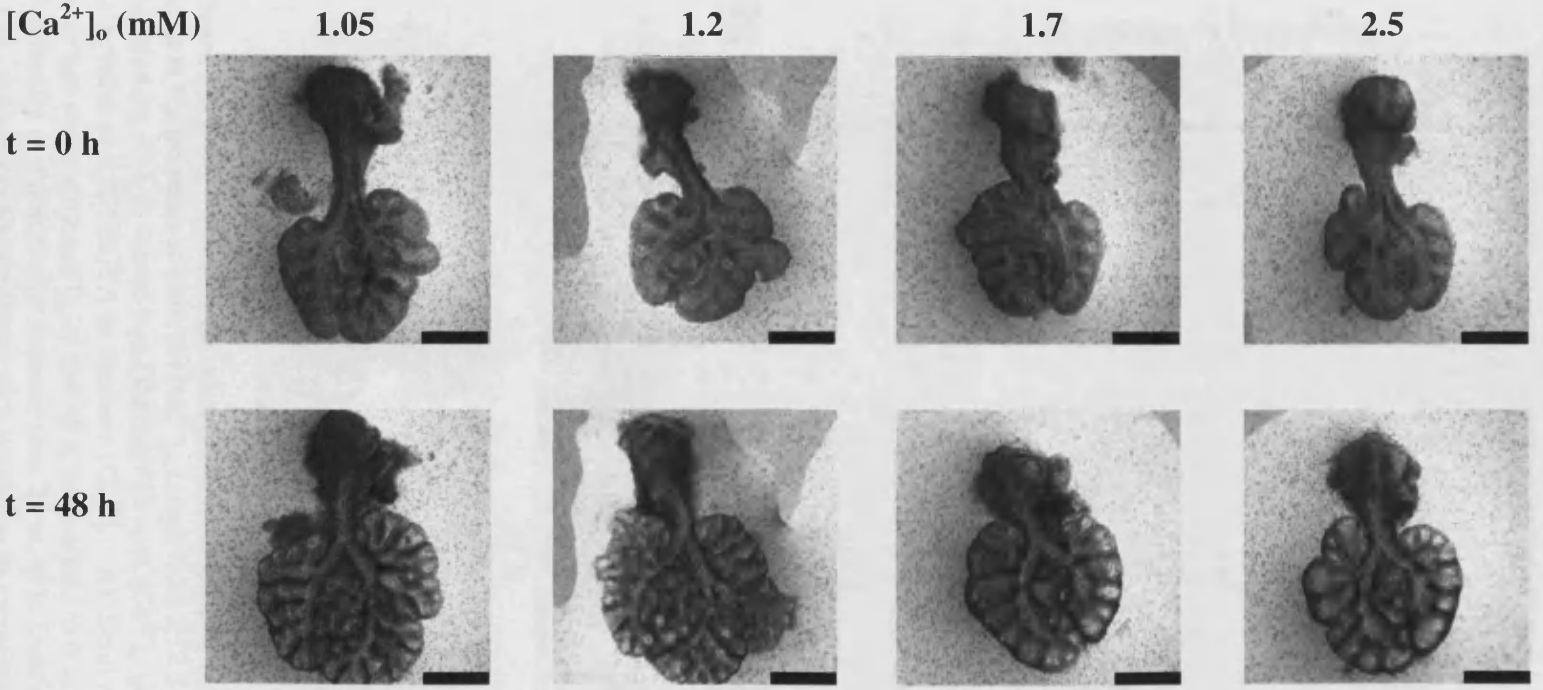

Figure 2.1: Initial determination of the effects of the $[Ca^{2+}]_o$ of culture medium on lung branching morphogenesis. A preliminary experiment was performed to determine if E12.5 mouse lung explant cultures are sensitive to changes in the $[Ca^{2+}]_o$ of culture medium. The upper panel of pictures represents the lungs at the time of dissection (E12.5, t = 0 h) and placement onto floating filters. The lower panel of pictures represents the same lungs after 48 h (t = 48 h) in culture in the presence of culture medium containing the $[Ca^{2+}]_o$ (mM) designated above the panels. Scale bars = 600 μm.

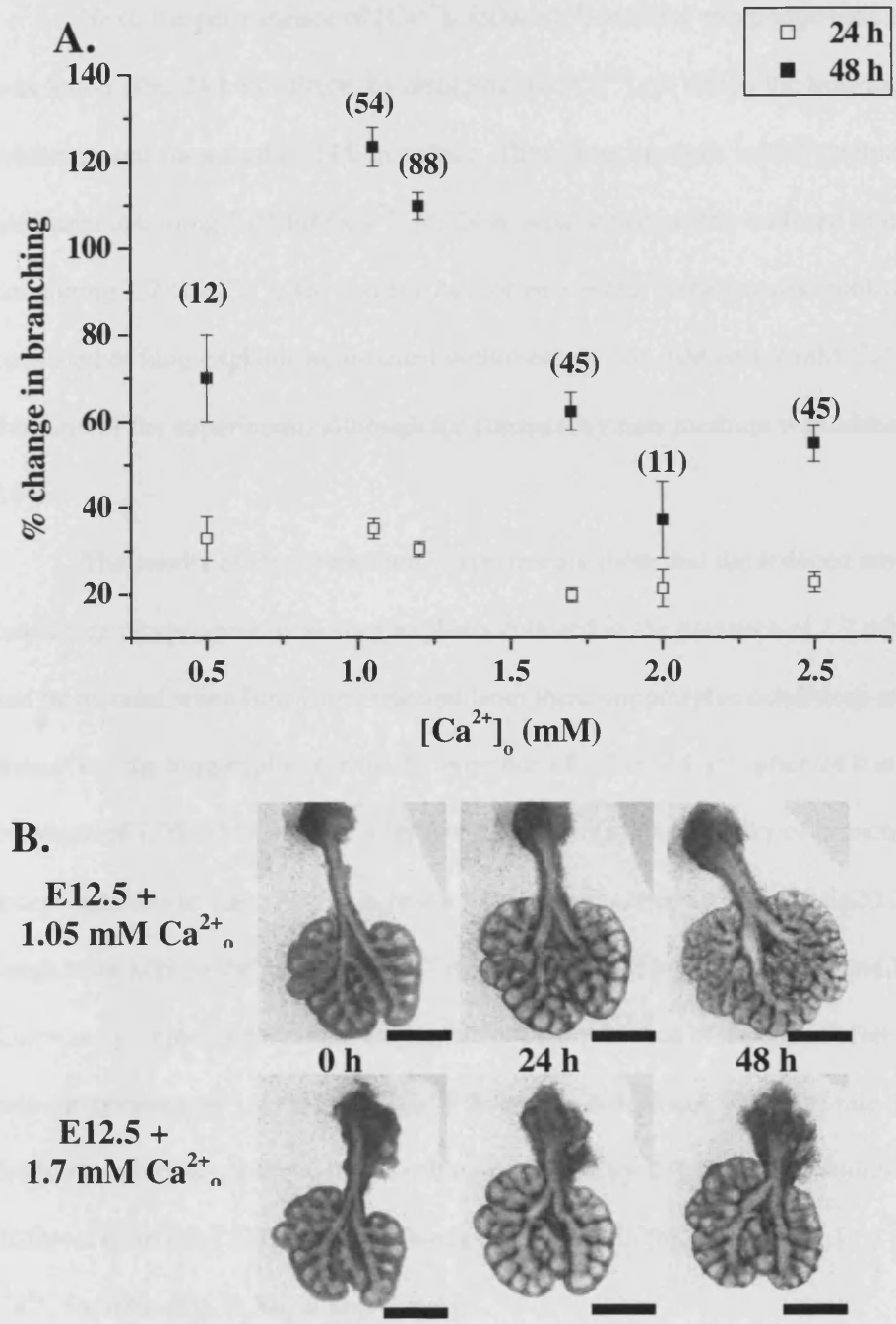

Figure 2.2: Lung branching morphogenesis is affected by incubating E12.5 mouse lungs in the presence of different $[Ca^{2+}]_o$. Lungs from E12.5 mouse embryos were cultured for 48 h in serum-free DMEM/F12 with $[Ca^{2+}]_o$ adjusted using 0.5M $CaCl_2$ to increase or 0.2M EGTA to decrease $[Ca^{2+}]_o$. **A).** Total number of terminal branches was counted at 0, 24 and 48 h, normalized to 0 h, and the change expressed graphically as a percentage increase over 24 or 48 h. Data shown are the mean ± s.e.m., n numbers shown above each condition in parentheses from ≥ 4 pooled experiments **B).** Representative pictures of lungs cultured in the presence of 1.05 mM Ca^{2+}_o (top row) or 1.7 mM Ca^{2+}_o (bottom row) at 0, 24 and 48 h. Scale bars = 700 μm.

Next, the permanence of $[Ca^{2+}]_o$-induced, branching morphogenesis effects was tested after 24 h in culture, by changing the $[Ca^{2+}]_o$ to which the lung explants were exposed for a further 24 h in culture. Thus, lung explants initially cultured with medium containing 1.05 mM Ca^{2+}_o for 24 h, were subsequently cultured in medium containing 1.7 mM Ca^{2+}_o for another 24 h or *vice versa*. Experimental controls consisted of lung explants maintained within either 1.05 mM or 1.7 mM Ca^{2+}_o for the duration of the experiment, although for consistency new medium was added after 24 h.

The results of the "switching" experiments show that the reduced amount of branching morphogenesis in lung explants cultured in the presence of 1.7 mM Ca^{2+}_o can be rescued when lungs are removed from these suppressive conditions after 24 h. Removing the lung explants from the presence of 1.7 mM Ca^{2+}_o after 24 h into the presence of 1.05 mM Ca^{2+}_o for a further 24 h, results in a recovery of branching morphogenesis to 154±19.6%, versus a branching increase of only 80.8±20.7% when lungs were kept in the presence of 1.7 mM Ca^{2+}_o for 48 h (Fig. 3.3A, D and E, n=5). Conversely, removing the lung explants from the presence of 1.05 mM after 24 h into the presence of 1.7 mM Ca^{2+}_o for a further 24 h does not affect the rate of branching morphogenesis with branching increased by 171.8±22.4%, which is not different from the 172.6±30.7% in lungs maintained in the presence of 1.05 mM Ca^{2+}_o for 48 h (Fig. 2.3A, B and C, n=5).

Lung explants cultured in 1.05 mM Ca^{2+}_o appeared to be larger than lung explants grown in 1.7 mM Ca^{2+}_o (Fig. 2.1). Therefore the total area and the luminal areas were measured by tracing both the external circumference and internal luminal area (Fig. 2.4A) and calculating the number of pixels contained within each area. There was a significant difference in the total area between lungs cultured in the

presence of 1.05 mM Ca^{2+}_o and 1.7 mM Ca^{2+}_o. The total area measured for lungs cultured in the presence of 1.05 mM Ca^{2+}_o was $1.22x10^5 \pm 4.2x10^3$ pixels (n=15), while the total area of lungs cultured in the presence of 1.7 mM Ca^{2+}_o was significantly decreased to $1.03x10^5 \pm 4.3x10^3$ pixels (n=14 from 4 separate isolations, p=0.003, Fig. 2.4B). The luminal space within lungs grown in the presence of 1.7 mM Ca^{2+}_o was also significantly smaller than the luminal space within lungs cultured in the presence of 1.05 mM Ca^{2+}_o. Lung explants cultured in the presence of 1.05 mM Ca^{2+}_o contained 61.04±1.04% lumen, while lungs cultured in the presence of 1.7 mM Ca^{2+}_o contained 57.95±0.87% lumen (p=0.033, Fig. 2.4C). The opposite was true for the percentage of mesenchyme making up the total lung area. Lungs cultured in the presence of 1.7 mM Ca^{2+}_o had a greater percentage of mesenchyme with 42.05±0.87% which was reduced to 38.97±1.04% in lungs cultured in the presence of 1.05 mM Ca^{2+}_o (p=0.033, Fig. 2.4C). Therefore, there was a 3% increase in the percentage of mesenchyme component within lungs cultured in the presence of 1.7 mM Ca^{2+}_o.

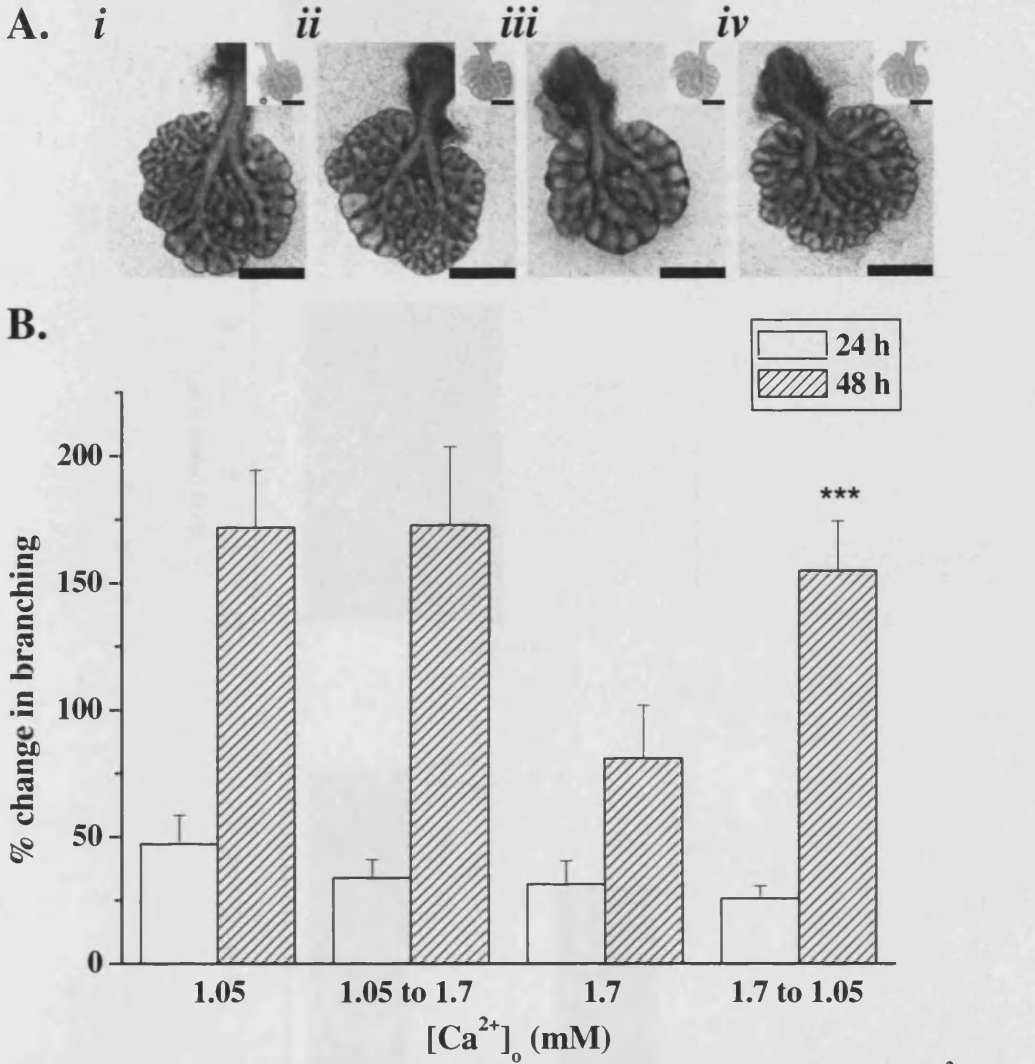

Figure 2.3: Lung branching morphogenesis can be rescued by manipulating $[Ca^{2+}]_o$. E12.5 mouse lungs were cultured for the first 24 h in the presence of 1.05 mM or 1.7 mM Ca^{2+}_o. At 24 h the culture medium was changed from 1.05 mM to 1.7 mM, 1.7 mM to 1.05 mM or replaced with medium containing the same $[Ca^{2+}]_o$ as the original medium. Lung explants were then cultured for another 24 h. **A).** Representative pictures of explants: ***i.*** 1.05 mM Ca^{2+}_o for 48 h, ***ii.*** 1.05 mM Ca^{2+}_o for 24 h then changed to 1.7 mM Ca^{2+}_o for a further 24 h, ***iii.*** 1.7 mM Ca^{2+}_o for 48 h, ***iv.*** 1.7 mM Ca^{2+}_o for 24 h then changed to 1.05 mM Ca^{2+}_o for a further 24 h. Inset pictures show each lung at 0 h showing a comparable number of initial terminal branches for each condition. **B).** Changing the $[Ca^{2+}]_o$ from 1.05mM to 1.7mM Ca^{2+}_o after 24 h had no effect on the amount of branching morphogenesis at 48 h. Changing the $[Ca^{2+}]_o$ from 1.7 mM to 1.05 mM Ca^{2+}_o after 24 h significantly increased the amount of terminal branching in the lung explants at 48 h. Data shown are mean± s.e.m. (n=5 lungs per condition from a single isolation), *** = $p<0.036$, in comparison to time-matched lung explants cultured in the presence of 1.7mM Ca^{2+}_o. Scale bars = 700 μm.

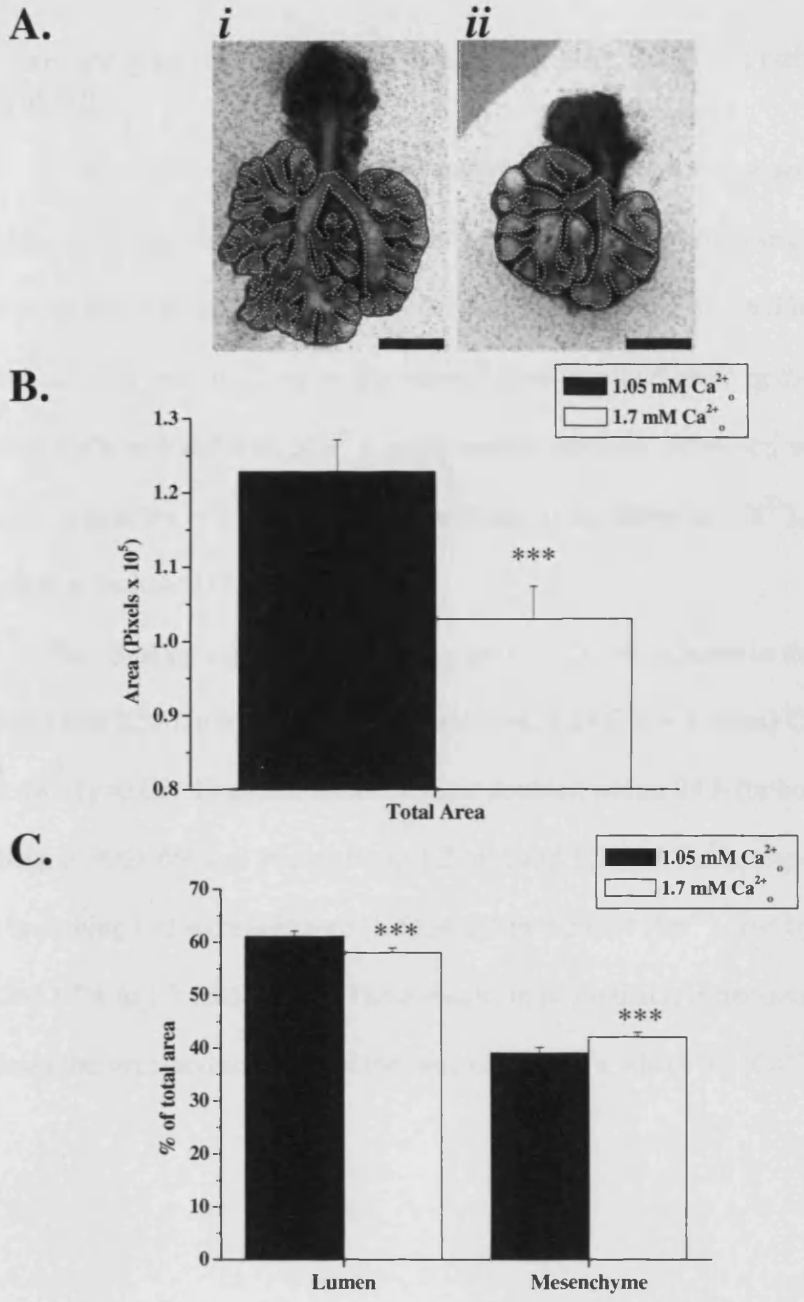

Figure 2.4: Total, luminal and mesenchymal area are affected by manipulating $[Ca^{2+}]_o$ of culture medium. Total lung area was measured by tracing the outside of (**A**, blue lines), and luminal area was measured by tracing the airways within, the lung (**A**, white dashed lines). **A).** Representative pictures of explants: ***i.*** 1.05 mM Ca^{2+}_o for 48 h, ***ii.*** 1.7 mM Ca^{2+}_o for 48 h. **B).** Total lung area is decreased when lungs are cultured in the presence of 1.7 mM Ca^{2+}_o for 48 h when compared to time-matched lungs cultured in the presence of 1.05 mM Ca^{2+}_o. **C).** Lungs cultured in the presence of 1.7 mM Ca^{2+}_o have a reduced percentage of lumen and an increased percentage of mesenchyme after 48 h when compared to time-matched lungs cultured in the presence of 1.05 mM Ca^{2+}_o. Data shown are mean± s.e.m. (n=15 for 1.05 mM Ca^{2+}_o and n=14 for 1.7 mM Ca^{2+}_o from 4 isolations), ***= $p \leq 0.033$ calculated by ANOVA with Tukey *post-hoc* test. Scale bars = 650 μm.

2.4 Sensitivity to $[Ca^{2+}]_o$ is abolished when lung lobes are cultured individually.

At one point in this study, it was thought that it may be more accurate to have different $[Ca^{2+}]_o$ applied to the same lung, as this would allow for a single lung to be the control and experimental sample at the same time. This was tested by separating individual lobes from the lungs at the time of dissection and growing them in separate wells with different $[Ca^{2+}]_o$ in the culture medium. However, when this was done the sensitivity of branching morphogenesis to the differing $[Ca^{2+}]_o$ was completely abolished (Fig. 2.5).

There was no significant difference between lobes cultured in the presence of 1.2 mM (Fig. 2.5A*i*, n = 8 lobes) or 1.7 mM (Fig. 2.5A*ii*, n = 5 lobes) $Ca^{2+}_{o,}$ at either 24 or 48 h ($p>0.05$). Branch numbers almost doubled within 24 h for both conditions resulting in 90±8.6% and 96±16.3% in 1.2 mM and 1.7 mM $Ca^{2+}_{o,}$ respectively. At 48 h branching had increased by 318.5±34.2% in 1.2 mM $[Ca^{2+}]_o$ and by 357.3±53.7% in 1.7 mM $[Ca^{2+}]_{o.}$ These results indicate that it is necessary to maintain the structural integrity of the lung explant as a whole for $[Ca^{2+}]_o$ sensitivity.

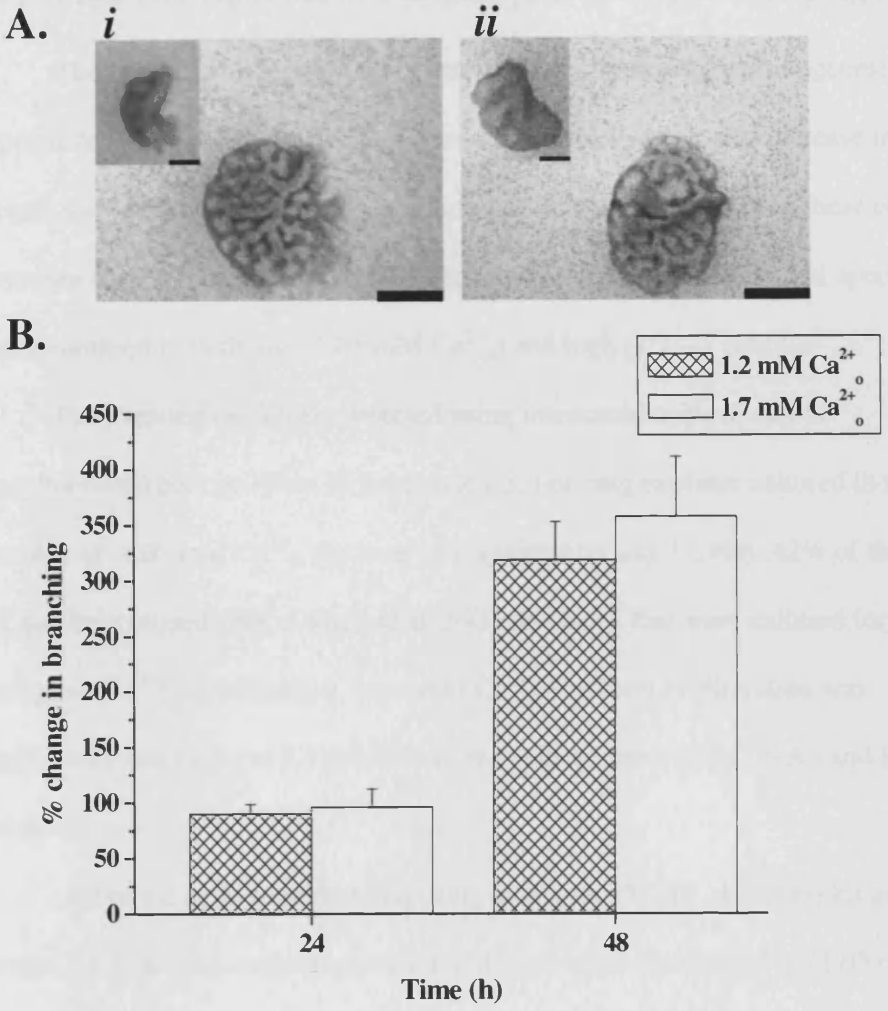

Figure 2.5: $[Ca^{2+}]_o$ sensitivity is requires an intact lung explant. Lungs from E12.5 mouse embryos were separated into individual lobes and cultured for 48 h in serum-free DMEM/F12 containing 1.2 or 1.7 mM Ca^{2+}_o. **A).** Representative pictures of lung lobes cultured in the presence of: ***i.*** 1.05 mM Ca^{2+}_o for 48 h, ***ii.*** 1.7 mM Ca^{2+}_o for 48 h. Inset pictures show each lung at 0 h (post-dissection) showing a comparable number of initial terminal branches for each condition. **B).** Total number of terminal branches was counted at 0, 24 and 48 h, normalized to 0 h, and the change expressed graphically as a percentage increase over 24 or 48 h. Data shown are the mean ± s.e.m. (n = 8 lobes for 1.2 mM Ca^{2+}_o and n = 5 lobes for 1.7 mM Ca^{2+}_o from a single isolation). Scale bars = 300 μm.

2.5 Cellular consequences of changing $[Ca^{2+}]_o$ on the developing lung.

The observed changes in the amount of lung branching morphogenesis in response to $[Ca^{2+}]_o$ could be due to a decrease in proliferation, and increase in apoptosis or a combination of the two. In order to determine which of these cellular responses occurred in response to $[Ca^{2+}]_o$, the levels of proliferation and apoptosis were quantified in both low (1.05 mM Ca^{2+}_o) and high (1.7 – 2 mM Ca^{2+}_o).

Proliferating cells were detected using immunohistochemistry of phosphorylated histone H3 as in Section 2.1.3. For lung explants cultured in the presence of 1.05 mM Ca^{2+}_o, the level of proliferation was 11.49±0.42% of the total cell number counted (Fig. 2.6A*i* and B, n=3). In Lungs that were cultured for 48 h in the higher $[Ca^{2+}]_o$ conditions, 1.7 to 2mM Ca^{2+}_o, the level proliferation was significantly decreased to 5.37±0.89% of the cells counted (Fig. 2.6 A*ii* and B, n=3, $p<0.004$).

Apoptotic cells were detected using an *in situ* TUNEL detection kit as in Section 2.1.3. In lung explants cultured in the presence of low $[Ca^{2+}]_o$ (1.05 mM) the percentage of apoptotic cells detected in the total cell number counted was 9.99±1.4% (Fig. 2.7 A*i*, B*i* and C). There was no significant difference in the number of apoptotic cells between lung explants cultured in the presence of either low or high $[Ca^{2+}]_o$. Indeed, lung explants cultured in the presence of high $[Ca^{2+}]_o$ (1.7-2 mM) had 12.15±3.04% apoptotic cells (Fig. 2.7 A*ii*, B*ii* and C).

2.6 Functional characterisation of lung explants.

Adequate lung growth requires fluid-dependent distension in the developing tissue (Harding & Hooper, 1996). The fluid causing this distension is secreted from the lung epithelium by secondary active Cl^- transport resulting in a negative trans-epithelial potential difference (TPD), the magnitude of which reflects the rate of Cl^- driven fluid secretion (Olver & Strang, 1974). Measurement of TPD has not been reported previously in a mouse lung culture model. Therefore, a protocol was developed and optimised for such measurements. Time lapse images from E12.5 mouse lungs cultured in low (1.05 mM) and high (1.7 mM) $[Ca^{2+}]_o$ illustrate that the rate and extent of branching are both significantly reduced in high $[Ca^{2+}]_o$ culture conditions (Figure 2.8). Additionally this figure shows that the terminal buds of lungs cultured in the presence of 1.7 mM Ca^{2+}_o appear to be more distended (Fig. 2.8B), with a higher luminal volume at each branch terminus, possibly indicative of fluid secretion which is visible after 24 h in culture.

The mean TPD of terminal branches from lungs incubated for 48 h in in the presence of 1.05 mM $[Ca^{2+}]_o$ was -1.24±0.15 mV. The mean TPD increased significantly to -1.68±0.16 mV when the lungs were cultured for 48 h in the presence of 1.7mM $[Ca^{2+}]_o$ (Fig.2.9A, $n \geq 17$ per condition, $p<0.05$). The increase in branching seen when lungs are switched from 1.7 mM Ca^{2+}_o to 1.05 mM Ca^{2+}_o after 24 h is not accompanied by similar changes in the TPD (Fig. 2.9 B). Once the TPD becomes more negatively charged after 24 h, from -1.07±0.1 mV in 1.05 mM Ca^{2+}_o to -1.49±0.23 mV in 1.7 mM Ca^{2+}_o, it remains at this level regardless of the $[Ca^{2+}]_o$ to which the lung is exposed for the next 24 h (n=5 for each condition).

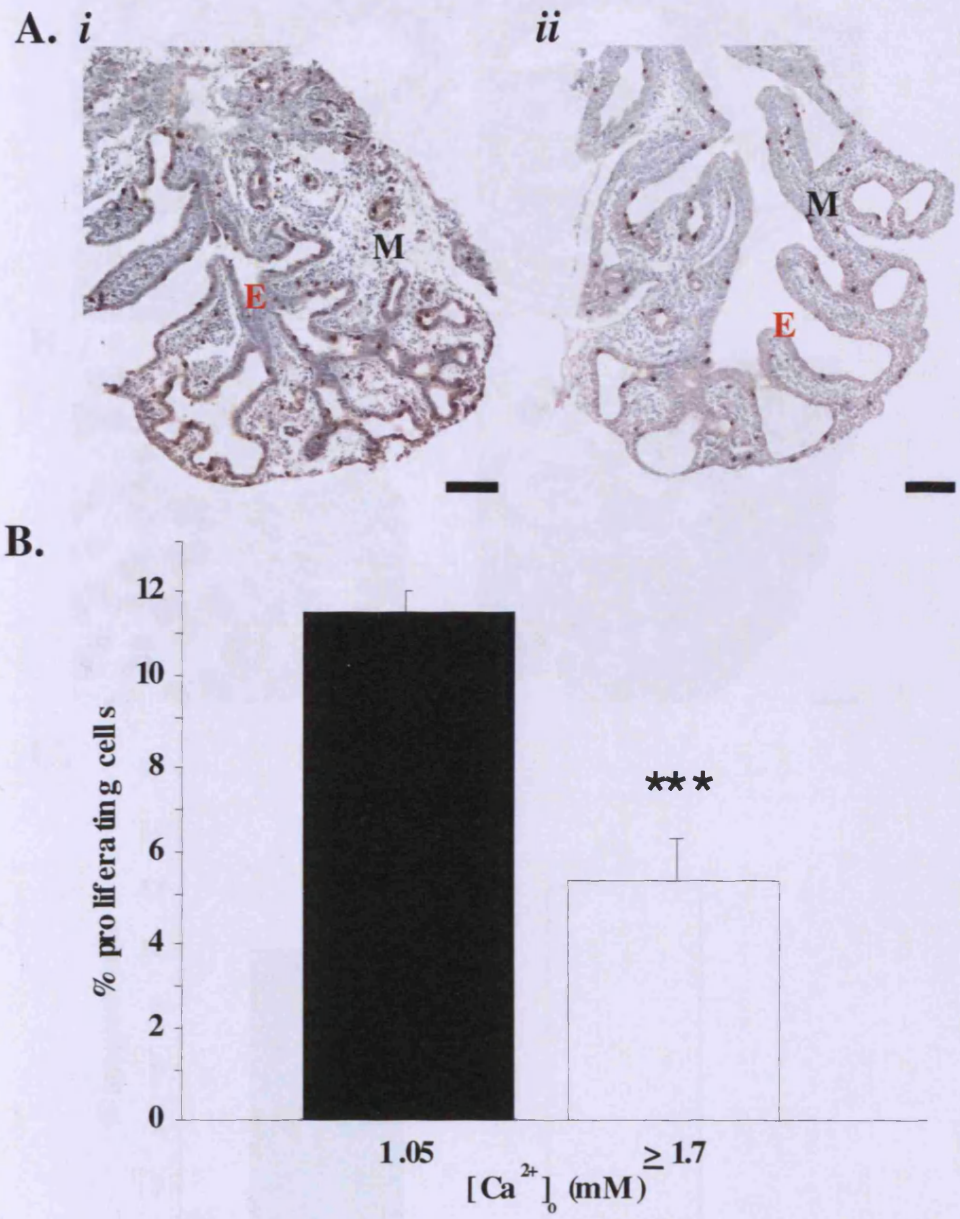

Figure 2.6: Proliferation of cells in lung explant cultures is $[Ca^{2+}]_o$ sensitive.

A). Representative detection of proliferating cells (brown pigment) in a 5µm section of an E12.5 mouse lung explant cultured in the presence of: ***i.*** 1.05 mM $Ca^{2+}{}_o$ for 48 h or ***ii.*** 1.7 mM $Ca^{2+}{}_o$. **B).** Proliferation, measured as the number of cells positive for anti-phosphorylated Histone H3 immunoreactivity is $Ca^{2+}{}_o$-sensitive and is greater when lungs are cultured in the presence of 1.05 mM $Ca^{2+}{}_o$ when compared to the number of proliferating cells in lungs cultured in the presence of 1.7 mM $Ca^{2+}{}_o$. Data shown are the mean ± s.e.m, n=3 lungs per condition, *** = $p<0.004$. **E** designates an area of epithelium, **M** designates an area of mesenchyme, Scale bars = 100 µm.

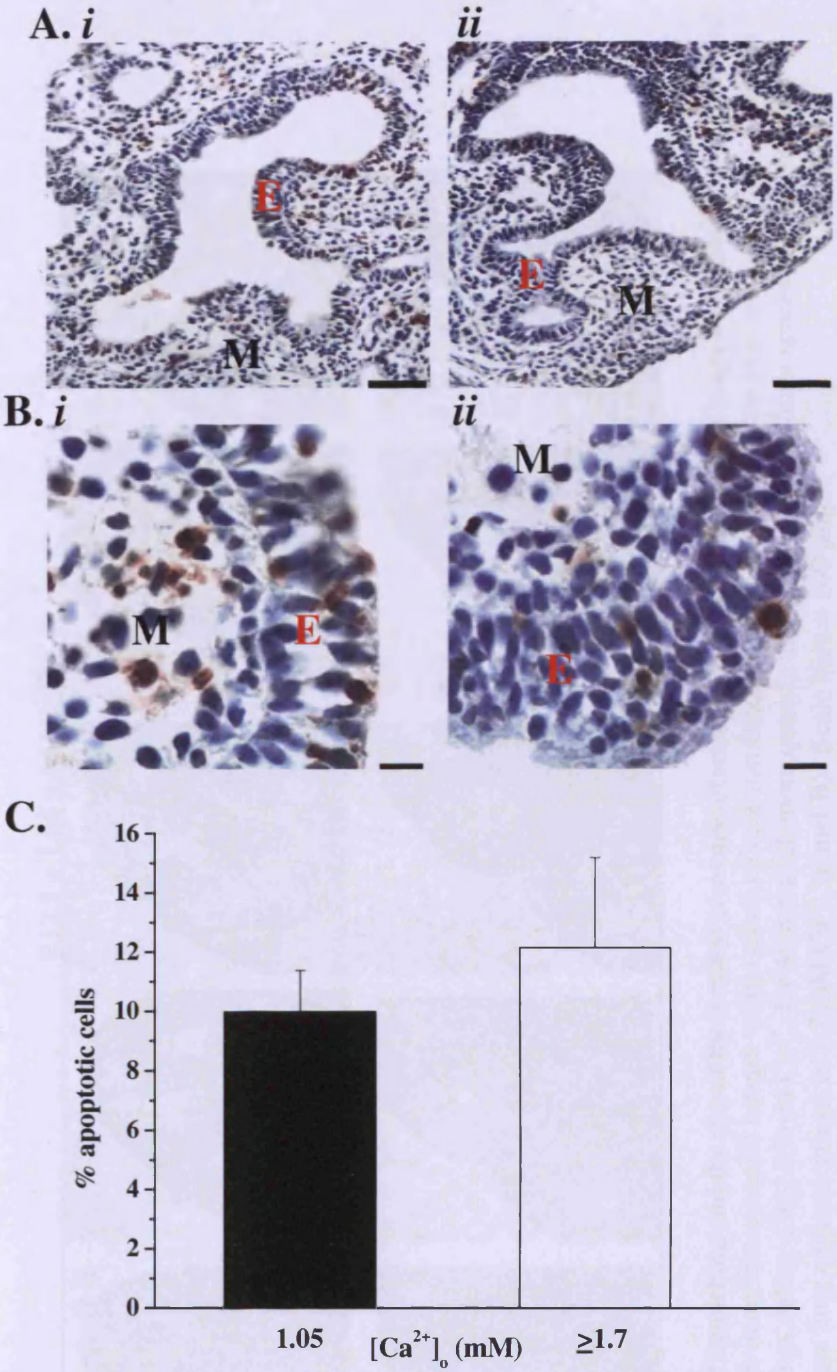

Figure 2.7: Apoptosis of cells in lung explant cultures is not $[Ca^{2+}]_o$ sensitive. A). Representative TUNEL detection of apoptotic cells (brown pigment) in a 5µm section of an E12.5 mouse lung explant cultured in the presence of: ***i.*** 1.05 mM $Ca^{2+}{}_o$or ***ii.*** 1.7 mM $Ca^{2+}{}_o$ for 48 h, scale bars = 100 µm. **B).** Higher magnification of apoptosis detection in lungs cultured in the presence of ***i.*** 1.05 mM $Ca^{2+}{}_o$or ***ii.*** 1.7 mM $Ca^{2+}{}_o$ for 48 h. **E** designates an area of epithelium, **M** designates an area of mesenchyme, Scale bars = 10 µm. **C).** Apoptosis measured as the number of cells detected by a TUNEL assay, is not $Ca^{2+}{}_o$-sensitive. Data shown are mean ± s.e.m., n=3 lungs for each condition.

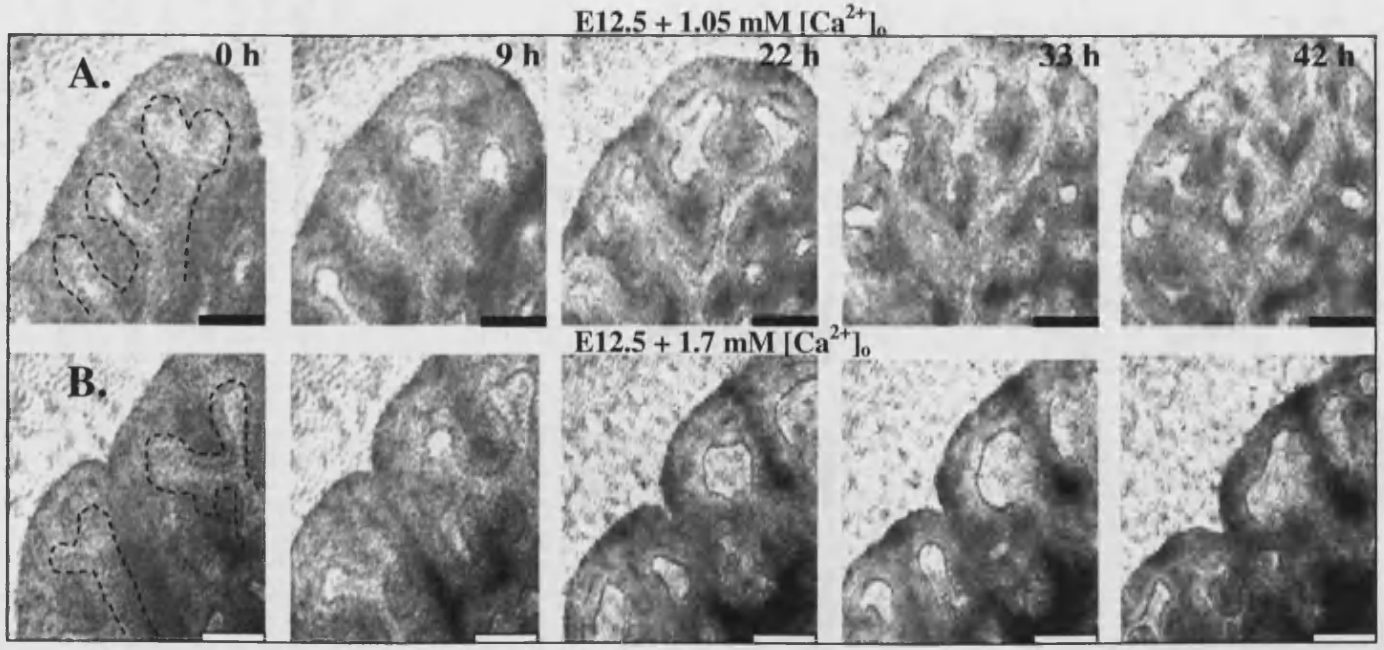

Figure 2.8: The rate of branching and the size of the luminal areas are affected by $[Ca^{2+}]_o$. E12.5 mouse lungs were dissected and cultured on Transwells for 48 h in an Incucyte cell imager within a cell culture incubator, and pictures were taken once every hour for a total of 48 h. E12.5 mouse lungs cultured in 1.05mM $Ca^{2+}{}_o$ for 48 h branch more quickly and have smaller luminal spaces in their terminal branches (Panel **A**) than lung explants grown in 1.7 mM $Ca^{2+}{}_o$ (Panel **B**). Scale bars = 100 μm.

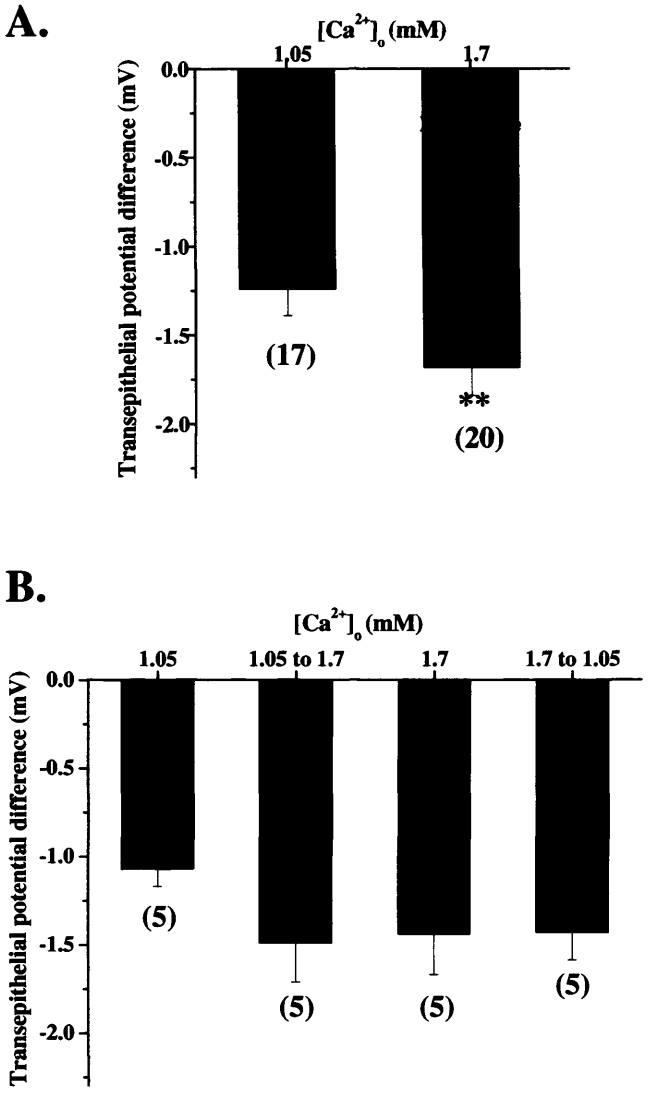

Figure 2.9: Trans-epithelial potential difference in lung explant cultures is $[Ca^{2+}]_o$-sensitive. TPD recordings were taken from E12.5 mouse lungs after 48 h in the culture conditions listed. **A).** TPD increases when lungs are cultured in the presence of 1.7 mM $Ca^{2+}{}_o$ (** = $p<0.05$) for 48 h. **B).** TPD is augmented when lungs are cultured in the presence of 1.7 mM $Ca^{2+}{}_o$ conditions which unlike branching morphogenesis, cannot be reversed by culturing explants in the presence of 1.05 mM $Ca^{2+}{}_o$ for 24 h after an initial 24 h in the presence of 1.7 mM $Ca^{2+}{}_o$. Data shown are mean ± s.e.m, n= shown in parentheses under each data point. (Data kindly provided by William Wilkinson, PhD)

2.7 Chapter Discussion

For the purpose of this discussion and the remainder of this report the term "low" refers to $[Ca^{2+}]_o$ in the range of 1.05 – 1.2 mM and "high" refers to $[Ca^{2+}]_o$ in the range of 1.7 – 2 mM.

This chapter shows that, lung branching morphogenesis and lung size are sensitive to changing $[Ca^{2+}]_o$ via a mechanism(s) that involves changes in proliferation levels and Cl^- secretion. These observations are completely novel. Also novel is the ability to reverse the suppression of branching morphogenesis observed in the presence of high Ca^{2+}_o after 24 h by reducing the Ca^{2+}_o to 1.05 mM. A summary chart of the results presented in this chapter is presented in Figure 2.10.

Interestingly, conditions which seem to be the most permissive for branching morphogenesis (1.05 – 1.2 mM Ca^{2+}_o) correspond to physiological adult $[Ca^{2+}]_o$; while concentrations of 0.5 mM and 1.7 – 2 mM Ca^{2+}_o seem to suppress the maximal response. The manner in which 0.5 mM Ca^{2+}_o suppresses branching morphogenesis has not been investigated in depth within this study. However this result suggests that there is both a minimum and maximum $[Ca^{2+}]_o$ required for optimal branching. This is supported by a preliminary experiment culturing lung explants in the presence of 0.1 mM Ca^{2+}_o that resulted in the death of the explants within 48 h. However, it is also possible that the mode of achieving reductions in $[Ca^{2+}]_o$, *i.e.* the introduction of 0.2 M EGTA into the culture medium, is in itself causing the suppression of branching morphogenesis and death of the explants.

Therefore, much of the experimentation has focused rather on 1.7 mM Ca^{2+}_o as this corresponds to $[Ca^{2+}]_o$ reported for the developing mouse fetus (Kovacs *et al.*, 1998). The results showing branching suppression at this $[Ca^{2+}]_o$ prompted the

question, why would conditions thought to be normal for the developing fetus be restrictive in this manner?

There is a need for the lung to maintain a balance in its final branch number for optimal development of alveoli. Many adverse factors, including oxygen exposure, abnormal growth factor signalling and regulation, can all cause the alveolar epithelial surface to be hypoplastic and deficient in its ability to perform gas exchange (Warburton *et al.*, 2006). However, there is also a danger of hyperplasia, with too many branches/alveoli, as seen in cultured lung explants that have been exposed to nicotine (Wuenschell *et al.*, 1998). In fact, children exposed to nicotine *in utero* also have trouble with efficient gas exchange (Cunningham *et al.*, 1994). Perhaps $[Ca^{2+}]_o$ is a factor that acts as a controller to ensure that the optimal number of branches is achieved.

It is unsurprising that the structural integrity of the lung explants needs to be maintained in order to retain the $[Ca^{2+}]_o$ sensitivity. It has been previously published that tracheal occlusion results accelerated lung growth, in part due to up-regulation of TGF-β (Quinn *et al.*, 1999). Breaking the lungs into individual lobes may provoke similar stimuli to that of tracheal occlusions. The bronchiole of E12.5 mouse lung explants contains smooth muscle, which will constrict upon breaking the lobe away from the rest of the lung, thereby shutting off any open lumen and increasing the pressure within the lobe. It is also possible that by dissociating the lung lobes there is an alteration in the activity of the peristaltic pacemaker (Jesudason *et al.*, 2005) within the smooth muscle of the lung airway that causes the increased branching morphogenesis noted in dissociated lung lobes.

What is the underlying cause of the branching differences that are seen in high vs low $[Ca^{2+}]_o$ cultures? Apoptosis levels in this study (9-12%) are greater than

the published approximated values for apoptosis occurring during the pseudoglandular stage of development of 1-2% (Wongtrakool & Roman, 2008). This increased apoptosis could be due to difference in the culturing conditions from those used in the Wongtrakool and Roman study, which cultured explants in DMEM with 10% bovine calf serum, which was not used in this study. Additional discrepancy could be produced by the differences in the sample sizes and modes of counting. However, apoptosis levels do not significantly differ in the low *versus* high $[Ca^{2+}]_o$ cultures indicating that increased apoptosis is not necessarily the cause for the reduced branching morphogenesis and lung size observed in high $[Ca^{2+}]_o$ cultures.

Proliferation levels detected in this study (6-12%) are lower than those previously published for proliferating epithelial cells in E11.5 lung explants grown for 4 days in BGJb medium, 35% (Chen *et al.*, 2005). This difference could be due to a difference in culturing conditions, or indeed in counting method as the Chen *et. al.* study did not detail the photomicrograph size used. However, as an assay for differences between high and low $[Ca^{2+}]_o$ cultures, the 50% difference in proliferation may be an indication of an attenuation of the amount of proliferating cells present in the developing lung by high $[Ca^{2+}]_o$, or conversely, an increase in proliferation mediated by lower $[Ca^{2+}]_o$. Proliferation levels are known to be affected by other manipulations of the lung developmental programme. Disruption of Bmp signalling, for example, decreases lung epithelial cell proliferation (Eblaghie *et al.*, 2006). There is also evidence for proliferation being regulated by $[Ca^{2+}]_o$. For example, Capan-1 cells, a model for human pancreatic exocrine cells, show a significant decrease in proliferation, when exposed to 4 mM $Ca^{2+}{}_o$ (Racz *et al.*, 2002).

The ability to determine the TPD of lung explants provides another layer of information on the lung explant's response to $[Ca^{2+}]_o$. The lung explants cultured in the presence of high $[Ca^{2+}]_o$ branch less and remain smaller, but their luminal volume at the terminus of each bud appears greater. However, measurements of the total luminal area show that there is a decrease in the amount of luminal space in 1.7 mM $Ca^{2+}{}_o$ indicating that although the terminal buds appear larger, overall, more branches translates into a larger luminal volume regardless of the bud size at the terminus. The TPD of lungs cultured in the presence of high $[Ca^{2+}]_o$ is more negative, possibly indicating an increase in Cl^- dependent fluid secretion; or it is possible that this increase in negativity could be due to an increase in Na^+ absorption. However, there is no published evidence for sodium absorption or the expression of epithelial sodium channels (ENACs) at this stage of development for review see : (Wilson *et al.*, 2007). Therefore in this study, it is assumed that TPD is a measure of Cl^- secretion and there appears to be no link between branch number and this measure. This is supported by a report which inhibited Cl^- secretion in rat lung explants by the application of bumetanide, which decreased overall lung growth, but did not affect branching morphogenesis (Souza *et al.*, 1995).

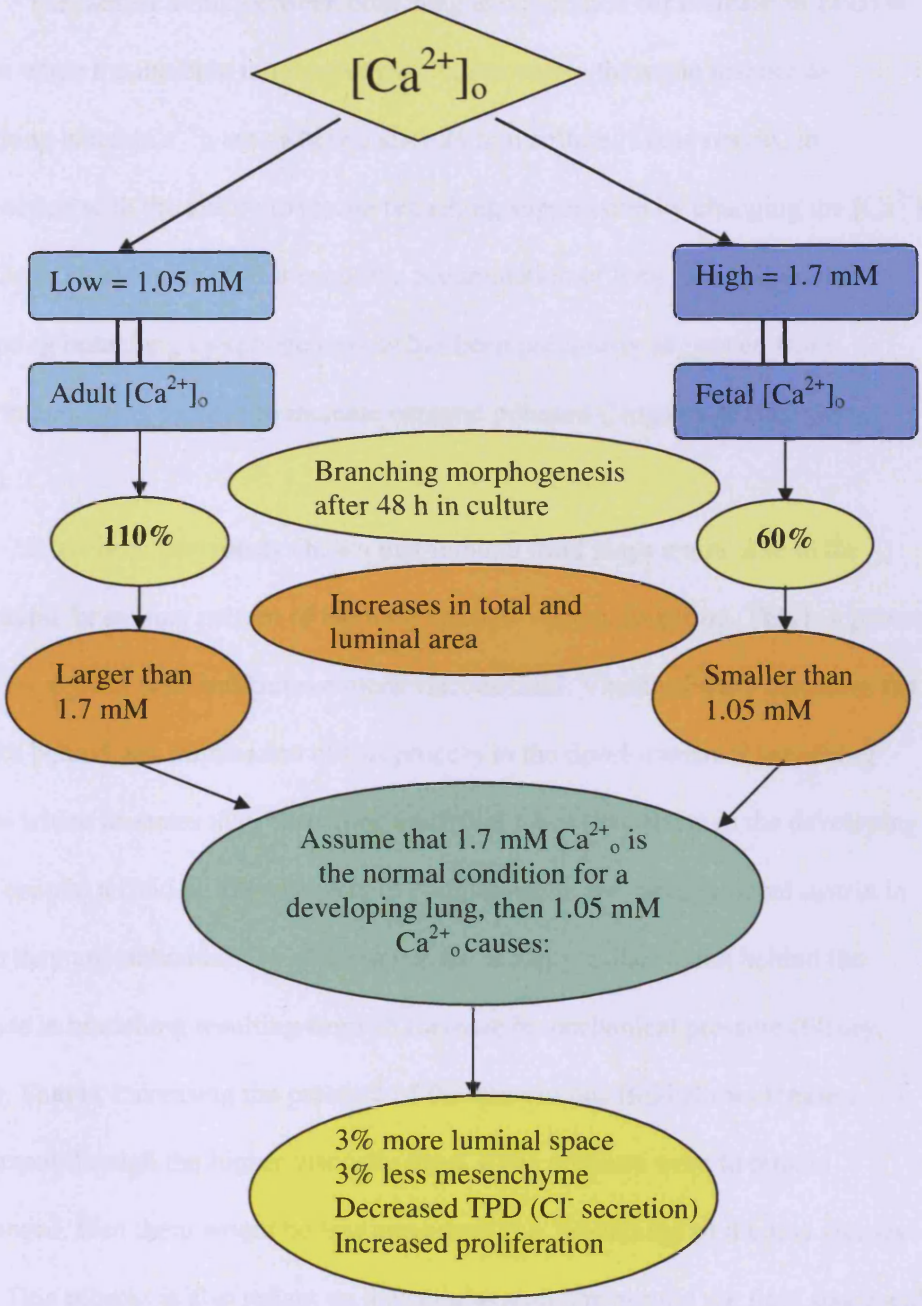

Figure 2.10 Diagrammatic summary of Chapter 2 results. Extracellular [Ca^{2+}] has effects on the development of the fetal lung effecting various aspects of development such as branching morphogenesis, lung size and proliferation.

The lack of a link between branching and secretion (or increase in TPD) is shown when the increase in negativity is not rescued in the same manner as branching when $[Ca^{2+}]_o$ are switched after 24 h in culture. These results, in conjunction with the ability to rescue branching suppression by changing the $[Ca^{2+}]_o$ after 24 h, would imply that it is not the accumulation of lung lumen fluid that is disrupting branching morphogenesis as has been previously suggested from experiments using sucrose to increase osmotic pressure (Nogawa & Hasegawa, 2002).

It has been previously shown that luminal fluid plays a vital role in the stereotypic branching pattern of the lung through viscous fingering. This is a process whereby a given fluid infiltrates a more viscous fluid. Vincent Fleury discusses the physics behind and implication of this process in the development of branching organs where he states that, branching epithelial tubes (like those in the developing lung) contain a fluid of low viscosity in comparison to the mesenchymal matrix in which they are embedded. This difference in viscosity is the reason behind the increase in branching resulting from an increase in mechanical pressure (Fleury, 2001). That is, increasing the pressure of the less viscous fluid allows it easier movement through the higher viscosity fluid. If the pressure were to remain unchanged, then there would be less movement (*i.e.* branching) of the less viscous fluid. This process is also reliant on the cellular structure around the fluid space and the cells must maintain connectivity as a solid sheet. As this sheet, they help create osmotic pressure with high pressure in the lumen and the cells must proliferate in order for the tube to continue to grow and branch (Fleury & Watanabe, 2002). It is possible that high $[Ca^{2+}]_o$ is affecting two parts of this process. Greater Cl^- secretion may not lead to an increase in pressure, but to a reduction of viscosity, and therefore

there is no pressure dependent increase in branching. Or there is the possibility that the pressure is increased in conjunction with Cl^- secretion in high $[Ca^{2+}]_o$, but the cellular structure and interactions surrounding the lumen have changed so that fluid fingering does not occur, possibly due to stretching of, or an increase in the viscosity of, the mesenchyme.

By determining the mechanism that is controlling the branching response, lung development may eventually be susceptible to pharmacological manipulation to help rescue defective branching *in vivo*. Indeed, the results showing that the inhibition of the branching programme by high $[Ca^{2+}]_o$ can be reversed by low $[Ca^{2+}]_o$ would imply just this. It seems that the branching process once started cannot be halted, but if suppressed, it can be "jump-started" by making the conditions to which the lung is exposed more favourable to branching. However the maturity of the lung also needs to be taken into account, *i.e.* are the branches supported by a vascular network that will eventually be capable of gas exchange? Therefore it is important to understand the underlying mechanism(s) by which the response to $[Ca^{2+}]_o$ is controlled in the normal developing lung.

CHAPTER 3: EXPRESSION OF THE EXTRACELLULAR CALCIUM-SENSING RECEPTOR DURING LUNG DEVELOPMENT

3.1 Methods

3.1.1 RNA Isolation and Reverse Transcriptase Polymerase Chain Reaction (RT-PCR)

RNA was isolated from pooled samples of mouse embryonic lungs using either Trizol reagent (Invitrogen, Paisley, UK) or RNeasy mini isolation kit (Qiagen, Crawley, West Sussex, UK). Both were used according to the manufacturer's instructions. After purification RNA was quantified and quality checked using spectrophotometry readings at 260 nm and 280 nm. cDNA was synthesised using Superscript first strand synthesis system for reverse transcriptase PCR (Invitrogen, Paisley, UK) according to manufacturer's instructions. PCR was performed using "intron-spanning" primer sequences designed against published CaR mouse sequences (NCBI Accession # NM_13803), at an annealing temperature of 55°C:

forward primer 5' - ACCTGCTTACCCGGAAGAGGGCTTT,

reverse primer 5' – GCACAAAGGCGGTCAGGAAAATGCC.

β-actin primers were used to amplify the housekeeping gene from all samples at an annealing temperature of 50 °C:

forward primer 5' – TCCTAGCACCATGAAGAT,

reverse primer 5' - AAACGCAGCTCAGTAACA.

PCR reactions were performed using the following PCR regime: an initial denaturing step of 95°C x 5 min; denaturing of 95°C x 1 min, annealing as specified above x 30 s, elongation 72°C x 1 min repeated for 35 cycles; final elongation of 72°C x 8 min.

The following method was developed and kindly provided by Pierre DelMoral, PhD. For quantitative PCR, RNA was purified from pooled samples of lungs (3 for each time point) aged between E11.5-E18.5 using RNeasy kits from Qiagen (Crawley, West Sussex, UK). After purification the RNA was quantified and

quality checked using a Nanodrop Spectrophotometer (Bio-Rad). Reverse transcription was carried out using 1μg RNA using the iScript select cDNA kit (Bio-Rad) according to manufacturer's instructions. The resulting cDNA was used for quantitative PCR in a Roche Light cycler (Roche, California, USA). Primers specific for CaR (NM_13803.2) and 18S (NR_003278.1) were designed using the Roche Assay Design Center (www.roche-applied-science.com) to be used in conjunction with PCR probes from the Roche Universal Probe Library. Both sets of primers were used in reactions with cycling conditions as follows: initial incubation of 95 °C x 5 min, then denaturation at 95 °C x 20 s, annealing at 60°C x 20 s, and elongation at 72 °C x 10 s which was repeated for 40 cycles. The Universal probes and primer sequences used were:

18S amplification; probe # 55,

forward primer 5' –AAATCAGTTATGGTTCCTTTGGTC,

reverse primer 5'-GCTCTAGAATTACCACAGTTATCCAA.

CaR amplification; probe # 32, intron-spanning,

forward primer 5'-GGTCCTGTGCAGACATCAAG,

reverse primer 5'- CCGCACTCATCGAAGGTC.

3.1.2 In Situ Hybridization (ISH)

Microdissected lungs were fixed in 4% PFA in PBS at 4 °C (fixation times were dependent on developmental stage and varied between 10 min to 1 h). The lungs were subsequently washed twice with PBS, dehydrated and stored in 70% ethanol at 4°C. The CaR antisense and sense probes (Method for production in Appendix A) were used along with RNase-free solutions, tubes and pipettes, in an attempt to prevent RNA degradation in the samples. The whole mount protocol was

based on a previously described method (Winnier *et al.*, 1995). The lungs were transferred to 2 ml tubes and bleached in a 4:1 mix of 100% EtOH and 30% H_2O_2 then washed with PBS containing 0.1% Tween-20. The lungs were then briefly digested with Proteinase K (Roche Applied Sciences, Burgess Hill, UK) then post-fixed in 0.2% glutaraldehyde mixed with 4% PFA. Pre-hybridisation was performed for 2 h at 68 °C in hybridisation buffer (Containing: deionised formamide, SSC, tRNA, SDS and heparin) after which the buffer was replaced with hybridisation buffer containing 1µg/ml DIG-labelled RNA-probe and left to hybridise overnight at 68 °C with shaking. The following morning the lungs were washed and treated with RNase A to remove any non-specific binding or un-hybridised RNA probe. The lungs were then treated to prevent any non-specific binding of the primary antibody for 1 h at room temperature while the anti-DIG antibody was pre-absorbed at 4 °C. After adding the pre-absorbed antibody to the samples, the complexes were incubated overnight at 4 °C with shaking. The following morning the antibody was removed and the samples washed for at least 24 h with hourly solution changes throughout the day. On the final day after washing, the samples were developed with BM purple at 37 °C to reveal hybridised probe and the samples were post-fixed in 4% PFA to preserve the colour for analysis.

3.1.3 Immunohistochemistry

Whole embryos or microdissected lungs were fixed in 4% PFA in PBS at 4 °C (fixation times dependent on developmental stage and varied from 10 min - overnight). The specimens were subsequently washed twice with PBS, then dehydrated and stored in 70% ethanol at 4°C. PFA fixed tissue was then embedded in paraffin wax and 5 µm thick sections were cut for histology on a standard microtome. Sections were mounted on Superfrost Plus glass sildes (Fisher Scientific,

UK) and once dry were de-paraffinized with Histochoice (Sigma-Aldrich, Gillingham, Dorset, UK) and re-hydrated through a series of graded alcohols. After rehydration, the slides were treated using citrate buffer antigen retrieval as in Section 2.1.3.

The slides were treated with 3% BSA in PBS (Sigma-Aldrich, Gillingham, Dorset, UK) containing 0.1% Triton-X100 (Sigma-Aldrich, Gillingham, Dorset, UK) for 1 h at room temperature to prevent non-specific binding of the primary antibody. Several primary antibodies were tested in order to determine and confirm the specificity of CaR staining. The 733 primary antibody was a rabbit polyclonal directed against a peptide corresponding to residues 215-237 in the extracellular domain of the bovine CaR protein (Riccardi *et al.*, 1998) diluted 1:200 and 1:400 in antibody dilution fluid (AbDF; 1% BSA, 3% Seablock (EastCoast Bio, Soham, Cambridgeshire, UK) in PBS with 0.1% Triton-X100). Negative controls for this antibody were omission of the primary antibody from the AbDF, and use of the pre-immunisation serum from the same rabbit that produced the 733 antibody (PIS; 1:400 in AbDF). Several commercially available antibodies were also tested for the immuno-detection of the CaR in mouse lungs. IMG-71169 and IMG-71168 (Imgenex, San Diego, CA, USA) were both used at a 1:400 dilution. Although the exact peptide sequences are proprietary of Imgenex, IMG-71169 is in the region of 370-420 residues and IMG-71168 is in the region of 200-250 amino acid residues of the human parathyroid CaR sequence. An antibody detecting amino acids12-27 at the very end of the CaR N-terminus was also tested (PA1-934A; Affinity BioReagents, Colorado, USA) at 1:50 and an antibody to 20 amino acids near the C-terminus of the protein (designated USB) was used at 1:200 dilution (CO117-15, US Biologicals, Massachusetts, USA). Negative controls for these antibodies were

performed by omitting the primary antibody and by using irrelevant Rabbit IgG complexes (Abcam plc., Cambridge, UK) diluted to the same extent as the primary antibody.

Primary antibodies were incubated overnight at 4°C, and then washed several times in PBS. The secondary antibody (supplied in the Dako Envision Kit mentioned below) was applied for 30 min at RT, and then removed in several washes of PBS. Visualization of the detected proteins was performed using an Envision Diaminobenzidine kit (DAB; Dako, Ely, Cambridgeshire, UK) according to the manufacturer's instructions. Once the DAB was developed to an adequate level, the slides were counterstained with Harris's haematoxylin, dehydrated and mounted with Clarion mounting medium (Sigma-Aldrich, Gillingham, Dorset, UK).

Photomicrographs were taken on a standard light microscope, attempting to maintain the same conditions for each set of pictures at each magnification. Photomicrographs were processed in Adobe Photoshop and subjected to a curves adjustment to remove background by selecting a reference area to be set as the white background for the picture. The pictures were then adjusted for brightness, contrast and size as needed. It was attempted to maintain the same image capture parameters for photomicrographs that were to be presented together.

3.2 Philosophy of Work

As stated in the previous chapter, activation of the CaR could be responsible for the differential sensitivity of mouse lungs to changes in $[Ca^{2+}]_o$ of the culture media. However, neither CaR protein nor RNA has been previously detected in the lung (Brown et al., 1993; Riccardi et al., 1995). In those studies, only adult lungs were investigated, no attempt to detect CaR in the developing lung has ever been published. The results in this chapter show that the both CaR RNA and protein are

expressed in a developmentally controlled manner for a period in the embryonic mouse lung, coinciding with the pseudoglandular phase of lung development during which the majority of branching morphogenesis occurs.

3.3 CaR RNA expression

3.3.1 RT-PCR

Initial RT-PCR experiments were performed using CD1 mouse embryos; as this strain produces large litters, less mice needed to be sacrificed to obtain adequate samples for each time point. The results from these mice indicated that CaR RNA was expressed at E11.5, E12.5 and E16.5, with no expression at E18.5 (Fig. 3.1A). Each sample was also used for a –RT negative control to determine if there was any DNA contamination in the RNA, and for amplification of β-actin as a positive control for each sample (Fig. 3.1B). All primers were intron-spanning as an additional control for any genomic DNA contamination in the samples.

3.3.2 Quantitative PCR

Quantitative PCR was performed on RNA which was extracted from 3 C57/Bl6 mouse lungs pooled for each time point. CaR specific and 18S (housekeeping gene) primers were used in conjunction with probes from the Universal Probe Library (Roche, California, USA) for detection of mRNA expression and relative quantification of CaR in these samples. Resulting PCR measurements were initially normalised to 18S expression levels to ensure that there was no initial difference in the amount of RNA. Following this normalisation, the amount of CaR mRNA expression was calculated relative to its expression level at E11.5, which was set to a value of 100%, as it was the earliest time point tested.

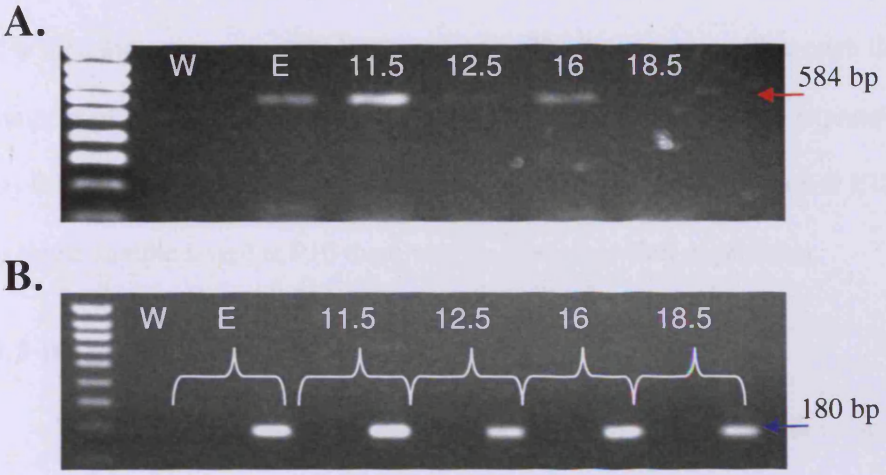

Figure 3.1: Initial RT-PCR amplification of CaR and β-actin. Total RNA was isolated from pooled CD1 strain embryonic mouse lung samples and reverse transcribed. The PCR reaction was performed using CaR specific primers resulting in a 584 bp product (red arrow, **A**) and β- actin primers resulting in a 180 bp product (blue arrow, **B**). As a negative control, water (W) was substituted for RNA, and as a positive control, total RNA from an E10.5 embryo (E) was used. Embryonic lungs at E11.5, E12.5, E16 and E18.5 were tested for their expression of CaR RNA. A DNA ladder in 100 bp increments from 100 – 1000 bp is the first lane on the left of each panel and indicates the size of amplicons. Panel **B** also shows in the lane to the left of each β-actin band the additional negative control of the samples where the reverse transcriptase was omitted from the 1st strand synthesis.

Table 3.1: CaR Expression levels determined by quantitative PCR. Total RNA was isolated from pooled lung samples (n=3 lungs for each time point). Complementary DNA was produced and used in PCR reactions for 18S and CaR mRNA detection. Data shown are the average of 2 reactions on the same cDNA samples. Data kindly provided by Pierre delMoral, Ph.D.

Lung Sample	Normalized expression level (% of E11.5)
E11.5	100
E12.5	261
E13.5	56
E14.5	7
E15.5	109
E16.5	30
E17.5	33
E18.5	27.5
P10	0

Expression of CaR was detected throughout the embryonic development of C57/Bl6 mouse lungs (Table 3.1) with a peak of expression at E12.5, which was an 161% increase over expression levels at E11.5. This peak tapers off through the remainder of development back down to E11.5 levels at E15.5, where expression is 109±14%. By E18.5 the expression decreases to 27.5±1% of expression at E11.5 and in a single sample tested at P10 there was no detectable CaR expression.

3.3.3 Whole Mount In Situ Hybridisation

Whole mount *in situ* hybridisation is a widely used method in developmental biology to detect and visualise the expression pattern of mRNA in early developmental stage tissues (Bellusci *et al.*, 1997b; Shi *et al.*, 2001; De Langhe *et al.*, 2005). A probe was made from a previously amplified segment of the human CaR corresponding to the nucleotide sequence 2332 – 2975 from human parathyroid CaR (Accession number U20759) to detect the expression of CaR mRNA in developing lung tissue (See Appendix A). As a negative control, the reverse complement of this sequence showed that there was no non-specific binding of probes within the lung tissue. Figure 3.2A shows that an E10.5 lung subjected to the sense probe and processed at the same time as the lung in Figure 3.2B shows no detection of CaR mRNA within the lung tissue. The E10.5 lung in Figure 3.2B shows detection of CaR mRNA expression in the epithelium lining the trachea and in the epithelium that lines the developing lung branches distally as well as punctuate points of expression throughout the mesenchyme. CaR mRNA expression is also detected in the epithelium lining the developing branches of lungs at E11.5, E12.5 and E14.5 (Fig. 3.2C, D and E).

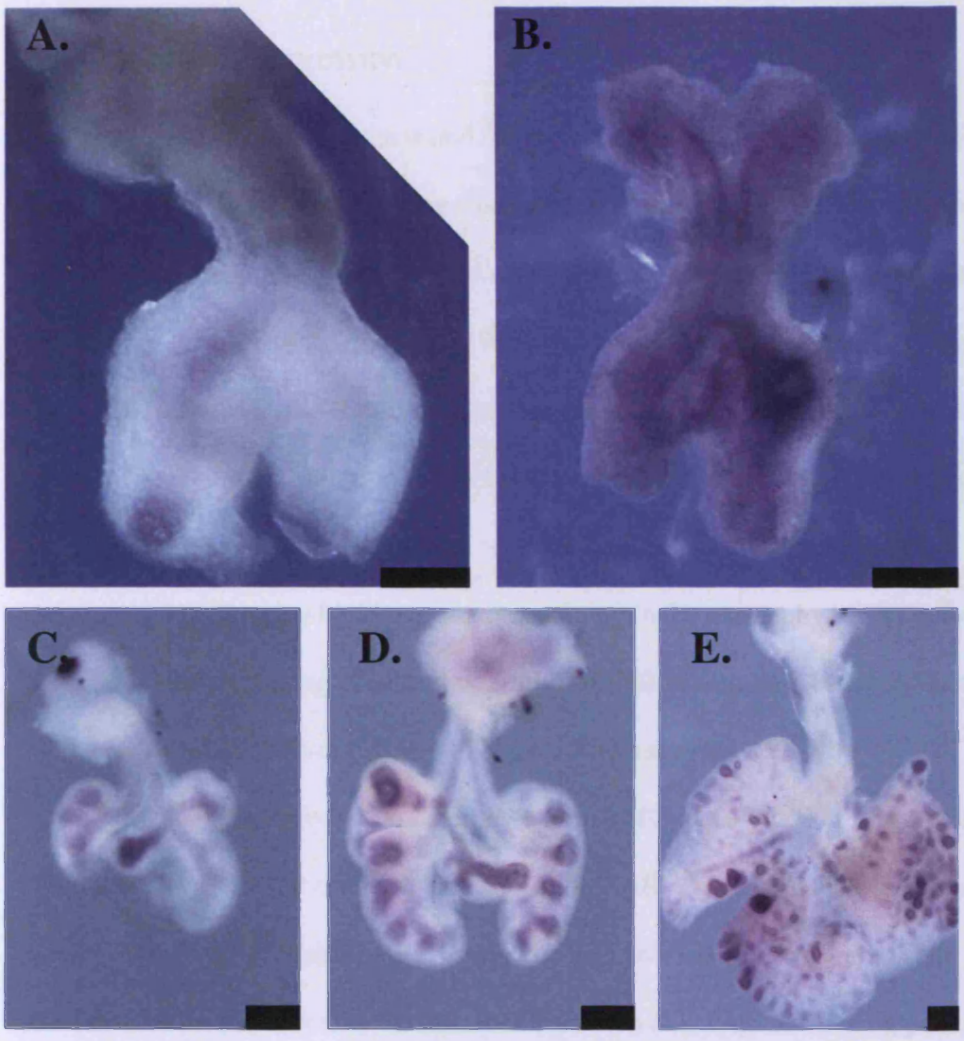

Figure 3.2: Whole mount *in situ* hybridization of CaR RNA in developing lungs.
PFA-fixed lungs were subjected to whole mount *in situ* hybridisation with CaR-specific RNA probes. **A).** Negative control, sense CaR probe applied to E10.5 lung shows no significant binding to CaR mRNA. Antisense CaR probe detects developmental CaR mRNA expression (purple) in mouse lungs at embryonic days 10.5 (**B.**), 11.5 (**C.**), 12.5 (**D.**) and 14.5. Scale bar = 200 μm.

3.4 CaR protein expression

Several antibodies were tested for their ability to specifically detect CaR in PFA-fixed, paraffin embedded lung tissue. The first antibodies tested were antiserum 733 (733), a rabbit polyclonal directed against amino acids 217-235 in the amino-terminus of the CaR (Riccardi *et al.*, 1998) and IMG-71169 (Imgenex, San Diego, CA, USA) also detecting a region in the N-terminus of the CaR protein, between amino acids 370-420. Figure 3.3 shows that both antibodies detected CaR expression in the same areas of serial E12.5 lung sections, mainly in the epithelium of the developing lung buds, with faint scattered staining in the mesenchyme. Negative controls, performed using pre-immune serum for 733 or omission of the primary antibody for the antiserum IMG-71169, detected no immunoreactivity.

Imgenex also produce another antiserum, IMG-71168, which is in the region of amino acids 200-250 of the N-terminus of the CaR. This antibody was not used initially due to the probability that it was directed toward the same amino acid residues as 733. However, in the interest of further validating the staining pattern for CaR in E12.5 lungs it was tested and yielded similar results to IMG-71169 (Fig. 3.4) with immunoreactivity mainly in epithelium and some scattered detection in the mesenchyme of E12.5 lung tissue.

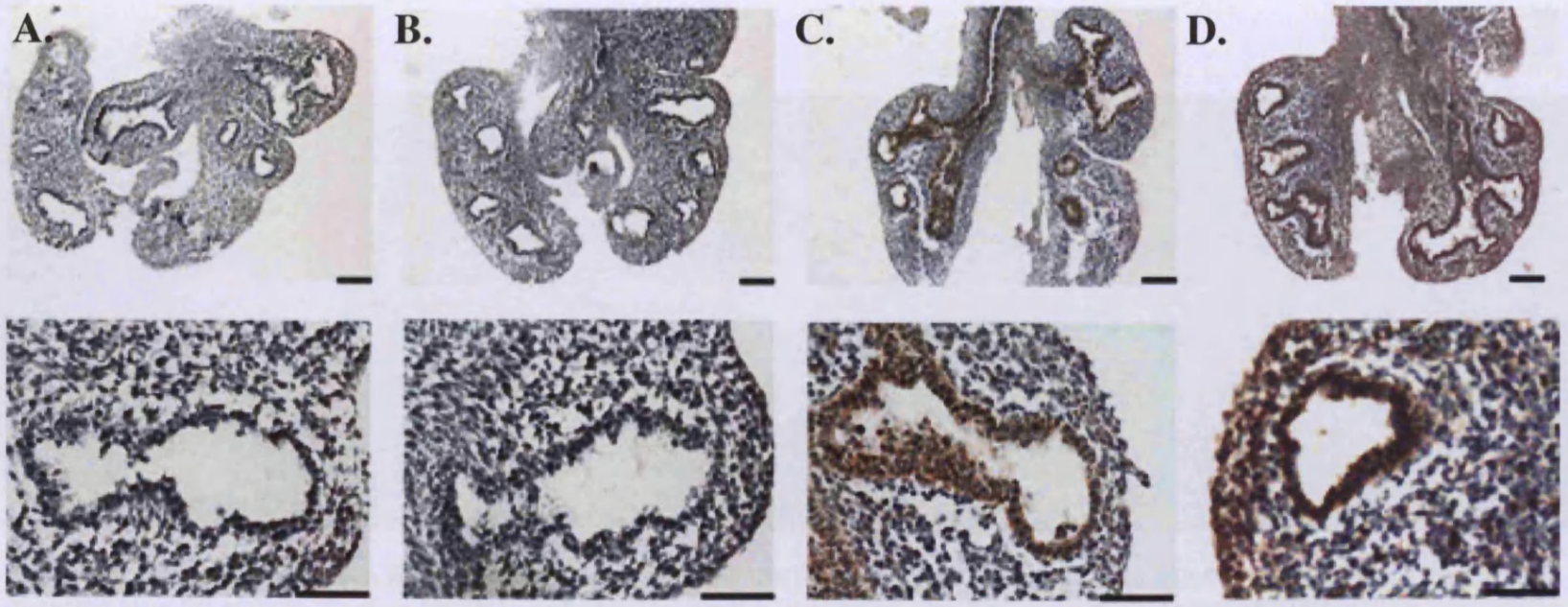

Figure 3.3: CaR protein detection by immunohistochemistry using IMG-71169 and 733 antisera on E12.5 mouse lung. E12.5 lungs were dissected from the embryo, fixed in 4% PFA, embedded in paraffin and sectioned to 5 microns thick. Immunohistochemistry was performed with IMG-71169 (**C**) and 733 (**D**) to detect CaR protein expression, visualised with DAB (brown pigment) and counterstained with Harris's hematoxylin (blue pigment). Negative controls were performed in tandem by omitting the primary antibody (**A**) and by applying pre-immunization serum from 733 production (**B**). The top row shows low magnification images of the whole mouse lung section. The bottom row of images shows greater detail of CaR immunoreactivity in the distal epithelium as well as in the mesenchyme of the E12.5 mouse lung. Top row scale bars = 100 μm, bottom row scale bars = 50 μm

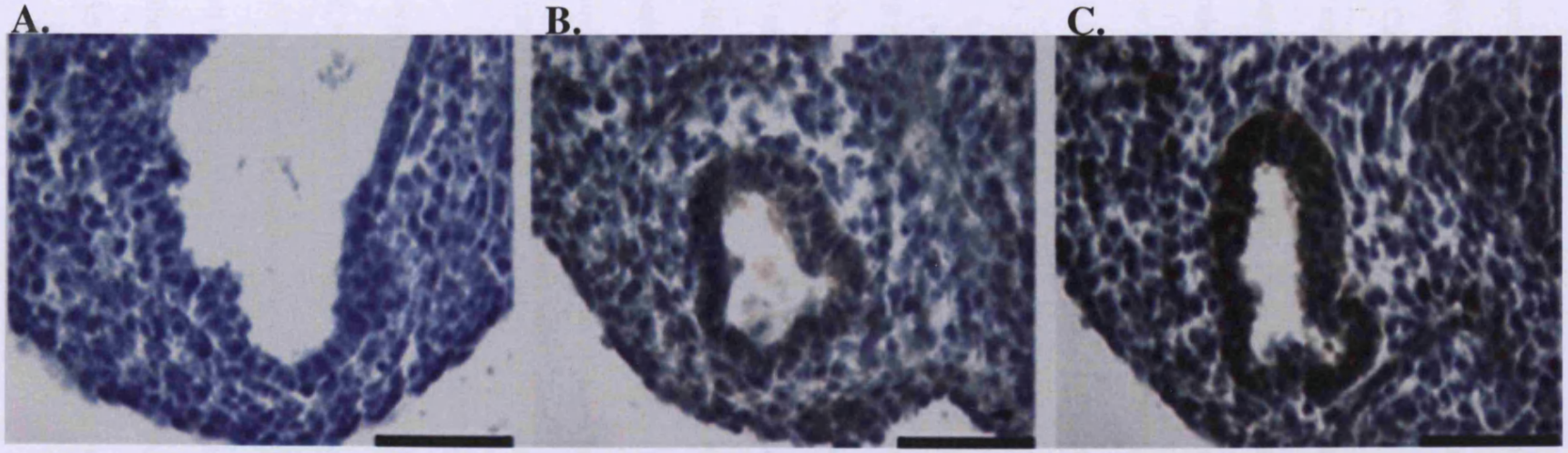

Figure 3.4: CaR protein detection by immunohistochemistry using IMG-71169 and – 71168 antisera on E12.5 mouse lung. E12.5 lungs were dissected from the embryo, fixed in 4% PFA, embedded in paraffin and sectioned to 5 microns thick. Immunohistochemistry was performed with IMG-71169 (**B**) and IMG-71168 (**C**) to detect CaR protein expression, visualised with DAB (brown pigment) and counterstained with Harris's hematoxylin (blue pigment). Negative control was performed in tandem by omitting the primary antibody (**A**). Scale bars = 50 μm.

There are several other commercially available polyclonal antibodies for the detection of the CaR. Two of these detect antigenic regions at opposite ends of the CaR protein (either the NH_2- or COOH-terminus) and were tested for validation of the CaR expression in E12.5 lungs; the ABR antibody detects amino acids12-27 at the end of the N-terminus and is commonly used for detection of the CaR by western blotting (Oda *et al.*, 1998), the USB antibody detects 20 amino acids near the C-terminus of the protein. Both antibodies, when used in reactions in tandem with 733 show the same patterns of immunoreactivity in the lung, with strong detection of CaR in the epithelium and some scattered detection of CaR in the mesenchyme (Fig. 3.5).

All of the antibodies tested on E12.5 gave a similar staining pattern in the lung which is a positive indicator that CaR protein is being detected by these antibodies regardless of the epitope against which the antibody is directed. Antisera 733 and IMG-71168 were tested at E16.5 to ensure that the same protocols were still applicable to larger tissue samples and that staining patterns remained the same for separate antibodies. Figure 3.6 shows that at this time point there is still immunoreactivity although the localisation is less concentrated in the epithelium, and more spread throughout the lung tissues as a whole.

The ontogeny of the CaR was determined on sections of whole embryo at embryonic stages, E10.5, E11.5, E12.5, E13.5, E14.5, E16.5 and E18.5. P0 and adult lung samples were used as negative controls, as previous PCR experiments indicated that CaR mRNA expression was decreased by E18.5 and undetectable in P10 or adult lungs. Using the 733 antibody, expression of the CaR can be seen in the epithelium of E10.5 – E16.5 lungs (Fig. 3.7A-F). At earlier time points, (E11.5-E13.5) slight expression is also detected in the mesenchyme of the lung which

increases through E16.5. By E18.5 CaR immunostaining is extremely faint (Fig. 3.7G) and is completely gone by P0 (Fig. 3.7H). The lack of CaR positive immunostaining is maintained in adult lung tissue (Fig. 3.7I).

There have been previous reports of CaR expression decreasing as cells are cultured (Mithal *et al.*, 1995). In order to ensure that the lung explant cultures maintained CaR expression in both low and high $[Ca^{2+}]_o$ culture conditions after 48 h, antiserum IMG-71169 was applied to sections from both 1.2 mM and 1.7 mM cultures. Results shown that in both experimental conditions CaR expression is maintained for 48 h (Fig. 3.8).

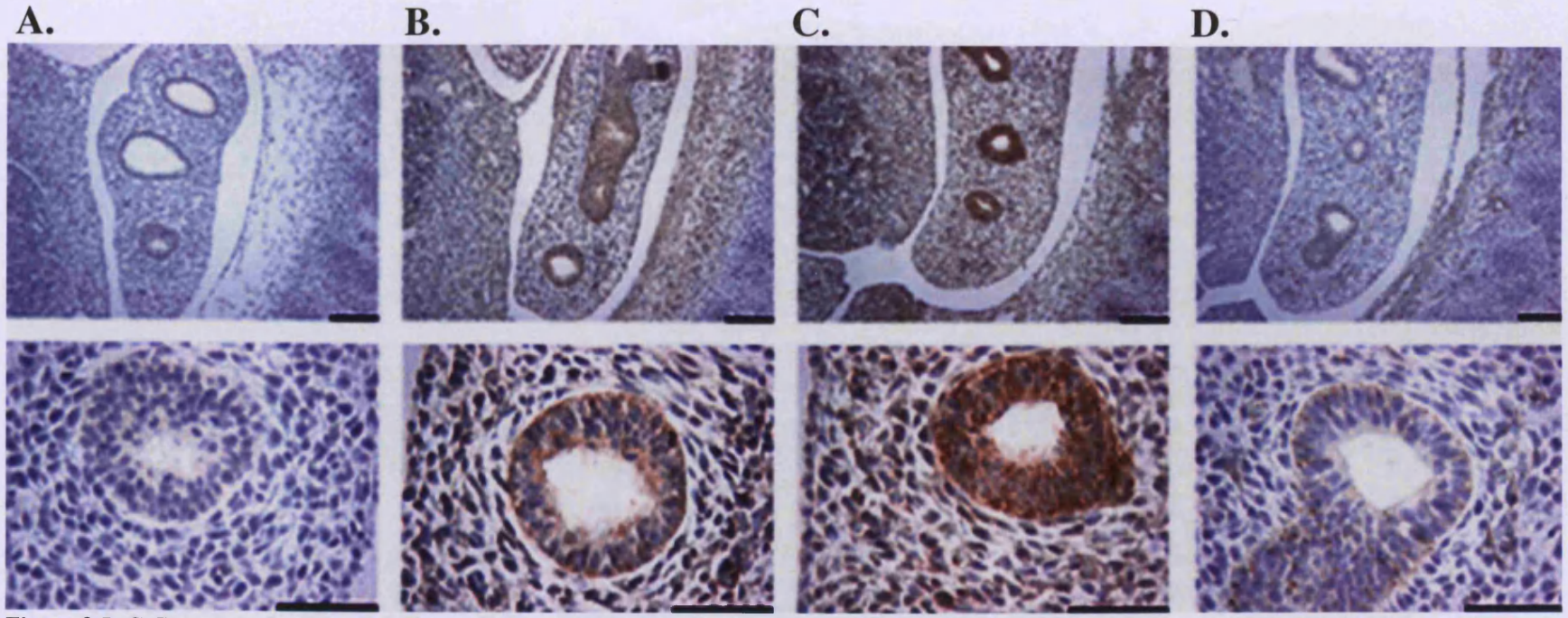

Figure 3.5: CaR protein detection by immunohistochemistry using 733, ABR and USB antisera in E12.5 mouse lungs. E12.5 embryos were fixed in 4% PFA, embedded in paraffin and sectioned to 5 microns thick. Immunohistochemistry was performed with antisera 733 (**B**), ABR (**C**) and USB (**D**) to detect CaR protein expression, visualised with DAB (brown pigment) and counterstained with Harris's hematoxylin (blue pigment). Negative control was performed in tandem by omitting the primary antibody (**A**). The top row shows low magnification images of the mouse lung in the context of the embryo. The bottom row of images shows greater detail of CaR immunoreactivity in the distal epithelium as well as in the mesenchyme of the E12.5 mouse lung. Top row scale bars = 100 μm, bottom row scale bars = 50 μm.

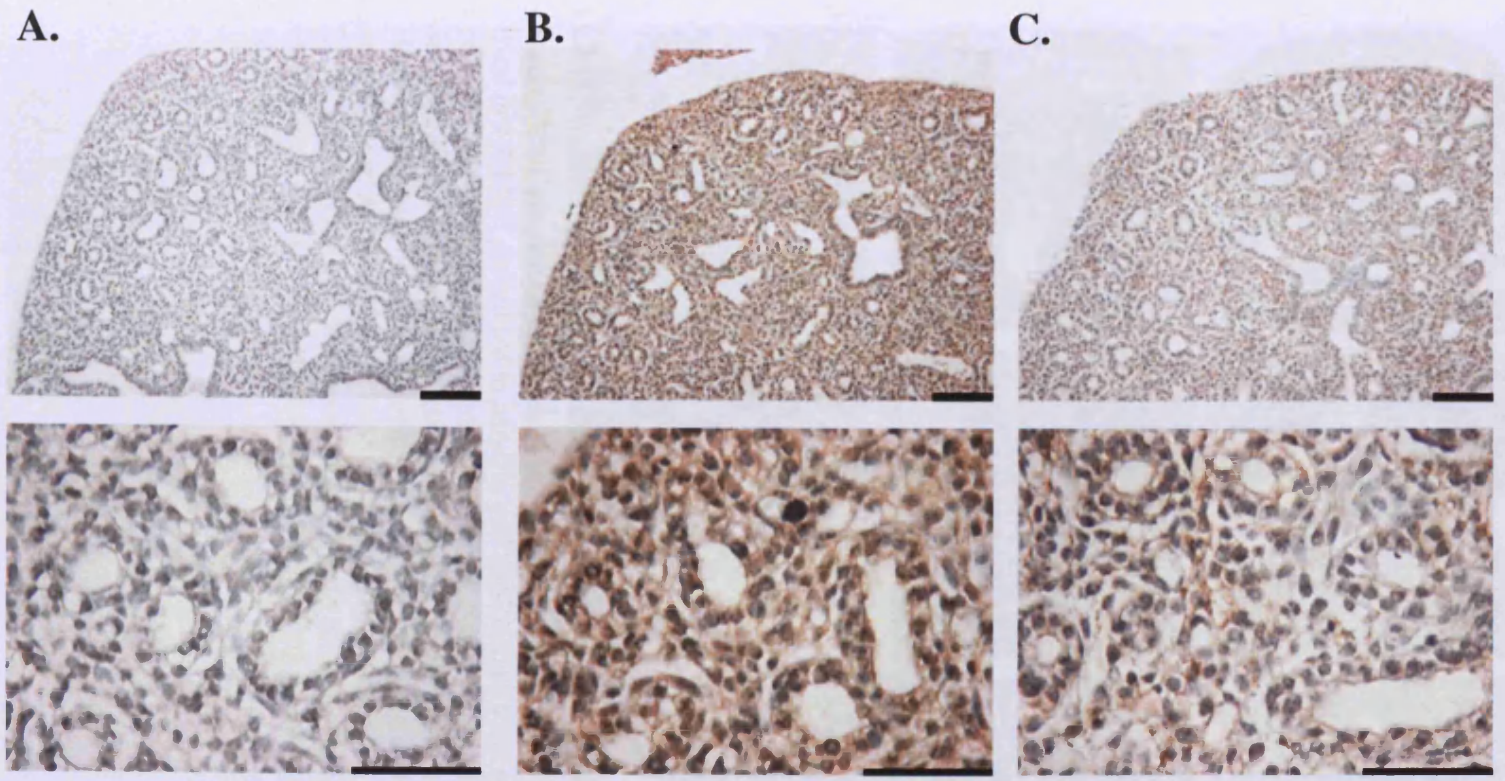

Figure 3.6: CaR protein detection by immunohistochemistry using 733 and IMG – 71168 antisera in E16.5 mouse lungs. E16.5 embryos were fixed in 4% PFA, embedded in paraffin and sectioned to 5 microns thick. Immunohistochemistry was performed with 733 (**B**) and IMG-71168 (**C**) antisera to detect CaR protein expression, visualised with DAB (brown pigment) and counterstained with Harris' hematoxylin (blue pigment). Negative control was performed in tandem by omitting the primary antibody (**A**). The top row shows low magnification images of the mouse lung at E16.5. The bottom row of images shows greater detail of CaR immunoreactivity in the distal epithelium as well as in the mesenchyme of the E12.5 mouse lung. Top row scale bars = 100 μm, bottom row scale bars = 50 μm.

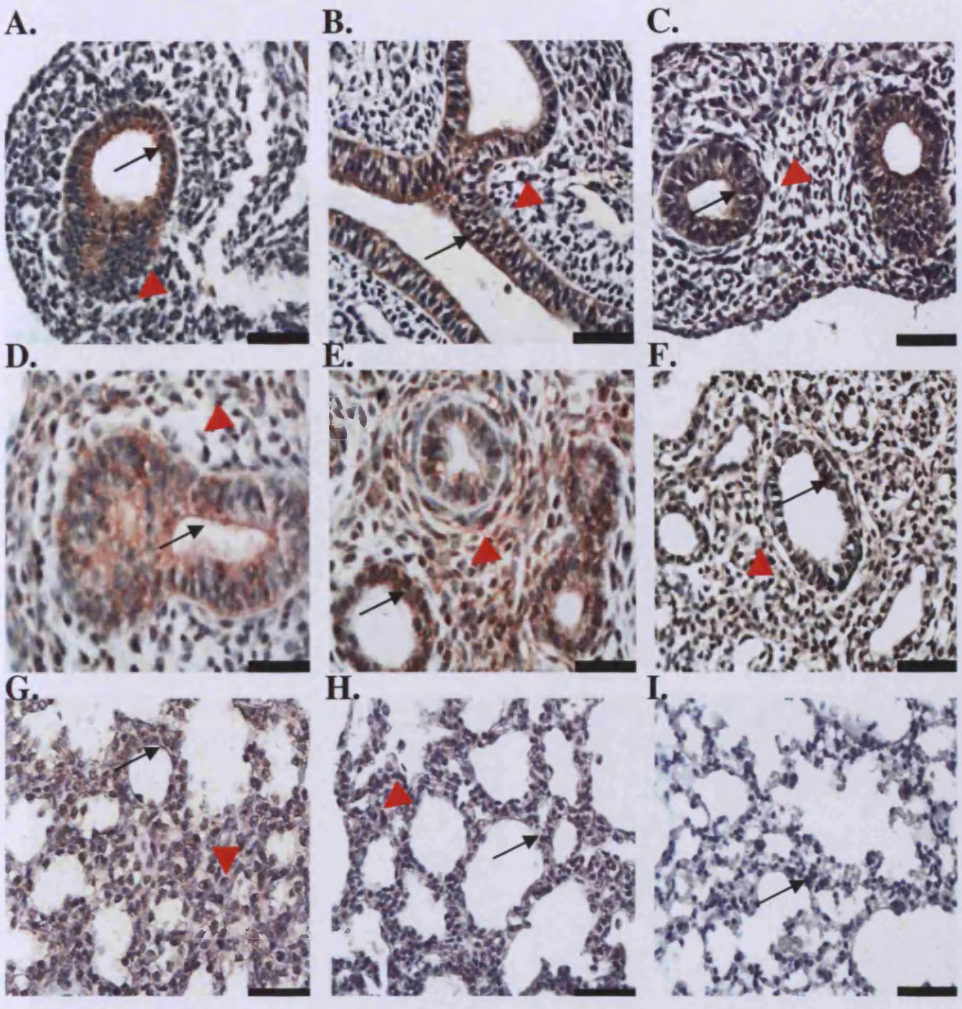

Figure: 3.7: CaR protein ontogeny in the developing mouse lung. Mouse lungs were fixed in 4% PFA, embedded in paraffin and sectioned to 5 microns thick. CaR protein was detected with 733 antiserum, a CaR N-terminal specific antibody, and developed with DAB substrate (brown pigment). Slides were counterstained with Harris' haematoxylin (blue pigment). Panel shows the lung at different stages of development. **A).** E10.5, **B).** E11.5, **C).** E12.5, **D).** E13.5, **E).** E14.5, **F).** E16.5, **G).** E18.5, **H).** P0, **I).** Adult. Red arrowheads refer to an area of lung mesenchyme in each section. Black arrows refer to an area of the lung epithelium in each section. Scale bars = 200μm.

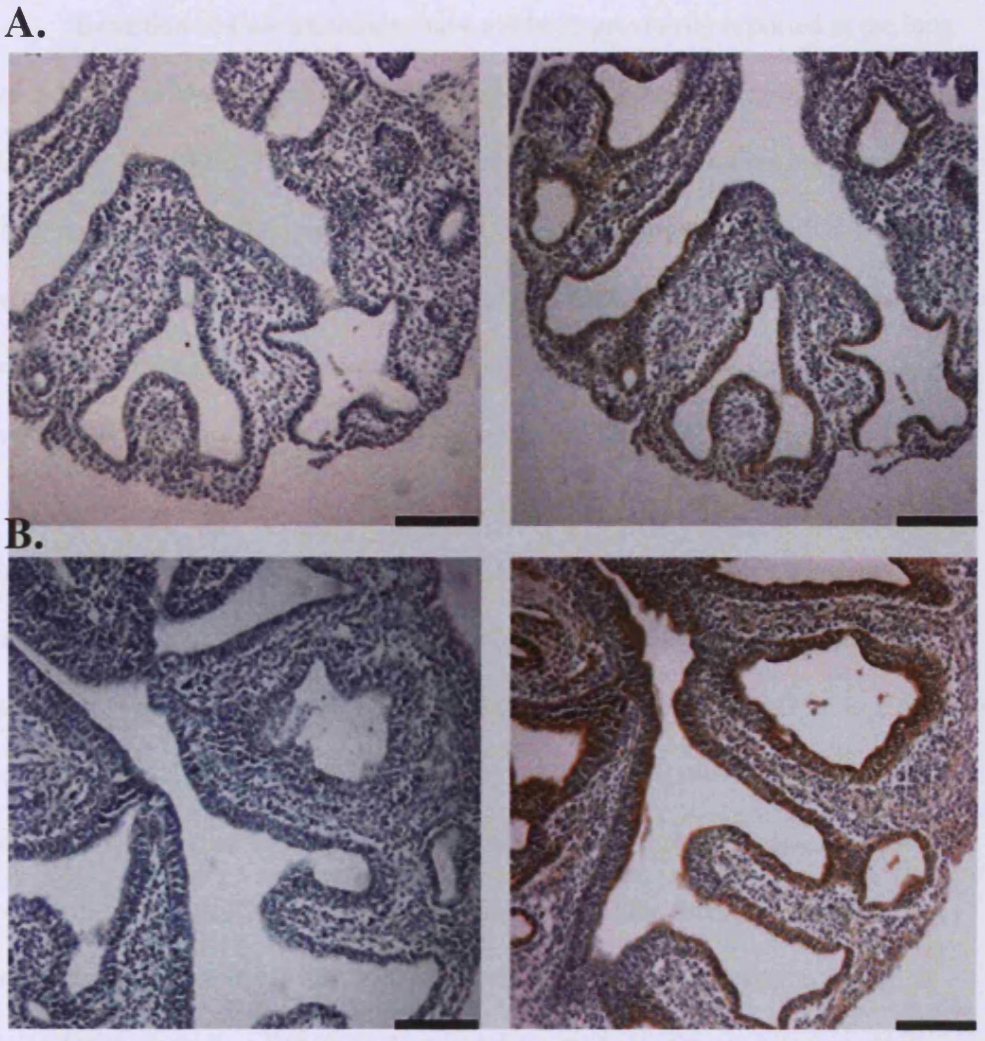

Figure 3.8 CaR expression is retained in culture for 48 h. After 48 h in culture, lung explants were fixed in 4% PFA, embedded in paraffin and sectioned to 5 microns thick. CaR protein expression was detected using IMG-71169 antiserum on lungs cultured in 1.2 mM Ca^{2+}_o (**A**, right panel) and 1.7 mM Ca^{2+}_o (**B**, right panel). Negative control was performed by omission of the primary antibody (**A** and **B**, left panels). Scale bars = 100 μm.

3.5 Chapter Discussion

Detection of CaR transcripts have not been previously reported in the lung when Northern blot analysis was performed on adult samples (Brown *et al.*, 1993; Riccardi *et al.*, 1995). The results presented in this chapter confirm previous findings showing a lack of CaR expression in adult tissue, but show that both RNA and protein are detected in the developing lung from E10.5 through E18.5. This detection was accomplished using a variety of methods in order to ensure that the results were genuine. A summary of the results is presented in Figure 3.9.

Initial RT-PCR results using CD1 embryonic lung total RNA indicated that the CaR was expressed in at least E11.5, E12.5 and E16.5 samples. Further experimentation using total RNA from C57/BL6 embryonic lungs subjected to quanitiative real-time PCR by my collaborator, Pierre delMoral PhD, in Los Angeles confirmed that CaR RNA was indeed expressed at E11.5, and that this expression peaked at E12.5, then tapered off through the remainder of development. By P10, there was no CaR mRNA detectable by this method. One further method of RNA detection, whole mount *in situ* hybridisation, detected CaR expression earlier, in E10.5 lungs, as well as E11.5, 12.5 and 14.5 lungs. Later time points were not attempted due to the limitations of the whole mount method on larger specimens.

This set of results shows that, by a combination of RNA detection techniques, CaR mRNA is indeed expressed in the developing mouse lung. However, mRNA expression does not necessarily translate into protein expression within a tissue, and aside from the whole mount *in situ* method, these modes of detection cannot show exactly what cell type is expressing the CaR at a certain time point. Therefore CaR protein detection was accomplished using standard immunohistochemical techniques.

One classic problem with immunohistochemistry is the specificity of the antibody used to detect the protein of interest. In order to ensure that the detection of CaR in the developing lung by immunohistochemistry was valid, different control applications, as well as several different antibodies were used. For the 733 antibody produced by Dr. Riccardi, a specific negative control was employed; the application of the pre-immune serum collected from the rabbit used to produce the polyclonal antibody prior to immunization with the 733 antigenic peptide. This negative control proves that any immunoreactivity seen is not due to an inherent antibody in the serum of the rabbit which was immunised to produce the 733 antiserum. Another way in which to confirm that the protein expression pattern detected is genuine, is to use antibodies produced to detect the same protein, but directed against different antigenic regions. In this study I used a total of 5 different CaR antibodies, all of which, when applied to E12.5 lung or whole embryo samples, gave a similar CaR staining pattern although with different intensities. CaR protein was mainly detected in the epithelium at early developmental time points, E10.5-12.5. At E13.5 and beyond CaR protein was detected in the mesenchyme as well.

Importantly after 48 h in culture, lungs removed at E12.5 still express CaR protein in their epithelium. This is probably due to the maintenance of the tissue structure instead of dispersing the cells for culture, as dispersed parathyroid cells lose CaR expression within 18 h of culture (Mithal *et al.*, 1995) whereas parathyroid cells cultured as pseudoglands maintain CaR expression and activity for much longer (Ritter *et al.*, 2004). It can therefore be assumed that any responsiveness to CaR agonists should be maintained throughout the length of the lung explant cultures used in the experimental program contained in this thesis.

What is the implication of this pattern of CaR expression within the developing lung? CaR is mostly expressed during the embryonic and pseudoglandular stages of lung development, E10.5-E16.5. During these stages the lung is undergoing branching morphogenesis, a process that involves the elongation and dichotomous branching of the lung epithelia, which over several branching generations forms the respiratory tree (Cardoso & Lu, 2006). As discussed in Section 1.10, this process requires the coordination of many signalling processes as well as the correct environmental stimuli in order to occur properly. Expression of the CaR during this time could be one factor which helps to coordinate the effects of environmental stimuli, *i.e.* $[Ca^{2+}]_o$, into cellular signalling responses. CaR activation has been previously shown to affect diverse cellular processes like proliferation and apoptosis, ion channel activity and secretion (Brown & MacLeod, 2001).

In early development, CaR expression appears to be maximal in the epithelium of the developing lung with faint detection in the mesenchyme, possibly reflecting a function for responding to $[Ca^{2+}]_o$ in the fluid of the lung lumen. Additionally, when the CaR is expressed in the epithelium at E12.5, there appears to be a fairly equal distribution between the apical and the basolateral membrane. After 48 h in culture, this distribution appears to shift with greater expression on the apical membrane. If this localisation shift is not an artefact of the staining protocol, the reason behind this shift remains to be determined. As the fetus continues to develop, CaR expression is more robustly detected within the mesenchyme. At these later time points (E13.5-E16.5) the lung mesenchyme is becoming vascularised (Colen *et al.*, 1999) and the expression of CaR in this compartment could represent a need to detect $[Ca^{2+}]_o$ from the infiltrating blood supply.

The role of the CaR at this point is purely speculative, but if the results of the previous chapter are taken into account, one can propose that changes in the branching morphogenesis, as well as changes in proliferation levels, TPD, and gene expression could all be mediated by the activation of CaR by high $[Ca^{2+}]_o$. The following chapters will focus on testing whether the CaR is indeed active in the developing lung and the possible mechanism(s) by which it could exert its effects.

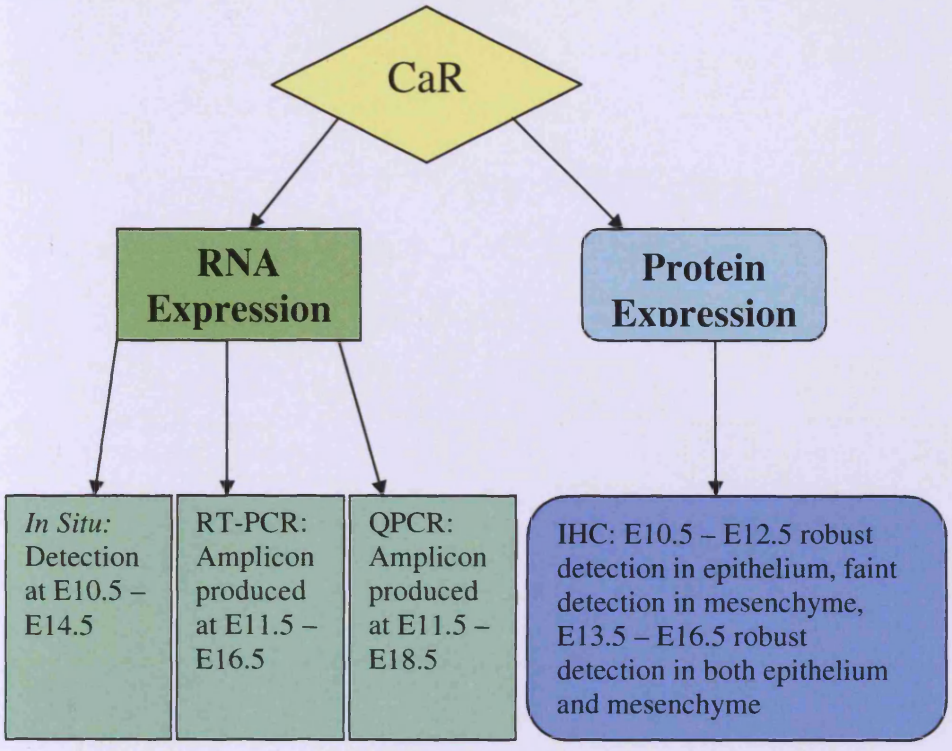

Figure 3.9: Diagrammatic summary of Chapter 3 results. CaR expression was detected using four different methods throughout embryonic development which resulted in a profile of developmentally regulated CaR expression in the lung.

CHAPTER 4:
EFFECT OF EXTRACELLULAR CALCIUM SENSING RECEPTOR ACTIVATION ON LUNG DEVELOPMENT

4.1 Methods

4.1.1 Lung Explant Cultures with CaR Agonists

Lungs were isolated from time-pregnant C57/BL6 females as in section 2.1.1. The calcimimetic NPS R-467 was a gift from NPS Pharmaceuticals. The calcimimetic, AMG R-568 was obtained from Amgen, Inc. An initial stock solution of each calcimimetic at 10 mM in DMSO was prepared and stored at -20°C. Prior to each experiment, fresh serial dilutions of the calcimimetics were prepared in water for addition to the culture medium at time = 0 h to the concentrations listed in figure legends. The culture medium was changed daily. Cultures were carried out in the same serum-free, chemically defined conditions as in section 2.1.1. The aminoglycoside antibiotics, gentamicin and neomycin (Sigma-Aldrich, Gillingham, Dorset, UK), were added to the culture medium of the lung explants to the concentrations specified in the text at t = 0 h and the medium was changed daily.

4.1.2 Lung Explant Cultures with Signalling Pathway Inhibitors

Lungs were isolated from time-pregnant C57/BL6 females and cultures carried out as in section 2.1.1. EC_{50} concentrations for signalling inhibitors are only available for cell culture models, thus initially inhibitors were added to the culture medium at time = 0 h in a range of concentrations for each inhibitor to determine the concentration appropriate (*i.e.* without achieving toxicity) for the explant culture method. All signalling inhibitors were obtained from Sigma-Aldrich (Gillingham, Dorset, UK) unless otherwise stated.

The following signalling inhibitors (listed with their target molecules) were used:

PD98059 – mitogen-activated protein kinase kinase (MEK)1/2 activation blocker; applied for 24 h at 25 or 50 μM and then medium replaced with Ca^{2+}_o adjusted medium alone at the desired $[Ca^{2+}]_o$ for the final 24 h;

U0126 – ERK1/2 inhibitor, applied for 24 h at 20, 30 or 40 μM and then medium replaced with Ca^{2+}_o adjusted medium alone at the desired $[Ca^{2+}]_o$ for the final 24 h;

BIRB 796 – p38 inhibitor (Kind gift of Dr. Mark Bagley, Cardiff University) , applied for 24 h at 1μM and then medium replaced with Ca^{2+}_o adjusted medium alone at the desired $[Ca^{2+}]_o$ for the final 24 h.

U73122 – PLC inhibitor, applied for 24 h at concentrations of 2.5, 5 or 10 μM and then medium replaced with Ca^{2+}_o adjusted medium alone at the desired $[Ca^{2+}]_o$ for the final 24 h;

U73343 – Inactive control analogue for U73122, applied for 24 h at concentrations of 2.5, 5 or 10 μM and then medium replaced with Ca^{2+}_o adjusted medium alone at the desired $[Ca^{2+}]_o$ for the final 24 h;

LY294002 – PI_3K inhibitor, applied for 48 h at concentrations of 5, 12.5 or 25 μM;

4.1.3 Intracellular Calcium Imaging

The mesenchyme was gently removed from the epithelium of E12.5 lungs using forceps and the remaining epithelial buds were cultured for 24 h free floating in DMEM/F-12 supplemented with 1% FCS. After 24 h epithelia were loaded with 6 μM fura-2 acetoxymethyl ester (Fura – 2AM; Molecular Probes, Eugene, OR., U.S.A.) for 60 min at 37 °C as described (Ward et al., 2002). The epithelial buds were then placed on glass coverslips and covered with Nucleopore filters (Whatman Intl. Ltd., Maidstone, Kent, UK) to prevent movement. These were placed in a perfusion chamber mounted upon a Nikon Diaphot equipped with a Cairn

monochromotor-based fluorescence system (Cairn Instruments, Faversham, Kent, U.K.) and were continuously superfused with a solution containing (in mM): 135 NaCl, 5 KCl, 0.8 $CaCl_2$, 0.8 $MgCl_2$, 5 HEPES, 10 glucose, pH 7.4. R-568 and carbachol were added to this solution to the final concentrations of 100 nM and 10 μM, respectively. Fura-2 was alternatively excited at 340 and 380 nm. Images at 510 nm were acquired at 0.2 Hz by a slow-scan CCD camera (Kinetic Imaging Ltd, Nottingham, U.K.). Following background subtraction, ratio of emission results from 340/380 excitation were calculated off-line using Andor IQ 1.3 software package (Andor Technology, UK).

4.1.4 Immunohistochemistry

Epithelial buds not used for intracellular calcium imaging studies were fixed in ice-cold methanol for 15 min, then washed in PBS at 4°C for 1 h. The primary antibodies, mouse monoclonal anti-smooth muscle actin antibody conjugated to cy3 (1:200, Sigma-Aldrich, Dorset, UK) co-incubated with a rabbit polyclonal anti-laminin antibody (1:200, Sigma-Aldrich, Dorset, UK), were applied to fixed epithelial buds overnight at 4°C. The following day the specimens were washed in PBS at RT for 1 h and then the secondary antibody, a donkey anti-rabbit conjugated to Alexa 488 (1:200, Molecular Probes, Eugene, OR., U.S.A.) was applied for 2 h at RT with gentle shaking. The final wash in PBS was done at RT for 1 h. The specimens were then mounted on a glass slide in Prolong anti-fade mounting medium (Molecular Probes, Eugene, OR., U.S.A.) and allowed to set at RT before being imaged by confocal microscopy.

4.1.5 Statistics

Graphic representations and statistics of the data were prepared with Origin 7 software. Data are presented as the mean (from multiple pooled experiments where indicated) ± s.e.m. Significance was determined using one-way ANOVA with Tukey *post-hoc* test and a p-value of ≤ 0.05 was deemed significant.

4.2 Philosophy of Work

The CaR has been previously shown to be activated, in a variety of systems, by $[Ca^{2+}]_o$ of 0.5 – 2.5 mM (Brown & MacLeod, 2001). This range is compatible with that used for the lung explant cultures in this project. To test the hypothesis that CaR activation is involved in the high $[Ca^{2+}]_o$- dependent suppression of lung branching morphogenesis, we utilised existing specific positive allosteric modulators of the CaR, NPS R-467 and AMG R-568. These compounds increase the sensitivity of the CaR to its classic agonist, Ca^{2+}, and they have been used in lung explant cultures grown in the presence of 1.05 and 1.2 mM Ca^{2+}_o to try and recapitulate the suppressive effect of high $[Ca^{2+}]_o$ on lung branching morphogenesis.

As a pleiotropic G-protein coupled receptor, CaR is known to mediate its effects via a number of different signalling pathways. These responses are generally dependent upon the G-protein subunits associated with the receptor in cell type or system tested (Ward, 2004). It was therefore decided to test a battery of well-characterised signalling inhibitors for their ability to rescue the suppressive effect of high $[Ca^{2+}]_o$ on lung branching morphogenesis in lung explant cultures, as an index for CaR activation. The pathways tested were MEK1/2, ERK1/2, p38, PLC and PI_3K, all of which are known to be activated by the CaR (Brown & MacLeod, 2001).

4.3 Lung Branching Morphogenesis is Responsive to Treatment with Calcimimetics.

In Chapter 3 it was demonstrated that CaR protein is present in the epithelium of E12.5 lungs. In order to determine if the suppression of branching morphogenesis by 1.7 mM Ca^{2+}_o is mediated by the CaR, lung explant cultures were treated with calcimimetic compounds, NPS R-467 and R-568 in the presence of either 1.05 or 1.2 mM Ca^{2+}_o. As positive allosteric modulators of the CaR, these calcimimetics would be expected to shift the dose response for Ca^{2+}_o to the left, thereby mimicking the effects of high Ca^{2+}_o and inhibiting branching morphogenesis.

Treatment with NPS R-467 resulted in a dose-dependent inhibition of branching morphogenesis at both 24 and 48 h when used at 100 or 1000 nM (n=3 for each concentration of NPS R-467 from a single isolation) in the presence of 1.05 mM Ca^{2+}_o (Fig. 4.1A). Branching was significantly decreased from 1.05 mM levels of 35.2±2.3% at 24 h and 123.3±4.5% at 48 h (taken from Fig. 2.2A); to 13.9±3.9% ($p = 0.04$) at 24 h and 77.8±7.7% ($p=0.02$) at 48 h with addition of 100 nM NPS R-467; to 14.17±11.8% at 24 h and 51.9±17.8% at 48 h with addition of 1000 nM NPS R-467 to culture medium containing 1.05 mM Ca^{2+}_o. Both of these concentrations of NPS R-467 resulted in branching increases which were not statistically different from those observed in lungs grown in 1.7 mM Ca^{2+}_o, 19.9±1.7% (24 h) and 62.2±4.4% (48 h, Fig. 2.2A).

When NPS R-467 was added to culture medium containing 1.2 mM Ca^{2+}_o a dose-dependent effect, similar to that in Figure 4.1A was not detected (Fig. 4.1B). A greater range of NPS R-467 concentrations resulted in significant decreases from 1.2 mM Ca^{2+}_o branching levels (30.4+1.8%± at 24 h and 109.2±3.1% at 48 h; Fig. 2.2A) after 48 h of treatment. The addition of both 10 and 30 nM NPS R-467 resulted in a

significant decrease from 1.2 mM Ca^{2+}_o levels of branching morphogenesis to 76.5±17.4% (n=6, p=0.01) and 83.4±12.2% (n=10, p=0.01) at 48 h respectively. The addition of 100 nM NPS R-467 resulted in significant decreases at both 24 h, to 15.5±5.3% (n=9, p=0.01) and at 48 h, 85.4±12.04% (p=0.02). The highest concentration of NPS R-467 tested was 1000 nM which only showed a significant decrease in branching levels at 48 h to 72.9±13.5% (n=6, p=0.004).

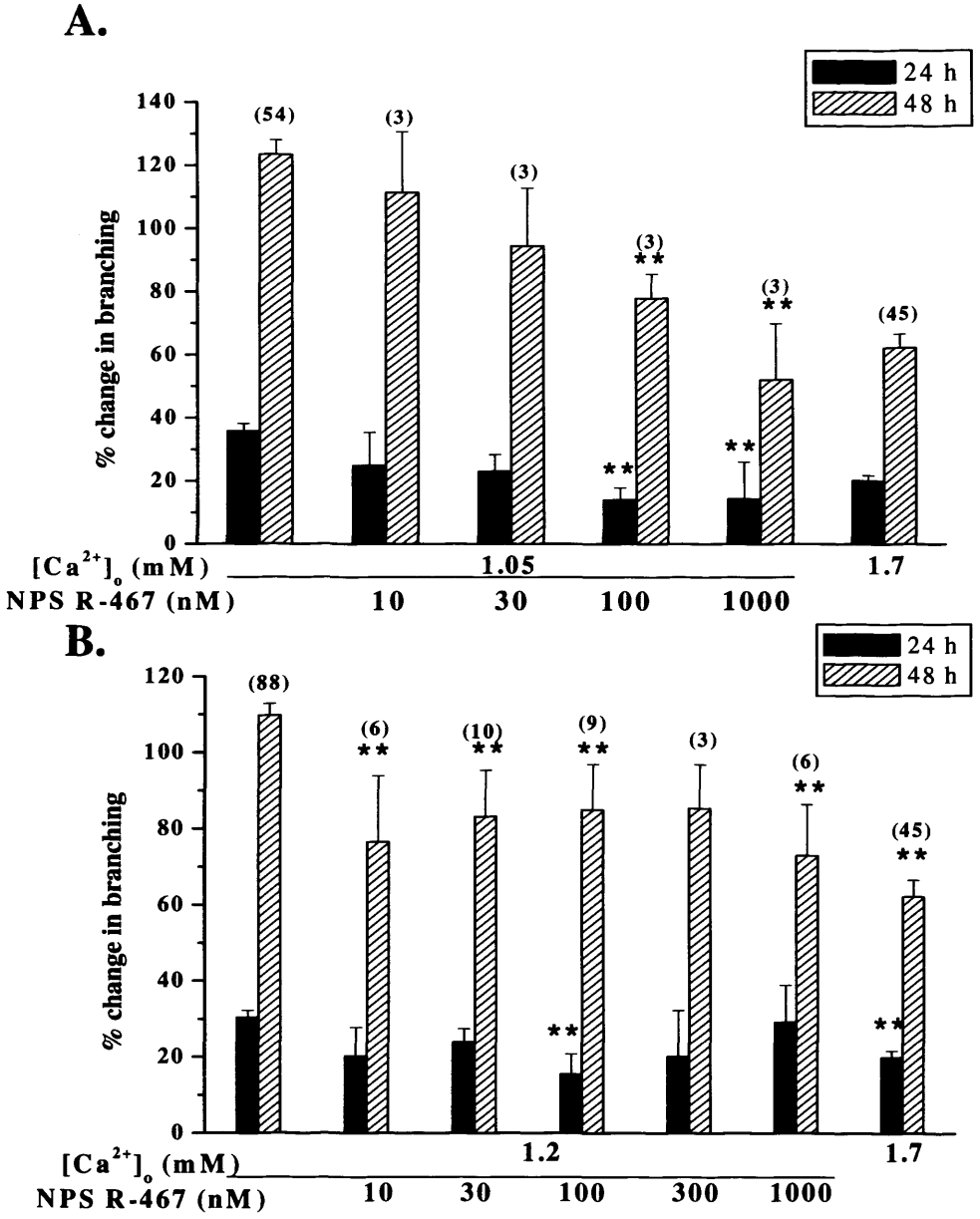

Figure 4.1: Effect of increasing concentrations of NPS R-467 on lung branching morphogenesis. Lungs from E12.5 mouse embryos were cultured for 48 h in the presence of either 1.05, 1.2 or 1.7 mM Ca^{2+}_o with or without the presence of NPS R-467. **A).** Graphic representation of branching morphogenesis induced when cultures are treated with 10-1000 nM NPS R-467 in 1.05 mM Ca^{2+}_o for 24 (black bar) and 48 h (hatched bar). **B).** Graphic representation of branching morphogenesis induced when lung explant cultures are treated with 10-1000 nM NPS R-467 in 1.2 mM Ca^{2+}_o for 24 (black bar) and 48 h (hatched bar). Terminal branch number at 24 and 48 h was normalised to branch number at 0 h and expressed as percent change in number of branches. Data shown as mean ± s.e.m from ≥ 1 separate experiments, n in parentheses above 48 h results, ** = $p \leq 0.05$ by ANOVA compared to 1.05 mM or 1.2 mM control values.

As an alternative positive allosteric modulator of the CaR, the calcimimetic Amgen R-568, was tested at 10, 30 and 50 nM in a single culture experiment grown in medium containing 1.2 mM Ca^{2+}_o (Fig. 4.2) for its ability to mimic the effects of 1.7 mM Ca^{2+}_o on lung branching morphogenesis. At all concentrations tested R-568 reduced the amount of branching although not all values reached statistical significance (Fig.4.2, n=3 lungs per condition). After 24 h lungs cultured in the presence of 1.2 mM Ca^{2+}_o+ 0.1% DMSO (control for the calcimimetic treatment) had increased branching by 41.2±18.3%, and after 48 h branching had increased by 101.2±15.5%, values similar to those observed in the presence of 1.2 mM Ca^{2+}_o without addition of DMSO in Figure 2.2A (30.4±1.8% and 109.7±3.1%). These results indicate that 0.1% DMSO application had no effect on branching morphogenesis. Application of 10 nM R-568 reduced the branching response to 17.2±8.6% at 24 h and 53.6±10.5% at 48 h, although these values were not significant different from control values. 30 nM R-568 evoked an increase in branching by 9.9±6.2% at 24 h and 40.2±9.4% (n=3, p=0.02) at 48 h, while 50 nM of the compound produced 16.7±5.5% at 24 h and 50±6.3% (n=3, p=0.03) at 48 h. These values are significantly different from 1.2 mM + 0.1% DMSO, but are not significantly different from the values induced by 30 nM R-568. Doses of 1, 10, 30 and 100 nM R-568 were also used in cultures with a basal $[Ca^{2+}]_o$ of 1.05 mM (Fig. 4.3). Significant changes in branching morphogenesis resulting in an increase of 79.6±15.7% (n=3, p=0.03) were seen with 10 nM R-568 and 96.5±9.1% (n=7 from two isolations, p=0.04) with 30 nM R-568 after 48 h in culture.

Figure 4.3B shows the results of TPD recordings from Chapter 2 with the addition of lungs cultured in the presence of 1.05 mM Ca^{2+}_o + 30 nM R-568 for 48 h. When lungs were cultured in the presence of 1.05 mM Ca^{2+}_o, their TPD was

-1.24±0.15 (n=17). This was significantly decreased when they were cultured in the presence of 1.7 mM Ca^{2+}_o where their TPD is -1.68±0.16 (n=20, p=0.048). The negativity of TPD recordings was increased further when 30 nM R-568 was added to culture medium containing a basal Ca^{2+}_o of 1.05 mM to -2.18±0.12 (n=4, p=0.007). This indicates that the increased negativity, or increases in secretion are mediated by activation of the CaR.

From the results of the previous experiments, it appeared that the concentration of R-568 needed to induce significant changes in branching morphogenesis was lower than that needed to produce a significant effect with NPS R-467. Therefore Figure 4.4B and D show the effect of specifically activating the CaR with a low dose of R-568 (10 nM) in the presence of 1.2 mM Ca^{2+}_o (n=15 from 5 separate isolations) on the branching morphogenesis of cultured lung explants. R-568 significantly suppressed the branching response at 24 h from 30.4±1.8% in the presence of 1.2 mM Ca^{2+}_o to 15.5±2.9% (p=0.001) in the presence of 1.2 mM Ca^{2+}_o + 10 nM R-568. This level of branching is not significantly different (p=0.2) from the 19.9±1.7% increase in branching seen in the presence of 1.7 mM Ca^{2+}_o. The suppression of branching by R-568 is maintained at 48 h where there is a 109.7±3.1% increase in the presence of 1.2 mM Ca^{2+}_o, and the branching suppression is shown by a branching increase of 72.9±5.9% ($p \leq 0.0001$) in the presence of 1.2 mM Ca^{2+}_o + 10 nM R-568. Again, this value is not significantly different (p=0.2) from the 62.2±4.4% branching increase in the presence of 1.7 mM Ca^{2+}_o (Fig. 4.4C and D).

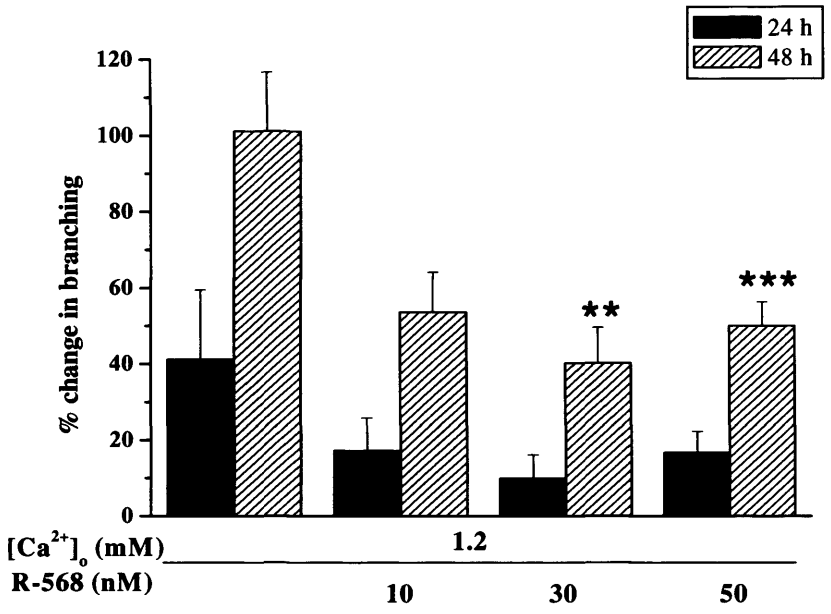

Figure 4.2: Effect of increasing concentrations of R-568 on lung branching morphogenesis in the presence of 1.2 mM Ca^{2+}_o. Lungs from E12.5 mouse embryos were cultured for a total of 48 h in the presence 1.2 mM Ca^{2+}_o. Parallel experiments were carried out with the addition of the calcimimetic R-568 in the presence of 1.2 mM Ca^{2+}_o. Terminal branch number at 24 and 48 h was normalised to branch number at 0 h and expressed as percent change in number of branches. Data presented as mean ± s.e.m. from a single experiment, n=3 for each condition, ** = $p \leq 0.03$, *** = $p \leq 0.02$ determined by ANOVA with Tukey *post-hoc* test.

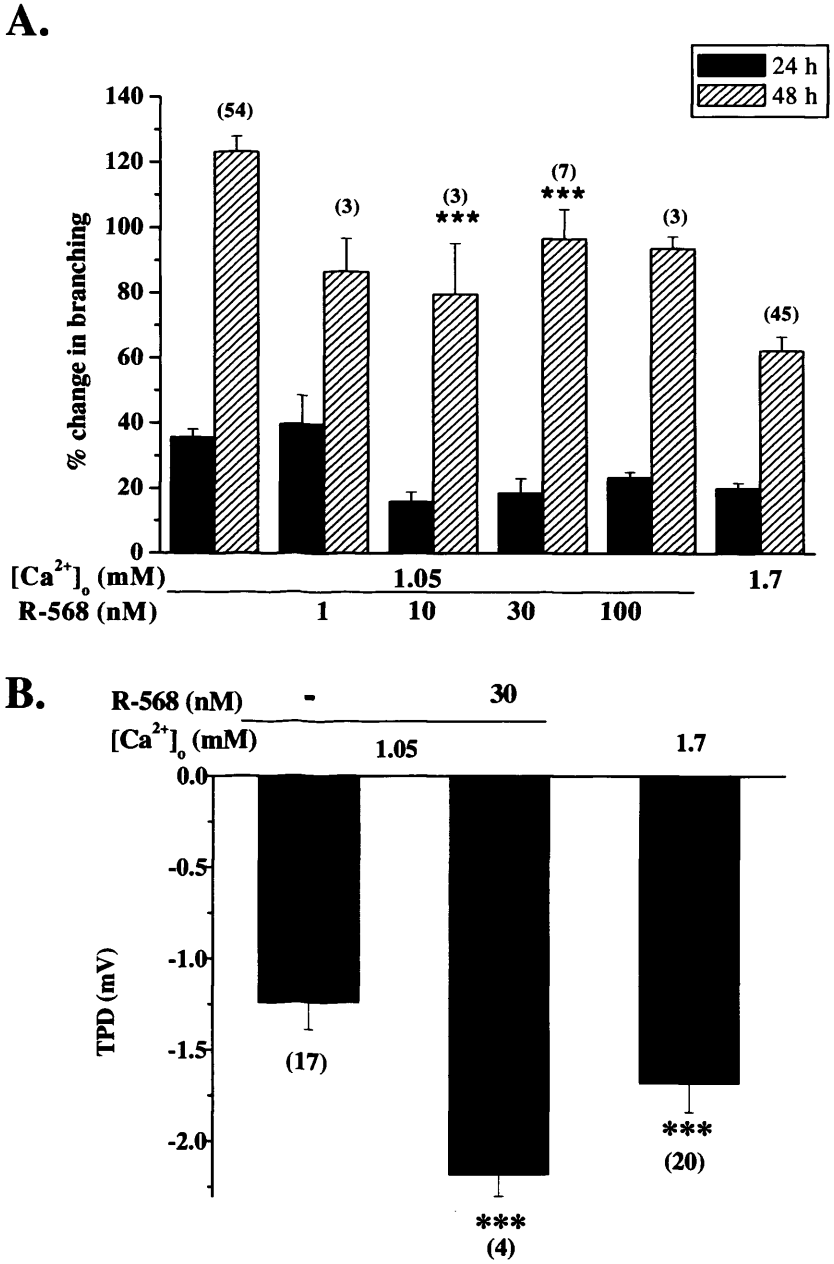

Figure 4.3: Effect of R-568 on lung branching morphogenesis and TPD in the presence of 1.05 mM Ca^{2+}_o. Lungs from E12.5 mouse embryos were cultured for a total of 48 h in the presence 1.05 mM Ca^{2+}_o with the addition of the listed concentrations of R-568. **A).** Terminal branch number at 24 and 48 h was normalised to branch number at 0 h and expressed as percent change in number of branches. **B).** TPD was measured after 48 h in culture and becomes more negative in cultures with the addition of 30 nM R-568 or in the presence of 1.7 mM Ca^{2+}_o for 48 h. Data presented are mean ± s.e.m. from ≥ 1 separate experiments, n shown in parentheses above/below 48 h results, *** = $p \leq 0.048$ determined by ANOVA with Tukey *post-hoc* test.

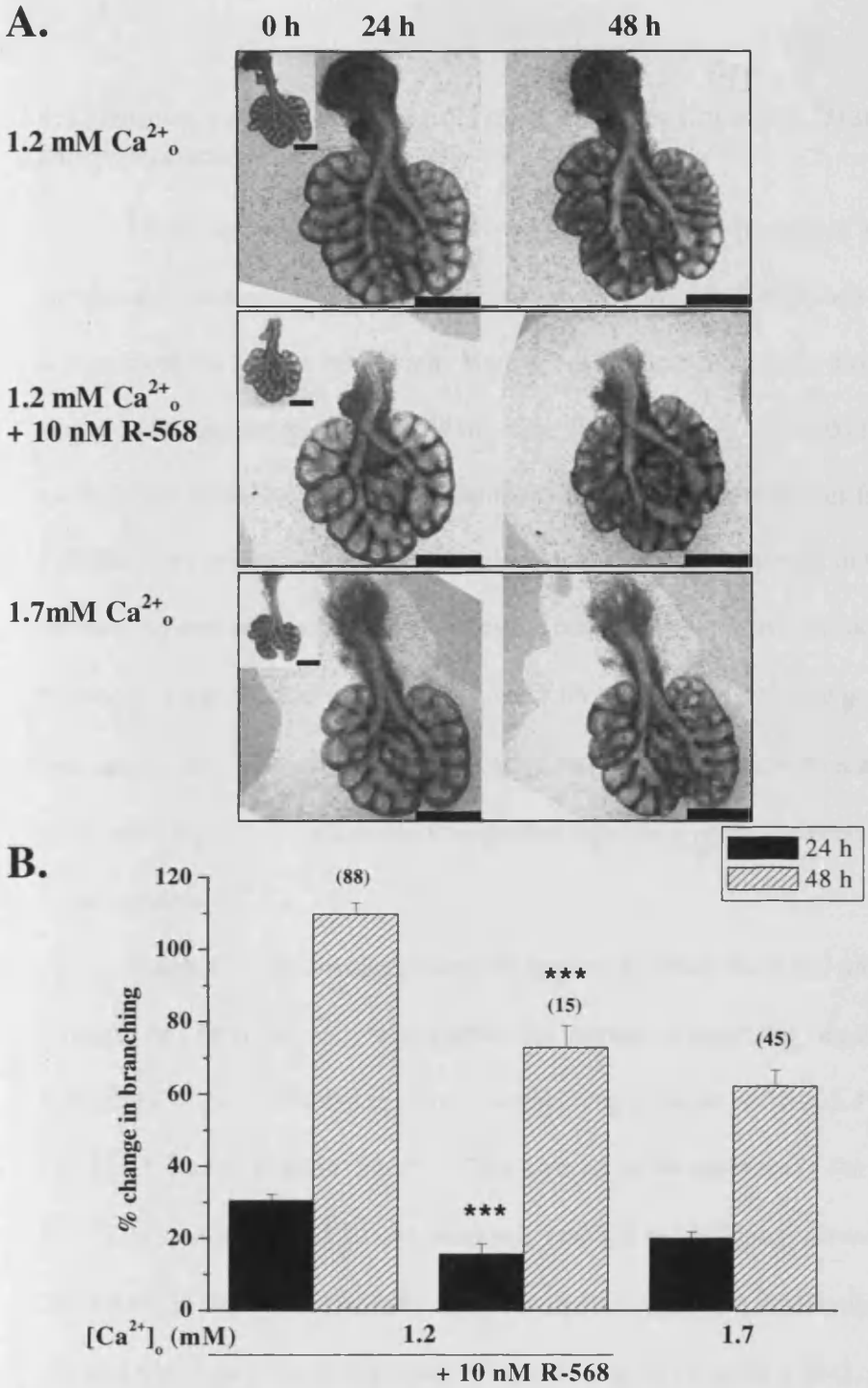

Figure 4.4: Lung branching morphogenesis is suppressed in the presence of 10 nM R-568 and high $[Ca^{2+}]_o$. Lungs from E12.5 mouse embryos were cultured for a total of 48 h in the presence 1.2 mM Ca^{2+}_o with 10 nM R-568. **A).** Representative pictures of lungs cultured in the presence of 1.2 mM Ca^{2+}_o, 1.2 mM Ca^{2+}_o + 10 nM R-568 and 1.7 mM Ca^{2+}_o at 0, 24 and 48 h. **B).** Terminal branch number at 24 and 48 h was normalised to branch number at 0 h and expressed as percent change in number of branches. Data presented are mean ± s.e.m., from ≥ 5 separate experiments, n in parentheses above 48 h results, *** = $p \leq 0.001$ in comparison to explants cultured in the presence of 1.2 mM Ca^{2+}_o determined by ANOVA with Tukey *post-hoc* test. Scale bars = 650 μm.

4.4 Aminoglycoside Antibiotic Treatment does not affect Branching Morphogenesis

As the previous studies have shown the CaR to be expressed in lung explant cultures and responsive to calcimimetic treatment, it was decided to test other activators of the CaR in this system. Both neomycin and gentamicin have been shown to be agonists of the CaR (Ward *et al.*, 2002; Ward *et al.*, 2005) in experiments involving homologous (kidney derived) and heterologous (CaR-HEK293) cell systems. Since these antibiotics are not routinely used in lung explant cultures, several concentrations were tested. Neomycin was used at concentrations between 30 and 100 μM in the presence of 1.05 or 1.2 mM Ca^{2+}_o and gentamicin was used at 20 – 100 μM at 1.05 mM Ca^{2+}_o. Neither aminoglycoside antibiotic produced a significant reduction in branching regardless of the concentration applied to the cultures.

Figure 4.5A shows that neomycin, applied at either 50 or 100 μM in the presence of 1.05 mM Ca^{2+}_o did not affect the amount of branching normally seen in 1.05 mM Ca^{2+}_o cultures where there is a branching increase of 35.7±2.4% at 24 h or 123.3±4.5% at 48 h (n=54, see Fig 2.2A). Indeed, in the presence of the same $[Ca^{2+}]_o$, administration of 50 μM neomycin resulted in branching increases of 21.7±8.5% at 24 h (p=0.2) and 91.4±25.7% at 48 h (n=3, p=0.12), similarly 100 μM allowed for 23.3±1.6% at 24 h (p=0.24) and 117.8±16.3% at 48 h (n=3, p=0.78). In the presence of 1.2 mM Ca^{2+}_o (values of 30.4±1.8% at 24 h or 109.2±3.1% at 48 h, n=88, see Fig. 2.2A), 30 (n=12) or 60 (n=3) μM neomycin treatment again did not produce any significant change in branching resulting in 20.9±3.9% (p=0.06) and 38.9±2.4% (p=0.37) at 24 h and 97.8±7.4% (0.18) and 89.3±1.8% (p=0.24) at 48 h respectively.

Gentamicin treatment was applied in the presence of 1.05 mM Ca^{2+}_o at 20, 50 and 100 μM but produced no significant changes to the level of branching morphogenesis normally seen in the presence of 1.05 mM Ca^{2+}_o (Fig. 4.5B). In the presence of 20 μM gentamicin (n=3) branching levels were 30.9±4% at 24 h (p=0.65) and 109.9±13.4% (p=0.5) at 48 h. Gentamicin concentrations of 50 (n=3) and 100 (n=6) μM produced much the same effects with increases in branching of 25.5±5.5% (p=0.33)or 29.5±5.1% (p=0.41) at 24 h and 122.6±2.5% (p=0.97) or 123±10.4% (p=0.98) at 48 h respectively.

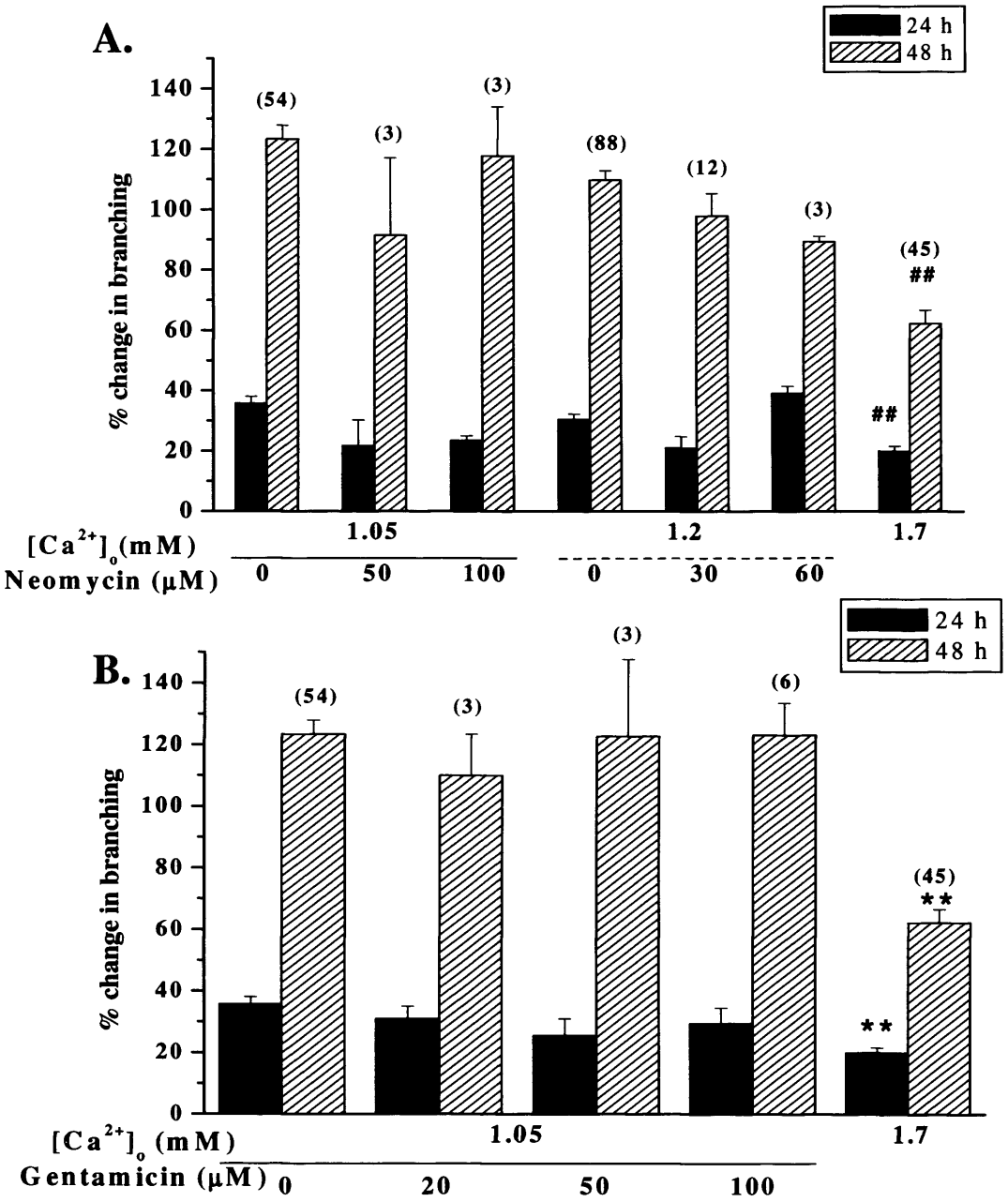

Figure 4.5: Aminoglycoside antibiotic treatment does not significantly affect branching morphogenesis. Lungs from E12.5 mouse embryos were cultured for 48 h in the presence of 1.05, 1.2 or 1.7 mM Ca^{2+}_o with or without the antibiotic indicated. **A).** Graphic representation of branching morphogenesis induced when cultures are treated with 30-100μM neomycin for 48 h. **B).** Graphic representation of branching morphogenesis induced when lung explant cultures are treated with 20-100 μM gentamicin for 48 h. Terminal branch number at 24 and 48 h was normalised to branch number at 0 h and expressed as percent change in number of branches. Data shown as mean ± s.e.m from multiple pooled experiments, n shown in parentheses above 48 h results, ## = $p \leq 0.001$ by ANOVA compared to both 1.05 and 1.2 mM control values; ** = $p \leq 0.001$ by ANOVA compared to 1.05 mM control values.

4.5 Inhibition of Signalling Pathways Downstream of CaR Activation

4.5.1 Effect of MEK and ERK1/2 Inhibition on Lung Branching Morphogenesis

In order to test the hypothesis that CaR was mediating its high $[Ca^{2+}]_o$ or calcimimetic induced suppression on lung branching morphogenesis via MEK signalling, PD98059, a MEK1/2 activation blocker was added to the culture medium of lung explant cultures containing either 1.7 mM Ca^{2+}_o or 1.2 mM Ca^{2+}_o + 10 nM R-568. Previously, concentrations of 25 and 75 μM PD98059 have been used in whole kidney explant culture models (Fisher *et al.*, 2001). In these experiments we used both 25 and 50 μM PD98059, neither of which rescued the branching morphogenesis suppression by high $[Ca^{2+}]_o$ or by calcimimetic.

In a single experiment (n=3), lung cultures exposed to 1.2 mM Ca^{2+}_o, with the addition of 50 μM PD98059 (Fig. 4.6A*iii*) resulted in branching increases of 31.5±2.8 % at 24 h and 70.1±11.2% at 48 h, which were not significantly different from values observed in control cultures of 19.3±3% at 24 h and 78.5±24% at 48 h (Fig. 4.6B). When lungs were cultured in the presence of 1.2 mM Ca^{2+}_o + 10 nM R-568, the level of branching was decreased slightly in comparison to control cultures, to 17.5±6.4% at 24 h and 60±6.6% at 48 h, although this was not statistically significant (Fig. 4.6A*ii* and B). Addition of 50 μM PD98059 to 1.2 mM Ca^{2+}_o with 10 nM R-568 did not significantly change the branching levels resulting in 19±3.4% change in branching at 24 h and 54.7±6.6% at 48 h (Fig. 4.6A*iv* and B).

Similarly, when 25 μM PD98059 was added to medium containing 1.7 mM Ca^{2+}_o, branching levels did not significantly differ from control cultures resulting in increases of 9.8±4.2% (control, n=7 from 2 separate isolations) and 15.1±2.4% (PD98059, n=8 from 2 separate isolations, p=0.28) at 24 h and 38.5±8.6% (control)

and 40.4±4.4% (PD98059, p=0.84) at 48 h (Fig. 4.7B). When 25 μM PD98059 is added to 1.7 mM Ca^{2+}_o or 1.7 mM Ca^{2+}_o + 10 nM R-568 (Fig. 4.7A*iii*), the amount of branching morphogenesis still remains similar to that observed in control conditions, with values of 9.8±2.3% at 24 h (n=3, p=0.24) and 37.9±15.8% (p=0.84) at 48 h.

A second compound, U1026 was used to test the hypothesis that the CaR was mediating its calcimimetic or high Ca^{2+}_o induced suppression on lung branching morphogenesis by initiating ERK1/2 signalling. U0126 is commonly used for inhibition of ERK1/2 activation at concentrations of 10 and 20 μM in both cell and organ explant cultures (Kling *et al.*, 2002; Bhagavathula *et al.*, 2005). U0126 was applied to E12.5 mouse lungs cultured in the presence of 1.7 mM Ca^{2+}_o in order to test if the diminished branching morphogenesis could be rescued by the inhibition of ERK1/2 activation (Fig. 4.8).

Treatment with either 20 or 30 μM U0126 in 1.7 mM Ca^{2+}_o resulted in further reductions in the amount of branching morphogenesis (Fig. 4.8A*ii* and *iii*). Lungs cultured in the presence of 1.7 mM Ca^{2+}_o showed branching increases of 9.5±5.7% at 24 h and 67.6±22.5% at 48 h (Fig. 4.8A*iv* and B, n=6 from 2 separate experiments). Application of 20 μM U0126 for 24 h decreased these values to 6.4±2.5 % at 24 h and 50.4±19.6% at 48 h (n=6 from 2 separate experiments); 30 μM U0126 for 24 h decreased these values even further to 2.1±6% at 24 h. At 48 h in one lung there was a loss of a branch due to the swelling of the bud, this resulted in an overall negative mean of -0.7±4% at 48 h (n=3). A single experiment with 40 μM U0126 was attempted, but this was toxic as the lungs died within 24 h (not shown).

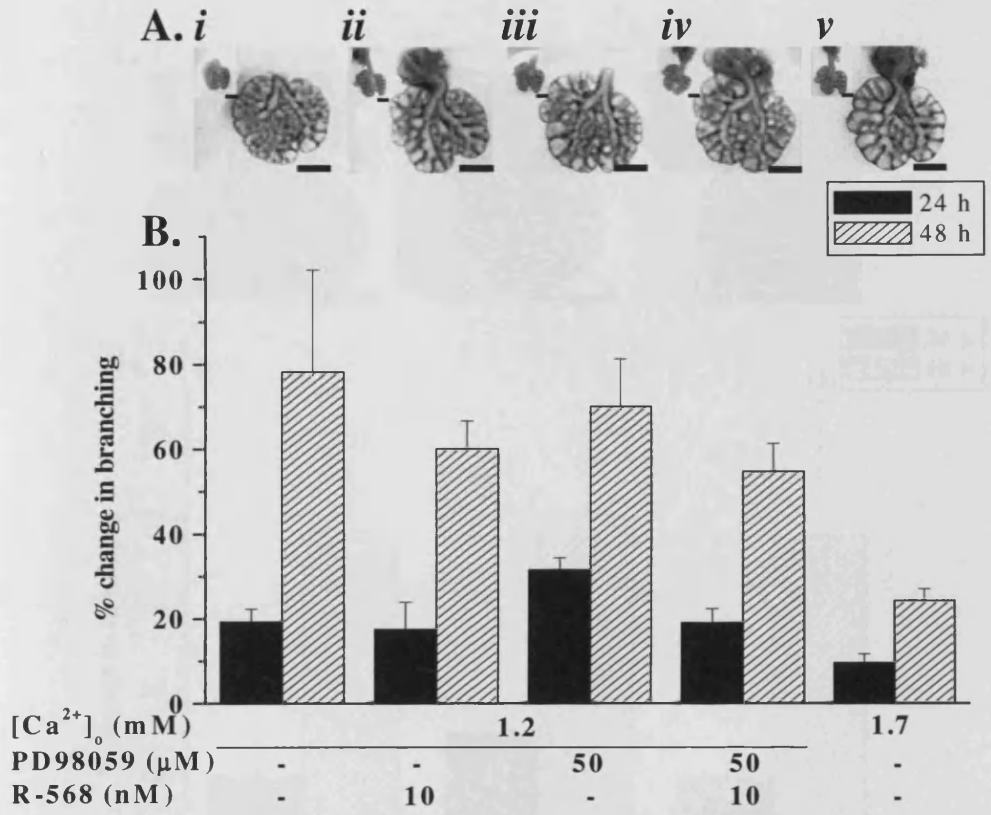

Figure 4.6: Effect of 50 μM PD98059 on $[Ca^{2+}]_o$- and calcimimetic-regulated branching morphogenesis. Lungs from E12.5 mouse embryos were cultured in the presence of 1.2 or 1.7 mM Ca^{2+}_o with 0.1% DMSO (negative control); and in the presence of 1.2 mM Ca^{2+}_o with 50 μM PD98059 (MEK activation blocker). **A).** Representative pictures of lungs cultured for 48 h in: ***i.*** 1.2 mM Ca^{2+}_o + 0.1% DMSO, ***ii*** 1.2 mM Ca^{2+}_o + 10 nM R-568, ***iii.*** 1.2 mM Ca^{2+}_o + 50μM PD98059, ***iv.*** 1.2 mM Ca^{2+}_o + 50 μM PD98059 + 10 nM R-568, ***v.*** 1.7 mM Ca^{2+}_o. Inset pictures show each lung at 0 h (post-dissection) showing a comparable number of initial terminal branches for each condition. **B).** Terminal branch number at 24 and 48 h was normalised to branch number at 0 h and expressed as a percent change in number of branches. Data shown are mean ± s.e.m., n=3 for all conditions, from a single isolation. Scale bars = 500 μm.

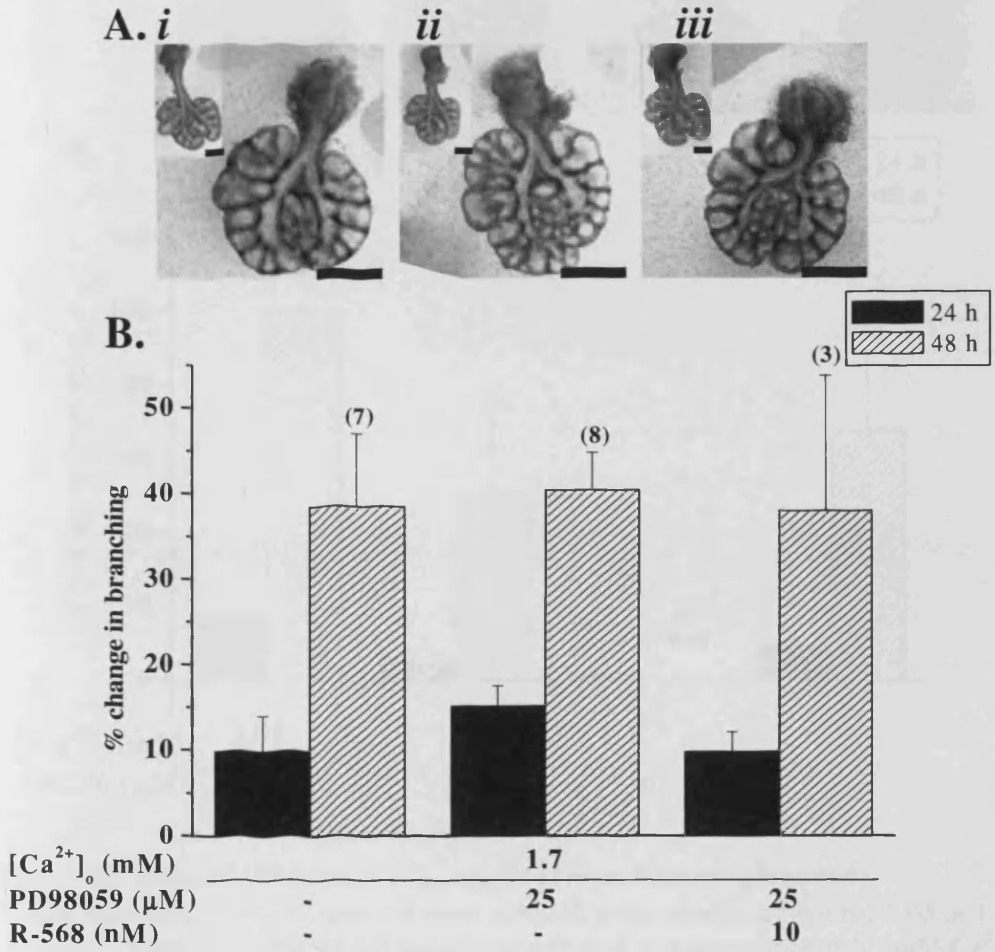

Figure 4.7: Effect of 25 μM PD98059 on $[Ca^{2+}]_o$- and calcimimetic-regulated branching morphogenesis. Lungs from E12.5 mouse embryos were cultured in the presence of 1.7 mM Ca^{2+}_o with 0.1% DMSO (negative control); or in the presence of 1.7 mM Ca^{2+}_o with the addition of 25 μM PD98059 (MEK activation blocker). **A).** Representative pictures of lungs cultured for 48 h at: ***i.*** 1.7 mM Ca^{2+}_o + 0.1% DMSO, ***ii.*** 1.7 mM Ca^{2+}_o + 25 μM PD98059, ***iii.*** 1.7 mM Ca^{2+}_o + 25 μM PD98059 + 10 nM R-568. Inset pictures show each lung at 0 h (post-dissection) showing a comparable number of initial terminal branches for each condition. **B).** Terminal branch number at 24 and 48 h was normalised to branch number at 0 h and expressed as a percent change in number of branches. Data shown are mean ± s.e.m., n in parentheses above 48 h results, from 2 separate experiments. Scale bars = 650 μm.

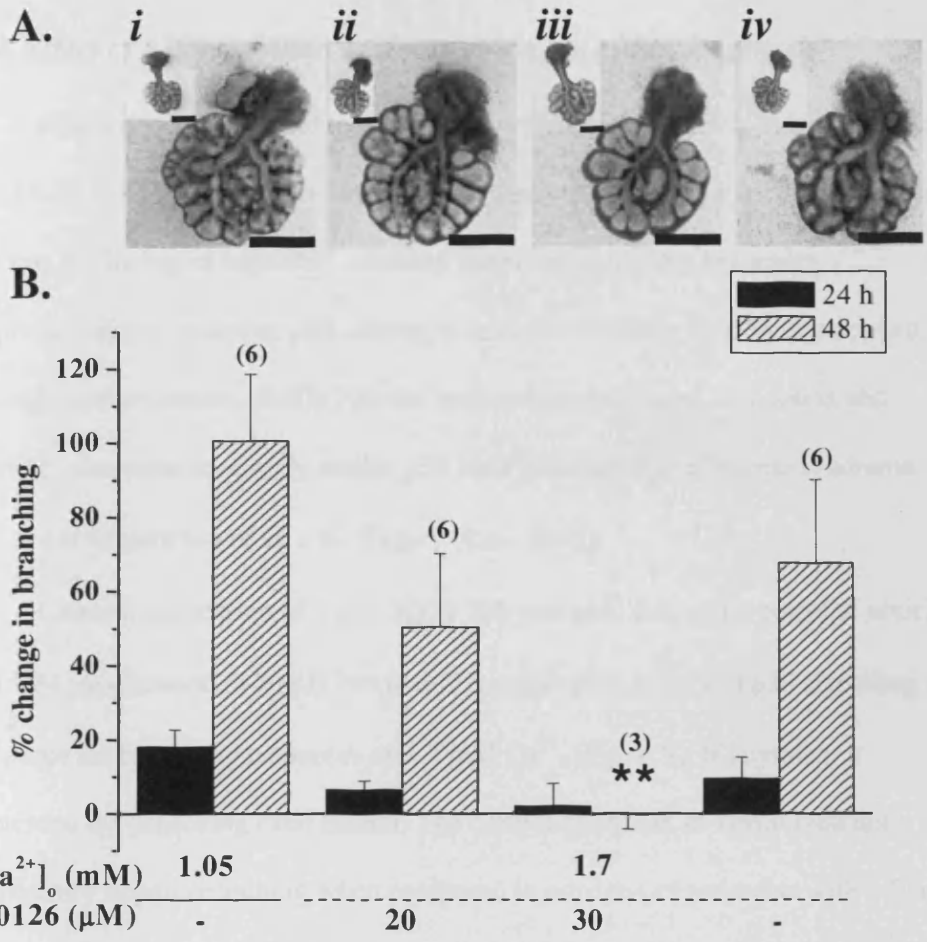

Figure 4.8: Effect of U0126 on $[Ca^{2+}]_o$ regulated branching morphogenesis.
Lungs from E12.5 mouse embryos were cultured in the presence of either 1.05 or 1.7 mM Ca^{2+}_o with 0.1% DMSO (negative control); and in the presence of 1.7 mM Ca^{2+}_o with 20 or 30 μM U0126 (ERK1/2 inhibitor). **A).** Representative pictures of lungs cultured for 48 h in: ***i.*** 1.05 mM Ca^{2+}_o+ 0.1% DMSO, ***ii.*** 1.7 mM Ca^{2+}_o+ 20 μM U0126, ***iii.*** 1.7 mM Ca^{2+}_o + 30 μM U0126, ***iv.*** 1.7mM Ca^{2+}_o + 0.1% DMSO. Inset pictures show each lung at 0 h (post-dissection) showing a comparable number of initial terminal branches for each condition. **B).**Terminal branch number at 24 and 48 h was normalised to branch number at 0 h and expressed as a percent change in number of branches. Data shown are mean ± s.e.m pooled from 2 separate experiments, n in parentheses above 48 h results. Significant inhibition of branching morphogenesis is induced by application of U0126 is indicated in time matched samples by the asterisks ($p<0.01$). Scale bars = 700 μm.

4.5.2 Effect of p38 Inhibition on Lung Branching Morphogenesis

CaR activation can lead to p38 phosphorylation and activity in osteoblastic MC3T3-E1 cells (Yamaguchi *et al.*, 2000). Therefore to test the hypothesis that the CaR was mediating its high Ca^{2+}_o induced suppression on lung branching morphogenesis by initiating p38 activity, a selective inhibitor for p38 was applied to the lung explant cultures. BIRB 796 has been successfully used as a potent and selective compound to acutely inhibit p38 MAPK signalling in Werner syndrome cells at a concentration of 10 μM (Bagley *et al.*, 2006).

Chronic application of 1 μM BIRB 796 was used due to the potential toxicity of 10 μM. Application of BIRB 796 at this concentration to inhibit p38 signalling did not rescue the branching responses of 1.7 mM Ca^{2+}_o (Fig. 4.9). If anything, it suppressed the branching even further. The control treatment of DMSO did not significantly impair branching when compared to previous experiments with 1.7 mM Ca^{2+}_o resulting in branching increases of 19.9±7.1% and 66.7±13.1% at 24 and 48 h (Fig. 4.9A*i* and ii). When 1 μM BIRB 796 was applied to lung cultures containing 1.7 mm Ca^{2+}_o, the percentage increases in branching were 20.5±6.5% and 35.9±20% at 24 and 48 h (Fig. 4.9 A and B, n=7 from two separate isolations).

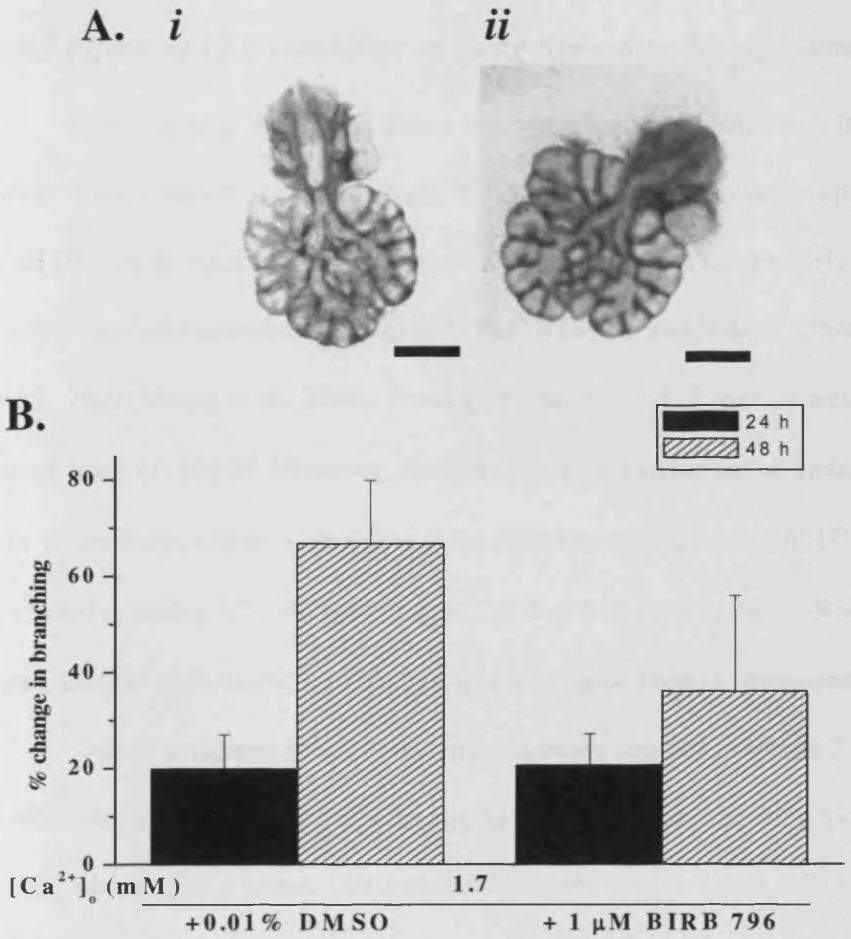

Figure 4.9 Inhibition of p38 signalling does not rescue 1.7 mM Ca^{2+}_o inhibition of branching morphogenesis. Lungs from E12.5 mouse embryos were cultured at 1.7 mM Ca^{2+}_o with 0.1% DMSO (negative control); and with 1 µM BIRB 796 (p38 inhibitor). **A).** Representative pictures of lungs cultured for 48 h in: ***i.*** 0.01% DMSO, ***ii.*** 1 µM BIRB. **B).** Terminal branch number at 24 and 48 h was normalised to branch number at 0 h and expressed as a percent change in number of branches. Data shown as mean ± s.e.m, n=7 lungs from two separate isolations. Scale bar = 600 µm.

4.5.3 Effects of PLC Inhibition on Lung Branching Morphogenesis

Activation of the CaR is linked to a phospholipase C-mediated increase in intracellular calcium concentration ($[Ca^{2+}]_i$) in almost every system expressing the CaR (Brown & MacLeod, 2001). The PLC inhibitor, U73122, is widely used to inhibit the CaR-dependent activation of PLC (Godwin and Soltoff, 2002; Handlogten et al., 2001; Huang et al., 2002). Concentrations of U73122 used in previous studies range from 1 – 10 μM. However, these studies were carried out on isolated cells and not whole tissue explants, therefore three different concentrations of U73122 and of its inactive analog U73343 were tested (2.5, 5 and 10 μM) in the studies presented here. DMSO (0.01-0.2%) was also used as a negative control compound.

When compared to the branching responses detailed in Figure 2.2A 0.1% DMSO did not have any significant effects on the level of branching morphogenesis at any concentration tested. Unfortunately at every dosage tested, U73343 treatment resulted in minimal branching increases (1-4%) at 24 h and by 48 h lung explants appeared dark and grainy, which is generally taken as an indicator that the lung has died (Fig. 4.10C, D and E). It was therefore decided that this did not demonstrate an applicable negative control and in subsequent cultures a relevant concentration of DMSO was added to culture medium.

Branching morphogenesis was sensitive to PLC inhibition by U73122 in a concentration-dependent manner (Fig. 4.11) at both 24 and 48 h in culture. At 24 h control explants exposed to 1.05 mM Ca^{2+}_o + 0.2% DMSO (n= 8 from 2 separate isolations) showed an increase in branching of 28.0±4.7%, at 48 h the number of terminal branches had doubled resulting in a 101.4±6.3% increase. There was no significant difference in the level of branching morphogenesis when 2.5 μM U73122 was added to the culture medium at either 24 or 48 h resulting in increases of

32.1±7.3% (n=3 from a single isolation, p=0.65) and 98.5±8.7% (p=0.81) respectively. However, both 5 and 10 μM U73122 caused an increase in branching morphogenesis that was significantly higher than that observed in the presence of 1.05mM Ca^{2+}_o + 0.2% DMSO. Treatment with 5 μM U73122 resulted in an increase of 55.6±7.1 % (n= 9 from 2 separate isolations, p≤0.001) at 24 h and 165.1±18% at 48 h (p≤0.001). 10 μM U73122 resulted in an even greater increase of 123.4±6% (n=11 from 3 separate isolations, p ≤0.001) at 24 h and 246.3±7.6% (p≤0.001) at 48 h.

In the presence of 1.7 mM Ca^{2+}_o + 0.2% DMSO branching is suppressed as expected from previous experiments (Fig. 2.2A, Fig. 4.12C), with only small increases in branch number, 16.1±5.3% at 24 h and 66.6±10.7% after 48 h (n=9 from 2 isolations). Addition of 2.5 μM U73122 does not significantly change these levels resulting in similar increases of 16.9±4.8% (n=4 from single isolation, p=0.94) at 24 h and 69.2±4.3% (p=0.89) after 48 h. With the addition of 5 μM U73122 the branching response is completely rescued to levels not statistically different from those observed in the presence of 1.05 mM Ca^{2+}_o (Fig. 4.12D), and were 88.7±10.08% at 24 h and 171.7±15.11% at 48 h (n=9 from 2 separate isolations, p≤0.001 compared to 1.7 mM Ca^{2+}_o + 0.2% DMSO). This rescue is made even more robust by the addition of 10 μM U73122, which results in branching increases of 117.5±6.9% (n=11 from 3 separate isolations, p≤0.001 compared to 1.7 mM Ca^{2+}_o + 0.2% DMSO) after 24 h and 215.5±5.4% after 48 h (p≤0.001 compared to 1.7 mM Ca^{2+}_o + 0.2% DMSO).

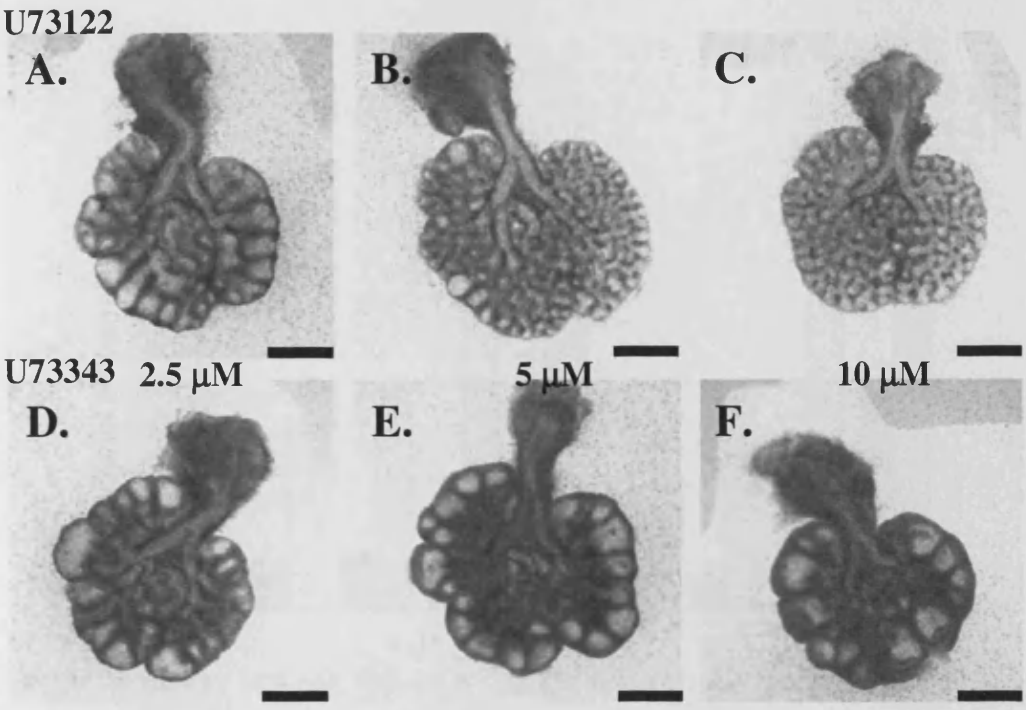

Figure 4.10: Effects of U73122 and U73343 on lung branching morphogenesis. The pictures are exemplar of E12.5 mouse lungs cultured for 48 h in the presence of 1.7 mM Ca^{2+}_{o} + U73122 (A-C) or + U73343 (D-F) at the concentrations indicated between the top and bottom row. Pictures are representative of n 3 lungs for each condition. Scale bars = 500 μm.

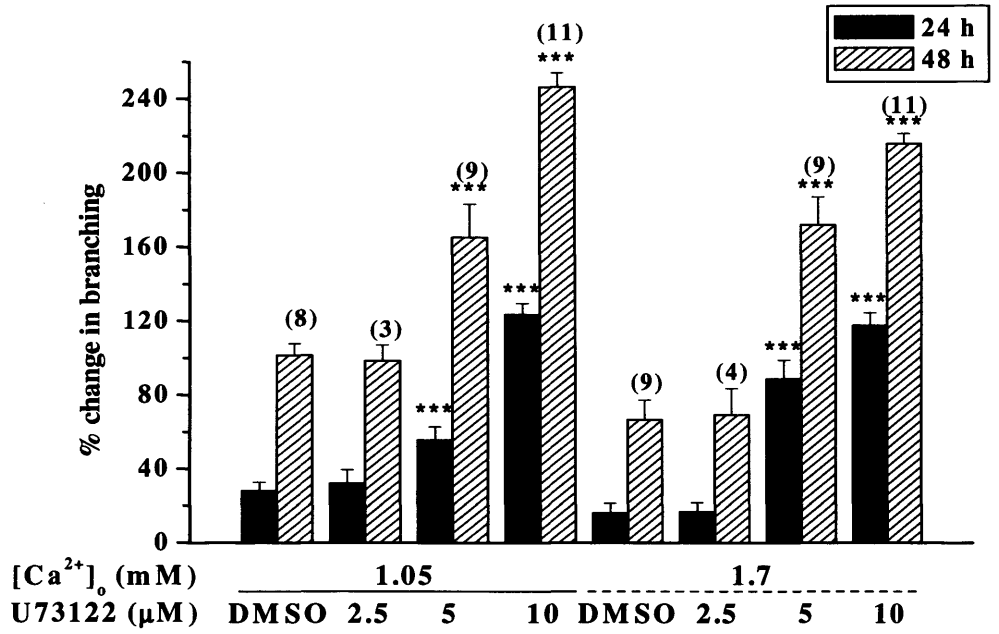

Figure 4.11: Branching morphogenesis is sensitive to PLC inhibition with U73122. Lungs from E12.5 mouse embryos were cultured in the presence of either 1.05 or 1.7 mM Ca^{2+}_o, with or without the addition of DMSO (0.2%) or U73122 (2.5, 5 and 10 μM). Graphic representation of branching increases seen in response to treatment with U73122. Branching responses are significantly increased with the addition of 5 or 10 μM U73122 at both 24 and 48 h. Terminal branch number at 24 and 48 h was normalised to branch number at 0 h and expressed as a percent change in number of branches. Data shown as mean ± s.e.m, from 1-3 separate experiments (n=3 or 4 then single experiment), n is shown in parentheses above 48 h results, *** = $p \leq 0.001$ by ANOVA with Tukey *post-hoc* test.

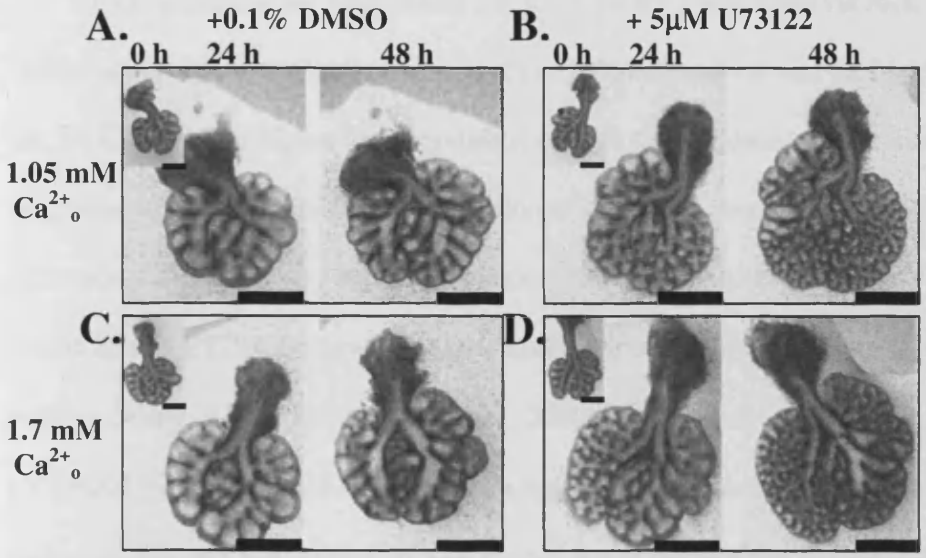

Figure 4.12: Exemplar lungs cultured with U73122. Lungs from E12.5 mouse embryos were cultured in the presence of 1.05mM Ca^{2+}_o (A and B) or 1.7mM Ca^{2+}_o (C and D) with 0.1% DMSO (A and C, negative control) or 5 μM U73122 (B and D, PLC inhibitor). Increased branching was visible after 24 h and continued to develop through to 48 h. These pictures are representative of two separate experiments where n=8 for A and n=9 for all other conditions. Scale bars = 725 μm.

4.5.4 Effect of PI3Kinase Inhibition on Lung Branching Morphogenesis

CaR activation has been shown to induce ERK1/2 activation via PI_3K induction in primate OSE cells (Hobson *et al.*, 2003). In order to test the hypothesis that the CaR was mediating its calcimimetic or high Ca^{2+}_o induced suppression on lung branching morphogenesis via activation of PI_3K, a known inhibitor of PI_3K activation, LY294002, was applied to lung explant cultures. Concentrations of both 10 and 20 μM LY294002 have been previously published for use on lung explant cultures (Wang *et al.*, 2005; Metzger *et al.*, 2007). In this study, concentrations of LY294002 from 5 – 25 μM were tested on lung explant cultures. The initial and highest dosage of LY294002 used was 25 μM. While this was not immediately toxic to the lungs, it did seem to be detrimental to their overall health as little branching morphogenesis was achieved and there was a dark, grainy appearance in their luminal area (Fig. 4.13A*ii* and *iv*).

In this single experiment, treatment with 25 μM LY294002 did not enhance branching morphogenesis at 24 h in the presence of 1.05 mM or 1.7 mM Ca^{2+}_o with 21.4±4.5% (n=3) and 23.7±7.1% (n=3) branching increases respectively. After 48 h, branching of explants incubated in 25 μM LY294002 in the presence of 1.05 mM Ca^{2+}_o had increased 38.2±5.9%, while the explants incubated in 25 μM LY294002 and in the presence of 1.7 mM Ca^{2+}_o remained unchanged from their 24 h increase of 23.7±7.1%. Both of these values were not statistically different from the amount of branching produced in the presence of 1.7 mM $[Ca^{2+}]_o$ + 0.1% DMSO, which was, 47.6±6.8% after 48 h ($p=0.38$ for 1.05 mM $[Ca^{2+}]_o$+ 25 μM LY294002 and $p=0.062$ for 1.7 mM $[Ca^{2+}]_o$+ 25 μM LY294002). In comparison, the percent change of branching morphogenesis in the presence of 1.05 mM (n=5) and 1.7 mM Ca^{2+}_o (n=5) containing 0.1% DMSO resulted in an increase in branching of 21.9±4.6% and

12.7±2.7% at 24 h with increases in branching of 98.1±24.5% and 47.6±6.8% after 48 h (Fig. 4.13B).

After the above experiment, lower concentrations of 5 and 12.5 μM LY294002 were used on lung explant cultures. At these concentrations, LY294002 application induced recovery from high Ca^{2+}_o- and calcimimetic- induced depression of branching morphogenesis. Figure 4.14 details the response of lung explant cultures to the application of 5 μM LY294002. There is no significant change in the amount of branching morphogenesis when 5 μM LY294002 is applied to cultures containing 1.05 mM Ca^{2+}_o for 48 h. Indeed, in the presence of 1.05 mM Ca^{2+}_o branching increases were 65.2±8.8% at 24 h and 170.33±23.4% at 48 h (n=3) while branching in the presence of 1.05 mM + 5 μM LY294002 (n=2) resulted in branching increases of 69.8% at 24 h and 131.3% at 48 h.

When 5 μM LY294002 was applied to cultures containing 1.2 mM Ca^{2+}_o + 10 nM R-568 there is a significant rise in the % increase in branch number at 24 h from 8.3±5.5% (1.2 mM + 10 nM R-568, n=3) to 39.8±5.3% (1.2 mM + 10 nM R-568 + 5 μM LY294002, n=4, p=0.01). The increase is maintained at 48 h where branching is increased from 66.1±5.1% to 137.6±14.3% (p=0.009). Lung explant cultures exposed to 1.7 mM Ca^{2+}_o resulted in the expected amount of branching morphogenesis with 9±3.2% at 24 h and 42.5±1.1% at 48 h. Treatment of lungs also grown in the presence of 1.7 mM Ca^{2+}_o, but with 5 μM LY294002 resulted in a robust rescue of the branching inhibition at both 24 h with 42.01±9.1% (n = 6 for both conditions from 2 separate isolations, p=0.007) and at 48 h, with a branching increase of 133.2±22.5% (n=6, p=0.005).

Experiments performed with 12.5 μM LY294002 did not show a concentration-dependent rescue of the branching morphogenesis as did experiments

with varying concentrations of U73122. However, there was still a rescue of branching suppression mediated by both the R-568 calcimimetic and by high (1.7 mM) Ca^{2+}_o (Fig. 4.15). As in the previous experiments, at 48 h there is no significant difference between branching observed in the presence of 1.05 mM Ca^{2+}_o (n=8; 135.2±19.9%) and that observed in the presence of 1.05 mM Ca^{2+}_o + 12.5 μM LY294002 (n=3; 137.9±2.8%). When 30 nM R-568 is added to the culture medium, branching morphogenesis decreases at 24 h from 41.2±7.9% in the presence of 1.05 mM Ca^{2+}_o alone, to 17.6±5.5% (n=7 p=0.03) in the presence of 1.05 mM Ca^{2+}_o + 30 nM R-568. At 48 h there is suppression from 135.2±19.9% in the presence of 1.05 mM Ca^{2+}_o alone, to 76.5±12.7% in the presence of 1.05 mM Ca^{2+}_o+ 30 nM R-568. Branching suppression at both time points is rescued in the presence of 1.05 mM Ca^{2+}_o + 30 nM R-568 + 12.5 μM LY294002, branching increased to 64.2±10.5% (n=7, p=0.001) at 24 h and 124.5±13.7% (p=0.03) at 48 h (Fig. 4.15 A - D and G). High (1.7 mM) Ca^{2+}_o suppression of branching morphogenesis was also abolished by co-incubation with 12.5 μM LY294002. Data pooled from 3 separate isolations (n=7 for each condition) show a rescue of branching rate from 12.9±2.8% to 57.1±5.9% (p=0.0002) at 24 h and from 50.6±5.9% to 139.2±14.7% (p=0.002) at 48 h when in the presence of 1.7 mM Ca^{2+}_o + 12.5 μM LY294002 (Fig. 4.15E, F and G).

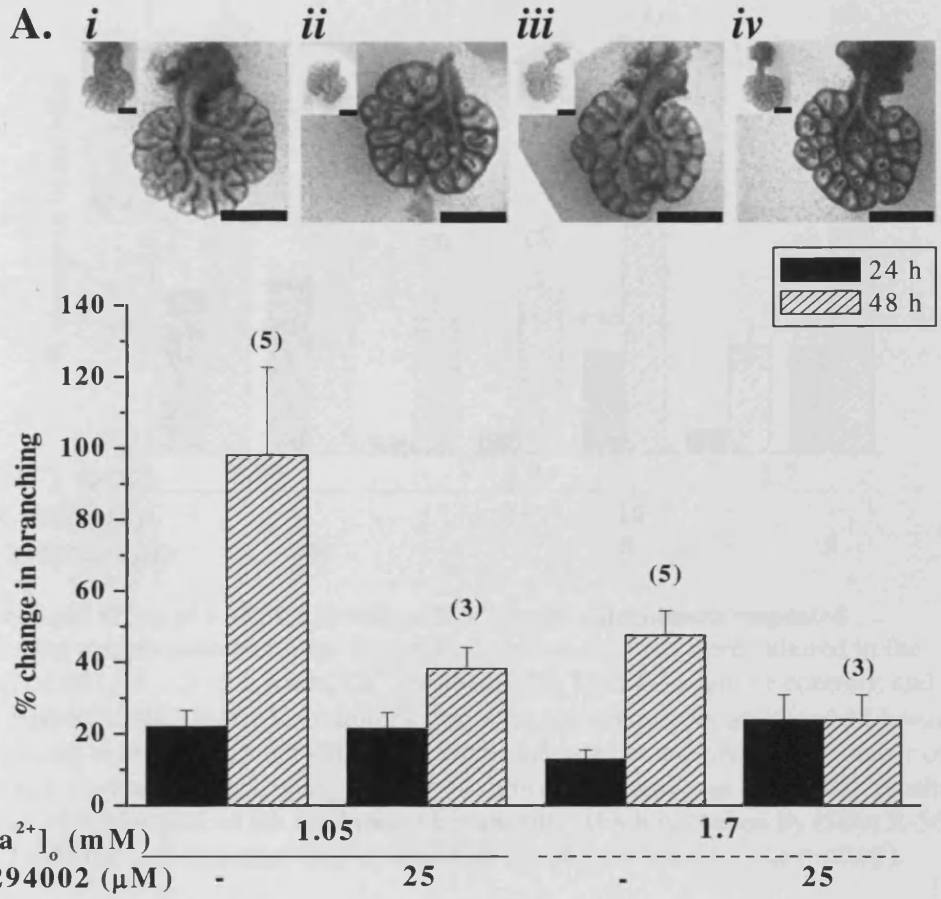

Figure 4.13: Treatment with 25 μM LY294002 does not rescue high $[Ca^{2+}]_o$ suppression of branching morphogenesis. Lungs from E12.5 mouse embryos were cultured in the presence of 1.05 mM Ca^{2+}_o with 0.1% DMSO (negative control); and 1.05 mM Ca^{2+}_o with 25 μM LY294002 (PI_3K inhibitor). **A).** Representative pictures of explants: ***i.*** 1.05 mM Ca^{2+}_o +0.1% DMSO lung after 48 h, ***ii.*** 1.05 mM Ca^{2+}_o with 25μM LY294002 after 48 h, ***iii.*** 1.7 mM Ca^{2+}_o +0.1% DMSO lung after 48 h, ***iv.*** 1.7mM Ca^{2+}_o with 25μM LY294002 after 48 h. Inset pictures show each lung at 0 h (post-dissection) showing a comparable number of initial terminal branches for each condition. **B).** Terminal branch number at 24 and 48 h was normalised to branch number at 0 h and expressed as a percent change in number of branches. Data shown are mean ± s.e.m, n is shown in parentheses above 48 h results. Scale bars = 750 μm.

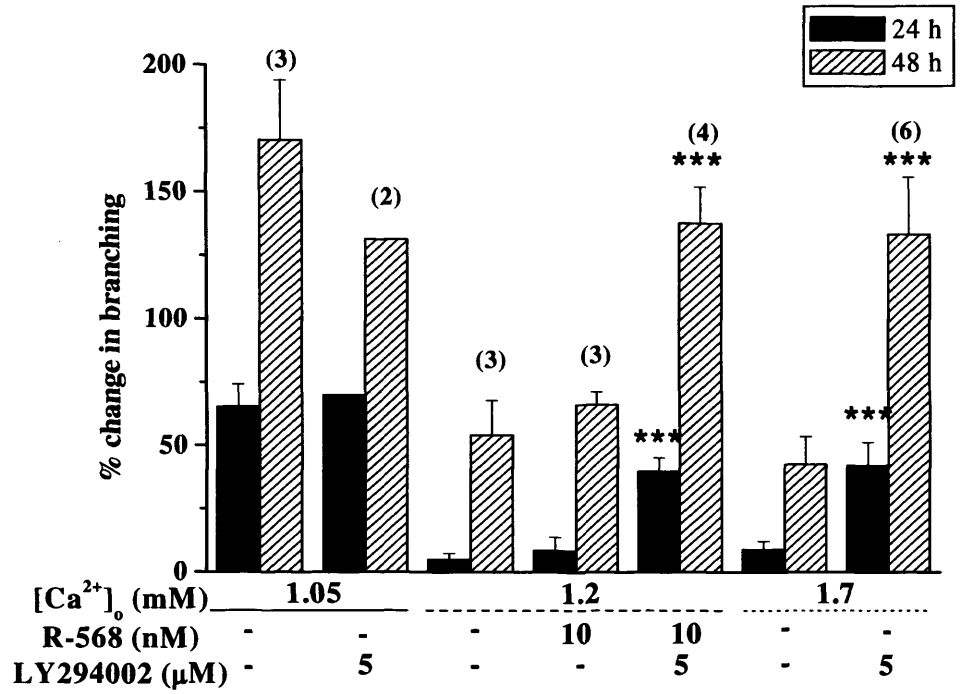

Figure 4.14: Effect of 5 μM LY294002 on $[Ca^{2+}]_o$- and calcimimetic-regulated branching morphogenesis. Lungs from E12.5 mouse embryos were cultured in the presence of 1.05, 1.2 or 1.7 mM $Ca^{2+}{}_o$ with 0.025% DMSO (negative control); and with 5 μM LY294002 (PI_3K inhibitor). Terminal branch number at 24 and 48 h was normalised to branch number at 0 h and expressed as a percent change in number of branches. Data shown as mean ± s.e.m, n is shown in parentheses above 48 h results. Rescue by LY294002 of the inhibition of branching which is evoked by either R-568 or 1.7 mM $Ca^{2+}{}_o$ is indicated in time-matched samples by the asterisks ($p<0.01$).

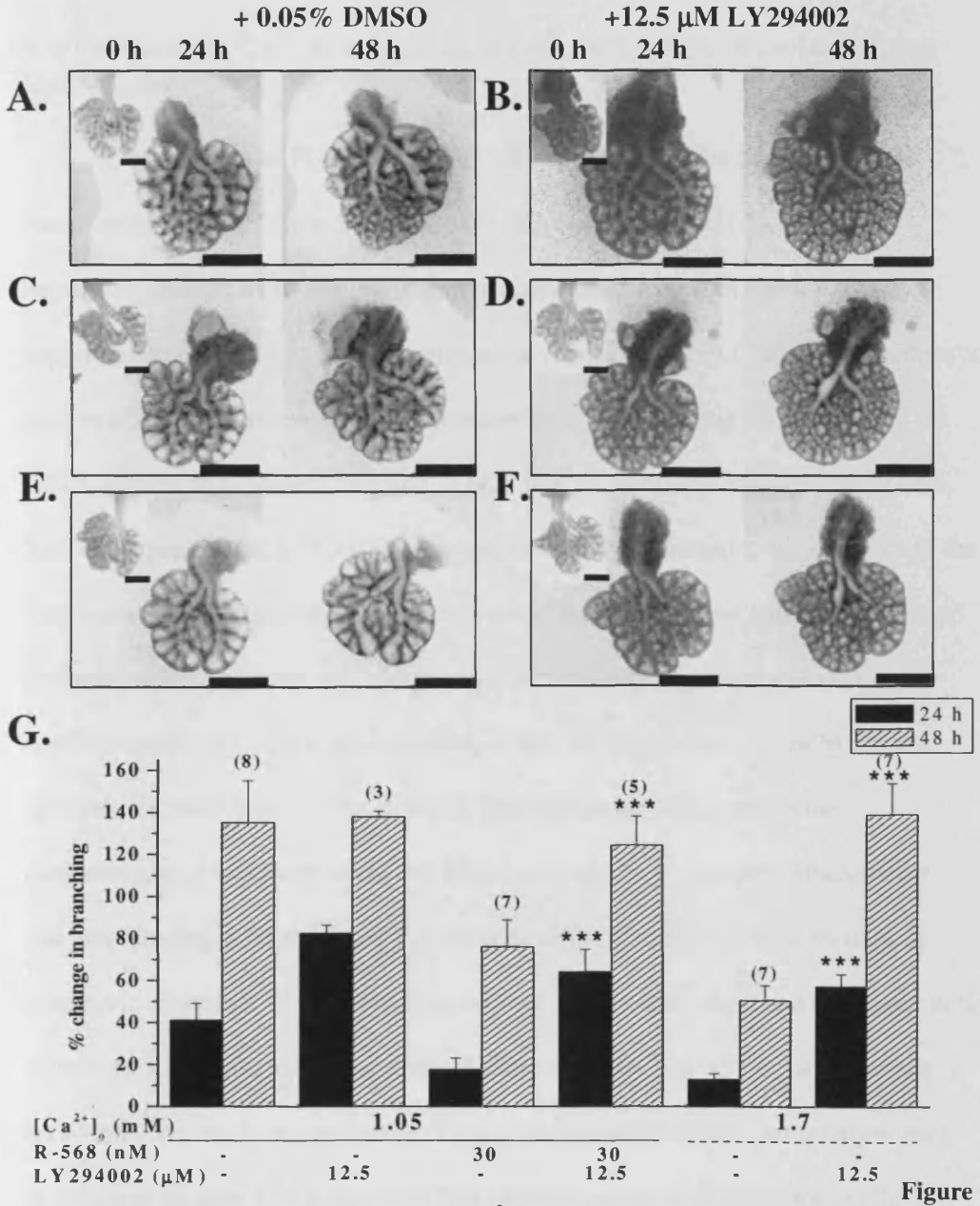

Figure 4.15: Effect of PI3 kinase inhibition on $[Ca^{2+}]_o$- and calcimimetic-regulated branching morphogenesis. Lungs from E12.5 mouse embryos were cultured in the presence of 1.05 or 1.7 mM Ca^{2+}_o with 0.1% DMSO; or with 12.5 μM LY294002. Effect of 1.05 mM (**A**, **B**), 30 nM R-568 (**C**, **D**) and 1.7 mM Ca^{2+}_o (**E**, **F**) in the absence (DMSO vehicle control; **A**, **C**, **E**) or presence (**B**, **D**, **F**) of 12.5 μM of LY294002 (LY), on branching. **G).** Terminal branch number at 24 and 48 h was normalised to branch number at 0 h and expressed as a percent change in number of branches. Data shown are mean ± s.e.m. from 3 separate experiments, n is shown in parentheses above 48 h results. Significant rescue of branching inhibition is indicated in time-matched samples by the asterisks ($p<0.01$). Scale bars = 750 μm.

4.6 Increases in Ca^{2+}_i as a readout of CaR Activation in Isolated Lung Epithelium

Downstream of PLC signalling, CaR activation evokes an increase in $[Ca^{2+}]_i$ due to release of Ca^{2+} from internal stores (Brown *et al.*, 1993). To test the hypothesis that the CaR was mediating its calcimimetic or high Ca^{2+}_o induced suppression on lung branching morphogenesis by initiating PLC signalling pathways and resulting in an increase in $[Ca^{2+}]_i$, ratiometric Ca^{2+} imaging was performed on E12.5 mouse lungs acutely exposed to high $[Ca^{2+}]_o$ and to the calcimimetic R-568. As CaR expression at E12.5 was shown to be mostly restricted to the epithelia of the lung buds (Fig. 3.6) and other studies by our collaborators have shown that isolated epithelial buds are viable and adequate for determining responses to externally applied stimuli (del Moral *et al.*, 2006a), it was decided to use mesenchyme-free epithelia for these studies (Fig. 4.16A). One significant difference in the methodology of this study to the del Moral et al. study, is that the epithelium for calcium imaging were mechanically stripped of their mesenchyme without prior enzymatic digestion. This preparation allowed for the epithelium and the lumen to be visualised by our microscope system on most samples (Fig. 4.16B). Additionally, a small hole was made, using the tip of a pipette normally used in electrophysiology, at an adjoining area of the epithelial bud to allow access of the solutions to the luminal surface of the epithelium. It should be noted that this preparation did not completely remove the smooth muscle cell layer that is closely associated with the lung epithelium (Fig. 4.16C) and therefore most of the lung samples still displayed contractions of the epithelial buds during Ca^{2+}_i recording.

After the lung bud was loaded with Fura – 2AM and mounted on the heated stage of the microscope, perfusion of the preparation was started with a pre-warmed

(32-35°C) physiological solution containing 0.8 mM basal Ca^{2+}_o and allowed to acclimatise under the microscope. When adequate visual resolution was achieved, recording of the epithelial bud began by taking initial readings of the basal Ca^{2+}_i fluorescence for 1 minute. When $[Ca^{2+}]_o$ was increased from 0.8 to 2 mM, isolated epithelia from E12.5 mouse lung explants demonstrated a mean increase in 340:380 ratio of 0.18 ± 0.04. In the presence of 0.8 mM Ca^{2+}_o, 100 nM R-568, evoked a mean increase of 0.090 ± 0.02. At the end of each experiment, as a control for viability of the preparation, isolated epithelial buds were treated with 10 μM carbachol, an activator of muscarinic acetylcholine receptors which have been shown to be expressed in the epithelia of the developing mouse respiratory system (Lammerding-Koppel *et al.*, 1995). When charbachol was applied the mean increase in 340:380 ratio was 0.16 ± 0.02 (Fig. 4.17B, n=6 for all conditions from three separate isolations).

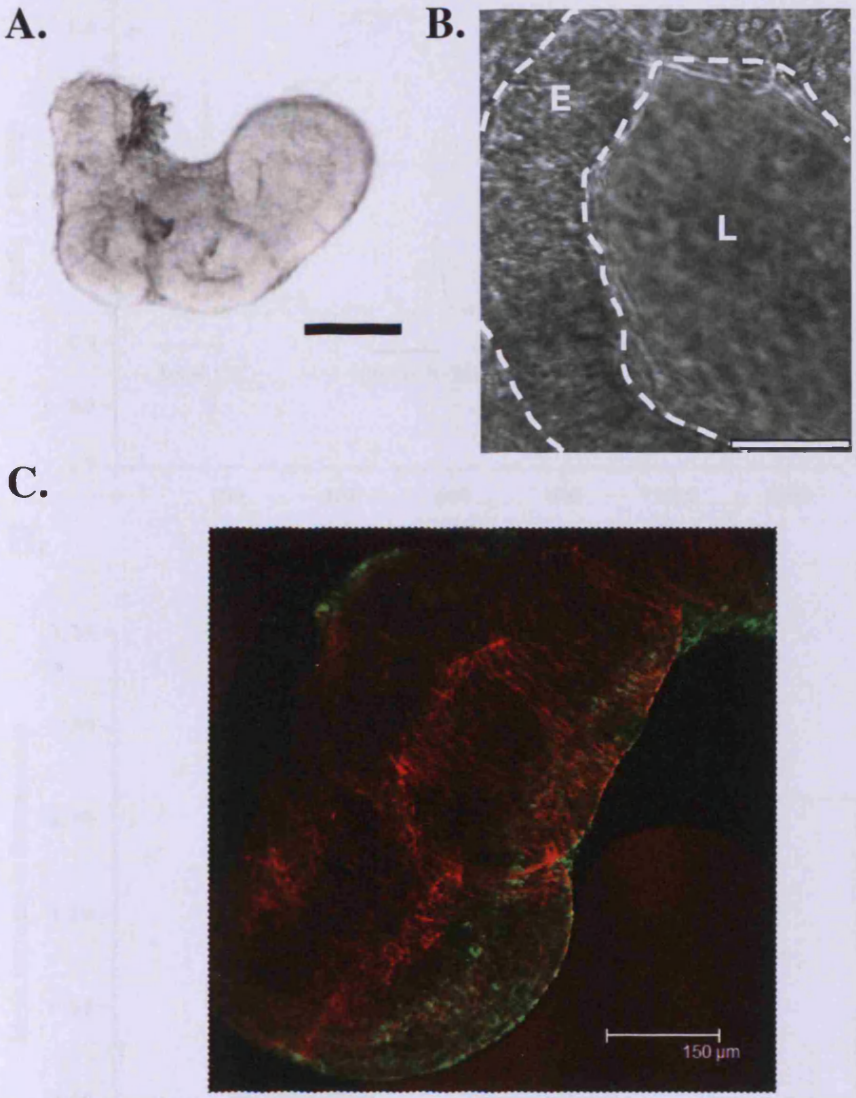

Figure 4.16: Exemplar photos of lung epithelia used in calcium imaging experiments. **A).** Freshly isolated lung epithelial bud, scale bar = 200 µM. **B).** Higher magnification phase contrast image of isolated epithelial bud after 24 h in culture. E designates the epithelium and L designates the lumen. Scale bar = 50 µM. **C).** Smooth muscle cells (anti- smooth muscle actin, 1:200 dilution, red) are not removed by mechanical dissection of the mesenchyme and remain closely associated with the basement membrane of the epithelium (anti-laminin, 1:200 dilution, green). Scale bar = 150 µm.

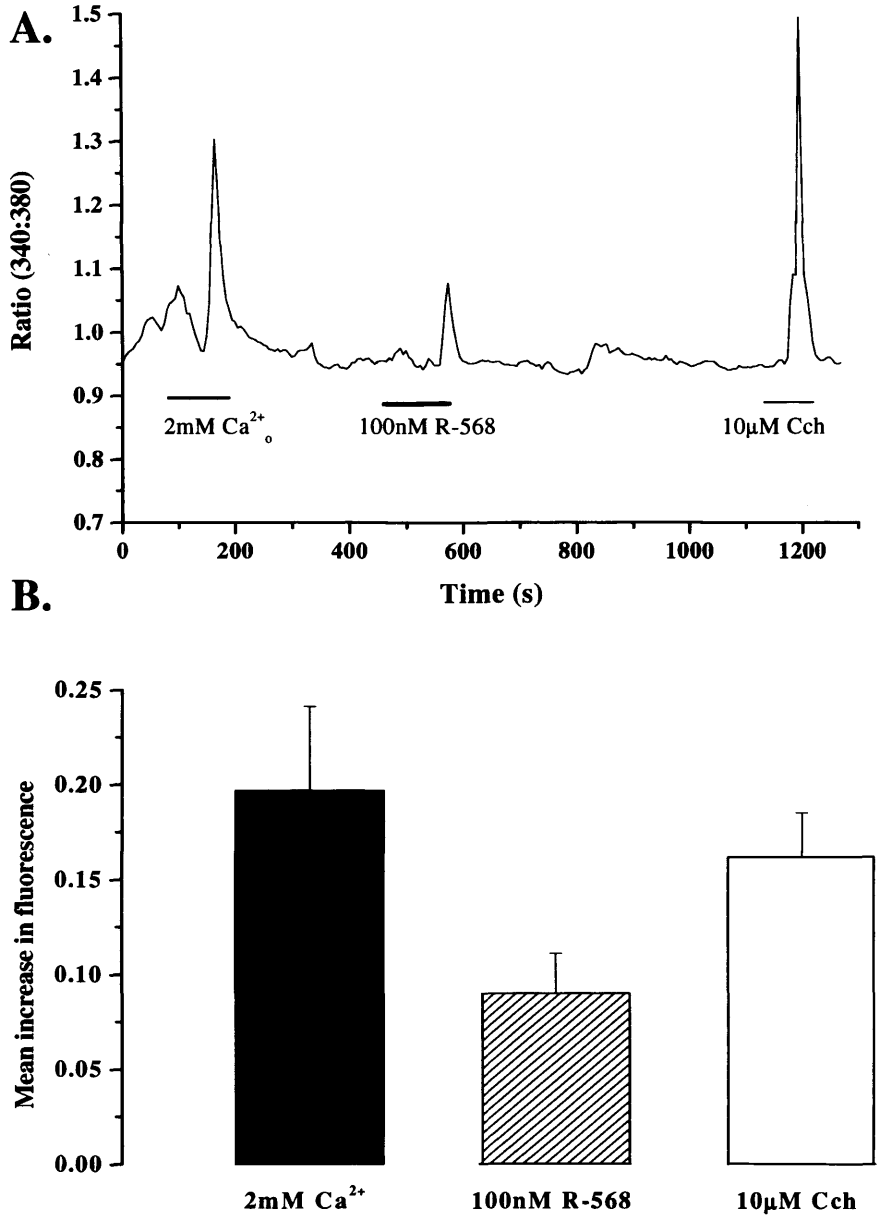

Figure 4.17: Effect of CaR activators on $[Ca^{2+}]_i$ signalling. A). Representative Fura-2 trace of epithelial buds loaded with the calcium-sensitive fluorescent dye after exposure to CaR activators showing that CaR-expressing epithelial cells exhibit rapid and transient increase in $[Ca^{2+}]_i$ (340:380 fura-2 fluorescence ratio) to acute (1-3 min) stimulation with Ca^{2+}_o (2 mM), and with the calcimimetic compound R-568 (100 nM). Carbachol treatment (Cch, 10 μM) confirms cell viability at the end of the experiment. **B).** Mean increase in fura-2 fluorescence ratio (6 epithelial buds from three separate isolations in three different days of experimentation). Only epithelial preparations that responded to the final carbachol stimulation have been considered.

4.7 Chapter Discussion

The purpose of this chapter was to elucidate the mechanism of action by which $[Ca^{2+}]_o$ exerts it effects on the branching morphogenesis programme of the lung and to test specifically the hypothesis that CaR activation was involved in this process. Results in Chapter 2 showed that lung branching morphogenesis is sensitive to changes in $[Ca^{2+}]_o$ and Chapter 3 showed that CaR is present in the lung across the pseudoglandular stage of lung development, when the majority of branching morphogenesis takes place, E10.5 – E16.5. The results in this chapter show that, by specifically activating the CaR using the calcimimetic R-568 in lung explant cultures, the branching suppression generally produced by high $[Ca^{2+}]_o$ can be recapitulated in the presence of low $[Ca^{2+}]_o$, that TPD increase is mediated by CaR activation, and that CaR activation potentially mediates its effects through activation of PLC and PI_3K (Fig. 4.20).

The main pharmacological tools for determining the function of the CaR are the calcimimetics, specific positive allosteric modulators of the CaR which shift the concentration response curve for $Ca^{2+}{}_o$ to the left (i.e. lower concentrations of classic agonists are needed to instigate signalling; see Section 1.5.2 for review). Most importantly, these compounds are specific for the CaR as the application of NPS-R-467 and Amgen R-568, at the concentrations used in this study, does not affect other GPCRs when they are expressed in HEK293 cells (Nemeth *et al.*, 1998).

Concentration response studies with R-568 revealed that the concentration required for effective suppression of branching morphogenesis was much lower than that needed when using NPS-R-467. This is in agreement with previously published data showing that R-568 is approximately twice as potent as NPS-R-467 (Nemeth *et al.*,

1998). Therefore, subsequent experiments only used R-568, as the supply of this compound was not rate-limiting. In TPD recording experiments, there was a link between increased secretion and activation of the CaR. That there is a link between CaR activation and Cl^- secretion is unsurprising, as a previously published report has shown that CaR activation can affect both the expression and current amplitude of volume-sensitive outwardly rectifying (VSOR) Cl^- channels in an intestinal epithelial cell line, Intestine 407 (Shimizu *et al.*, 2000).

In my hands, the use of alternative membrane-impermeant CaR agonists, the aminoglycoside antibiotics neomycin and gentamicin, did not affect the branching morphogenesis programme of the lung explant cultures at any concentration tested. This lack of affect could be ascribed to the phenotypic pharmacology displayed by the CaR. A similar lack of response of the CaR to neomycin has been reported in cultured human aortic endothelial cells (Ziegelstein *et al.*, 2006). It is possible that these antibiotics induce some CaR mediated signalling, but that this does not have an effect on the branching morphogenesis readout which I am using.

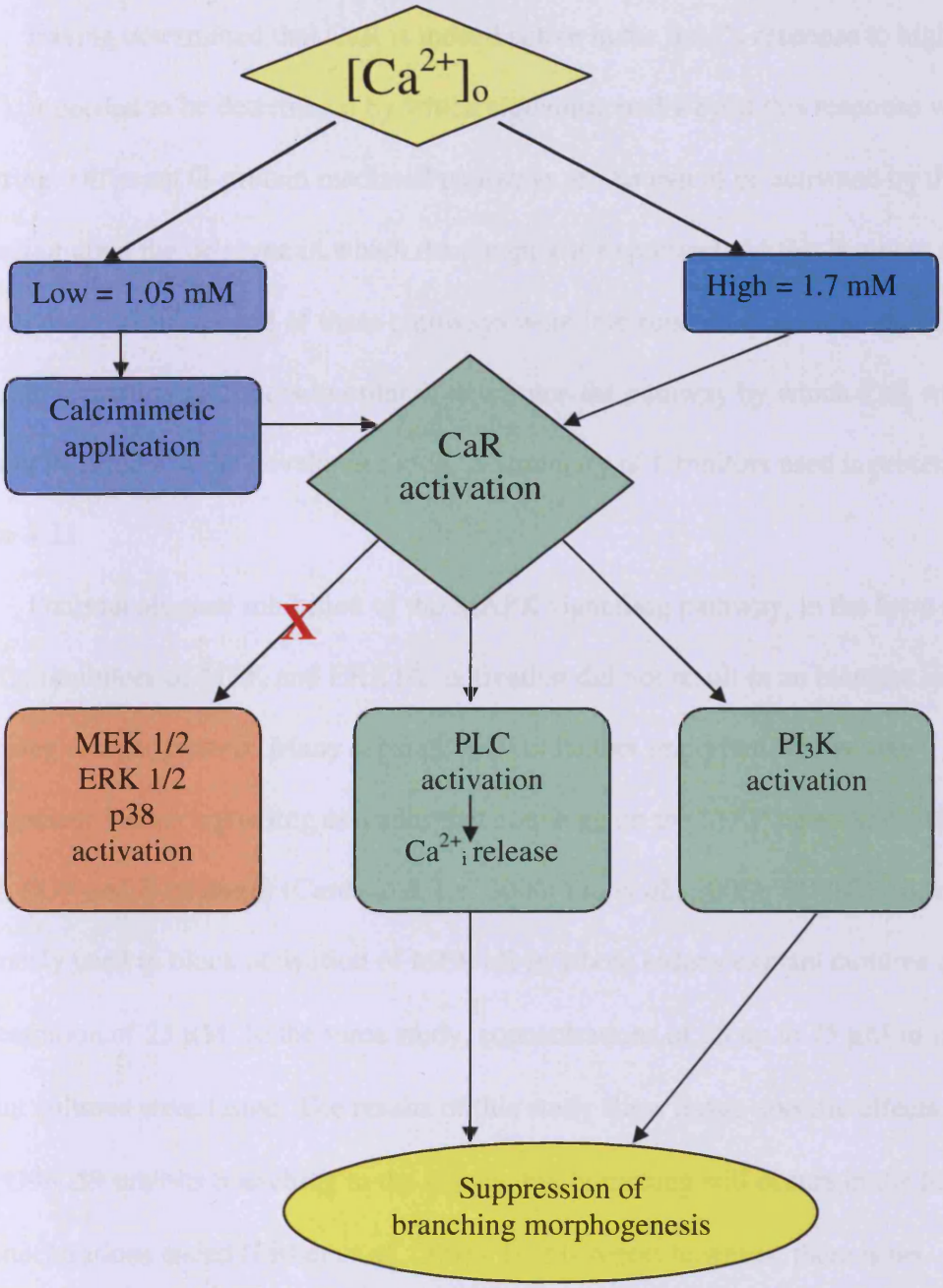

Figure 4.20: Diagrammatic summary of Chapter 4 results. High $[Ca^{2+}]_o$, or low $[Ca^{2+}]_o$ with the addition of calcimimetics, induces CaR activation in lung explant cultures. This activation results in the downstream activation of PLC, with resultant increases in $[Ca^{2+}]_i$, PI_3K activation and suppression of branching morphogenesis. In these conditions, CaR activation does not appear induce the MEK1/2, ERK1/2 or p38 activation.

Having determined that CaR is indeed active in the lung's response to high $[Ca^{2+}]_o$ it needed to be determined by which signalling pathway(s) this response was occurring. Different G-protein mediated pathways are known to be activated by the CaR depending upon the cell type in which the receptor is expressed. As this is a new system for CaR expression, several of these pathways were interrupted using commercially available signalling inhibitors in order to determine the pathway by which CaR was exerting its effects in the developing lung. A summary of inhibitors used is presented in Figure 4.21.

Pharmacological inhibition of the MAPK signalling pathway, in the form of specific inhibitors of MEK and ERK1/2, activation did not result in an increase in branching morphogenesis. Many separate growth factors important within lung development induce signalling cascades that converge on the MAP kinases including FGFs, EGF and E-cadherin (Cardoso & Lu, 2006; Liu *et al.*, 2008). PD98059 has been previously used to block activation of MEK1/2 in whole kidney explant cultures at a concentration of 25 μM. In the same study, concentrations of 25 up to 75 μM in lung explant cultures were tested. The results of this study show tissue-specific effects, 25 μM PD98059 inhibits branching in the kidney, but branching still occurs in the lung at all concentrations tested (Fisher *et al.*, 2001). In this report however, there is no quantification of the rate or amount of branching that occurs in the absence of PD98059 application. Therefore it is possible that an inhibition of the default branching rate in the group's standard culture medium was overlooked. Since minimal branching did still occur at the concentrations I tested, it might be assumed that the branching observed by Fisher *et al.* (2001) was at a similar level.

In the context of branching morphogenesis, the results obtained from application of U0126 were much the same as Kling *et al.* (2002), where it was used on E13 rat lung explants at a concentration of 20 μM. Similar to my results, U0126 treatment diminished branching morphogenesis. This group determined that the suppression of branching morphogenesis was due to ERK1/2 inhibition decreasing proliferation, and inducing mesenchymal apoptosis (Kling *et al.*, 2002). Something much the same could be occurring in the lung explants treated with U0126 in this study.

There does appear to be a differential type of morphological presentation when treating lung explants with PD98059 and U0126, which was unexpected due to the fact that they both target the same signalling pathway. Lungs treated with U0126 have a higher inhibition of branching morphogenesis and qualitative changes in the presentation of their mesenchyme after 48 h. This differential morphology could be due to the concentrations at which these inhibitors were used in the current study as both PD98059 and U0126 can also inhibit ERK5 (Mody *et al.*, 2001). In the current study, PD98059 was used below the concentration at which it inhibits ERK5 activation (100μM) and U0126 was used at a concentration which would completely inhibit ERK5 (20 and 30 μM).

The last MAP kinase inhibitor used was BIRB 796, an inhibitor of p38 (Bagley *et al.*, 2006). My results showing that p38 inhibition slightly increases the branching inhibition of 1.7 mM Ca^{2+}_o are supported by a previously published report using a different p38 inhibitor, SB203580. Application of 10 μM SB203580 significantly impairs branching morphogenesis by impairing cell-cell interactions (Liu *et al.*, 2008).

Therefore, taking into consideration the results using PD98059, U0126 and BIRB 796, CaR activation is not exerting its effects via MEK-ERK1/2 or p38 activation.

Blocking PLC signalling using U73122 on lung explants rescued the suppression of branching morphogenesis by high $[Ca^{2+}]_o$ back to and above levels seen in the presence of 1.05 mM Ca^{2+}_o. U73122 is a widely used inhibitor of PLC activity, repetitively used for determining if CaR activation results in PLC activity and the downstream effects of this for the cell (Ward, 2004).

Unexpectedly, although sold as an inactive compound for use as a negative control along side of U73122; U73343 has lethal effects on lung explant cultures. The differential effects seen in treating lungs with these compounds could be the result of differential activities of the compounds due to the complexity of the system in which they are applied. There is some precedent for U73343 having a non-PLC related effect. When applied to isolated pyramidal cells expressing G-protein activated inwardly rectifying K^+ (GIRK) channels, U73122 inhibited PLC but also suppressed channel activity. In the same system, application of U73343 did not inhibit PLC but was even more effective at blocking GIRK channel activity than U73122 (Sickmann *et al.*, 2008).

Another possibility is that the toxicity of U73343 is a non-specific effect due to impurities present in the preparation purchased. The U73343 supplied by Sigma-Aldrich is reported to be $\geq$ 90% pure, where as the U73122 is $\geq$98% pure. In the 10% of the U73343 preparation unaccounted for there could be a toxic by-product that is producing the effect seen. However, the rescue of branching morphogenesis seen when U73122 is applied does not appear to mediated by the DMSO in which it is dissolved, therefore the effect is most likely due to the inhibition of PLC signalling.

The activation of PI_3K is another CaR associated signalling pathway which appears to be intimately connected with the CaR mediated suppression of branching morphogenesis. LY294002 has been shown to inhibit casein kinase 2 to a similar extent as PI_3K (Davies *et al.*, 2000) and a second inhibitor of PI_3K, wortmannin, has not been used. Therefore, it is not possible to definitively state the involvement of PI_3K in CaR – mediated suppression of branching morphogenesis. However, the use of LY294002 rescued both high $[Ca^{2+}]_o$ and calcimimetic induced suppression of branching morphogenesis. As PI_3K inhibition is the most commonly reported affect of LY294002 application, these results imply that the activation of PI_3K was induced by CaR activation.

Not only do the results in this Chapter show the potential involvement of PLC and PI_3K, $Ca^{2+}{}_i$- imaging experiments performed here showed transient activation of $Ca^{2+}{}_i$ in response to both $Ca^{2+}{}_o$ and R-568. Results produced by performing ratiometric imaging of $Ca^{2+}{}_i$ release in epithelial buds were much in line with a previous study showing that $[Ca^{2+}]_o$ similar to that used in my experiments (0.8 – 2 mM) resulted in transient, small, nanomolar $[Ca^{2+}]_i$ increases. Additionally, in the dispersed bovine parathyroid cells used for that study, the EC_{50} of $Ca^{2+}{}_o$ which increases $[Ca^{2+}]_i$ was 1.66±0.34 mM and when 100 nM R-568 was added this decreased to 0.61±0.04 mM, values that are in line with the results in Section 4.7 (Nemeth *et al.*, 1998).

While the specific effect of smooth muscle on the response was not investigated in this study, it could be argued that, in this preparation smooth muscle cells are not removed from interacting with the epithelium. Therefore, any response to $Ca^{2+}{}_o$ and R-568 recorded could be due to $Ca^{2+}{}_o$ influx from outside of the smooth muscle cell. This

is a possibility however, I would argue that R-568 is a membrane- impermeant agonist and therefore must interact with a receptor at the cellular membrane in order to exert its effects. Additionally, this compound requires the presence of a type 1 calcimimetic (Ca^{2+}_o etc.) to produce any signal within the cell by CaR (McLarnon & Riccardi, 2002) and therefore cannot be acting independently especially at the relatively low concentration used in this study (100 nM).

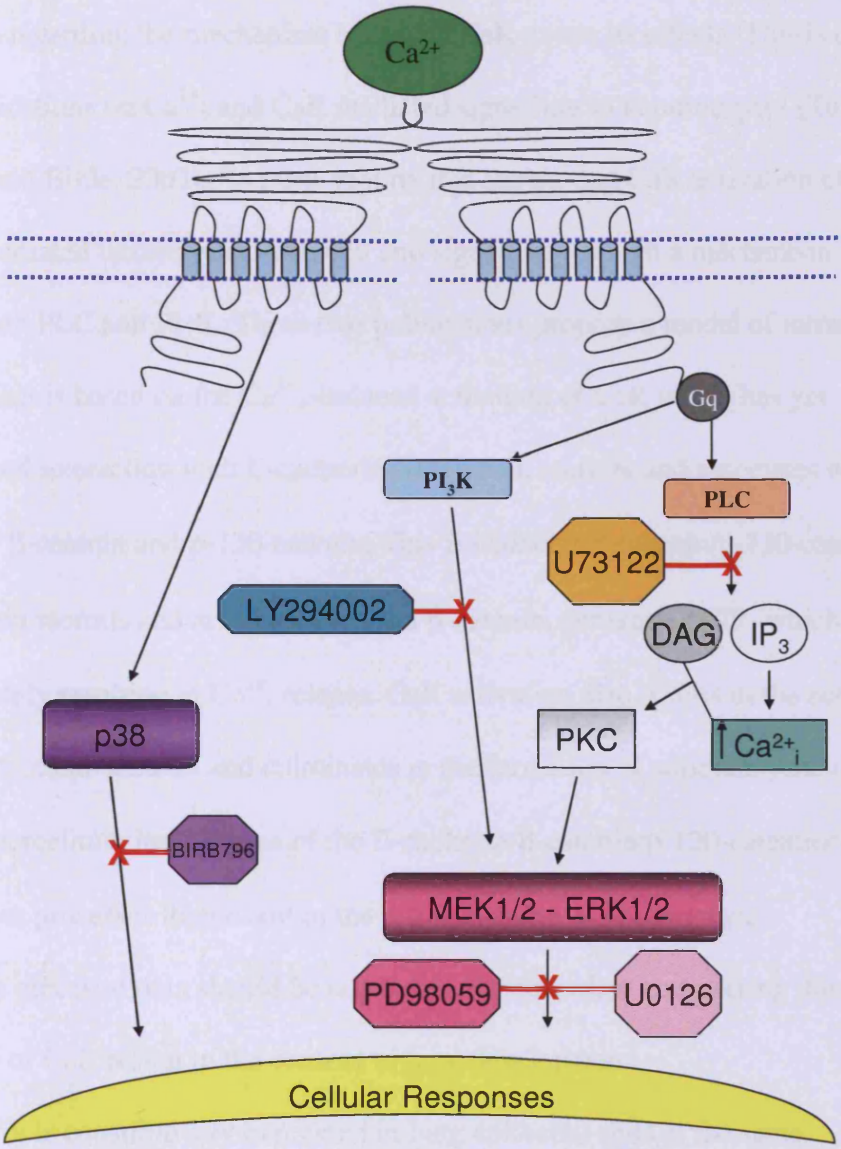

Figure 4.21 Diagrammatic summary of the signalling pathways inhibited in lung explant cultures. The CaR is known to activate several different signalling pathways dependent upon the cell type in which it is expressed. G_q-mediated PLC activation was inhibited using U73122. G_q-mediated PI_3K signalling was inhibited using LY294002. MEK1/2 and ERK1/2 activation were inhibited by PD98059 and U0126, while p38 activation was blocked by BIRB 796.

The likely involvement of both PLC and PI_3K with the attendant Ca^{2+}_i increases in the CaR mediated effects on branching morphogenesis provides a candidate route for speculation regarding the mechanism by which CaR exerts its effects. This is due to recent publications on Ca^{2+}_o and CaR mediated signalling in keratinocytes (Tu et al., 2008; Xie and Bikle, 2007). In these reports it is shown that CaR activation effects E-cadherin mediated intracellular adhesion and signalling through a mechanism which involves both PLC and PI_3K. These two publications propose a model of intracellular signalling that is based on the Ca^{2+}_o-induced activation of CaR which has yet undetermined interaction with E-cadherin which then recruits and associates with a complex of β-catenin and p-120-catenin. This E-cadherin/β-catenin/p-120-catenin complex then recruits and activates PI_3K via β-catenin, generating PIP_3 which activates PLC ultimately resulting in Ca^{2+}_i release. CaR activation also results in the activation of Src family tyrosine kinases and culminates in the formation of adherens junctions reliant upon the intercellular interactions of the E-cadherin/β-catenin/p-120-catenin complex. Both of these processes then result in the differentiation of keratinocytes.

Five pieces of data should be taken into account when considering this possible mechanism of CaR action in the context of lung development:

1. E-cadherin is constitutively expressed in lung epithelial cells at the same developmental time point as CaR (Hirai *et al.*, 1989), this is also shown in Chapter 6 of this report;

2. application of active antibodies to perturb E-cadherin activity results in disrupted morphogenesis with deformed tubules (limited luminal space) most likely resulting from the reduced efficacy of intracellular connection (Hirai *et al.*, 1989);

3. ectopic over-expression of E-cadherin in isolated epithelial cultures impairs branching (Liu *et al.*, 2008) and results in large cyst-like epithelial cultures;

4. CaR activation in keratinocytes is related to E-cadherin mediated PI_3K-PLC activation (Tu *et al.*, 2008);

5. rescue of high Ca^{2+}_o branching morphogenesis suppression can be promoted by the inhibition of both PLC and PI_3K.

In the light of those pieces of data it is possible that CaR is mediating its effects in a similar fashion to that which occurs in keratinocytes; although in order to definitively elucidate the role of the CaR in lung development it would be useful to investigate how the lung develops in its absence. Experiments attempting this are the subject of the next chapter.

CHAPTER 5:
THE EFFECTS OF CALCIUM-SENSING RECEPTOR ABLATION ON LUNG DEVELOPMENT

5.1 Methods

5.1.1 Addition of CaR-specific Oligodeoxynucleotides (ODNs) to Lung Cultures

In order to reduce expression of the CaR in cultured lungs, previously described ODNs against the CaR (Ritchie *et al.*, 2001) were added to the culture medium to a final concentration of 50μM and left for 48h, as per section 2.1. The antisense sequence was designed to bind specifically to the complementary CaR mRNA, which in turn impairs the expression of native CaR protein. As controls, both sense and missense sequences were used to show that application of the ODNs did not impact on the responses of the lung explant cultures. The missense sequence was designed to have no homology to any known sequence in the mouse, but contained the same nucleotide components of the antisense sequence in a scrambled order. All of these ODNs were phosphorothiolated at the 3'- end to ensure their stability in the culture medium.

Antisense ODN sequence; 5'-CCATGCCATGGCTCTGCCTTCTC;

Sense sequence; 5'- GAGAAGGCAGAGCCATGGCATGG;

Missense ODN sequence 5'- CTCCGATCCCATTTCGGTCCGCT.

5.1.2 Genotyping CaR Knockout Mice

Mice heterozygous for CaR deletion on a C57/BL6J background strain were maintained in conventional housing, climate controlled environment with a laboratory diet. Ear biopsy of mice provided tissue to be used for the genotyping adult and weanling animals. DNA for genotyping embryos was isolated from limb tissue taken at the time of dissection. DNA isolation was performed using either a

Wizard SV Genomic DNA isolation system (Promega, Southhampton, UK) or a DirectPCR DNA extraction system (Viagen Biotech, Los Angeles, CA, USA).

Isolated DNA was used in two separate PCR reactions. The reaction using the CaR6HF and CaR6HR primers resulted in a ~215 bp amplicon demonstrating the presence of the wild-type (WT) CaR gene. The other set of primers, CaR6HR and Neo, resulted in a ~280 bp amplicon that indicated the presence of the neomycin resistance cassette (NEO) used to produce the CaR knockout.

The PCR primer sequences are as follows:

CaR6HF –5' -TCTGTTCTCTTTAGGTCCTGAAACA

CaR6HR –5' –TCATTGATGAACAGTCTTTCTCCCT

Neo - 5' –TCTTGATTCCCACTTTGTGGTTCTA

PCR reactions were performed with BioTaq (Bioline, London, UK), in a reaction mix containing 2 mM Mg^{2+}as specified by the manufacturer. Reactions containing 1 µl genomic DNA, extracted as above, were subjected to the following PCR regime: 95°C x 5 min; 95°C x 30 s, 55°C x 30 s, 72°C x 1 min repeated for 35 cycles; 72°C x 8 min. Resultant PCR products were separated by electrophoresis using a 2% agarose gel. Wild-type mice (WT) were designated by the presence of the WT band alone, heterozygous mice (HET) produced both the WT and NEO bands, and homozygous null mice (NULL) produced only the NEO band (Fig. 5.1). In order to confirm the identity of the resultant PCR products, individual bands were cut from the agarose gel and purified using a gel extraction kit (Qiagen, Crawley, UK) according to the manufacturer's instructions. Purified PCR products were sequenced by Cogenics (Essex, ,UK) and resultant sequences are shown in Appendix C.

5.1.3 Calculation of Lung:Body Weight Ratio

After removal from the uterus, embryos at various developmental stages were placed into individual wells of a multi-well tissue culture dish. Embryos were weighed in a Petri dish on a Sartorius Series balance (d = 1mg, Acculab, Epsom, Surrey, UK) and then humanely sacrificed. Tissue was then collected for genotyping and the heart and lungs dissected *en-bloc* from the chest cavity. The heart and associated blood vessels were carefully removed from the lungs which were then weighed on either the Sartorius balance (for embryos >E14.5) or B1204 balance (for embryos $\leq$ E14.5; d = 0.1mg, Analytical Products, Oxford, UK). Lung:body weight ratio was calculated as the wet weight of the lungs divided by the wet weight of the freshly isolated embryo.

5.1.4 Lung Explant Cultures

Lungs were dissected and cultured as described in Section 2.1.1 and cultured in the presence or absence of the calcimimetic R-568 as per Section 4.1.1. Lungs from the entire litter were exposed to the same $[Ca^{2+}]_o$, as genotypes were not revealed until the end of the study, to reduce experimenter bias. Lungs to be used for RNA isolation were immersed in RNAlater (Sigma-Aldrich, UK) and frozen at -20°C until a sufficient number was gathered for isolation.

5.1.5 Immunohistochemistry

Immunohistochemical detection and quantification of proliferating and apoptotic cells in CaR WT, HET and NULL lungs was performed as in Section 2.1.3.

5.1.6 Optimisation of PCR for the detection of CaR Splice Variant Expression

As it has been reported that certain tissues of the current mouse model of CaR knockout express a functionally active, exon-5- less splice variant of the CaR, lung samples used for explant cultures were collected to determine its expression in this system. RNA was isolated from pooled lung and kidney samples using RNeasy Mini-Prep kits (Qiagen,Crawley, West Sussex, UK) according to manufacturer's instructions. Reverse transcription was performed with either Stratascript QPCR cDNA synthesis kit (Stratagene, CA, USA) or BioScript One-step RT-PCR kit (Bioline, London, UK). PCR primers previously used in WT samples for the detection of CaR RNA can also be used to detect the exon-5-less splice variant of the CaR, as they span the sequence which is deleted in the splice variant (Fig 5.2A; See Section 3.1.1 for primer sequences).

PCR reactions were performed with Velocity Taq polymerase (Bioline, London, UK) in a reaction mix specified by the manufacturer. Annealing temperature and Mg^{2+} concentration gradients were performed with RNA from kidney samples to determine the best conditions for the clearest amplification of desired bands. Other reaction temperatures were as specified for the Velocity taq polymerase and all reactions were carried out for a total of 35 cycles. Two amplicon sizes were possible; 584 bp for the full-length CaR and 354 bp for the splice variant CaR (Fig. 5.2B). After amplification the resulting products were separated on a 2% agarose gel by electrophoresis along with Hyperladder IV (Bioline, London, UK) as molecular weight markers for size comparison.

To confirm the presence of *bona fide* full-length and splice-variant CaR transcripts, amplicon bands of each size were cut from the agarose gel and purified using a Gel Extraction kit (Qiagen, Crawley, UK) according to manufacturer's

instructions. This DNA was then sub-cloned into a pGEM vector (Promega, Southhampton, UK) and used to transform Alpha-select competent bacterial cells (Bioline, London, UK). Cells which incorporated the vector and produced colonies on ampicillin containing agar plates were grown overnight in LB medium (Sigma-Aldrich, Dorset, UK). DNA was isolated from the bacterial cultures using a QIAprep spin mini-prep kit (Qiagen, Crawley, UK) according to manufacturer's instructions. This DNA was then sent to Cogenics (Essex, UK) for sequencing. The sequencing results are presented in Appendix C.

5.1.7 Statistics

Graphic representations and statistics of the data were prepared with Origin 7 software. Data are presented as the mean (from multiple pooled experiments where indicated) ± s.e.m. Significance was determined using one-way ANOVA with Tukey *post-hoc* test and a p-value of ≤ 0.05 was deemed significant.

5.2 Philosophy of Work

The previous chapters have shown that the CaR was expressed in lung explant cultures and that activation of the receptor using Ca^{2+}_o and calcimimetic suppressed branching via a mechanism involving PLC and PI_3K. Experiments in this chapter were designed to test the hypothesis that, by abrogating CaR expression, the CaR-mediated suppression of lung branching morphogenesis would no longer occur. Any resultant changes would inform further on the role that the CaR may be playing in lung development and its modes of action. Two different approaches to abrogate CaR expression were used in this chapter;

1. Application of CaR specific ODNs to reduce/ inhibit functionality of the native CaR in WT lung cultures;

2. Lung explant cultures from CaR knockout mice where there is no endogenous expression of the full-length CaR transcript.

Due to the maintained responsiveness of the lung explant cultures of CaR knockout mice to Ca^{2+}_o and calcimimetic, a PCR reaction to detect the expression of the exon-5-less splice variant of the CaR was optimised and employed. Furthermore, as a lung phenotype has never been investigated in embryonic CaR knockout mice, lung and body weight of embryos were measured to detect any gross physical differences between the genotypes. The amount of proliferation and apoptosis occurring at different stages of development and in response to culture in 1.7 mM Ca^{2+}_o was also investigated to characterize any potential phenotypic differences underpinning the different genotypes.

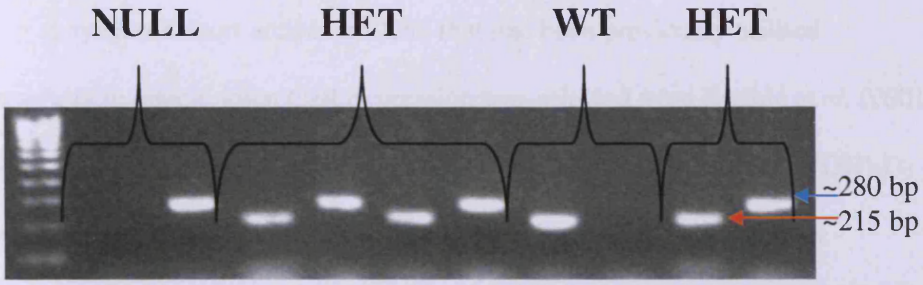

Figure 5.1: Exemplar CaR mouse genotyping results. After PCR reaction, 10 µl of PCR product was mixed with 5x loading buffer and electrophoresed on a 2% agarose gel. Resultant bands were visualised on a UV light box and photographed. Genotypes were recognised as indicated above. Molecular weight markers of 100 – 1000 bp in 100 bp increments are shown in the first lane on the left.

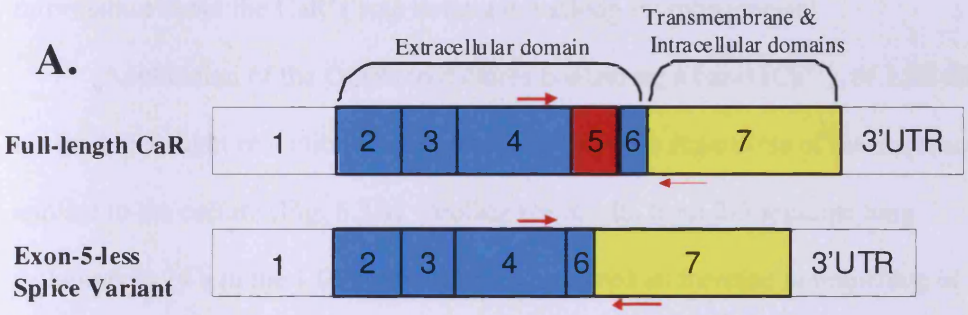

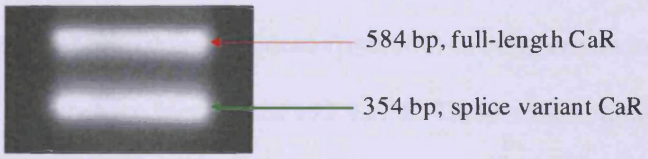

Figure 5.2: Schematic representation of full-length and splice variant isoforms of the CaR with primer placement and exemplar PCR products. A). Schematic diagram of both the full-length CaR and the exon-5-less splice variant CaR. Exon-5 is highlighted in red and primer locations are indicated with the red arrows. Exon 1 is a non-coding exon, exons 2-6 form the extracellular domain of the protein and exon 7 comprises the transmembrane and intracellular domains of the CaR protein. **B).** Exemplar PCR products at expected sizes amplified from adult heterozygous kidney RNA. (Figure adapted with permission from Dr.Thomas Vizard.)

5.3 ODN Treatment of Lung Explant Cultures

A synthetic short antisense ODN that had been previously utilised successfully to knock down CaR expression was selected from Ritchie *et al.* (2001). As a functional readout, the authors measured the effect of Ca^{2+}_o on $1,25(OH)_2D_3$ – responsive Mg^{2+} entry in mouse distal convoluted tubule cells, which was diminished by application of the CaR antisense ODN (Ritchie *et al.*, 2001). As this ODN should inhibit any endogenous expression of the CaR in embryonic lungs, experiments treating the lung explants in culture could provide more detailed information about the CaR's role in lung branching morphogenesis.

Application of the ODNs to cultures containing a basal $[Ca^{2+}]_o$ of 1.05 mM resulted in a slight reduction of the branching response regardless of the sequence applied to the culture (Fig. 5.3A). Pooling the results from 2-3 separate lung isolations at 24 h in the 1.05 mM control, I observed an increase in branching of 38.1±5.6% (n=12). When sense (n=9), missense (n=6) or antisense (n=9) ODNs were added to the culture, the branching response decreased to 22±6.5%, 20.6±5.6% and 9.8±3.2% respectively. After 48 h all cultures containing ODN's had a significantly decreased branching response ($p \leq 0.004$) in comparison to 1.05 mM Ca^{2+}_o which had a branching increase of 127.9±7%. These values, although different from the 1.05 mM Ca^{2+}_o culture, were not significantly different from each other, with sense cultures increasing to 86.3±7.3%, missense cultures increasing to 92.8±3.3% and antisense cultures increasing to 78.8±5.5% ($p \geq 0.08$). In a single experiment (n=4 for each condition) where ODNs were added to cultures containing 1.7 mM Ca^{2+}_o, there was only one significant change in the branching response from the 16.5±3.1% at 24 h and 53.3±5.9% at 48 h of the 1.7 mM Ca^{2+}_o control (Fig.

5.3B). There was a significant decrease in the amount of branching morphogenesis after 24 h where antisense ODNs had been applied, with a small branching increase of 3.3±3.3% (p=0.03) however this significant reduction was abolished by 48 h when the explants had an increase in branching morphogenesis of 63.1±11.2% (p=0.5). The sense ODN cultures had increases of 7.9±2.9% (p=0.09) at 24 h and 59.2±4.9% (p=0.5) at 48 h; missense ODN cultures had increases of 5±5% (p=0.1) at 24 h and 59.1±5.5% (p=0.5) at 48 h none of these values were significantly different from 1.7 mM Ca^{2+}_o control culture values. Although the level of branching morphogenesis in the antisense ODN culture was significantly different from the 1.7 mM Ca^{2+}_o control culture at 24 h, it was not significantly different from the levels of branching morphogenesis in either the sense or missense ODN containing cultures at either time point (p=0.7 at 24 h and p=0.9 at 48 h). These results indicate that any changes in the branching response of cultures where ODNs have been applied are due to an ODN treatment effect, not due to the specificity or binding of the ODN to the target CaR sequence.

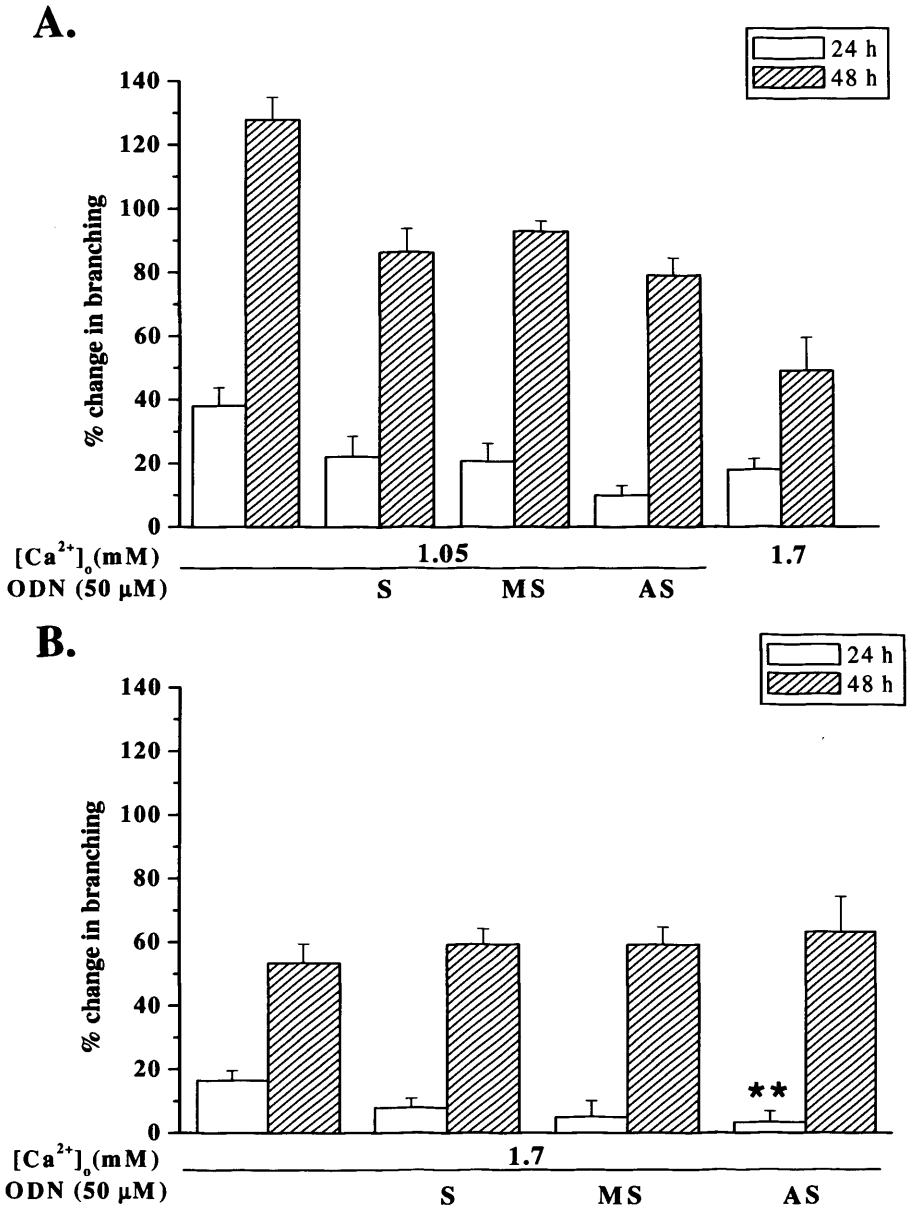

Figure 5.3: CaR ODN treatment is not sufficient to change $[Ca^{2+}]_o$ dependent branching responses. Lungs from E12.5 mouse embryos were cultured for a total of 48 h in the presence 1.05 or 1.7 mM $Ca^{2+}{}_o$ with the addition of CaR specific ODNs applied to a 50 µM final concentration in culture medium. Percent change in branching is defined as the number of branches in each explant at 24 and 48 h divided by number branches at 0 h. Data presented are mean ± s.e.m., from ≥2 pooled experiments at 1.05 mM $Ca^{2+}{}_o$ (n≥6 for each condition) and a single experiment at 1.7 mM $Ca^{2+}{}_o$ (n=4), ** = p=0.03 by ANOVA.

5.4 Effect of $[Ca^{2+}]_o$ and Calcimimetic on Lung Explant Cultures from CaR Knockout Mice

As there was a DNA-toxicity effect when treating lung explant cultures from C57/BL6 mice with ODNs, the next logical step was to look at the branching responses of lungs from mice genetically engineered to lack CaR expression. The hypothesis was that, as the lungs of these mice must lack CaR expression, then the branching morphogenesis responses in lung explant cultures would be similar to the branching morphogenesis responses observed when PLC and PI_3K signalling are inhibited, regardless of the $[Ca^{2+}]_o$ in which the knockout lungs are cultured. Therefore, CaR knockout lung explants were cultured for 48 h in the presence of 1.2 mM or 1.7 mM Ca^{2+}_o.

For many of the CaR knockout experiments, C57/BL6 mice were used as a control for the culture conditions as this is the background strain on which the CaR knockout line is kept. When grown in the presence of 1.2 mM Ca^{2+}_o, all three genotypes responded with similar percentage branching increases after 48 h to those observed in E12.5 lungs from C57/BL6 (Fig. 5.4A). WT lungs from CaR knockout litters had branching increases of 111.2±10.5% (n=11) while HET lung branching increased by 113.3±11.9% (n=18) and NULL lungs kept up with their counterparts with an increase in branching of 106.3±16.7% (n=6). The C57/BL6 column in Figure 5.4A is from a separate experiment (n=6) and for reference only showing that C57/BL6 lungs in 1.2 mM Ca^{2+}_o double their branch number after 48 h (See also Fig.2.2A).

When grown in the presence of 1.7 mM Ca^{2+}_o, none of the genotypes branches significantly more than C57/BL6 lungs grown in the same conditions ($p \geq 0.06$). In this experiment, C57/BL6 lungs had a branching increase of 57.9±7.7%

(n=3, similar to that seen in Fig. 2.2A) after 48 h, while WT lungs increased by 74.5±22.1% (n=4), HET lungs increased 53.5±11.7% (n=8) and NULL lungs increased 45.1±15.6% (n=5, Fig. 5.4B).

Since the genotype (and therefore CaR expression) of the lungs did not seem to contribute to a differential branching morphogenesis response evoked by Ca^{2+}_o than that of normal C57/BL6 mice, CaR knockout and littermate lungs were treated with the calcimimetic R-568. By exposing the lungs to this CaR specific positive allosteric modulator, the hypothesis that there was a functional CaR still present in these lungs, despite their genetic status, could be tested. This does indeed appear to be the case from the results detailed in Figure 5.5.

In two separate experiments, four separate CaR knockout litters were used. C57/BL6 lungs grown for 48 h in the presence of 1.2 mM Ca^{2+}_o increase their branching by 102.4±8.1% (Fig. 5.5A, n=6), when grown in the presence of 1.7 mM Ca^{2+}_o for 48 h this is decreased to 56.7±8.8% (Fig. 5.5E, n=3). When CaR knockout and littermate lungs were cultured in the presence of 1.2 mM Ca^{2+}_o with 10 nM R-568, all of the genotypes showed a branching response reduced from that of C57/BL6 lungs grown in the presence of 1.2 mM Ca^{2+}_o alone. WT lungs responded with a decrease in branching morphogenesis to 85.4±6.9% (Fig. 5.5B, n=8) which although showing a shift, was not statistically different from that of 1.2 mM Ca^{2+}_o lungs alone. However, both HET and NULL lungs responded to R-568 with statistically significant decreases in the amount of branching morphogenesis at 48 h, indicating the residual presence of a functional CaR. After 48 h of R-568 treatment, HET lungs responded with an increase in branching of 69.7±8.03% (Fig. 5.5C, n=14, p=0.0030). In the same conditions, NULL lungs had an increase in branching morphogenesis of 72.6±4.6% (Fig. 5.5D, n=7, p=0.04) after 48 h.

Although branching morphogenesis levels do not vary between embryos of different genotypes, it was thought that perhaps the response seen would have differential effects on the amount of proliferation and apoptosis within lungs from knockout litters. Therefore the amount of proliferation and apoptosis was determined as in Section 2.1.3 on lung explants after culture for 48 h in the presence of 1.7 mM Ca^{2+}_{o}. It was thought at one point early in this analysis that the genotype of the mother might have been influencing the proliferation and apoptosis of the response, therefore both WT pups and HET pups from C57/BL6 mothers were also tested for comparison against WT, HET and NULL embryos from a HET mother (Fig. 5.6). No changes in proliferation or apoptosis resulted from the differences in either maternal or fetal genotype.

The percentage of proliferating cells in WT embryos from a C57/BL6 mother, used as control values, was 5.3±0.7% (n=7, similar to the value presented in Figure 2.6), HET pups, also from a C57/BL6 mother, had 4.4±0.5% proliferating cells, a value not statistically different from their WT littermates (n=5, p=0.37). These values did not change significantly when embryos were born from a HET mother with the percentage of proliferating cells in WT lungs at 3.9±0.6% (n=6, p=0.16), HET lungs at 3.8±0.5% (n=8, p=0.1) and NULL lungs at 4.6±0.3% (n=4, p=0.5).

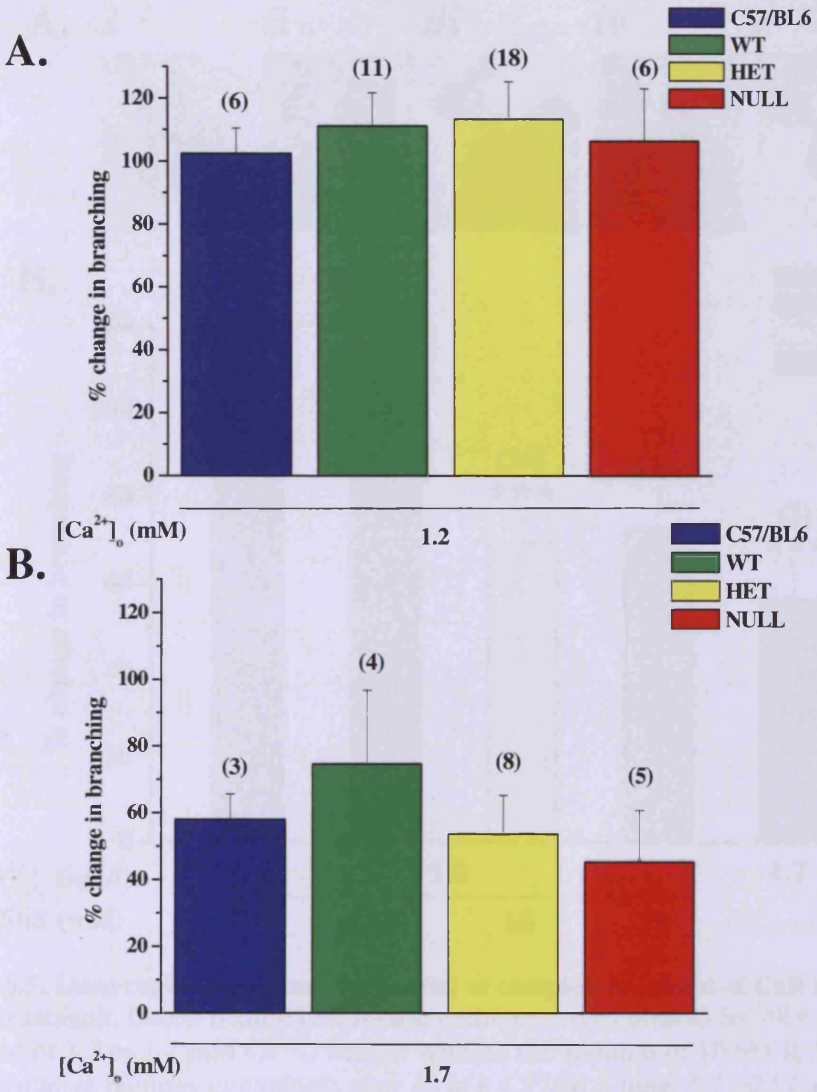

Figure 5.4: Lung explants with partial or complete knockout of CaR show similar $[Ca^{2+}]_o$-mediated branching responses to wild-type C57/BL6 lungs. Lungs from E12.5 mouse embryos were cultured for 48 h in the presence of 1.2 or 1.7 mM Ca^{2+}_o. **A).** The branching response of CaR knockouts, littermates and C57/BL6 controls was comparable in the presence of 1.2 mM Ca^{2+}_o after 48 h in culture. **B).** The branching response of CaR knockouts, littermates and C57/BL6 controls was comparable in the presence of 1.7 mM Ca^{2+}_o. Total number of terminal branches was counted at 0 and 48 h, normalized to 0 h, and the change expressed graphically as a percentage increase over 48 h. Data shown are the mean ± s.e.m., n numbers shown above each result in parentheses from pooled experiments.

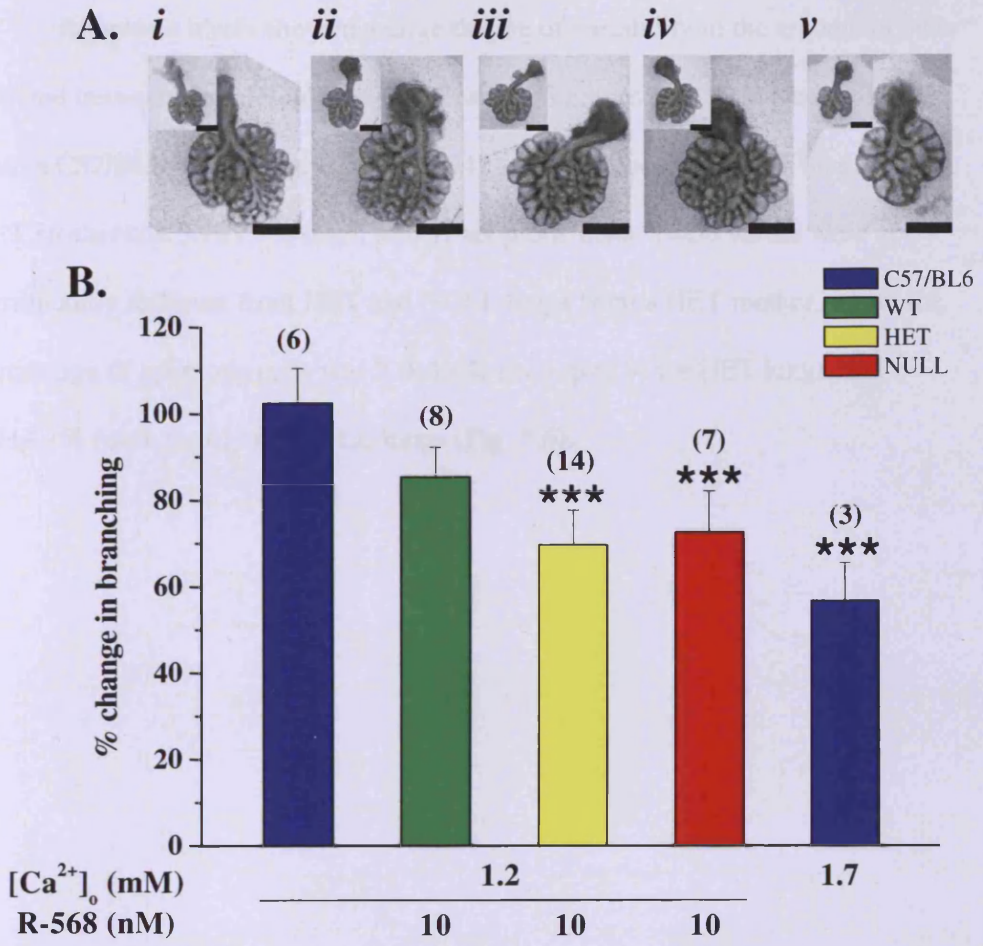

Figure 5.5: Lung explant cultures with partial or complete knockout of CaR respond to R-568 treatment. Lungs from E12.5 mouse embryos were cultured for 48 h in the presence of 1.2 or 1.7 mM Ca^{2+}_o, with or without the addition of 10 nM R-568. **A).** Representative pictures of explants after 48 h: ***i.*** C57/BL6 lung, 1.2 mM Ca^{2+}_o, ***ii.*** WT lung, 1.2 mM Ca^{2+}_o + 10 nM R-568, ***iii.*** HET lung, 1.2 mM Ca^{2+}_o + 10 nM R-568, ***iv.*** NULL lung, 1.2 mM Ca^{2+}_o + 10 nM R-568, ***v.*** C57/BL6 lung, 1.7 mM Ca^{2+}_o. Inset pictures present each lung at 0 h (post-dissection) showing a comparable number of initial terminal branches for each genotype and culture condition. **B).** Graphical presentation of the branching response of CaR knockouts, littermates and C57/BL6 controls in the presence of 1.2 mM Ca^{2+}_o, with or without 10 nM R-568, and 1.7 mM Ca^{2+}_o after 48 h in culture. Total number of terminal branches was counted at 0 and 48 h, normalized to 0 h, and the change expressed graphically as a percentage increase over 48 h. Data shown are the mean ± s.e.m from 2 pooled experiments, n shown in parentheses above results, *** = $p \leq 0.04$ in comparison to time-matched samples cultured in 1.2 mM Ca^{2+}_o, determined by ANOVA. Scale bars = 800 μm.

Apoptosis levels showed a large degree of variability in the amount of cells detected between samples and no significant differences were achieved. WT lungs from a C57/BL6 mother had 3.7±3% (n=4) apoptotic cells while WT lungs from a HET mother had 3.7±1.7% (n=3, p=0.1) apoptotic cells. These values were not significantly different from HET and NULL lungs from a HET mother, where the percentage of apoptotic cells was 2.0±1.6% (n=3, p=0.9) for HET lungs, and 4.7±4.1% (n=3, p=0.1) for NULL lungs (Fig. 5.6).

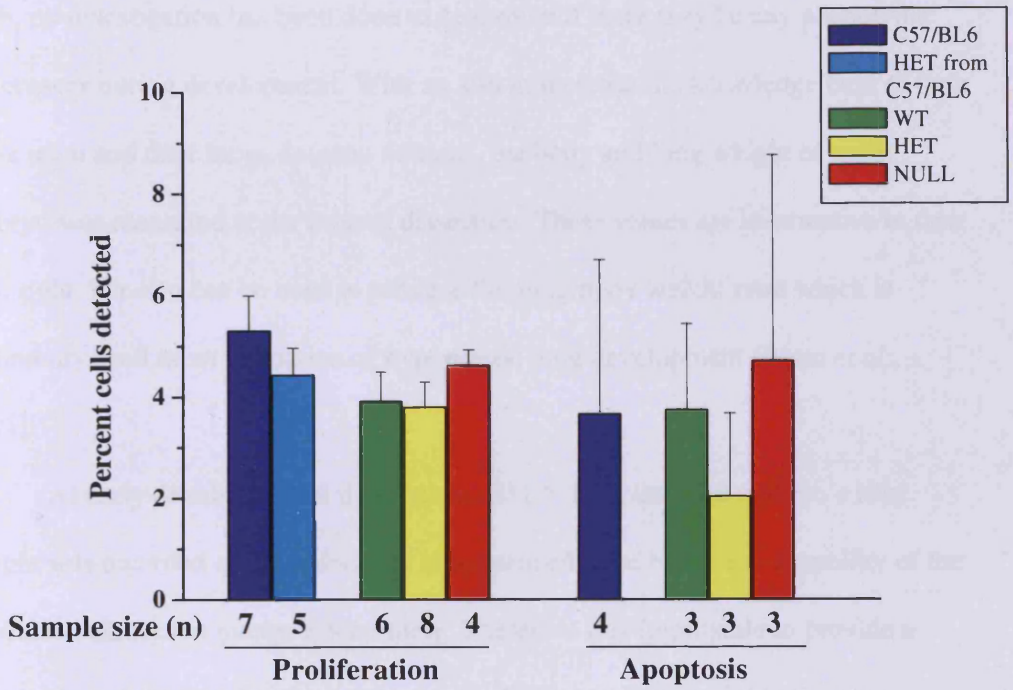

Figure 5.6: Levels of proliferation and apoptosis in lung explants cultured in the presence of 1.7 mM Ca^{2+}_o are not dependent upon fetal or maternal genotype. Lungs from E12.5 mouse embryos were cultured in the presence of 1.7 mM Ca^{2+}_o for 48 h. After culture the lungs were fixed in 4% PFA and embedded into paraffin. 5 µm sections were subjected to immunohistochemistry to detect proliferation (phospho-histone H3) and apoptosis (TUNEL assay as described in Chapter 2). The number of cells detected is expressed as a percentage of the total number of cells counted. Data presented are the mean ± s.e.m from 3 separate litters for proliferation and a single litter for apoptosis.

5.5 Physical Measurements of Development in CaR Knockout Mice

As the gross physical appearance (*i.e.* size and shape) of CaR NULL knockout mice is not overtly different to that of their WT and HET counterparts at birth, no investigation has been done to determine if there may be any phenotypic differences during development. With an aim to increase the knowledge base of how these mice and their lungs develop *in utero*, the body and lung weight of each embryo was measured at the time of dissection. These values are informative in their own right, but also can be used to produce the lung:body weight ratio which is commonly used as an indication of hypoplastic lung development (Bratu *et al.*, 2001).

At early developmental time points, E11.5-12.5, only the embryo's total weight was recorded as the individual lungs proved to be below the capability of the available balances to measure accurately. Therefore it is impossible to provide a lung:body weight ratio for these time points. However, body weights show no significant difference between the genotypes with E11.5 embryos weighing on average between 37.6 and 41.3 mg (Fig. 5.7A) and E12.5 embryos weighing on average between 79.2 and 87.2 mg (Fig. 5.7B). At E13.5, WT embryos weigh 147.5±6.7 mg, HET embryos weigh 158.4±6.6 mg and NULL embryos weigh 164.2±10.6 mg ($p>0.05$). As the embryos continue to develop, the lack of a statistically significant weight difference between the genotypes is maintained ($p>0.05$, Fig 5.8A). At P0, WT embryos weigh 1402±67.8mg, HET embryos weigh 1298.8±37.3 mg and NULL embryos weigh 1302.6±70.8 mg (Fig. 5.8A).

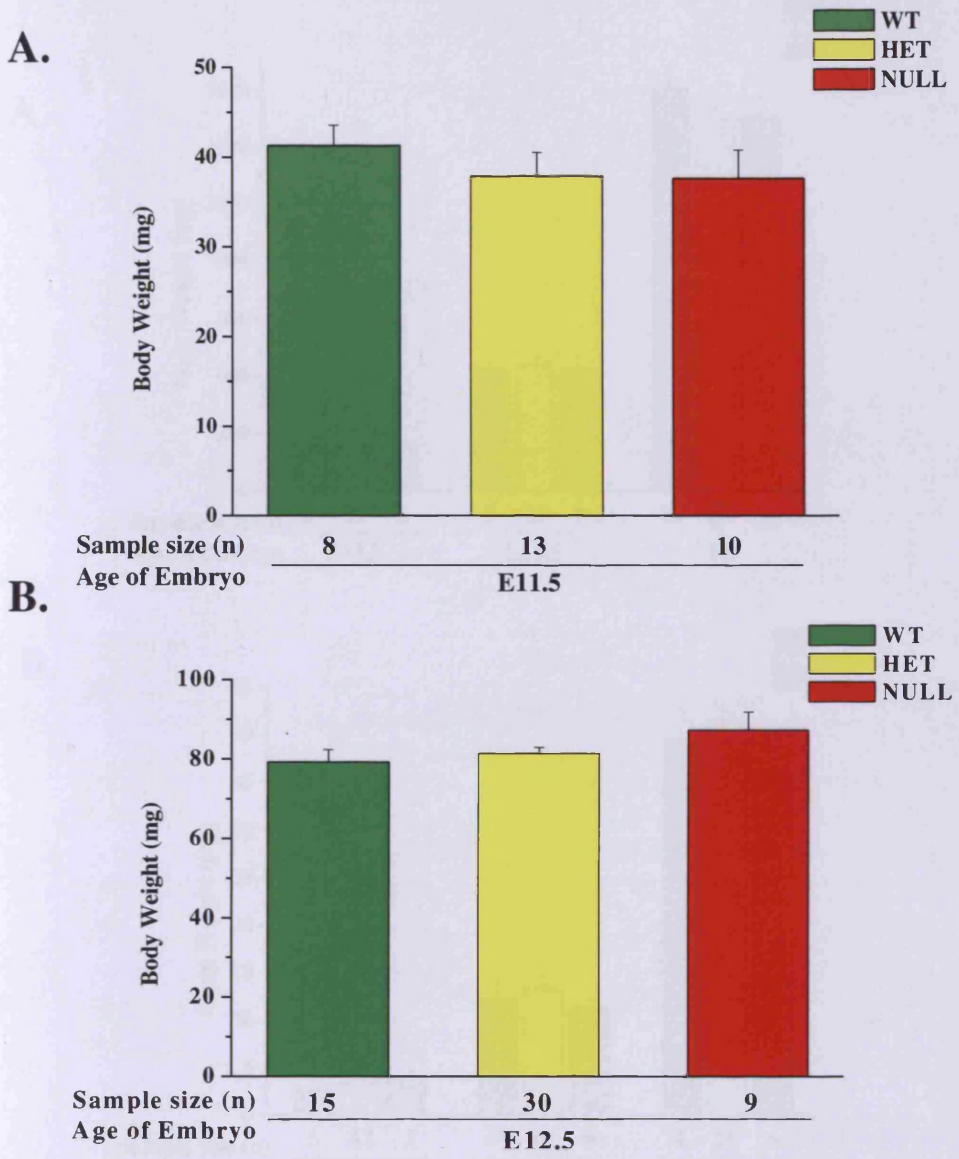

Figure 5.7: Body Weight comparison of WT, HET and NULL CaR mice at E11.5 and E12.5. Embryos were removed from time-mated females, washed in HBSS and weighed immediately before lung dissection. **A).** Weights of embryos harvested at E11.5. **B).** Weights of embryos harvested at E12.5. Data shown are mean ± s.e.m pooled from at least 3 different litters.

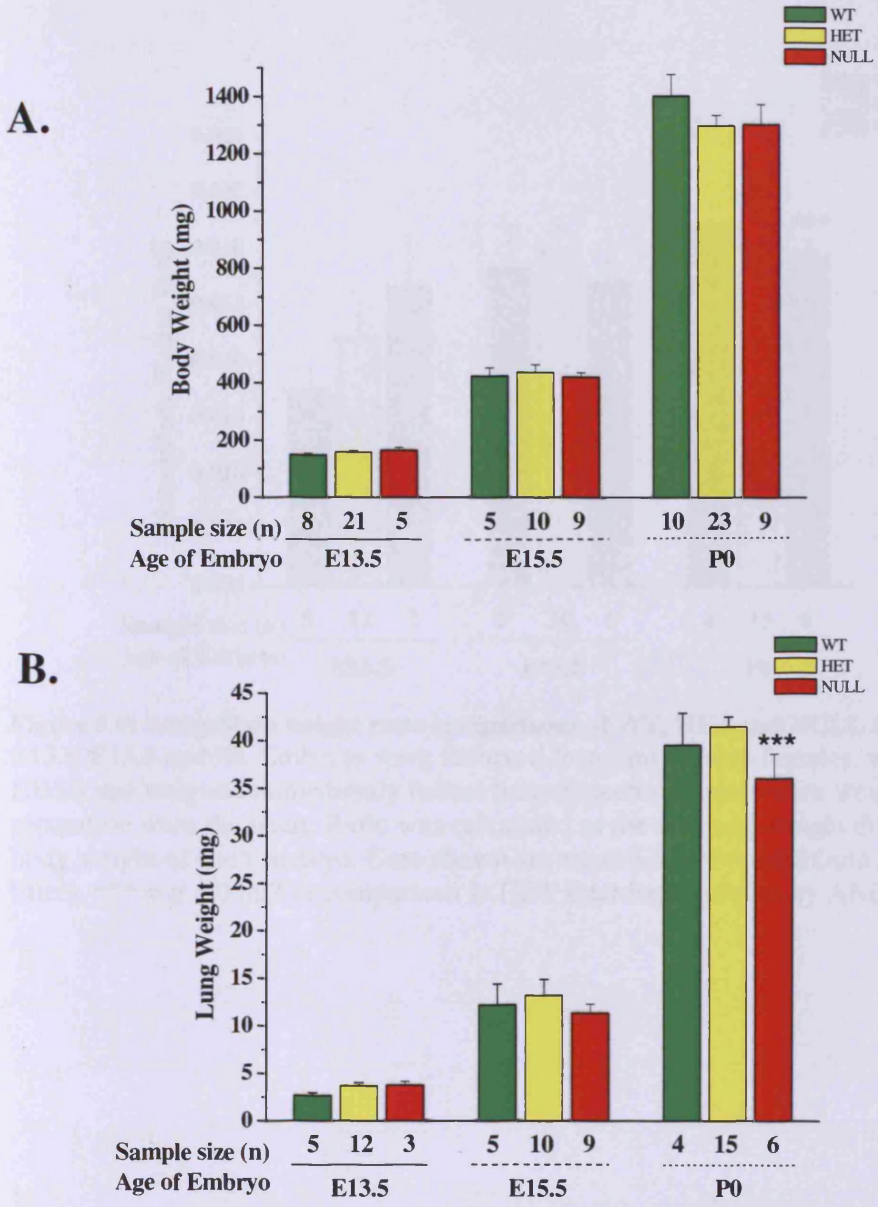

Figure 5.8: Body and lung weight comparisons of WT, HET and NULL CaR mice at E13.5, E15.5 and P0. Embryos were removed from time-mated females, washed in HBSS and weighed immediately before lung dissection. Lungs were weighed post-separation from the heart. **A).** Body weight of embryos removed at E13.5, E15.5 and P0. **B).** Lung weights from E13.5, E15.5 and P0 embryos. Data shown are mean ± s.e.m pooled from ≥ 3 different litters, *** = p=0.03 in comparison to HET littermate samples by ANOVA.

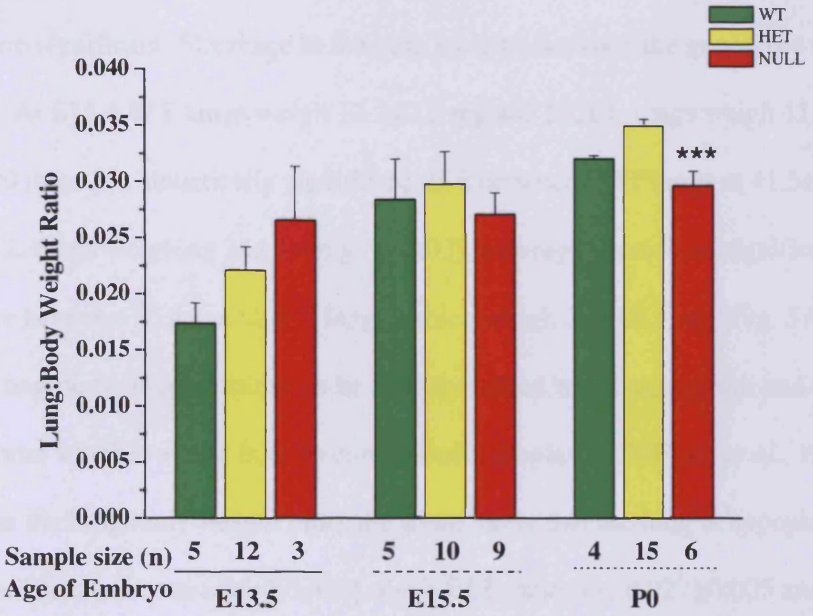

Figure 5.9: Lung:Body weight ratio comparisons of WT, HET and NULL CaR mice at E13.5, E15.5 and P0. Embryos were removed from time-mated females, washed in HBSS and weighed immediately before lung dissection. Lungs were weighed post-separation from the heart. Ratio was calculated as the wet lung weight divided by the body weight of each embryo. Data shown are mean ± s.e.m pooled from ≥3 different litters, *** = p = 0.003 in comparison to HET littermate samples by ANOVA.

The weight of individual lungs was also measured at E13.5, 15.5 and P0. There is no significant difference in the lung weights between the genotypes at E13.5 or E15.5. At E15.5 WT lungs weigh 12.2±2.2 mg and NULL lungs weigh 11.3±0.9 mg. At P0 there is a statistically significant shift between HET lungs at 41.5±1.1 mg and NULL lungs weighing 36±2.6 mg (p=0.03), although there is no significant difference between NULL and WT lungs, which weigh 39.5±3.3 mg (Fig. 5.8B).

Lung:body weight ratios can be directly linked with lung growth and are used to determine whether a lung is to be considered hypoplastic (DiFiore *et al.*, 1994). The lower the lung:body weight ratio, the more likely that the lung is hypoplastic. At the earliest time point measured, E13.5, the NULL ratio was 0.027±0.005 and the HET ratio was 0.022±0.002, their WT littermates had a ratio of 0.017±0.02 but this was not statistically significant (p>0.05, Fig. 5.9). At E15.5 all of the genotypes have similar ratios with WT at 0.028±0.004, HET at 0.029±0.003 and NULL at 0.027±0.002. At P0 WT lungs have a ratio of 0.032±0.0003 and their HET littermate's lung:body weight ratio is 0.035±0.0006 (p=0.14). However, NULL embryos have a significantly lower lung:body weight ratio than their HET counterparts, with a value of 0.0296±0.001 (p=0.003). This indicates that, at P0, the lighter lung weight measured in NULL embryos does not completely correspond with a decrease in total body weight (Fig. 5.9), and therefore the lungs are more likely to be hypoplastic than the lungs of their HET littermates.

The amount of cellular proliferation was determined by immunohistochemical detection of cells expressing phosphorylated Histone H3 in order to elucidate any differences in the developmental programme of the genotypes (Fig. 5.10A). No statistically significant differences were detected at any stage tested. E15.5 lungs all had similar levels of proliferation when compared with WT, at

2.39±0.4% (n=5) cells proliferating, HET at 2.65±0.5% (n=6, p=0.68) and NULL at 2.39±0.7% (n=4, p=0.99) cells proliferating. E17.5 lungs also had similar levels of proliferation with WT at 2.86±0.57% (n=8) cells proliferating, HET at 2.19±0.3% (n=8, p=0.34) and NULL at 2.82±0.05% (n=8, p=0.8) cells proliferating. At P0 levels of proliferation were reduced across all genotypes by approximately 50%, but levels were not statistically different across the genotypes. At this time point, the percentage of proliferating cells out of the total cell number counted in WT lungs was 1.04±0.5% (n=7), in HET lungs this was 1.25±0.5% (n=5, p=0.78) and in NULL lungs was 0.4±0.1% (n=3, p=0.4).

Apoptosis levels were quantified at both E15.5 and P0 by TUNEL immunohistochemistry (Fig. 5.10B). At E15.5 there was significantly more apoptosis (50-100%) detected in HET and NULL lungs than in their WT counterparts. At this time point WT lungs had 1.0±0.2% (n=5) apoptotic cells while HET lungs had 2.56±0.6% (n=6, p=0.035) apoptotic cells and NULL lungs had 1.61±0.1% (n=4, p=0.025) apoptotic cells. This trend looks likely to continue as the lungs develop, although at P0 due to the large variability, in HET and NULL samples there is no statistical difference between genotypes. At this time point WT lungs had 1.78±0.5% (n=7) apoptotic cells while HET lungs had 2.85±1.2% (n=5, p=0.38) apoptotic cells and NULL lungs had 2.86±1.5% (n=3, p=0.4) apoptotic cells.

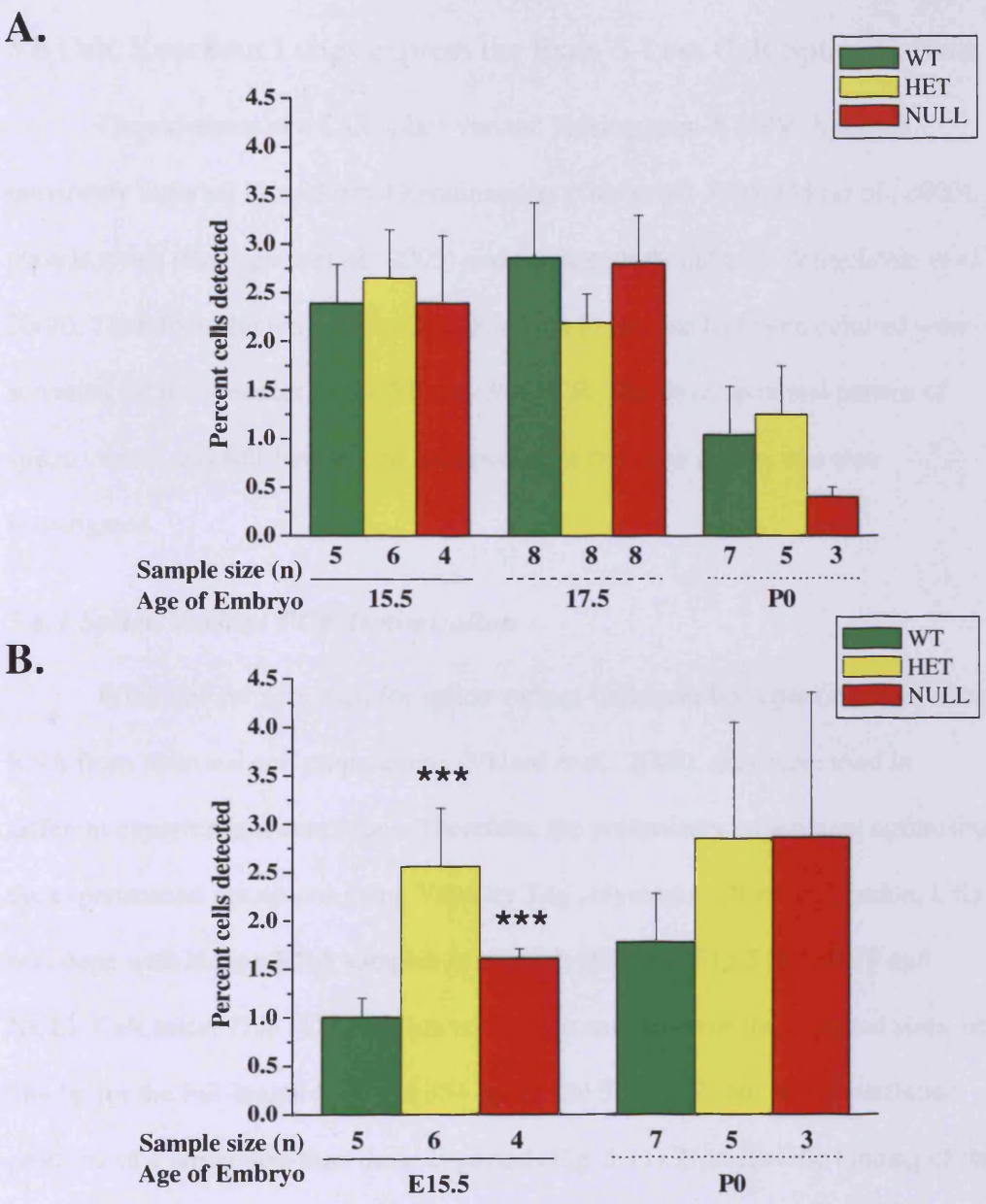

Figure 5.10: Proliferation and apoptosis levels in the developing lungs of WT, HET and NULL CaR mice. A). Proliferating cells were detected in paraffin sections of E15.5, E17.5 and P0 lungs from WT, HET and NULL CaR mice by immunohistochemical detection of phosphorylated Histone H3. **B).** Apoptotic cells were detected in paraffin sections of E15.5 and P0 lungs from WT, HET and NULL CaR mice by TUNEL immunohistochemical detection. Data presented are mean ± s.e.m. from 2 separate litters of mice. *** = $p \leq 0.04$ by ANOVA.

5.6 CaR Knockout Lungs express the Exon-5-Less CaR Splice Variant

The existence of a CaR splice variant, lacking exon-5 (SPV) has been previously reported in epidermal keratinocytes (Oda *et al.*, 1998; Oda *et al.*, 2000), chondrocytes (Rodriguez *et al.*, 2005) and aortic endothelial cells (Ziegelstein *et al.*, 2006). Therefore, the lungs from CaR knockout litters that had been cultured were screened for the presence of the SPV by RT-PCR. The developmental pattern of splice variant and full-length CaR expression, at two time points, was also investigated.

5.6.1 Splice Variant PCR Optimization

While the primers used for splice-variant CaR have been previously used on RNA from neuronal cell preparations (Vizard *et al.*, 2008), they were used in different experimental conditions. Therefore, the preliminary experiment optimising the experimental conditions using Velocity Taq polymerase (Bioline, London, UK) was done with kidney RNA samples from adult HET and E15.5 WT, HET and NULL CaR mice. This PCR reaction resulted in amplicons of the expected sizes, of 584 bp for the full-length CaR and 354 bp for the SPV CaR, but also superfluous products of a larger size than those expected (Fig. 5.11). Non-specific binding of the primers, due to an inadequate annealing temperature, or genomic contamination of the RNA samples, could cause the production of non-specific PCR products seen in this reaction. Therefore the next PCR used a broader temperature gradient, as well as a gradient of [Mg^{2+}] within the PCR reaction mix. This PCR showed that the optimal reaction conditions were 2 mM Mg^{2+} in the reaction mix with 68°C annealing temperature (Fig. 5.12).

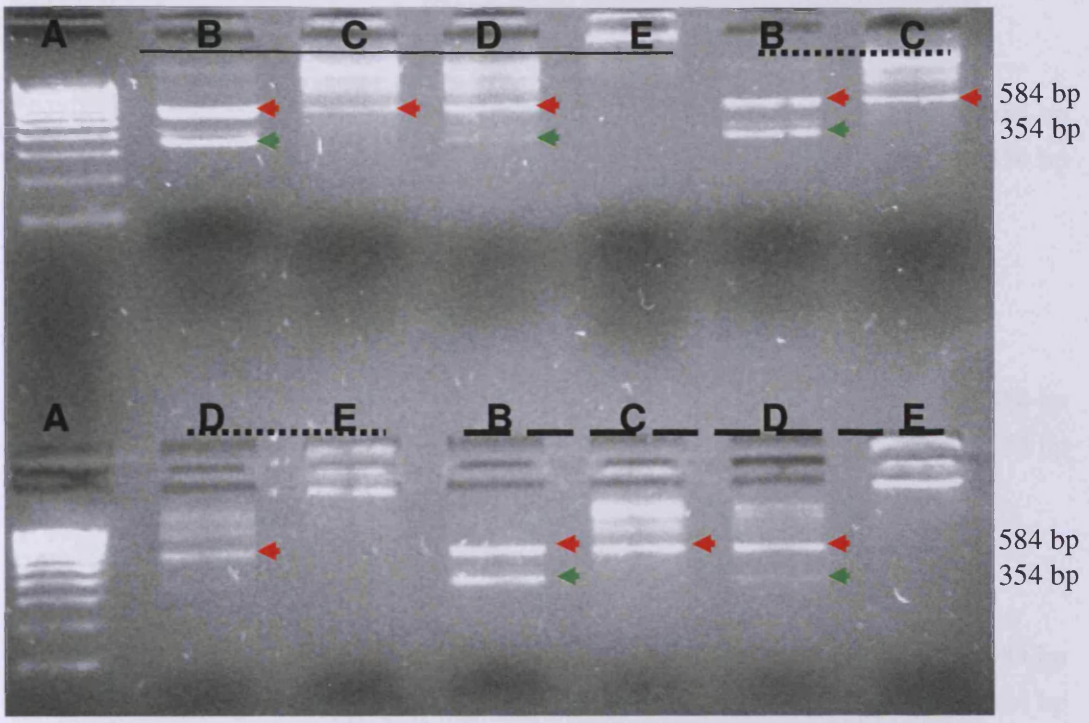

Figure 5.11: Initial temperature gradient for optimisation of PCR conditions for the detection of the CaR SPV. Total RNA was isolated from an adult HET kidney (B), E15.5 WT (C), E15.5 HET (D) and E15.5 NULL (E) pooled kidney samples and reverse transcribed. The resulting cDNA was used in PCR reactions with varying annealing temperatures. DNA ladder (A) 100 – 1000 bp in 100 bp increments indicates size of products. Top row- solid line is annealing temperature = 56°, Top and bottom row- dotted line is annealing temperature = 58.4°, Bottom Row- dashed line is annealing temperature = 60°. Full-length CaR expected size of the amplicon = 584 bp, red arrowheads, SPV CaR expected size of the amplicon = 354 bp, green arrowheads.

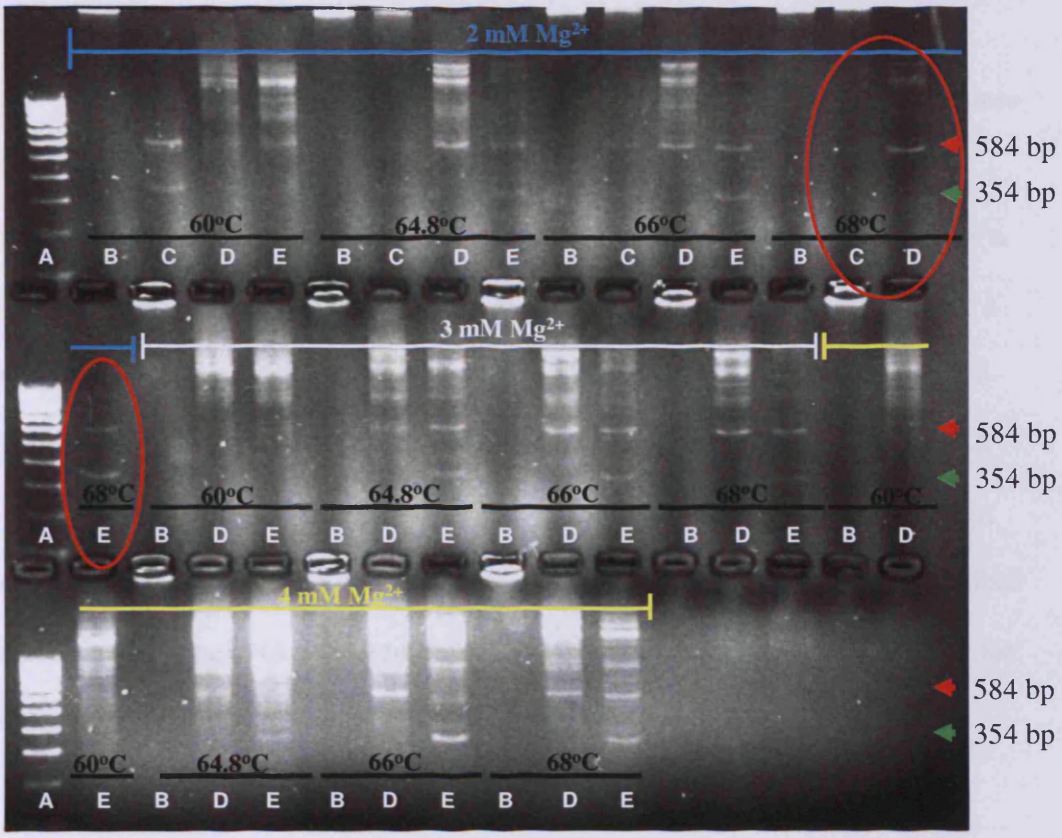

Figure 5.12: Temperature and [Mg^{2+}] gradient for optimal detection of CaR SPV by PCR. Total RNA was isolated from each of the following: adult HET kidney (C), E15.5 WT (D), E15.5 HET (E) pooled kidney samples and reverse transcribed, the resulting cDNA was used in PCR reactions with varying annealing temperatures and [Mg^{2+}]. Negative control was performed with water replacement of cDNA (B). DNA ladder (A) 100 – 1000 bp in 100 bp increments indicates size of products. Full-length CaR amplicon expected size = 584 bp (red arrowhead), SPV CaR amplicon expected size = 354 bp (green arrowhead), [Mg^{2+}] of 2, 3 and 4 mM were tested and are indicated above products. Annealing temperature sets, 60 °C, 64.8 °C, 66 °C and 68 °C are indicated below the products. The clearest amplicons were produced by 2 mM Mg^{2+} and 68°C annealing temperature (red circles).

5.6.2 Developmental detection of SPV CaR expression by RT- PCR

As branching morphogenesis studies using WT, HET and NULL CaR mouse lung showed that sensitivity to high $[Ca^{2+}]_o$ and calcimimetics is maintained regardless of genotypic status, I performed a PCR reaction to detect expression of a CaR splice-variant lacking exon 5. This exon-5-less splice-variant could result in a functionally active protein mediating the branching response to $[Ca^{2+}]_o$ and R-568. As a positive control, a PCR reaction for β-actin was also performed (Fig. 5.13A).

Total RNA was isolated from WT, HET and NULL lungs which had been cultured in 1.2 mM Ca^{2+}_o + 10 nM R-568 for 48 h. The RNA was reverse transcribed and the resulting cDNA was used in the PCR reaction optimised in Section 5.7.1 for detecting both full-length and SPV CaR. The products of this reaction were separated on a 2% agarose gel by electrophoresis and visualised. This reaction showed that cultured WT CaR lungs continue to express the CaR after 48 h in culture, while HET CaR lungs express both the full-length and SPV CaR and NULL CaR lungs only express the SPV CaR after 48 h (Fig. 5.13B).

Developmental expression of SPV RNA was also investigated to determine if SPV expression was maintained across the genotypes at different time points. Full-length CaR expression was confirmed in E11.5 and E15.5 WT lung samples while SPV CaR expression was detected in HET and NULL lungs of the same time points (Fig. 5.14).

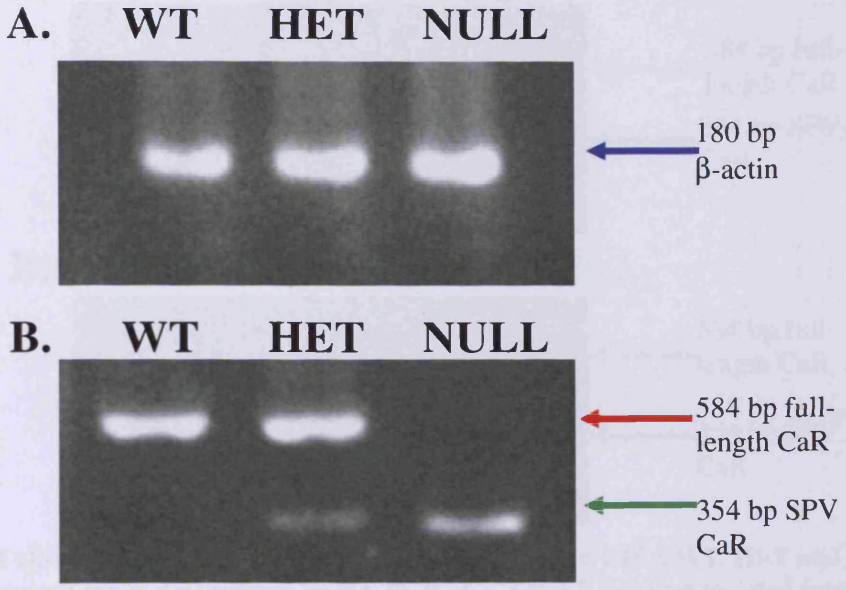

Figure 5.13: Full-length CaR, SPV CaR and β-actin expression in cultured WT, HET and NULL CaR mouse lungs determined by RT-PCR. Total RNA was isolated from pooled lung samples and subjected to RT-PCR. **A).** β-actin expression in WT, HET and NULL (also used in B), amplicon size = 180 bp (blue arrow). **B).** Full-length and SPV CaR expression in WT (single lung), HET (3 lungs pooled) and NULL (3 lungs pooled) littermates after culture in 1.2 mM Ca^{2+}_o + 10 nM R-568 for 48 h. Expected amplicon size for full-length CaR = 584 bp (red arrow). Expected amplicon size for SPV CaR = 354 bp (green arrow).

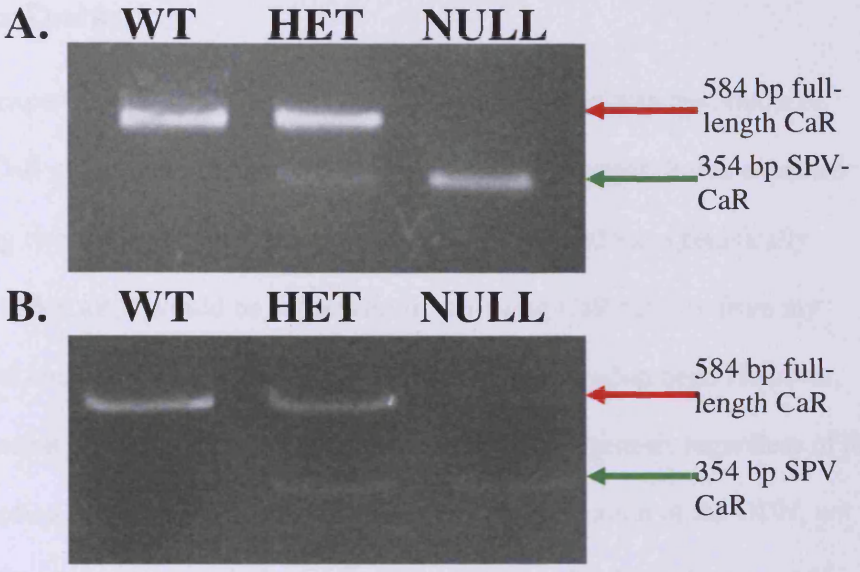

Figure 5.14 Full-length and SPV CaR expression in E11.5 and E15.5 WT, HET and NULL CaR mouse lungs determined by RT-PCR. A). Total RNA was isolated from pooled (8 lungs each) samples of E11.5 WT, HET and NULL CaR knockout littermate lungs and subjected to RT-PCR for detection of full-length and SPV CaR expression. **B).** Total RNA was isolated from pooled E15.5 WT (3 lungs), HET (8 lungs) and Null (4 lungs) CaR knockout littermate lungs and subjected to RT-PCR for detection of full-length and SPV CaR expression. Expected amplicon size for full-length CaR = 584 bp (red arrow). Expected amplicon size for SPV CaR = 354 bp (green arrow).

5.7 Chapter Discussion

The experiments in this chapter were designed to elucidate the effects of abrogating CaR expression and activity within lung development. It was expected that, by using two different approaches, ODN application and mice genetically modified to lack CaR, I would be successful in removing CaR activity from my culture model and determine any effects this had on lung development. However, ODN application resulted in decreases in branching morphogenesis regardless of the sequence applied, implying that this effect was due to application of the ODN, not due to specific interactions with the target CaR. Additionally, lungs harvested from CaR knockout mice responded to both changes in $[Ca^{2+}]_o$ and the specific positive allosteric modulator of the CaR, R-568. Proliferation levels, as well as embryo size, did not differ between the genotypes regardless of the time-point investigated. Subtle differences between WT/HET and NULL embryos were detected in lung weight and lung:body weight ratios, apoptosis levels mid-gestation (E15.5) were also significantly higher in both HET and NULL embryos in comparison to their WT littermates. The lack of a robust phenotypic difference between the genotypes implies that CaR HET and NULL embryonic lungs either have a redundant mechanism with which to respond to CaR agonists, or they are incomplete knockouts for the CaR. One possible component of the response of the knockout lungs, expression of the exon-5-less splice variant of the CaR, was detected in both cultured and *in vivo* lung samples using RT-PCR.

The lack of response to ODN application may be due to technical difficulties in applying the ODN sequence to the locality of CaR expression. Previously, Rothenpieler and Dressler (1993) used FITC-labelled ODNs to determine how they are distributed in several cultured organs, including the lung. Their study showed

that after 48h with ODNs in the culture medium, there was high expression of their labelled ODN in the mesenchyme of the lung, but very little in the epithelium (Rothenpieler & Dressler, 1993). Therefore lack of ODN access to the epithelium, where the majority of CaR protein is expressed at E12.5, could be causing the results in Figure 5.3. Further experiments could improve the method of ODN delivery to the lung epithelium, including direct injection into the lung lumen of the ODN alone and/or use of surfactants to promote ODN uptake or application of ODNs to isolated epithelial bud cultures.

After the lack of success with the CaR ODN knockdown experiments, it was thought that using the CaR knockout mice would be more informative in conclusively determining the role of CaR in lung development. The logic being that, by using a model where CaR expression had been completely removed from the embryo, the technical issues surrounding exogenous knockdown of CaR expression would be overcome. Therefore it was surprising that lungs hetero- and homo-zygous for CaR knockout branched to the same extent as their WT counterparts in culture, regardless of the $[Ca^{2+}]_o$ and application of R-568. Data obtained from the physical measurement of body weight, as well as developmental measurements such as proliferation and apoptosis, also did not differ between the genotypes at the stage (E12.5) used for lung explant culture.

Significant differences were never detected in the body weight of embryos, and it was not until later in development that differences in lung weight and lung:body weight ratio were noted. These differences were again subtle, with the HET embryos remaining more similar to the WT, while the NULL embryos showed reductions in both lung weight and lung:body weight ratios in comparison to their HET littermates. The lack of statistical significance between the lung:body weight

ratios of WT and NULL embryos is possibly due to the large variability in the data obtained for the WT embryos. For an unknown reason, measurements of both HET and NULL embryos was within a more consistent range, especially in the body weight measurements despite a fairly large sample size (WT n=10, HET n=23, NULL n=9).

Although there were no overt differences in the physical aspects of CaR knockout mice aside from slightly smaller lungs, Appendix B details the numbers of each genotype that were harvested for a period in 2007. This information was gathered because; during the process of harvesting embryos I noted that there seemed to be an abnormally large number of aborted fetuses within the uterus of each HET mother. Additionally it seemed to take a large number of litters to obtain sample sizes large enough for each genotype. After compilation of the genotyping data, embryos aged E14.5 and younger resulted in the expected Mendelian genotyping ratio of approximately 1 WT: 2 HET: 1 NULL. However, there were a large number of aborted fetuses within this group and almost invariably they were either HET (19 to 1 WT) or NULL (7 to 1 WT) embryos. This implies that embryos with disrupted activity of the CaR may be more susceptible to death than those which maintain normal CaR activity.

HET and NULL embryos that are not aborted begin to show signs of a phenotypic difference in their lungs at E15.5. At this time point HET and NULL lungs have significantly increased levels of apoptosis in their lungs. Although it is at a low level, 2-2.7% of cells counted, apoptosis is still 50-100% more in these embryos than their WT counterparts. It is possible that the decrease in lung size noted in NULL lungs at P0 could be the result of increased apoptosis through the latter stages of development. Indeed the trend towards a higher level of apoptosis in

HET and NULL lungs seems to be preserved at P0, however at this point is not significant, potentially due to high variability and could be improved by the addition of several samples for each genotype. However, what the increase in apoptosis does not explain is that the greatest difference at P0 is between HET and NULL embryos, not NULL and WT embryos. Therefore, if apoptosis is increased in both genotypes why are they different from each other?

The answer could be as simple as the fact that HET embryos have at least one copy of a functioning CaR. This allows for at least partial control of calcium homeostasis with a phenotype of greatly reduced severity in HET pups after birth (Ho *et al.*, 1995) and could be compensating in the developing lung as well, reducing the severity of any phenotype induced by disrupted CaR expression. There could also be a compensation effect within the *in vivo* developmental situation, by the exon-5 less splice variant of CaR. This has been recently suggested by the increased severity of hyperparathyroidism in a conditional CaR knockout which removes both full-length and SPV CaR from the targeted tissues (Chang *et al.*, 2008) in comparison to the hyperparathyroidism in the CaR knockout mouse used in this study.

Compensatory mechanisms could also be a part of the reason why lungs NULL for CaR still respond to R-568 application. WT lungs were expected to present with a lower amount of branching in 1.2 mM Ca^{2+}_{o} when R-568 was applied, some decrease could also be expected in the HET lungs as they too express some CaR, however NULL lungs should have responded as if R-568 was not present, with a doubling of branching morphogenesis in 48 h. E12.5 HET and NULL lungs after 48 h in culture express RNA for the exon-5 less SPV of the CaR as do E11.5 and E15.5 lungs. Presumably expression of the SPV in HET and NULL lungs

corresponds to the same expression pattern as full length CaR, E10.5-E18.5, and experiments to determine this definitively are ongoing.

While in some systems of the CaR knockout mouse the SPV is not expressed, such as SCG neurons (Vizard *et al.*, 2008), expression has been detected in others including keratinocytes (Oda *et al.*, 1998), chondrocytes (Rodriguez *et al.*, 2005) as well as both E15.5 and adult kidney (Fig. 4.11-12). Studies using heterologous systems to express the SPV, such as HEK293 cells, have shown that it is not trafficked to the membrane, whereas in native systems, such as chondrocytes, it is expressed at the membrane and is functional (Rodriguez *et al.*, 2005). Functionality was determined in this study by treatment of NULL chondrocytes with Ca^{2+}, Mn^{2+} and Sr^{2+}, as well as neomycin, all of which resulted in the production of inositiol phosphates in a similar fashion to full length CaR. Indeed, embryos with complete ablation of CaR expression in their chondrocytes die by E13, implying not only a vital role for CaR activity during development, but that the SPV can functionally compensate for loss of the full-length CaR in this tissue (Chang *et al.*, 2008).

That this SPV CaR receptor is functional in the developing lung is supported by the response of the NULL lungs to both high $[Ca^{2+}]_o$ and R-568. R-568 should be able to modulate allosterically the SPV in the same fashion as the full-length CaR because, studies using site-directed mutagenesis have shown that one of the primary residues for binding R-568 is Glu837 at the junction between extracellular loop 3 and the seventh transmembrane domain of the protein (Hu *et al.*, 2002; Petrel *et al.*, 2004). The loss of exon-5 does not affect this area of the protein, but removes only a small part of the large extracellular domain (Oda *et al.*, 2000). Indeed, long term application of R-568 has been shown to rescue plasma membrane expression and

function of several loss-of-function CaR mutants in HEK293 cells (Huang & Breitwieser, 2007).

It may be interesting for the CaR research field as a whole to determine in which systems the SPV is active and whether the lung compensation effects are by other receptors or the involvement of the SPV, but how relevant this information would be to the research of lung branching morphogenesis is unclear. Studies may pursue the $[Ca^{2+}]_i$ signalling behaviour of isolated epithelial buds from these mice, but presumably they would respond in a similar way to their WT counterparts as they did with branching. Overall, the major drawback to using this particular mouse model for lung branching morphogenesis studies is that any phenotype is going to be very subtle, and clear, timely results are not going to be provided by its continued use.

Therefore several other options are to be considered for the progression of elucidating the role of CaR in lung development. *Nuf* mice, with constitutively active CaR, have been characterised for their ectopic calcification and hypocalcaemia, but specific morphology of their lungs, except in the context of calcification, has never been studied (Hough *et al.*, 2004). The hypothesis to be tested with these mice would be, that their developing lungs should have lower levels of branching morphogenesis at lower $[Ca^{2+}]_o$ than their WT counterparts, *i.e.* in 1.05 mM Ca^{2+}_o for 48 h, their level of branching should be more like WT lungs in 1.7 mM Ca^{2+}_o. Experiments to characterise the $[Ca^{2+}]_o$ response of the *Nuf* mouse background strain, Balb/C, have begun in order eventually to test the hypothesis that reduced branching results from constitutive CaR activation in *Nuf* mice.

There is also the possibility of injecting WT lungs with an adenoviral dominant negative CaR, such as, the dominant negative CaR construct that was

transfected into WT SCG neurons in order to successfully knockdown activity of the receptor in a native system (Vizard *et al.*, 2008). While having technical issues of its own, such as titration of viral dose etc., an adenoviral dominant negative construct would remove the technical difficulty of transfecting the lung epithelium in a whole lung explant based culture system. Also as mentioned earlier in this section, CaR ODNs could be applied to isolated epithelial buds, where the access to the epithelium would be much less restricted than in the whole lung explant system. The dominant negative CaR construct could also be applied to this system.

By far the most effective means of removing CaR expression from the developing lung would be to use the recently published floxed CaR mouse (Chang *et al.*, 2008). The use of this transgenic mouse line would allow for lung specific knockdown of both the CaR and the SPV CaR. This could be achieved by crossing the floxed CaR mouse with a mouse containing Cre-recombinase linked to a SP-C promoter, producing CaR knockout in the developing epithelium, or other promoters could be used to generate mesenchyme-specific or total lung knockout of CaR. However, due to potential difficulties with Intellectual Property arrangements, this mouse may not be widely available for some time.

In summary, the results presented within this chapter have not as yet conclusively demonstrated a specific role of the CaR in lung development due to the inability to successfully knockdown CaR expression. Therefore, until a complete CaR knockout mouse becomes available, other modes of interfering with natural CaR expression and activity, by using knockdown strategies in native CaR expressing lung tissue or by use of a mouse model with constitutively active CaR should be attempted in order to help determine the specific role of CaR in lung development.

CHAPTER 6:
PRELIMINARY EXPERIMENTS FOR PROGRESSION OF THE PROJECT

6.1 Methods

6.1.1 Lung Explant Cultures

Embryos at day 12.5 of development (E12.5) were removed from time-mated females for gene expression studies from 3 different lines of transgenic mice:

1. Mlc1vnLacz^{v24} mice, hereafter referred to as Fgf10$^{+/LacZ}$ (Kelly *et al.*, 2001), contain an Mlcv-nLacZ gene encoding for β-galactosidase 114 kb upstream of FGF-10 and are reporters for FGF-10 expression. Confirmation that the pattern of β-galactosidase expression is specific for FGF-10 in the lung has been previously demonstrated (Mailleux *et al.*, 2005). FGF-10 protein is expressed throughout lung development and has been specifically localised to the mesoderm where it induces budding and growth of lung endoderm (Bellusci *et al.*, 1997b).

2. TOPGAL mice (DasGupta & Fuchs, 1999) are used as a reporter line for β-catenin and LEF/TCF transcription factor activation. These mice have been used as a reporter for canonical Wnt signalling; canonical Wnts inhibit glycogen-synthase kinase-3β (GSK-3β) from phosphorylating β-catenin, which then accumulates in the cytoplasm, translocates to the nucleus and activates transcription of LEF/TCF target genes. TOPGAL expression in lung at E12.5 is present in the distal epithelium (De Langhe *et al.*, 2005).

3. Flk-1$^{+/LacZ}$ mice (Shalaby *et al.*, 1995) are a reporter line for Flk-1 marking vasculogenesis. Flk-1, also known as VEGF-R2, is a receptor for VEGF-A which is exclusively expressed in the mesenchyme of the developing lung (Del Moral *et al.*, 2006b) and is an early marker of endothelial cell precursors with very high expression during vasculogenesis and angiogenesis (Yamaguchi *et al.*, 1993).

The morning of plug was considered E0.5, all females were humanely sacrificed in accordance with Home Office or Children's Hospital Los Angeles Institutional Animal Care and Use Committee regulations. E12.5 lungs from each transgenic line were cultured in the presence of either 1.05 mM Ca^{2+}_o or 1.7 mM Ca^{2+}_o for 48 h as in section 2.1.1. The level of branching morphogenesis was counted at 0, 24 and 48 h to ensure that the effect of $[Ca^{2+}]_o$ on branching morphogenesis was maintained despite their transgenic status.

6.1.2 X-gal Staining of Cultured LacZ Positive Lungs

After 48 h in culture, the lung explants from reporter mice (Section 6.1.1) were washed briefly in PBS and fixed in 4% PFA for 3 minutes at RT. Freshly prepared X-gal solution (0.1M phosphate buffer (pH 7.3) with 2 mM $MgCl_2$, 5mM $C_6N_6FeK_4$, 5mM $C_6N_6FeK_3$, and 1 mg/ml X-gal [5-bromo-4-chloro-3-indolyl-β-D-galactoside]) was applied to the lungs and they were stained in the dark for 2-48 h with rocking at 37°C. After sufficient staining was achieved the tissue was washed briefly in PBS and then post-fixed and stored in 4% PFA at 4 °C.

6.1.3 Immunohistochemistry

E11.5 lung buds and isolated epithelium were fixed in ice-cold methanol for 15 min, then washed in PBS at 4°C for 1 h. Specimens were exposed to the following primary antibodies; mouse monoclonal anti-smooth muscle actin antibody conjugated to cy3 (1:200, Sigma-Aldrich, Dorset, UK), or rat monoclonal antibody to E-cadherin (1:200, Abcam, Cambridge, UK), both antibodies were co-applied with a rabbit polyclonal anti-CaR antibody (1:200, US Biologicals, Massachusetts, USA). Primary

antibodies were incubated overnight at 4°C. The following day the specimens were washed in PBS at RT for 1 h and then the secondary antibodies, goat anti-rat conjugated to CY3 (1:200, Jackson Laboratories, Pennsylvania, USA) or donkey anti-rabbit conjugated to Alexa 488 (1:200, Molecular Probes, Eugene, OR., U.S.A.) was applied for 2 h at RT with gentle shaking. The final wash in PBS was done at RT for 1 h. The specimens were then mounted on a glass slide in Prolong anti-fade mounting medium (Molecular Probes, Eugene, OR., U.S.A.) and allowed to set at RT before being imaged by confocal microscopy.

6.2 Philosophy of Work

The contents of this chapter address two separate lines of experimental inquiry. Firstly, changes in $[Ca^{2+}]_o$ and CaR activation have been previously shown to affect gene expression (Brown & MacLeod, 2001; Peterlik & Cross, 2005). Therefore, in order to test the hypothesis that gene expression patterns are differentially regulated by $[Ca^{2+}]_o$ in the lung explant culture model, transgenic LacZ-expressing reporter mice were used to demonstrate global changes in FGF-10, β-catenin and Flk-1 expression. Secondly, as a preliminary investigation into the possible mechanism of CaR action, I also performed immunofluorecent detection of CaR in conjunction with α-smooth muscle actin, or E-cadherin on E11.5 lungs to determine if there was any co-localisation between these proteins.

6.3 Effects of $[Ca^{2+}]_o$ on Gene Expression

The effects of $[Ca^{2+}]_o$ on gene expression during lung development were tested using three different transgenic mice which express β-galactosidase under the control of a gene specific promoter. For all three strains, branching morphogenesis increased approximately 100% after culture for 48 h in the presence of 1.05 mM Ca^{2+}_o, while branching morphogenesis in the presence of 1.7 mM Ca^{2+}_o for 48 h was approximately 60%. These levels of branching morphogenesis were comparable to the levels previously obtained from C57/BL6 lung explant cultures.

In preliminary experiments (n=3 lungs per Ca^{2+}_o condition), lung explants from $Fgf10^{+/LacZ}$ mice cultured in the presence of 1.7 mM Ca^{2+}_o showed an increase in FGF-10 expression in their distal mesenchyme, without an attendant increase in branching morphogenesis (Fig. 6.1). Lung explants from TOPGAL mice, cultured for 48 h in the presence of 1.05 mM Ca^{2+}_o ($n \geq 11$) show a substantial amount of staining in their distal epithelium and main bronchi (Fig. 6.2B and C, left panels). When cultured in the presence of 1.7 mM Ca^{2+}_o, this expression appears decreased in the distal epithelium, although the levels of β-galactosidase staining in the main bronchi appear unchanged (Fig. 6.2B and C, right panels).

Lung explants from $Flk\text{-}1^{+/LacZ}$ mice, cultured for 48 h in the presence of 1.7 mM Ca^{2+}_o had greatly increased expression of Flk-1 in comparison to the staining present in lungs cultured in the presence of 1.05 mM Ca^{2+}_o (n = 7, Fig. 6.3) for 48 h. In the presence of 1.7 mM Ca^{2+}_o the localisation of Flk-1 also changes, with strands of vasculature criss-crossing over and around the developing branches (Fig. 6.3C, right

panel) while expression in the presence of 1.05 mM Ca^{2+}_o is limited to the mesenchymal spaces between the developing branches (n = 7, Fig. 6.3C, left panel).

6.4 Immunofluorescent Detection of CaR, α-smooth muscle actin and E-cadherin in E11.5 Mouse Lung.

In order to begin the experimental programme to define definitively the mechanism by which the CaR is mediating its effects, preliminary detection of CaR in conjunction with α-smooth muscle actin and E-cadherin was performed using a protocol for whole mount immunofluorescence in freshly isolated E11.5 lungs and isolated epithelium. CaR expression was visualised using the USB antibody which detects a region in the C-terminal portion of the protein. In all whole mount samples there was robust detection of the CaR in both the epithelium and the mesenchyme (Fig. 6.4-6.7). CaR and α-smooth muscle actin expression did not appear to co-localise, with α-smooth muscle actin expression restricted to the proximal airways (Fig. 6.4). CaR expression in the mesenchyme appeared stellate with the strands of expression following the contours of the developing branches (Fig. 6.4-6.7). CaR expression in the epithelium was adjacent to areas of E-cadherin expression at the plasma membrane (Fig. 6.6-6.8) and appeared to be fairly uniform in distribution between the luminal and basolateral membranes.

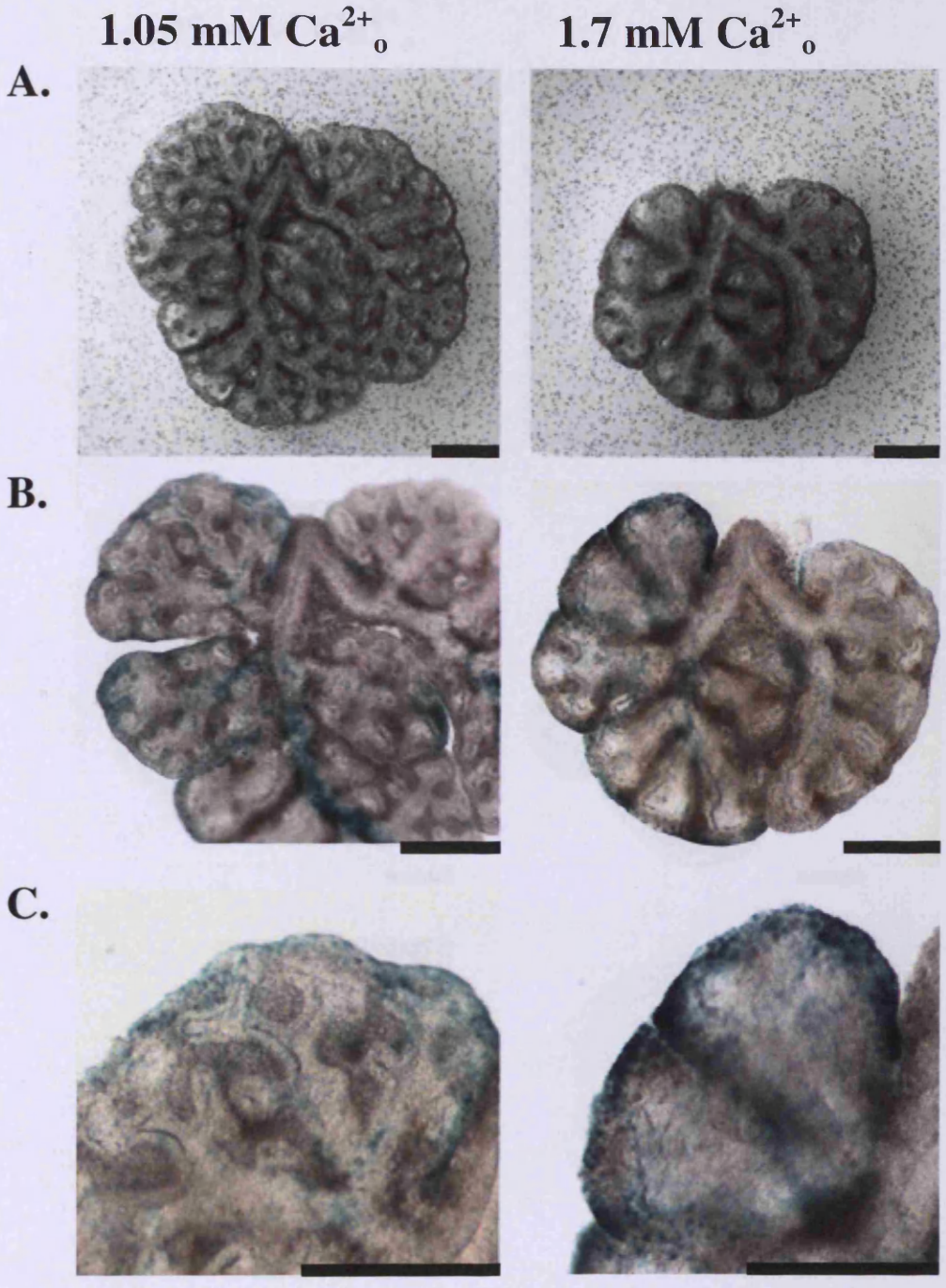

Figure 6.1: FGF-10 expression is $[Ca^{2+}]_o$-sensitive. E12.5 lungs were removed from $Fgf10^{+/LacZ}$ mice and cultured in the presence of 1.05 mM (left panel) or 1.7 mM Ca^{2+}_o (right panel) for 48 h and responded with expected levels of branching morphogenesis relative to $[Ca^{2+}]_o$ (**A**). FGF-10 expression was visualised with β-galactosidase staining (**B** and **C**) showing increased expression in lungs cultured in 1.7 mM Ca^{2+}_o. Lungs shown are representative of 3 lungs per condition from a single isolation. Scale bars = 300 μm.

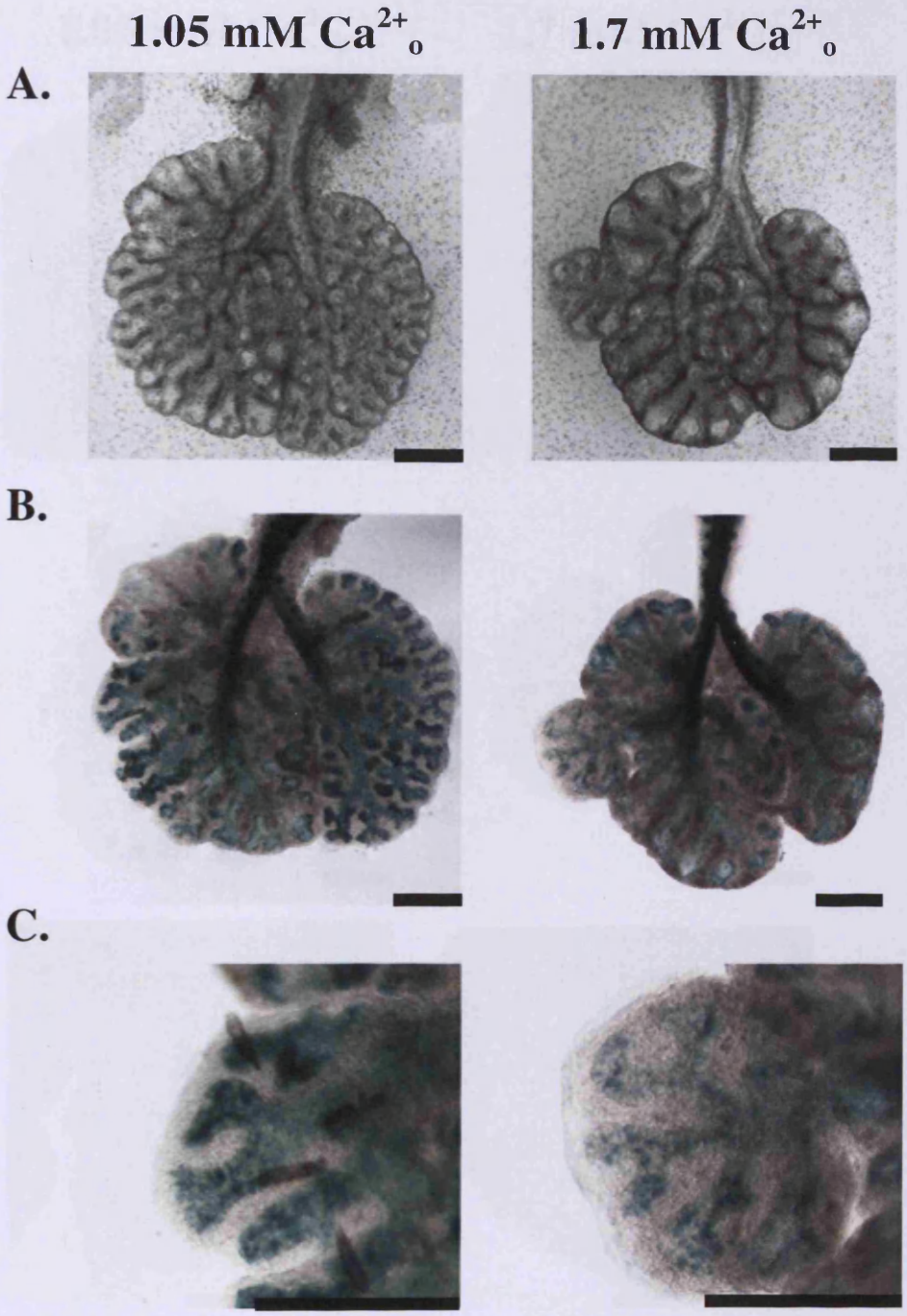

Figure 6.2: β-Catenin-LEF/TCF complex expression is $[Ca^{2+}]_o$-sensitive. E12.5 lungs were removed from TOPGAL mice and cultured in 1.05 mM (left panel) or 1.7 mM Ca^{2+}_o (right panel) for 48 h and responded with expected levels of branching morphogenesis relative to $[Ca^{2+}]_o$ (A). β-Catenin-LEF/TCF complex expression was visualised with β-galactosidase staining (B and C higher magnification) showing decreased β-Catenin-LEF/TCF complex expression in lungs cultured in 1.7 mM Ca^{2+}_o. Lungs shown are representative of >11 lungs per condition from 3 separate isolations. Scale bars = 300 μm.

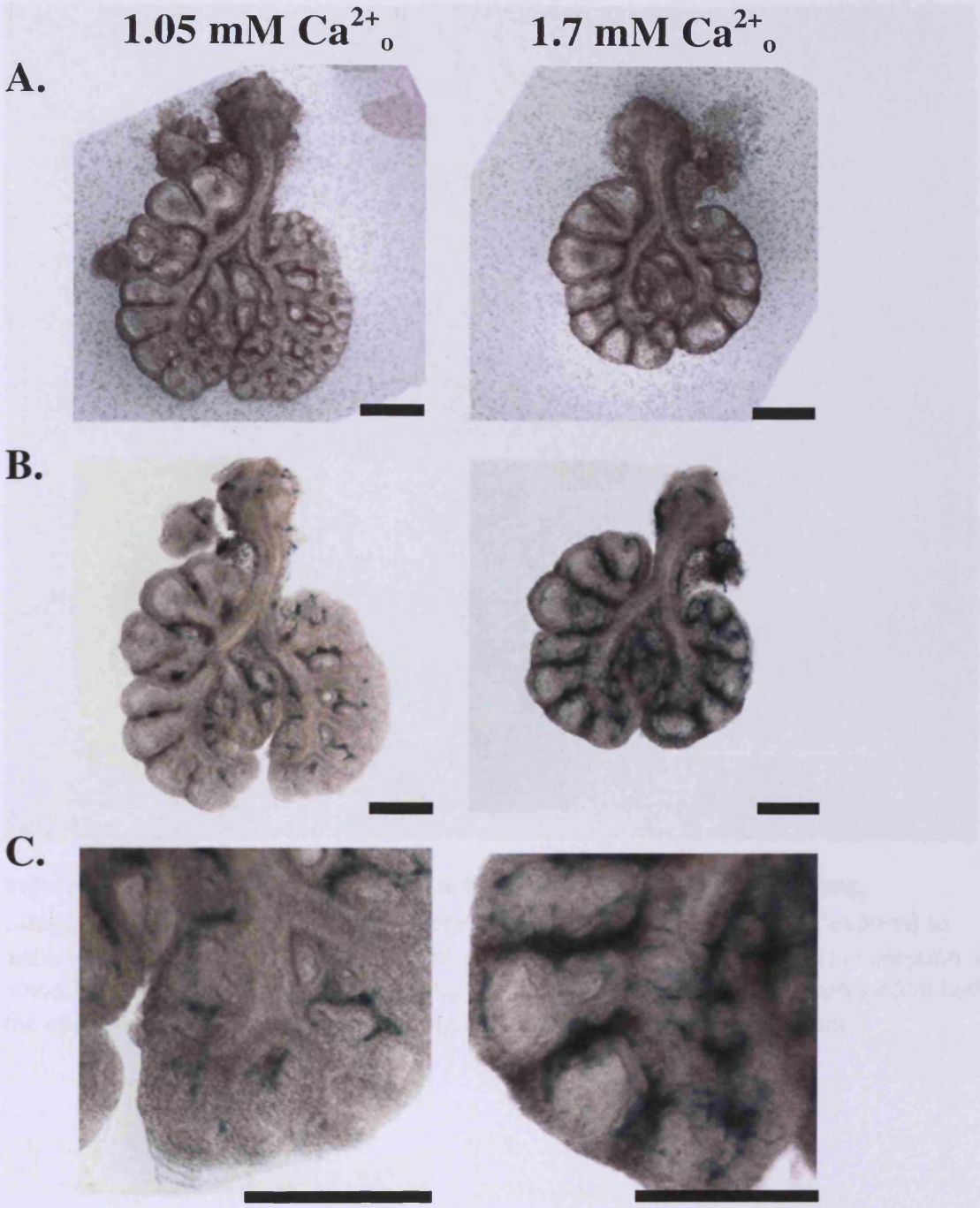

Figure 6.3: 1.7 mM Ca^{2+}_o induced vasculogenesis shown by an increase in Flk-1 expression. E12.5 lungs were removed from Flk-$1^{+/LacZ}$ mice and cultured in 1.05 mM (left panel) or 1.7 mM Ca^{2+}_o (right panel) for 48 h and responded with expected levels of branching morphogenesis relative to $[Ca^{2+}]_o$ (A). Flk-1 expression was visualised with β-galactosidase staining (B and C higher magnification) showing increased vasculogenesis in lungs cultured in 1.7 mM Ca^{2+}_o. Lungs shown are representative of 7 lungs per condition from 2 separate isolations. Scale bars = 500 μm.

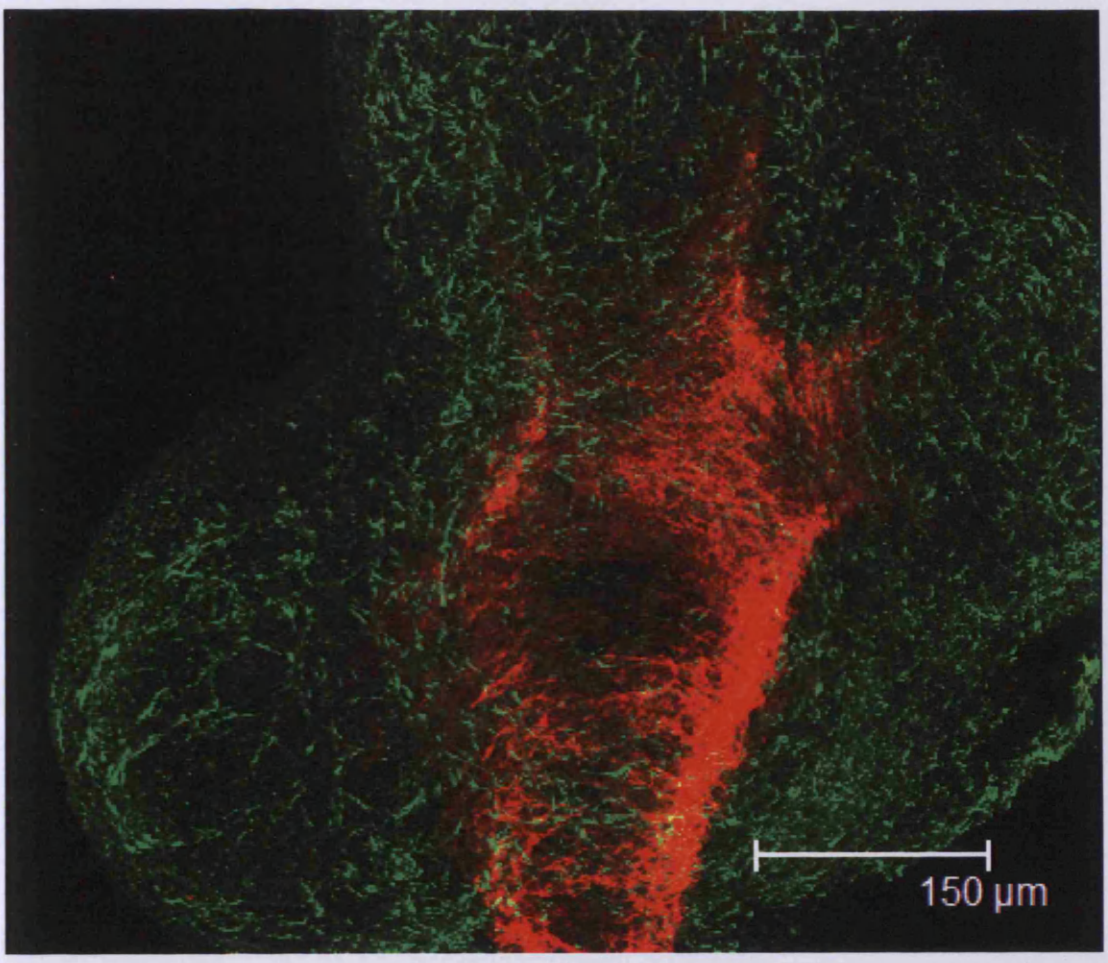

Figure 6.4: CaR and α-smooth muscle actin localisation in E11.5 mouse lung.
Lungs from E11.5 mouse embryos were fixed in ice-cold methanol and exposed to antibodies for detection of CaR (green) and α-smooth muscle actin (red) expression. α-smooth muscle actin is expressed in the proximal airway and CaR is expressed in both the epithelium and mesenchyme throughout the lung. Scale bar = 150 µm.

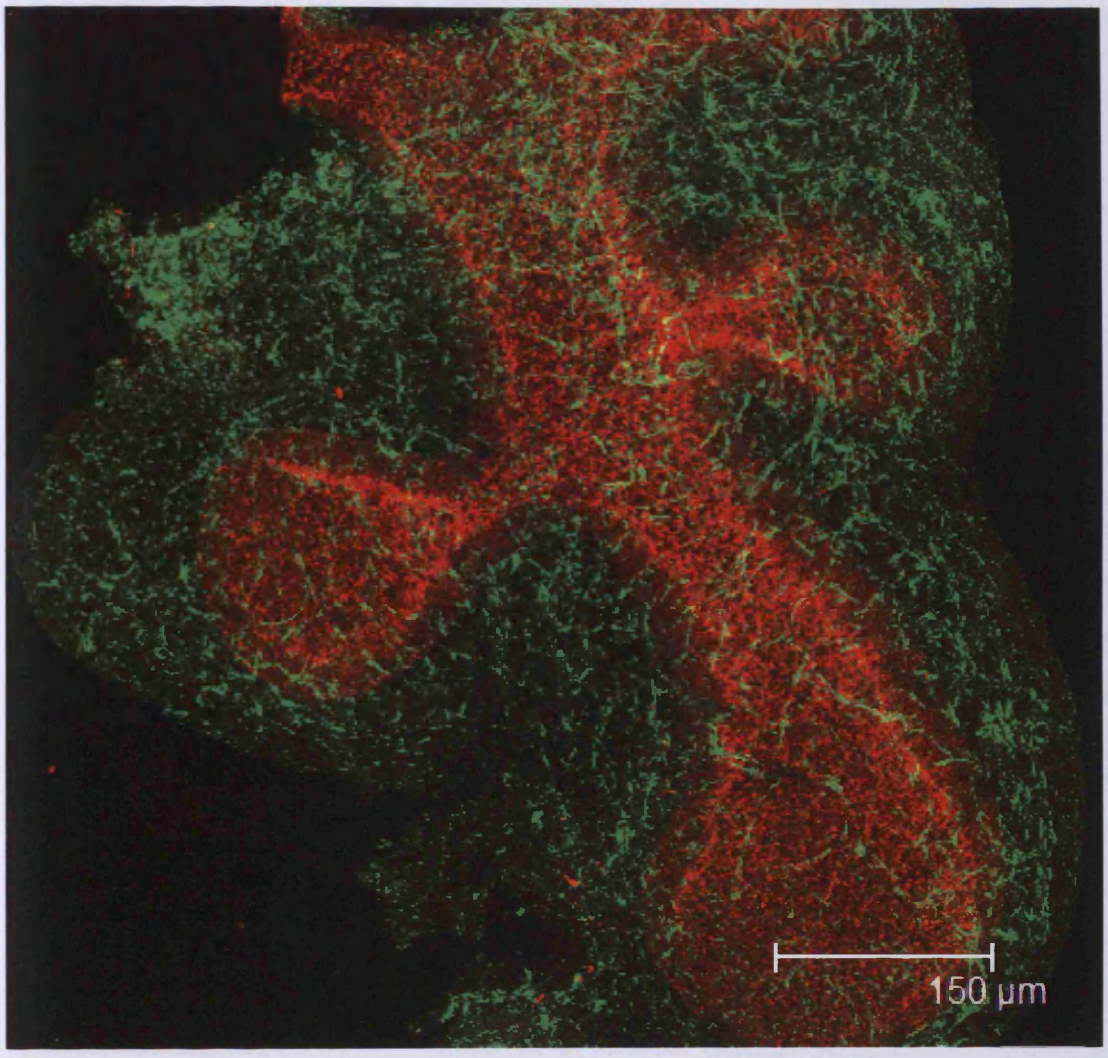

Figure 6.5: CaR and E-cadherin localisation in E11.5 mouse lung. Lungs from E11.5 mouse embryos were fixed in ice-cold methanol and exposed to antibodies for detection of CaR (green) and E-cadherin (red) expression. E-cadherin is expressed throughout the developing epithelium and CaR is expressed in both the epithelium and mesenchyme throughout the lung. Scale bar = 150 µm.

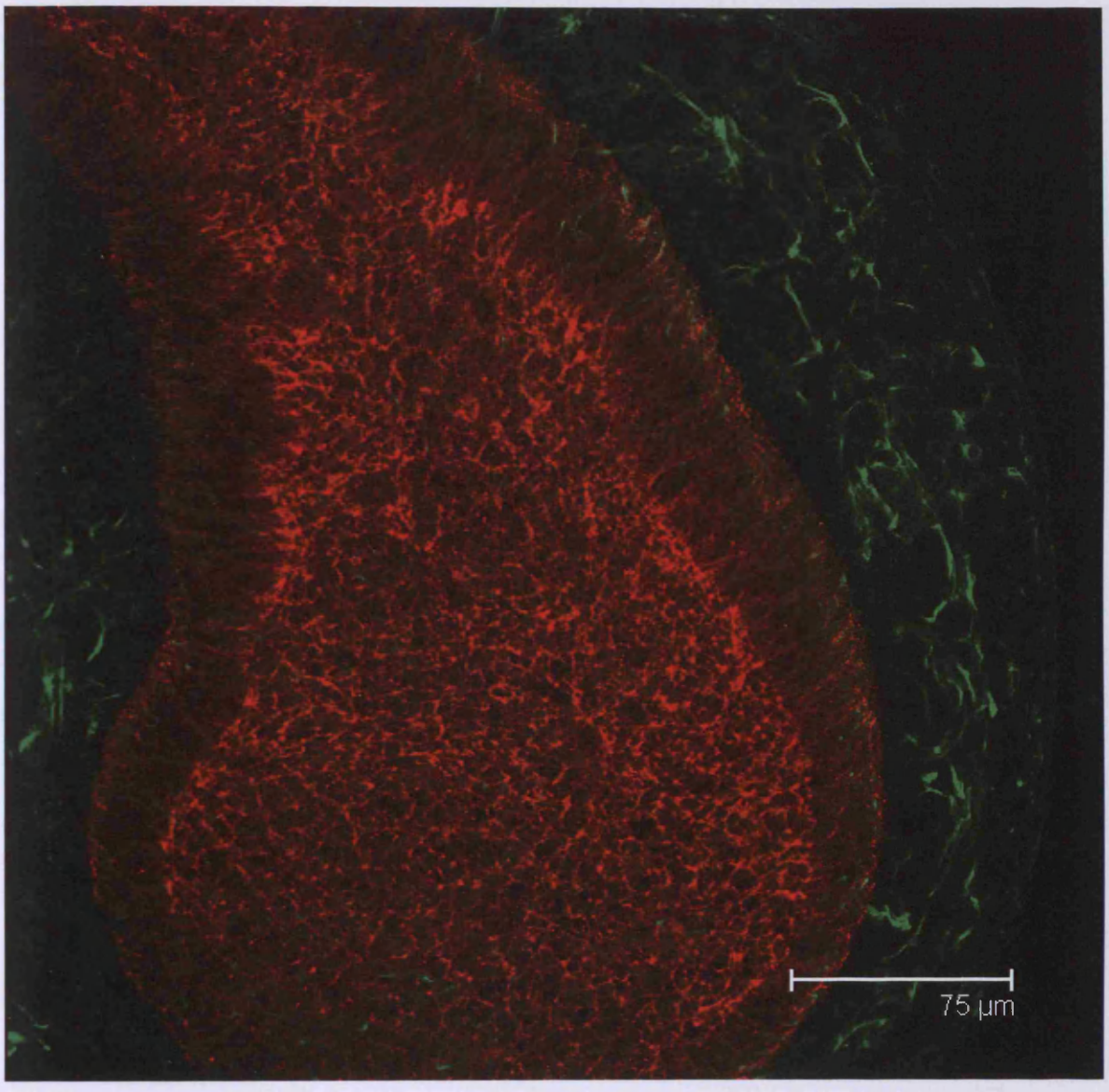

Figure 6.6: CaR and E-cadherin localisation in E11.5 mouse lung terminal bud. Lungs from E11.5 mouse embryos were fixed in ice-cold methanol and exposed to antibodies for detection of CaR (green) and E-cadherin (red) expression. E-cadherin is expressed throughout the developing epithelium and CaR is expressed in both the epithelium and mesenchyme throughout the lung. Scale bar = 75 µm.

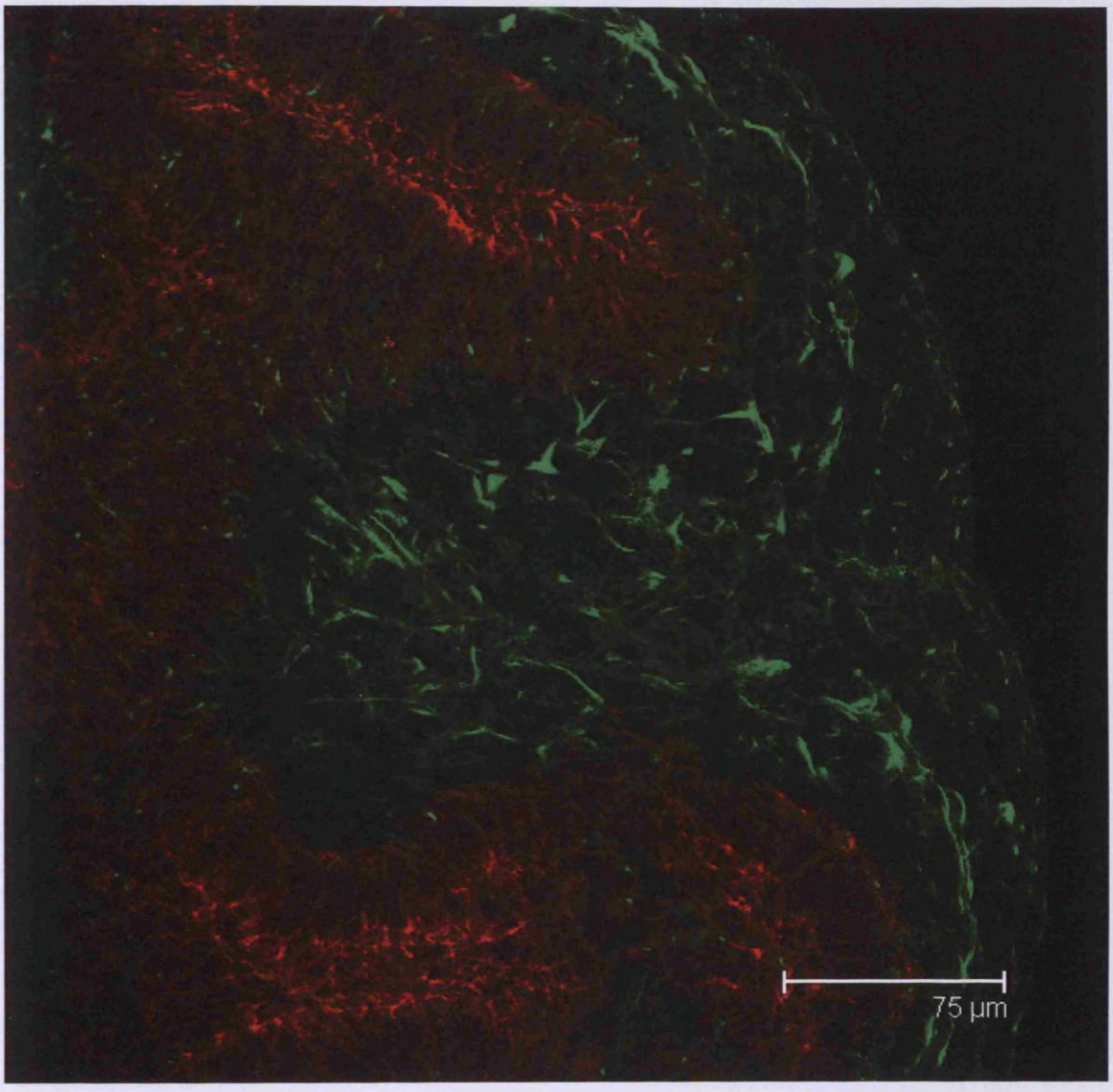

Figure 6.7: CaR and E-cadherin localisation in E11.5 mouse lung terminal buds and proximal airway. Lungs from E11.5 mouse embryos were fixed in ice-cold methanol and exposed to antibodies for detection of CaR (green) and E-cadherin (red) expression. E-cadherin is expressed throughout the developing epithelium and CaR is expressed in both the epithelium and mesenchyme throughout the lung. Scale bar = 75 µm.

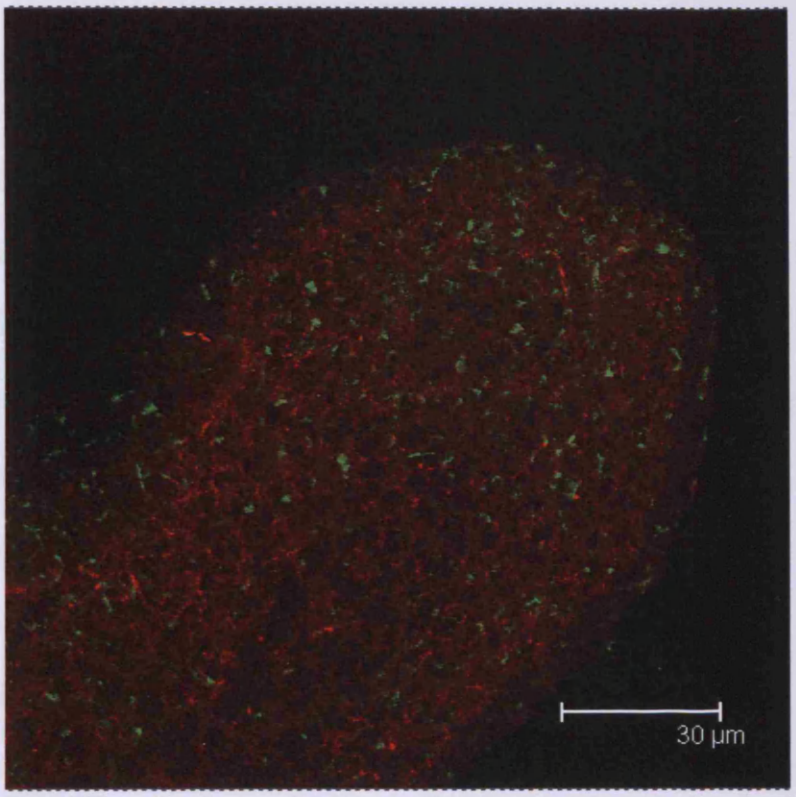

Figure 6.8: CaR and E-cadherin localisation in E11.5 mouse lung isolated epithelial buds. Epithelial buds from E11.5 mouse embryos were stripped of their mesenchyme, fixed in ice-cold methanol and exposed to antibodies for detection of CaR (green) and E-cadherin (red) expression. E-cadherin is expressed throughout the epithelium as is CaR. Scale bar = 30 µm.

6.5 Chapter Discussion

While preliminary, the results presented in this chapter show that $[Ca^{2+}]_o$, possibly acting through the CaR, can affect gene expression levels of two developmentally important proteins, FGF-10 and β-catenin, as well as influence the quantity and locality of vascularisation in the developing lung. Also, using immunofluorescence on freshly isolated tissue has allowed for a clearer localization of the CaR protein, and demonstrated its proximity to α-smooth muscle actin and E-cadherin in freshly isolated E11.5 lungs.

The possibility of $[Ca^{2+}]_o$ affecting the cellular processes occurring in lung development is supported by the changes in gene expression seen in the studies with the LacZ reporter mice. Although still preliminary, the results suggest that there is increased and diffuse FGF-10 expression in lungs cultured in the presence of 1.7 mM Ca^{2+}_o. These results would fit into a model where increased $[Ca^{2+}]_o$ is linked to airway expansion. Indeed, mice which lack expression of Shh, a negative regulator of FGF-10 expression, have lungs with greatly dilated airways (Pepicelli *et al.*, 1998). It is also possible that increased FGF-10 expression could cause the differentiation of epithelial cells and impede branching due to a change in cellular identity. This possibility is supported by data from cultures of human skin keratinocytes, where exogenous FGF-10 application, in conjunction with increased $[Ca^{2+}]_o$ promotes differentiation (Marchese *et al.*, 2001).

A further indication that high $[Ca^{2+}]_o$ may be impacting the differentiation of the high Ca^{2+}_o lung explant cultures is the decrease in TOPGAL expression seen when lungs are cultured in the presence of 1.7 mM Ca^{2+}_o. TOPGAL expression is dependent upon stabilisation of β-catenin and is also responsive to TCF3/LEF1 transcription factor

activation (DasGupta & Fuchs, 1999). In the mouse lung, TOPGAL expression is strong in the distal epithelium at E12.5, but by E14.5 it is restricted to the proximal epithelium (De Langhe *et al.*, 2005). Therefore it is possible that the decrease in TOPGAL expression seen in mouse lungs cultured in the presence of 1.7 mM Ca^{2+}_o correlates to these lungs moving on to a later point of development. It is also possible that Wnt5a secretion and signalling is interfering with canonical Wnt activity in the stabilisation of β-catenin, as it does in the intestine (MacLeod *et al.*, 2007; Pacheco *et al.*, 2007), although this possibility remains to be tested.

The most convincing and complete experiment from these preliminary data shows that physiological fetal $[Ca^{2+}]_o$ induces vascular development, as shown by the results using reporter mice expressing LacZ under the control of the Flk-1 promoter. Flk-1 expression, and therefore the amount of developing vasculature, is greatly increased in cultures exposed to 1.7 mM Ca^{2+}_o. The increase in Flk-1 expression correlates with a larger quantity of endothelial cell precursors. In 1.7 mM Ca^{2+}_o, instead of being concentrated only in the proximal mesenchyme and between branches, as these precursors are in 1.05 mM Ca^{2+}_o, they surround the branches with a diffuse, net-like pattern. This induction of vascular development by high Ca^{2+}_o could be important in the developing fetus to ensure optimal matching between branches and vasculature for eventual gas exchange surfaces.

Not only may high Ca^{2+}_o change the expression patterns of these proteins, but it may also impact on the cellular structure of the epithelial sheet by activating CaR interaction with E-cadherin (See Chapter 4). To begin investigating if the interaction between CaR and E-cadherin occurs in the developing lung, I performed

immunofluorescence on E11.5 lungs in order to determine the baseline localisation of these two proteins. The results presented here show that CaR and E-cadherin are located in the same cellular compartment, the epithelium, and are closely associated, but not over-lapping (using this antibody for detection), at the cellular membrane. Using this detection protocol, mesenchymal expression of CaR is also robust at this time point. Previous immunohistochemistry of CaR did not show a robust mesenchymal presence until E13.5, however, as the prior detection was performed on 5 μM thick sections it may not have been possible to appreciate fully the stellate expression pattern seen in this chapter.

Finally, the results of this chapter show that by using transgenic mouse models and improved immunohistochemistry protocols, I have started the programme of work to carry this project forward. The potential implications of the results of this project and the continuation of this programme of work are discussed in the following chapter.

CHAPTER 7:
GENERAL DISCUSSION

7.1 $[Ca^{2+}]_o$ in Culture Conditions and the Developing Fetus

Currently many laboratories that routinely perform lung explant cultures do not consider $[Ca^{2+}]_o$ as an important factor within their culture conditions. This may be a mistake, because different types of culture media contain $[Ca^{2+}]_o$ that differ greatly. As seen within the results from Chapter 2, variations in the $[Ca^{2+}]_o$ of the culture medium used can alter the amount of lung growth within explant cultures quite dramatically. For instance, the routinely used BGJb medium contains 2.5 mM calcium, as calcium lactate (www.invitrogen.com, catalogue number 12591038), a concentration which this study has shown to be an inhibitory $[Ca^{2+}]_o$ for the branching morphogenesis of lung explants.

One study that has published results using this medium, supplemented their explants with serum (Nogawa & Hasegawa, 2002). Indeed, when BGJb medium is used alone, the airways of lung explants develop poorly without any definable acinar structure (Chinoy *et al.*, 1998). The addition of a combination of growth factors (EGF and TGF-β1, as may be present in serum) to this preparation results is a normal pattern of branching and differentiation (Chinoy *et al.*, 1998). Therefore, at least some inhibitory effects of culture conditions could be overcome by the addition of serum and/or growth factors. In conjunction with this idea, the results of the experiments in Chapter 2 imply that branching morphogenesis can be rescued by reducing the $[Ca^{2+}]_o$ in the culture medium, without adding growth factors or serum. How this rescue occurs is currently unknown, but it could be due to an effect on the composition of the luminal fluid within the lung.

It is accepted that the fluid within the developing lung is important for the formation of an optimally functioning lung (Hooper & Harding, 1995). The exact composition of the mouse's lung fluid, and therefore the exact $[Ca^{2+}]_o$ to which the

developing lung is exposed, remains unresolved. Classic studies done on late gestation sheep fetuses (Adamson *et al.*, 1969) showed that alveolar fluid is of a distinctly different composition to either amniotic fluid or blood plasma. Total $[Ca^{2+}]$, [phosphates], and $[HCO_3^-]$ were all lower in alveolar fluid, regardless of the age at which the samples were collected. Total $[Ca^{2+}]$ was 0.8 mM in alveolar fluid, as opposed to 1.6 mM in amniotic fluid and 3.3 mM in plasma.

The composition of alveolar fluid has not yet been confirmed in the developing mouse for practical reasons of sample size or in human subjects for ethical reasons. If these values could be obtained, it would go some way to putting the responses observed in this study into the physiological context. In the absence of these data, it might be inferred from the above sheep studies, that the $[Ca^{2+}]_o$ of the lung lumen is substantially lower than that of plasma, providing a low $[Ca^{2+}]_o$ environment ideal for branching morphogenesis. Until the practicalities of determining $[Ca^{2+}]_o$ from scant microlitres of alveolar fluid can be overcome, it is best that research is focused on understanding the phenomena as they are witnessed *in vitro*.

Considering Kovacs *et al.* (1998), it was assumed that the developing mouse and human lung, at the early pseudoglandular phase (in mice, E11.5-12.5), develops in a relatively hypercalcaemic environment. Therefore, it was assumed that the serum $[Ca^{2+}]_o$ of the developing embryos is approximately 1.7 mM, as previously published for late gestation (E18.5) mice (Kovacs *et al.*, 1998).

7.2 Mechanisms of Ca^{2+}_o effects on Lung Development

Taking the results presented in this study into consideration with previously published observations, there are potentially two different mechanisms by which the CaR can be exerting its influence on the branching morphogenesis of the lung. It is entirely possible that the physiological condition of the developing lung is a combination of these two mechanisms. However, for clarity the following two possibilities will be discussed separately:

1. A CaR and E-cadherin mechanism (Fig. 7.1);
2. A CaR and Wnt5a mechanism (Fig. 7.2).

At the end of Chapter 4, there are listed five pieces of data that need to be considered to interpret the mode of CaR activation in lung explant cultures. These are:

1. E-cadherin is constitutively expressed in epithelial cells at the same developmental time point as CaR (Hirai *et al.*, 1989);
2. application of active antibodies to perturb E-cadherin activity results in disrupted morphogenesis with deformed tubules (limited luminal space) most likely resulting from the reduced efficacy of intracellular connection (Hirai *et al.*, 1989);
3. ectopic over-expression of E-cadherin in isolated epithelial cultures impairs branching (Liu *et al.*, 2008) and results in large cyst-like epithelial cultures;
4. CaR activation in keratinocytes is related to E-cadherin mediated PI_3K-PLC activation (Tu *et al.*, 2008);
5. rescue of high Ca^{2+}_o branching morphogenesis suppression can be instigated through the inhibition of both PLC and PI_3K.

In addition to these five points, the TPD data from Chapter 2 and 4 should also be considered. These data showed that Cl^- secretion increases in response to CaR activation by high $[Ca^{2+}]_o$ and R-568, but without a concurrent increase in branching.

Considering all of these factors, one possible model for the mode of CaR exerting is effects on lung branching morphogenesis is that CaR activation increases Cl^- secretion in response to high $[Ca^{2+}]_o$ (possibly via ion channel activity in the epithelial cell membrane, Fig. 7.1). In conjunction with this activation, if similar to skin epithelial keratinocytes (Xie & Bikle, 2007; Tu *et al.*, 2008), then the following two pathways are also activated.

1. CaR interacts with E-cadherin, through an as yet unidentified mechanism, which associates with β-catenin and p-120-catenin. This complex recruits and associates with PI_3K, produces PIP_3, which in turn causes the activation of PLC. This ultimately results in an increase in $[Ca^{2+}]_i$ which could affect the cell cycle and differentiation programme of the developing lung.
2. Activation of CaR promotes the formation of E-cadherin mediated intercellular adherens junctions by activation of Src family tyrosine kinase signalling. This change in the epithelial cell-cell interaction alters the ability of the epithelium to respond to the increase in Cl^- secretion with an increase in branching, as has been previously reported in other situations of increased pressure (Blewett *et al.*, 1996). Therefore, the terminal buds swell, in a similar manner to epithelium where E-cadherin is over-expressed (Liu *et al.*, 2008).

This inability to respond to increased secretion/pressure with branching is possibly due to a difference in the physics of the branching situation, as described by Fleury and Wantanabe (2002). That is, the increase in intercellular junctions increases the viscosity/rigidity of the developing epithelium. Therefore, there are no

positions of reduced viscosity/rigidity from which the cells can protrude and form branches.

The second possible mode of CaR action involves the CaR-mediated secretion of Wnt5a, a non-canonical Wnt protein that can negatively impact canonical Wnt signalling (Fig. 7.2). CaR activation has been shown to up-regulate Wnt5a secretion in both adenocarcinoma cells (MacLeod *et al.*, 2007; Pacheco *et al.*, 2007) and colonic myofibroblasts (Pacheco & MacLeod, 2008). In the lung, Wnt5a over-expression increases the expression of FGF-10. The ability of the epithelium to respond to the signalling activity of FGF-10 is reduced, possibly by direct effects on FGF-10, and/or interfering with the interaction of FGF-10 and Shh signals (Li *et al.*, 2005). Within lung explant cultures exposed to high $[Ca^{2+}]_o$, CaR activation could lead to secretion of Wnt5a. Wnt5a antagonises the interactions between FGF-10 and Shh, as well as the activity of Bmp4, all of which are vital for inducing branching morphogenesis in the distal bud tips. It is also possible that Wnt5a secretion could be involved in the suppression of branching morphogenesis by high $[Ca^{2+}]_o$ by decreasing the stabilisation of β-catenin. However, there is, as yet, no published data to support this idea.

Both of these models provide possible mechanisms of action for the CaR mediated suppression of branching morphogenesis. Further experimentation will help determine if either, or a combination, of these models is a viable representation of the *in vivo* developmental situation. By continuing to investigate the role of the CaR in lung development, it may be possible to determine if manipulations of these pathways can result in better developmental outcomes in situations of lung hypo- or hyper-plasia.

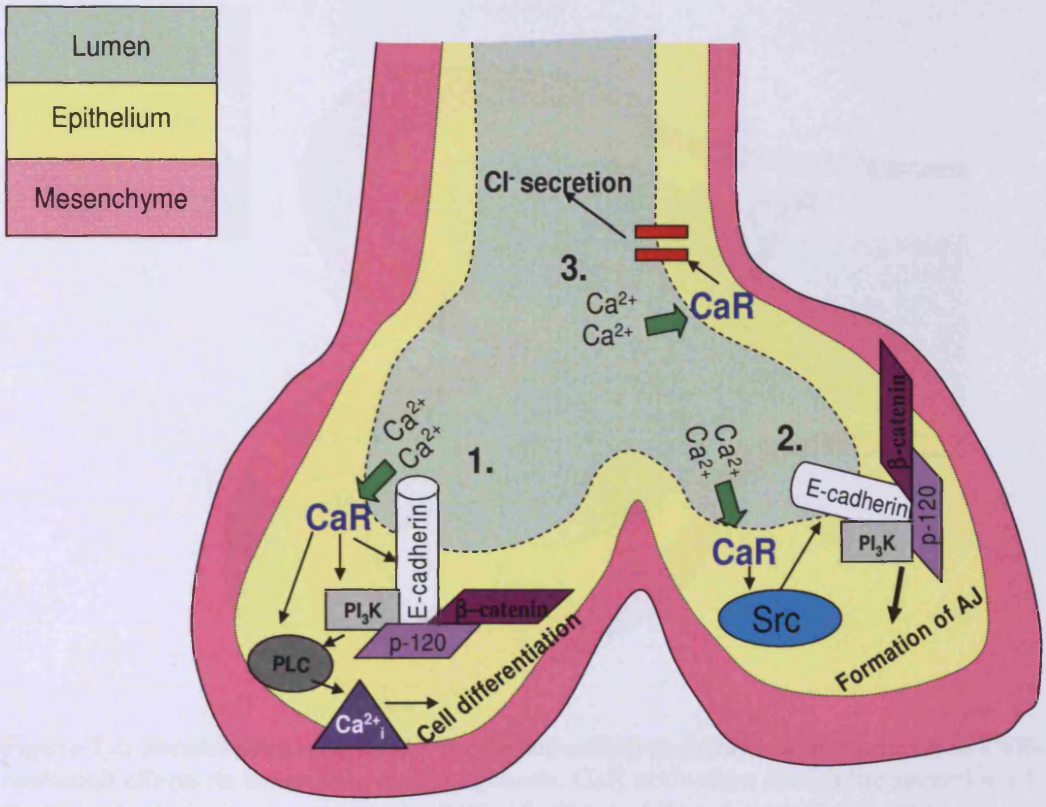

Figure 7.1: Proposed model for the signalling pathway and mechanism of CaR-mediated effects on branching morphogenesis. CaR activation causes E-cadherin to associate with PI_3K and induce PLC activation resulting in increases in $[Ca^{2+}]_i$ and cell differentiation (**1.**). Concurrently CaR activation initiates Src tyrosine kinase phosphorylation causing E-cadherin and its associated catenins (p-120 and β-catenin) with PI3K to form adherens junctions with neighbouring cells (**2.**). These cell-cell interaction changes decrease the ability of the epithelium to branch in response to the CaR-mediated increase in Cl^- secretion which is the result of activation of ion channels (red bars, **3.**).

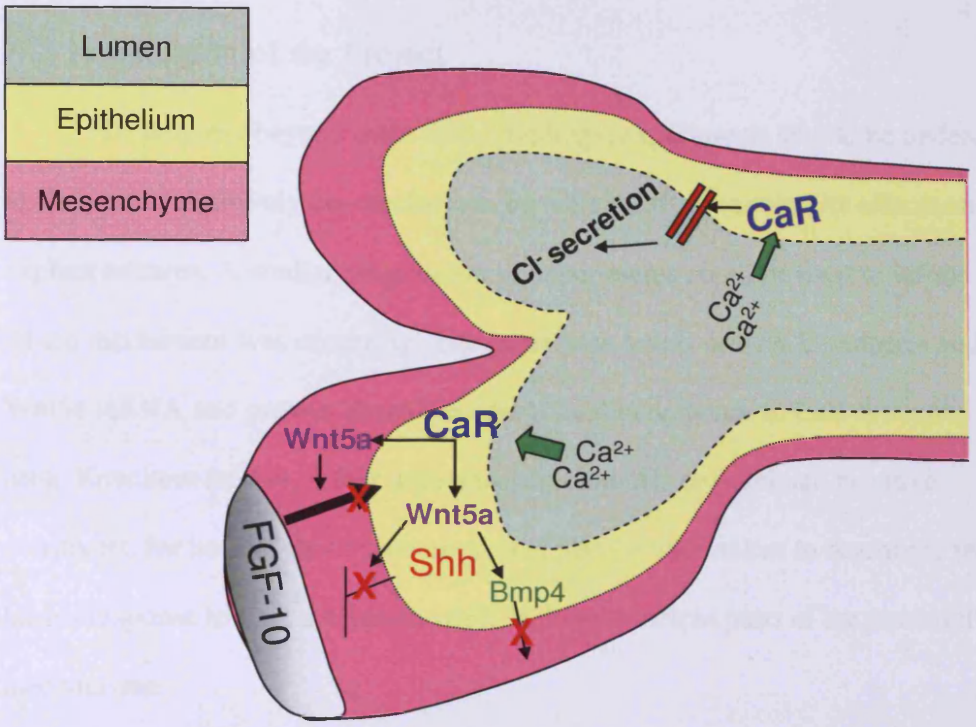

Figure 7.2: Second proposed model for the signalling pathway and mechanism of CaR-mediated effects on branching morphogenesis. CaR activation causes the secretion of Wnt5a which then antagonises the FGF-10, Shh and Bmp4 signalling activities which are vital for branching morphogenesis. Therefore the lung does not respond to the increase in Cl^- secretion by ion channels (red bars) activated by CaR with an increase in branching morphogenesis.

7.3 Progression of the Project

To progress beyond these initial findings, experiments should be undertaken to elucidate definitively the mechanism by which CaR is exerting its effects on lung explant cultures. A similar progression of experiments could be used to inform as to which mechanism was occurring. The expression levels of both E-cadherin and Wnt5a mRNA and protein should be determined in response to CaR activation in the lung. Knockout studies, either with transgenic models or dominant negative constructs, for both of these proteins should also be undertaken to determine the lung's response to CaR activation while lacking principle parts of the potential mechanisms.

Determining the exact mechanisms of CaR mediated effects on branching morphogenesis is important for understanding the pharmacology of this receptor within the context of the lung development. There are also possible downstream effects by both CaR activation and direct actions of Ca^{2+}_o alone, on gene expression and the formation of the vascular network. Definitive distinction between the role of Ca^{2+}_o and the role of CaR action in lung development requires two separate lines of enquiry to be undertaken. Firstly, test the hypothesis that Ca^{2+}_o, acting through CaR activation, is responsible for changes in gene expression. This can be accomplished by using transgenic reporter mouse lungs for explant culture, as in Chapter 6. The repetition of lung explant cultures on FGF-$10^{+/LacZ}$ and TOPGAL mouse strains will improve the robustness of the data for the observed effects of $[Ca^{2+}]_o$ on their expression levels and localities. Along with this, lung explants from these mice should be used in cultures with R-568 application to determine if any of the observed changes in expression are mediated by the activation of the CaR.

Further explant culture studies with lung explants from Flk-$1^{+/LacZ}$ mice should be performed in the presence of R-568 to determine if the increase in vascularisation observed in the presence of high $[Ca^{2+}]_o$ is due to CaR activation. These studies could provide an underlying role for CaR in lung development. This role could be that CaR activation is a physiological brake to control the level of branching morphogenesis, so that optimal matching occurs between branch development and vasculogenesis.

The level and locality of Wnt5a expression in lung explant cultured should be determined to test the hypothesis that Wnt5a secretion and/or signalling are activated in response to CaR activation. This should be determined in response to both low and high $[Ca^{2+}]_o$, as well as in response to specific activation of CaR by R-568. Transgenic models, PCR, western blotting and immunohistochemistry techniques could all be used to test this hypothesis. Possible downstream constituents of Wnt5a activities include Bmp4 and Shh. Their expression levels and localisation should also be determined under the same conditions (*i.e.* in response to $Ca^{2+}{}_o$ and CaR activation), with or without the presence of Wnt5a. These studies would inform on changes, resulting from activation of CaR and Wnt5a, in their patterns (of expression or localisation) that could be affecting the lung developmental programme.

Finally, in order to demonstrate conclusively the role of CaR in lung development, without the complicating factor of CaR splice variant activity, there are two other mouse models with aberrant CaR expression or activity. These transgenic mouse lines are:

1. Mice with an activating mutation of CaR, *i.e. Nuf* mice (Hough *et al.*, 2004);
2. Mice with a tissue-specific, conditional CaR knockout due to loxP sites flanking exon 7 of CaR gene (Chang *et al.*, 2008).

Lungs from both of these transgenic mouse lines should be used for explant cultures to determine the branching response to $[Ca^{2+}]_o$ and R-568 application. Additionally, the investigation for lung pathology should be undertaken in adult animals. This could lead to the discovery of post-natal consequences after developmental perturbation of CaR activity.

7.4 Implications for the Advancement of Medicine

While specific effects of CaR on the lung have not been reported, there is some circumstantial evidence to suggest that patients with FHH or NSHPT may be pre-disposed to having lung pathology. Section 1.11 detailed two case studies that reported severe respiratory complications resulting in the death of two NSHPT babies, despite intervention to resolve their hyperparathyroidism. Additionally, in a familial cohort study of FHH patients, there were several instances of early death from respiratory problems (Auwerx *et al.*, 1985b). In these circumstances it is impossible to perform retrospective studies to inform on the role of CaR mutation in their respiratory mortality. It may be possible to look longitudinally at cohorts of FHH families and determine if there is a higher instance of infant mortality due to respiratory pathology, and/or predisposition to respiratory conditions, than in the rest of the population. The link has already been made between FHH and interstitial lung disease in these cohorts, but perhaps other respiratory pathologies (such as a predisposition to asthma or recurrent respiratory infection) have been overlooked due to the symptoms from which these patients suffer. If a positive link can be made between these cohorts and an increased instance of neo-natal mortality, interventions could be taken for monitoring in early pregnancy and delivery in order to prevent mortality from FHH expectant mothers.

The potential for medical intervention in cases of lung hypo- or hyper-plasia is another reason for determining the role of the CaR in lung development. Advantageously for this possibility, the calcimimetics such as Cinacalcet are already proven, have been approved by the FDA and EMEA, and are commercially available. If the findings of this report hold true in human lung development, with CaR expression and activity playing a role in branching morphogenesis and possibly vasculogenesis, it presents a unique opportunity to quickly develop early pre-natal interventions without having to start clinical trials *ex novo.*

7.5 Final Thoughts

"Bodies are not jigsawed together as mosaics of phenotypic pieces, each one contributed by a different gene. There is no one to one mapping between genes and units of anatomy or behaviour. Genes 'collaborate' with hundreds of other genes in programming the developmental *processes* that culminate in a body, in the same kind of way as the words of a recipe collaborate in a cookery process that culminates in a dish."

- Richard Dawkins *The God Delusion* (Dawkins, 2006)

For the first time this project has shown that the CaR is expressed and is active during fetal lung development. It can be therefore be hypothesized that Ca^{2+}_{o} and CaR activation are two pieces of the jigsaw puzzle that represents the coordination of intrinsic and extrinsic factors, resolving into an organ that is responsible for the gas exchange that keeps us all alive.

APPENDIX A:
PRODUCTION OF A CaR SPECIFIC *IN SITU* HYBRIDIZATION PROBE

Methods:

JM109 *E. Coli* (Promega, Southhampton, UK) containing previously cloned full length CaR tagged with GFP (Maldonado-Perez *et al.*, 2003) were grown overnight in 200ml of LB medium and DNA purified using a maxi-prep protocol (Qiagen, Crawley, West Sussex, UK). This DNA was then digested using Sph 1 and Sac 1 restriction enzymes. The resulting 484 bp fragment was subcloned into pGem-T vector (Promega, Southhampton, UK). Once the CaR fragment was cloned into the pGem-T vector (Fig.1), RNA probes could be generated from the SP6 and T7 promoter regions on either side of the multiple cloning sites. Where transcription of either sense or antisense digoxigenin-labelled RNA probes were produced from the SP6 and T7 promoters respectively. Initially, the plasmid was linearised using Sph 1 (for SP6/sense probe) or Sac 1 (for T7/antisense probe; Fig. 2 A). The linearised vectors were then transcribed with DIG-11-UTP with SP6 and T7 RNA polymerases using a DIG T7/SP6 kit (Roche Applied Science, Burgess Hill, UK) according to the manufacturer's instructions. 1 µl of resulting product was then checked via electrophoresis on a 1% agarose gel stained with ethidium bromide. According to the product insert, using 1µg of plasmid DNA under standard reaction conditions should result in approximately 10µg of labelled product, however this was not the case for this particular probe, initially there was not enough labelled probe to use in subsequent experiments (Fig. 2B).

In order to resolve the lack of sufficient probe, purification and cleaning (PCR Purification kit, Qiagen, Crawley, West Sussex, UK) was added post linearization but this did not result in any additional probe labelling. However, the control DNA provided within the kit resulted in a significant amount of labelled RNA probe; therefore the kit components were all working properly (Fig. 2C). The reaction was then scaled up to use double the amount of reagents on the same starting amount (1µg) of plasmid DNA. Scaling up the reaction resulted in an appropriate amount of labelled RNA probe for the 1µg of starting DNA (Fig. 2D). This was then purified using Quick Spin Columns (Roche Applied Science, Burgess Hill, UK). Quantification and determination of labelling efficiency was performed as in the DIG labelling kit package insert. Briefly, the amount of resultant probe was assumed to be 10µg per 1µg of starting material. This was diluted to 10ng/µl, as was the control labelled RNA provided within the kit. A set of serial dilutions was performed on the control RNA from 10ng/µl down to 0.01pg/µl using a 5:3:2 mix of water: 20x SSC: 10% formaldehyde as the RNA dilution buffer. 10µl of each of the probes and dilutions was applied to a small piece of Hybond N+ nylon membrane (GE Healthcare, Chalfont St. Giles, Buckinghamshire, UK) and dried at 60°C for 1 hour. The membrane was then washed, blocked and exposed to the DIG antibody for 30 minutes at room temperature. After the excess antibody was washed from the membrane, it was equilibrated in detection buffer for 5 minutes. The color reaction was performed at room temperature using BM purple (Roche Applied Sciences, Burgess Hill, UK) as a colour substrate. This reaction took approximately 45 minutes, after which it was stopped by washing with distilled water and the membrane was allowed to dry for storage.

The membrane showed that both probes had indeed labelled to a high concentration of 10ng/µl in the diluted sample, meaning that there was approximately 10µg total of labelled RNA in the purified sample (Fig. 2E).

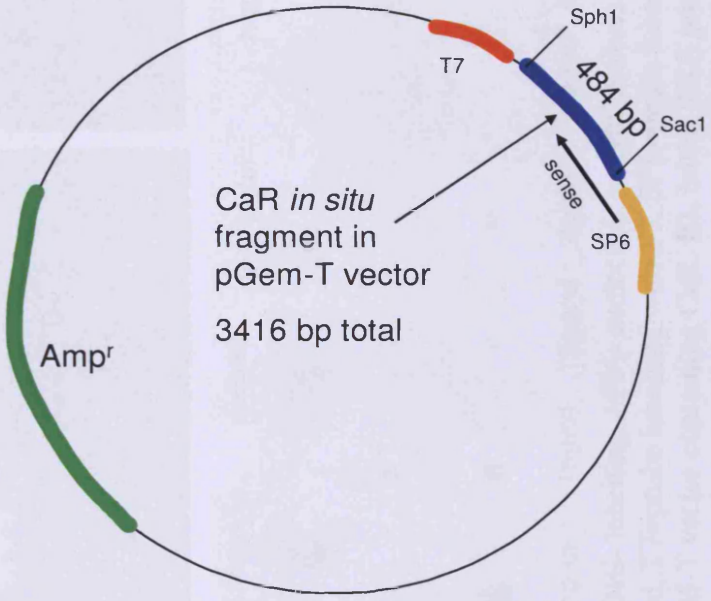

Appendix A, Figure 1: Schematic diagram of CaR fragment for *in situ* probe in pGem-T vector.

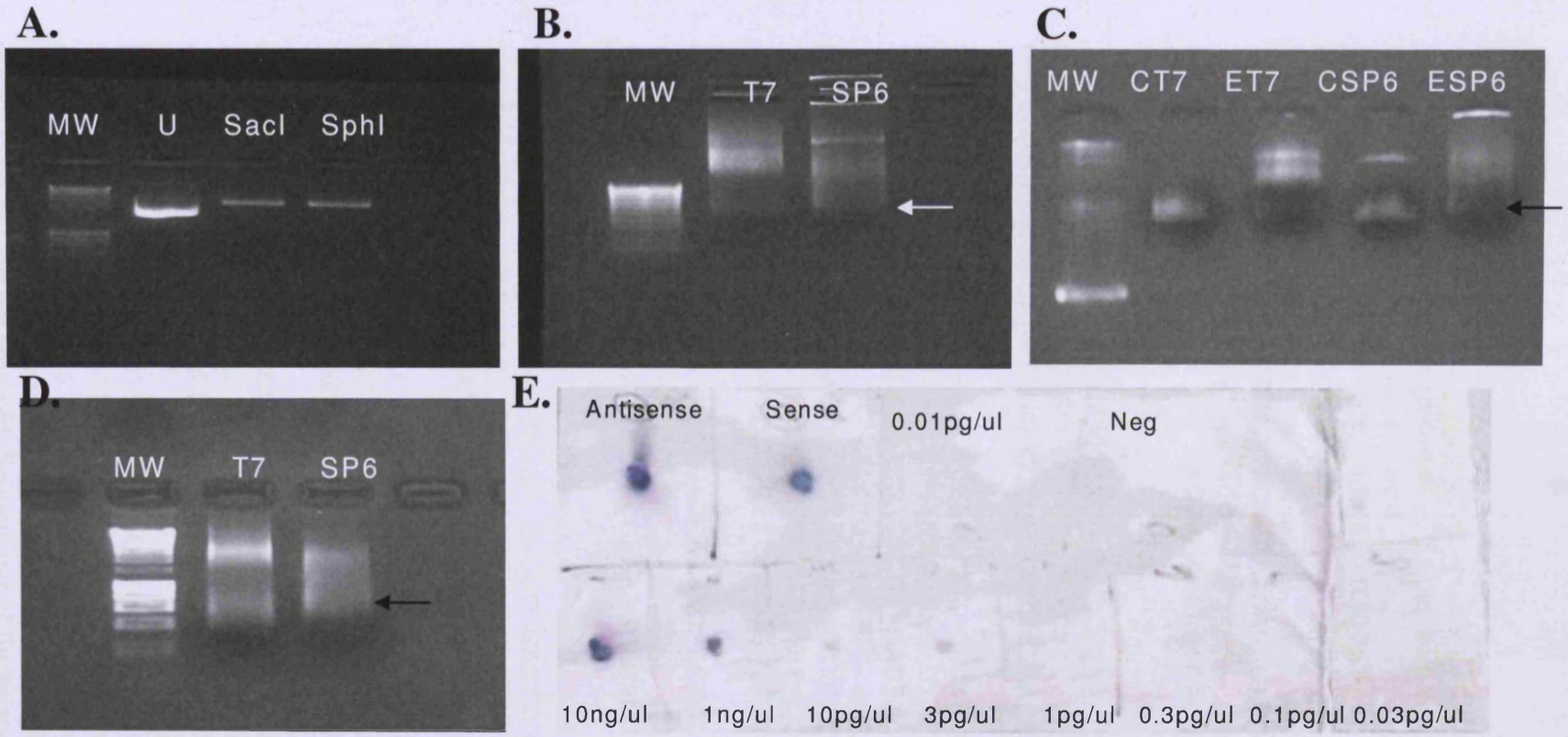

Appendix A, Figure 2: Optimization of RNA probe DIG- labelling. MW= molecular weight markers **A, C, D**=Hyperladder I; B=Hyperladder IV (Bioline), U=undigested plasmid, T7=probe labelling with T7, SP6=probe labelling with SP6 **A).** Linearization digests using Sac1 and Sph1 of pGEM-T vector containing CaR. **B).** Initial RNA probe labelling with faint 500 base band (arrow). **C).** Test of labelling kit with Control (CT7, CSP6) and Experimental (ET7, ESP6) CaR RNA 500 base band (arrow). **D).** Increased amount of probe labelling with scaling up of the labelling reaction with 500 base band (arrow). **E).** Quantification and determination of labelling efficiency with Antisense and Sense probes matching 10 ng/µl dilutions of control probes.

CaR-GFP Plasmid sequence - from David Maldonado-Perez
CaR *in situ* probe sequence
Human Parathyroid CaR, mRNA, U20759
YELLOW - Restriction enzyme sites

```
SACI - CTCGAGAGGATGGAGGAGGAGAAGAGGGACGAGACGAGACGACGAAGA
       CTCGA-AGGATGGAGGAGGAGAAGAGGGACGAGACGA--CGA------
2332-                  GAGGAGAAGAGGGACGAGACGA--CGA--AAGA

GGTCGAGGGACAAGAAGTAGCCCCTCGGGGTCCTGACCTGCACGGCGGACGCGGTC
GGTCGAGGGACAAGAAGTAGCCCCTCGGGGTCCTGACCTGCACGGCGGACGCGGTC
GGTCGAGGGACAAGAAGTAGCCCCTCGGGGTCCTGACCTGCACGGCGGACGCGGTC

GGCCGGAAACCGTAGTCGAAGCACGAGACGTAGAGTACGTAGGACCACTTTTGGTT
GGCCGGAAACCGTAGTCGAAGCACGAGACGTAGAGTACGTAGGACCACTTTTGGTT
GGCCGGAAACCGTAGTCGAAGCACGAGACGTAGAGTACGTAGGACCACTTTTGGTT

GGCACAGGAGGACCACAAACTCCGGTTCTAGGGGTGGTCGAAGGTGGCGTTCACCA
GGCACAGGAGGACCACAAACTCCGGTTCTAGGGGTGGTCGAAGGTGGCGTTCACCA
GGCACAGGAGGACCACAAACTCCGGTTCTAGGGGTGGTCGAAGGTGGCGTTCACCA

CCCCCGAGTTGGACGTCAAGGACGACCAAAAGGAGACGTGGAAGTACGTGTAACAG
CCCCCGAGTTGGACGTCAAGGACGACCAAAAGGAGACGTGGAAGTACGTCTAACAG
CCCCCGAGTTGGACGTCAAGGACGACCAAAAGGAGACGTGGAAGTACGTCTAACAG

TAGACACACTAGACCGAGATGTGGCGCGGGGGGAGTTCGATGGCGTTGGTGGTCGA
TAGACACACTACACCGAGATGTGGCGCGGGGGGAGTTCGATGGCGTTGGTCCTCGA
TAGACACACTACACCGAGATGTGGCGCGGGGGGAGTTCGATGGCGTTGGTCCTCGA

CCTCCTACTCTAGTAGAAGTAGTGCACGGTGCTCCCGAGGGAGTACCGGGACCCGA
CCTCCTACTCTAGTAGAAGTAGTGCACGGTGCTCCCGAGGGAGTACCGGGACCCGA
CCTCCTACTCTAGTAGAAGTAGTGCACGGTGCTCCCGAGGGAGTACCGGGACCCGA

AGGACTAGCCGATGTGGACGGACGACCGACGGTAGACGAAGAAGAAACGGAAGTTC
AGGACTAGCCGATGTGGACGGACGACCGACGGTAGACGAAGAAGAAACGGAAGTTC
AGGACTAGCCGATGTGGACGGACGACCGACGGTAGACGAAGAAGAAACGGAAGTTC

AGGGCCTTCGACGGCCTCTTGAAGTTACTTCGGTTCAAGTAGTGGAAGTC-SPHI
AGGGCCTTCGACGGCCTCTTGAAGTT-CTTC-GTTCAAGTAGTG-AAGTC
AGGGCCTTCGACGGCCTCTTGAAGTTACTTCGGTTCAAGTAGTG      -2795
```

Appendix A, Figure 3: Sequencing line-up of CaR in situ probe with CaR-GFP and CaR mRNA from human parathyroid. Sequencing of linearized pGem-T vector containing CaR fragment for *in situ* shows high sequence homology with original cloned fragment and published sequences for CaR mRNA.

APPENDIX B:
CAR KNOCKOUT EMBRYO GENOTYPE RATIOS

Methods:

DNA isolation and Genotyping PCR was performed as in Section 5.1.2. For abortuses, DNA was isolated from any tissue remaining in an intact amniotic sac that could be distinguished from the placenta. The graph is representative of a sample of embryos harvested at E14.5 and younger. Ratio of HET and NULL genotypes were calculated as the number of HET or NULL embryos divided by the number of WT embryos.

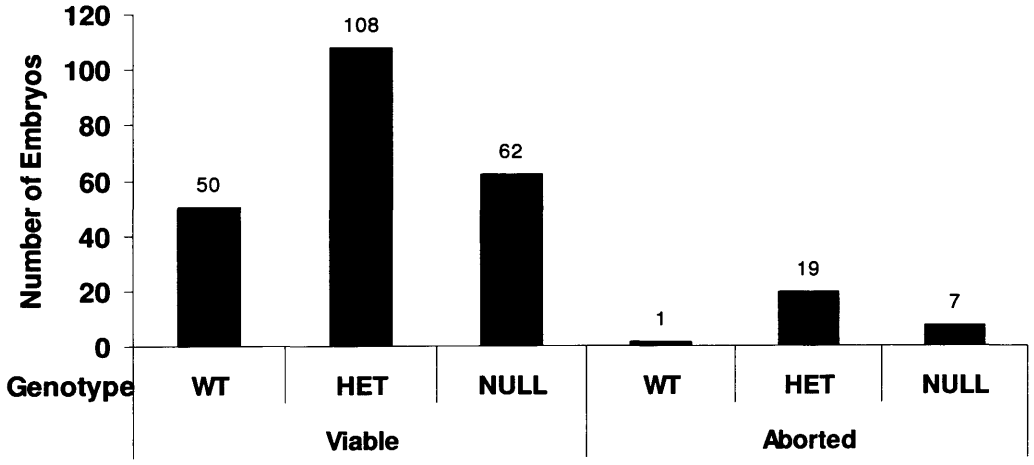

Appendix B, Figure 1: Numbers of each genotype harvested from CaR HET mothers. Mendelian ratios of genotypes maintained in viable embryos with 1 WT: 2.2 HET: 1.2 NULL, but higher numbers of heterozygotes (19 HET: 1WT) and null (7 NULL: 1 WT) embryos are aborted.

APPENDIX C:
SEQUENCING OF GENOTYPING AND SPLICE VARIANT PCR PRODUCTS

Methods:

After PCR amplification of genomic or cDNA the products were electrophoresed on a 2% agarose gel. Once separated and photographed the products of the desired sizes were cut from the agarose gel and purified using a Gel Extraction kit (Qiagen, Crawley, UK) according to the manufacturer's instructions. PCR products from the genotyping PCR were sent for sequencing after this purification. SPV PCR products were subcloned into a p-GEM vector (Promega, UK) and E.coli were transformed to produce this vector. After plating on agar-ampicillin plates, one resultant colony for each PCR product was sent for sequencing.

Sequencing reactions were performed by Cogenics, Essex, UK. When sequences for genotyping PCR products were returned a Nucleotide BLAST search was performed on the NIH, NCBI website.

A. The sequence for the CaR6HF-CaR6HR PCR product (Wildtype CaR)

corresponded to the genomic sequence NT_ 039624.7 *Mus Musculus* chromosome 16 genomic contig, strain C57BL/6J as well as the transcript NM_013803.1 *Mus Musculus*, calcium-sensing receptor, mRNA. Shown below is the PCR product sequence in RED and the genomic (NT_039624.7) CaR sequence from BLAST search in black.

```
ACAACATGGGGGAGCAGGTGACCTTCGATGAGTGCGGTGACCTGGTGGGGAACTACTCCA
33500469-
ACAACATGGGGGAGCAGGTGACCTTCGATGAGTGCGGTGACCTGGTGGGGAACTACTCCA

TCATCAACTGGCACCTCTCCCCAGAGGACGGCTCCATTGTGTTCAAGGAAGTTGGGTACT
TCATCAACTGGCACCTCTCCCCAGAGGACGGCTCCATTGTGTTCAAGGAAGTTGGGTACT

ACAATGTGTATGCCAAGAAGGGAGAAAGACTGTTCATCAATGA
ACAATGTGTATGCCAAGAAGGGAGAAAGACTGTTCATCAATGA-33500297
```

B. The sequence for the Neo-CaR6HR PCR product (Neo Cassette containing CaR)

corresponded to both cloning vector sequences as well as Car sequences. The initial bases 1-111 correspond to several different types of cloning vectors, for simplicity only one vector sequence is shown below.

The Neo PCR product sequence to base 111 is in GREEN and the cloning vector, pEFBos-IRESGFPNEO, sequence is in BLUE.

```
     GGTTT-CNAATGTGTCAGTTT-NTAGCCTGAAGAACGAGATCAGCAGCCTCTGTTCCACA
4278-GGTTTCCAAATGTGTCAGTTTCATAGCCTGAAGAACGAGATCAGCAGCCTCTGTTCCACA

TACACTTCATTCTCAGTATTGTTTTGCCAAGTTCTAATTCCATCAGAAGCTG
TACACTTCATTCTCAGTATTGTTTTGCCAAGTTCTAATTCCATCAGAAGCTG-4389
```

From base number 112 onwards the Neo-PCR product sequence corresponded to the genomic sequence NT_ 039624.7 *Mus Musculus* chromosome 16 genomic contig, strain C57BL/6J as well as the transcript NM_013803.1 *Mus Musculus*, calcium-sensing receptor, mRNA. Neo PCR product sequence is in GREEN and the genomic (NT_039624.7) CaR sequence from BLAST search in black.

GTGACCTGGTGGGGAACTACTCCATCATCAACTGGCACCTCTCCCCAGAGGACGGCTCCA
33500423-
GTGACCTGGTGGGGAACTACTCCATCATCAACTGGCACCTCTCCCCAGAGGACGGCTCCA

TTGTGTTCAAGGAAGTTGGGTACTACAATGTGTATGCCAAGAAGGGAGAAAGACTGTTCA
TTGTGTTCAAGGAAGTTGGGTACTACAATGTGTATGCCAAGAAGGGAGAAAGACTGTTCA

TCAATGA
TCAATGA-33500297

C. Sequence for Ensembl Transcript ID ENZMUST00000063597 Extracellular Calcium-sensing receptor, Mus Musculus

EXON 4

ATGGTTTTGCCAAAGAGTTTTGGGAAGAAACATTTAATTGCCACCTGCAAGACGGCGCA
AAAGGACCTTTACCCGTGGACACCTTCGTGAGAAGTCACGAGGAAGGCGGCAACAGGTTA
CTCAATAGCTCCACTGCCTTCCGACCCCTCTGCACGGGGGATGAAAACATCAATAGTGTC
GAGACCCCTTACATGGACTACGAACATTTACGGATATCCTACAACGTGTACTTAGCCGTC
TACTCCATTGCGCACGCCCTGCAAGATATATACACCTGCTTACCCGGAAGAGGGCTTTTC

SPV PCR Product Sequence :ACCTGCTTACCCGGAAGAGGGCTTTTC
WT PCR Product Sequence :ACCTGCTTACCCGGAAGAGGGCTTTTC

ACCAACGGGTCCTGTGCAGACATCAAGAAGGTTGAGGCCTGGCAG
ACCAACGGGTCCTGTGCAGACATCAAGAAGGTTGAGGCCTGGCAG
ACCAACGGGTCCTGTGCAGACATCAAGAAGGTTGAGGCCTGGCAG

EXON 5

GTCCTGAAACACCTACGGCACCTGAATTTCACCAACAACATGGGGGAGCAGGTGACCTTC
GTCCTGAAACACCTACGGCACCTGAATTTCACCAACAACATGGGGGAGCAGGTGACCTTC

GATGAGTGCGGTGACCTGGTGGGGAACTACTCCATCATCAACTGGCACCTCTCCCCAGAG
GATGAGTGCGGTGACCTGGTGGGGAACTACTCCATCATCAACTGGCACCTCTCCCCAGAG

GACGGCTCCATTGTGTTCAAGGAAGTTGGGTACTACAATGTGTATGCCAAGAAGGGAGAA
GACGGCTCCATTGTGTTCAAGGAAGTTGGGTACTACAATGTGTATGCCAAGAAGGGAGAA

AGACTGTTCATCAATGAGGGGAAGATCTTGTGGAGTGGGTTCTCCAGAGAG
AGACTGTTCATCAATGAGGGGAAGATCTTGTGGAGTGGGTTCTCCAGAGAG

EXON 6

GTGCCCTTCTCCAACTGCAGCCGGGACTGTCAGGCAGGGACCAGGAAGGGCATCATTGAG
GTGCCCTTCTCCAACTGCAGCCGGGACTGTCAGGCAGGGACCAGGAAGGGCATCATTGAG
GTGCCCTTCTCCAACTGCAGCCGGGACTGTCAGGCAGGGACCAGGAAGGGCATCATTGAG

GGAGAGCCCACCTGCTGTTTTGAGTGTGTGGAGTGTCCTGACGGCGAGTACAGTGGTGAG
GGAGAGCCCACCTGCTGTTTTGAGTGTGTGGAGTGTCCTGACGGCGAGTACAGTGGTGAG
GGAGAGCCCACCTGCTGTTTTGAGTGTGTGGAGTGTCCTGACGGCGAGTACAGTGGTGAG

ACAG
ACAG
ACAG

EXON 7

ATGCGAGTGCCTGTGACAAGTGCCCGGATGACTTCTGGTCCAATGAGAACCACACTTCCT
ATGCGAGTGCCTGTGACAAGTGCCCGGATGACTTCTGGTCCAATGAGAACCACACTTCCT
ATGCGAGTGCCTGTGACAAGTGCCCGGATGACTTCTGGTCCAATGAGAACCACACTTCCT

GCATTGCCAAGGAGATTGAGTTCCTGGCGTGGACTGAGCCCTTTGGAATCGCTCTCACTC
GCATTGCCAAGGAGATTGAGTTCCTGGCGTGGACTGAGCCCTTTGGAATCGCTCTCACTC
GCATTGCCAAGGAGATTGAGTTCCTGGCGTGGACTGAGCCCTTTGGAATCGCTCTCACTC

TCTTTGCGGTGCTGGGCATTTTCCTGACCGCCTTTGTGCTGGGCGTCTTCATCAAGTTCC
TNTTTGCGGTGCTGGGCATTTTCCTGACCGCCTTTGTGC
TCTTTGCGGTGCTGGGCATTTTCCTGACCGCCTTTGTGC

References

Acarregui MJ, Penisten ST, Goss KL, Ramirez K & Snyder JM. (1999). Vascular Endothelial Growth Factor Gene Expression in Human Fetal Lung In Vitro. *Am J Respir Cell Mol Biol* **20,** 14-23.

Acarregui MJ, Snyder JM & Mendelson CR. (1993). Oxygen modulates the differentiation of human fetal lung in vitro and its responsiveness to cAMP. *Am J Physiol Lung Cell Mol Physiol* **264,** L465-474.

Adams GB, Chabner KT, Alley IR, Olson DP, Szczepiorkowski ZM, Poznansky MC, Kos CH, Pollak MR, Brown EM & Scadden DT. (2006). Stem cell engraftment at the endosteal niche is specified by the calcium-sensing receptor. *Nature* **439,** 599-603.

Adamson TM, Boyd RDH, Platt HS & Strang LB. (1969). Composition of alveolar liquid in the foetal lamb. *J Physiol* **204,** 159-168.

Aida K, Koishi S, Tawata M & Onaya T. (1995). Molecular cloning of a putative Ca(2+)-sensing receptor cDNA from human kidney. *Biochem Biophys Res Commun* **214,** 524-529.

Akeson AL, Greenberg JM, Cameron JE, Thompson FY, Brooks SK, Wiginton D & Whitsett JA. (2003). Temporal and spatial regulation of VEGF-A controls vascular patterning in the embryonic lung. *Dev Biol* **264,** 443-455.

Albert PR & Robillard L. (2002). G protein specificity: Traffic direction required. *Cell Signal* **14,** 407-418.

Arthur JM, Collinsworth GP, Gettys TW, Quarles LD & Raymond JR. (1997). Specific coupling of a cation-sensing receptor to G protein alpha-subunits in MDCK cells. *Am J Physiol Renal Physiol* **273,** F129-135.

Arthur JM, Lawrence MS, Payne CR, Rane MJ & McLeish KR. (2000). The calcium-sensing receptor stimulates JNK in MDCK cells. *Biochem Biophys Res Commun* **275,** 538-541.

Attie MF, Gill JR, Jr., Stock JL, Spiegel AM, Downs RW, Jr., Levine MA & Marx SJ. (1983). Urinary calcium excretion in familial hypocalciuric hypercalcemia. Persistence of relative hypocalciuria after induction of hypoparathyroidism. *J Clin Invest* **72,** 667-676.

Auwerx J, Boogaerts M, Ceuppens JL & Demedts M. (1985a). Defective host defence mechanisms in a family with hypocalciuric hypercalcaemia and coexisting interstitial lung disease. *Clin Exp Immunol* **62,** 57-64.

Auwerx J, Demedts M, Bouillon R & Desmet J. (1985b). Coexistence of hypocalciuric hypercalcaemia and interstitial lung disease in a family: a cross-sectional study. *Eur J Clin Invest* **15,** 6-14.

Bagley MC, Davis T, Dix MC, Widdowson CS & Kipling D. (2006). Microwave-assisted synthesis of N-pyrazole ureas and the p38[small alpha] inhibitor BIRB 796 for study into accelerated cell ageing. *Organic & Biomolecular Chemistry* **4,** 4158-4164.

Bai M, Janicic N, Trivedi S, Quinn SJ, Cole DEC, Brown EM & Hendy GN. (1997). Markedly reduced activity of mutant calcium-sensing receptor with an inserted Alu element from a kindred with familial hypocalciuric hypercalcemia and neonatal severe hyperparathyroidism. *J Clin Invest* **99,** 1917-1925.

Bai M, Quinn S, Trivedi S, Kifor O, Pearce SHS, Pollak MR, Krapcho K, Hebert SC & Brown EM. (1996). Expression and characterization of inactivating and activating mutations in the human Ca-0(2+)-sensing receptor. *J Biol Chem* **271,** 19537-19545.

Bai M, Trivedi S & Brown EM. (1998). Dimerization of the extracellular calcium-sensing receptor (CaR) on the cell surface of CaR-transfected HEK293 cells. *J Biol Chem* **273,** 23605-23610.

Bellusci S, Furuta Y, Rush MG, Henderson R, Winnier G & Hogan BLM. (1997a). Involvement of Sonic hedgehog (Shh) in mouse embryonic lung growth and morphogenesis. *Development* **124,** 53-63.

Bellusci S, Grindley J, Emoto H, Itoh N & Hogan BLM. (1997b). Fibroblast Growth Factor 10(FGF10) and branching morphogenesis in the embryonic mouse lung. *Development* **124,** 4867-4878.

Bellusci S, Henderson R, Winnier G, Oikawa T & Hogan BLM. (1996). Evidence from normal expression and targeted misexpression that bone morphogenetic protein-4 (Bmp-4) plays a role in mouse embryonic lung morphogenesis. *Development* **122,** 1693-1702.

Bhagavathula N, Kelley EA, Reddy M, Nerusu KC, Leonard C, Fay K, Chakrabarty S & Varani J. (2005). Upregulation of calcium-sensing receptor and mitogen-activated protein kinase signalling in the regulation of growth and differentiation in colon carcinoma. *Br J Cancer* **93,** 1364-1371.

Bikle DD & Pillai S. (1993). Vitamin D, calcium, and epidermal differentiation. *Endocr Rev* **14,** 3-19.

Blewett CJ, Zgleszewski SE, Chinoy MR, Krummel TM & Cilley RE. (1996). Bronchial ligation enhances murine fetal lung development in whole-organ culture. *J Pediatr Surg* **31,** 869-877.

Bradbury RA, Sunn KL, Crossley M, Bai M, Brown EM, Delbridge L & Conigrave AD. (1998). Expression of the parathyroid Ca2+-sensing receptor in cytotrophoblasts from human term placenta. *J Endocrinol* **156,** 425-430.

Bragg AD, Moses HL & Serra R. (2001). Signaling to the epithelium is not sufficient to mediate all of the effects of transforming growth factor beta and bone morphogenetic protein 4 on murine embryonic lung development. *Mech Dev* **109,** 13-26.

Bratu I, Flageole H, Laberge J-M, Possmayer F, Harbottle R, Kay S, Khalife S & Piedboeuf B. (2001). Surfactant levels after reversible tracheal occlusion and prenatal steroids in experimental diaphragmatic hernia. *J Pediatr Surg* **36,** 122-127.

Brauner-Osborne H, Jensen AA, Sheppard PO, O'Hara P & Krogsgaard-Larsen P. (1999). The agonist-binding domain of the calcium-sensing receptor is located at the amino-terminal domain. *J Biol Chem* **274,** 18382-18386.

Brown E, Enyedi P, LeBoff M, Rotberg J, Preston J & Chen C. (1987). High extracellular Ca2+ and Mg2+ stimulate accumulation of inositol phosphates in bovine parathyroid cells. *FEBS Lett* **218,** 113-118.

Brown EM, Gamba G, Riccardi D, Lombardi M, Butters R, Kifor O, Sun A, Hediger MA, Lytton J & Hebert SC. (1993). Cloning and characterization of an extracellular Ca(2+)-sensing receptor from bovine parathyroid. *Nature* **366,** 575-580.

Brown EM & MacLeod RJ. (2001). Extracellular Calcium Sensing and Extracellular Calcium Signaling. *Physiol Rev* **81,** 239-297.

Bruce JI, Yang X, Ferguson CJ, Elliott AC, Steward MC, Case RM & Riccardi D. (1999). Molecular and functional identification of a Ca2+ (polyvalent cation)-sensing receptor in rat pancreas. *J Biol Chem* **274,** 20561-20568.

Butters RR, Chattopadhyay N, Nielsen P, Smith CP, Mithal A, Kifor O, Bai M, Quinn S, Goldsmith P, Hurwitz S, Krapcho K, Busby J & Brown EM. (1997). Cloning and characterization of a calcium-sensing receptor from the hypercalcemic New Zealand white rabbit reveals unaltered responsiveness to extracellular calcium. *J Bone Miner Res* **12,** 568-579.

Carafoli E. (2002). Calcium signaling: a tale for all seasons. *Proc Natl Acad Sci U S A* **99,** 1115-1122.

Cardoso WV, Itoh A, Nogawa H, Mason I & Brody JS. (1997). FGF-1 and FGF-7 induce distinct patterns of growth and differentiation in embryonic lung epithelium. *Dev Dyn* **208,** 398-405.

Cardoso WV & Lu JN. (2006). Regulation of early lung morphogenesis: questions, facts and controversies. *Development* **133,** 1611-1624.

Chakrabarty S, Radjendirane V, Appelman H & Varani J. (2003). Extracellular calcium and calcium sensing receptor function in human colon carcinomas: Promotion of E-cadherin expression and suppression of beta-catenin/TCF activation. *Cancer Res* **63,** 67-71.

Chang W, Tu C, Bajra R, Komuves L, Miller S, Strewler G & Shoback D. (1999a). Calcium Sensing in Cultured Chondrogenic RCJ3.1C5.18 Cells. *Endocrinology* **140,** 1911-1919.

Chang W, Tu C, Chen T-H, Bikle D & Shoback D. (2008). The Extracellular Calcium-Sensing Receptor (CaSR) Is a Critical Modulator of Skeletal Development. *Sci Signal* **1,** ra1-.

Chang WH & Shoback D. (2004). Extracellular Ca2+-sensing receptors - an overview. *Cell Calcium* **35,** 183-196.

Chang WH, Tu CL, Bajra R, Komuves L, Miller S, Strewler G & Shoback D. (1999b). Calcium sensing in cultured chondrogenic RCJ3.1C5.18 cells. *Endocrinology* **140,** 1911-1919.

Chattopadhyay N, Baum M, Bai M, Riccardi D, Hebert SC, Harris HW & Brown EM. (1996). Ontogeny of the extracellular calcium-sensing receptor in rat kidney. *Am J Physiol* **271,** F736-743.

Chattopadhyay N, Cheng I, Rogers K, Riccardi D, Hall A, Diaz R, Hebert SC, Soybel DI & Brown EM. (1998). Identification and localization of extracellular Ca(2+)-sensing receptor in rat intestine. *Am J Physiol* **274,** G122-130.

Chattopadhyay N, Ye CP, Singh DP, Kifor O, Vassilev PM, Shinohara T, Chylack LT & Brown EM. (1997). Expression of extracellular calcium-sensing receptor by human lens epithelial cells. *Biochem Biophys Res Commun* **233,** 801-805.

Chen C, Chen H, Sun JP, Bringas P, Chen YH, Warburton D & Shi W. (2005). Smad1 expression and function during mouse embryonic lung branching morphogenesis.

American Journal of Physiology-Lung Cellular and Molecular Physiology **288,** L1033-L1039.

Cheng I, Qureshi I, Chattopadhyay N, Qureshi A, Butters RR, Hall AE, Cima RR, Rogers KV, Hebert SC, Geibel JP, Brown EM & Soybel DI. (1999). Expression of an extracellular calcium-sensing receptor in rat stomach. *Gastroenterology* **116,** 118-126.

Cheng SX, Geibel JP & Hebert SC. (2004). Extracellular polyamines regulate fluid secretion in rat colonic crypts via the extracellular calcium-sensing receptor. *Gastroenterology* **126,** 148-158.

Cheng SX, Okuda M, Hall AE, Geibel JP & Hebert SC. (2002). Expression of calcium-sensing receptor in rat colonic epithelium: evidence for modulation of fluid secretion. *American Journal of Physiology-Gastrointestinal and Liver Physiology* **283,** G240-G250.

Chinoy MR, Zgleszewski SE, Cilley RE, Blewett CJ, Krummel TM, Reisher SR & Feinstein SI. (1998). Influence of epidermal growth factor and transforming growth factor beta-1 on patterns of fetal mouse lung branching morphogenesis in organ culture. *Pediatr Pulmonol* **25,** 244-256.

Chopra DP, Sullivan JK & Reece-Kooyer S. (1990). Regulation by calcium of proliferation and morphology of normal human tracheobronchial epithelial cell cultures. *J Cell Sci* **96,** 509-517.

Cole DE, Janicic N, Salisbury SR & Hendy GN. (1997). Neonatal severe hyperparathyroidism, secondary hyperparathyroidism, and familial hypocalciuric hypercalcemia: multiple different phenotypes associated with an inactivating Alu insertion mutation of the calcium-sensing receptor gene. *Am J Med Genet* **71,** 202-210.

Colen KL, Crisera CA, Rose MI, Connelly PR, Longaker MT & Gittes GK. (1999). Vascular development in the mouse embryonic pancreas and lung. *J Pediatr Surg* **34,** 781-785.

Colvin JS, White AC, Pratt SJ & Ornitz DM. (2001). Lung hypoplasia and neonatal death in Fgf9-null mice identify this gene as an essential regulator of lung mesenchyme. *Development* **128,** 2095-2106.

Conigrave AD, Mun HC, Delbridge L, Quinn SJ, Wilkinson M & Brown EM. (2004). L-amino acids regulate parathyroid hormone secretion. *J Biol Chem* **279,** 38151-38159.

Conigrave AD, Quinn SJ & Brown EM. (2000). From the Cover: L-Amino acid sensing by the extracellular Ca2+-sensing receptor. *Proceedings of the National Academy of Sciences* **97,** 4814-4819.

Corbetta S, Lania A, Filopanti M, Vicentini L, Ballare E & Spada A. (2002). Mitogen-activated protein kinase cascade in human normal and tumoral parathyroid cells. *J Clin Endocrinol Metab* **87,** 2201-2205.

Cunningham J, Dockery DW & Speizer FE. (1994). Maternal Smoking during Pregnancy as a Predictor of Lung Function in Children. *Am J Epidemiol* **139,** 1139-1152.

DasGupta R & Fuchs E. (1999). Multiple roles for activated LEF/TCF transcription complexes during hair follicle development and differentiation. *Development* **126,** 4557-4568.

Davies SL, Gibbons CE, Vizard T & Ward DT. (2006). Ca2+-sensing receptor induces Rho kinase-mediated actin stress fiber assembly and altered cell morphology, but not in response to aromatic amino acids. *American Journal of Physiology-Cell Physiology* **290,** C1543-C1551.

Davies SP, Reddy H, Caivano M & Cohen P. (2000). Specificity and mechanism of action of some commonly used protein kinase inhibitors. *Biochem J* **351,** 95-105.

Dawkins R. (2006). *The God Delusion.* Transworld Publishers.

De Langhe SP, Sala FG, Del Moral PM, Fairbanks TJ, Yamada KM, Warburton D, Burns RC & Bellusci S. (2005). Dickkopf-1 (DKK1) reveals that fibronectin is a major target of Wnt signaling in branching morphogenesis of the mouse embryonic lung. *Dev Biol* **277,** 316-331.

De Moerlooze L, Spencer-Dene B, Revest JM, Hajihosseini M, Rosewell I & Dickson C. (2000). An important role for the IIIb isoform of fibroblast growth factor receptor 2 (FGFR2) in mesenchymal-epithelial signalling during mouse organogenesis. *Development* **127,** 483-492.

del Moral PM, De Langhe SP, Sala FG, Veltmaat JM, Tefft D, Wang K, Warburton D & Bellusci S. (2006a). Differential role of FGF9 on epithelium and mesenchyme in mouse embryonic lung. *Dev Biol* **293,** 77-89.

Del Moral PM, Sala FG, Tefft D, Shi W, Keshet E, Bellusci S & Warburton D. (2006b). VEGF-A signaling through Flk-1 is a critical facilitator of early embryonic lung epithelial to endothelial crosstalk and branching morphogenesis. *Dev Biol* **290,** 177-188.

Demedts M, Lissens W, Wuyts W, Matthijs G, Thomeer M & Bouillon R. (2008). A New Missense Mutation in the CASR Gene in Familial Interstitial Lung Disease with

Hypocalciuric Hypercalcemia and Defective Granulocyte Function. *Am J Respir Crit Care Med* **177,** 558-559.

Diaz R, Hurwitz S, Chattopadhyay N, Pines M, Yang YH, Kifor O, Einat MS, Butters R, Hebert SC & Brown EM. (1997). Cloning, expression, and tissue localization of the calcium-sensing receptor in chicken (Gallus domesticus). *American Journal of Physiology-Regulatory Integrative and Comparative Physiology* **42,** R1008-R1016.

DiFiore JW, Fauza DO, Slavin R, Peters CA, Fackler JC & Wilson JM. (1994). Experimental fetal tracheal ligation reverses the structural and physiological effects of pulmonary hypoplasia in congenital diaphragmatic hernia. *J Pediatr Surg* **29,** 248-257.

Douglas WW. (1978). Stimulus-secretion coupling: variations on the theme of calcium-activated exocytosis involving cellular and extracellular sources of calcium. *Ciba Found Symp* **54,** 61-90.

Dvorak MM, Chen T-H, Orwoll B, Garvey C, Chang W, Bikle DD & Shoback DM. (2007). Constitutive Activity of the Osteoblast Ca2+-Sensing Receptor Promotes Loss of Cancellous Bone. *Endocrinology* **148,** 3156-3163.

Dvorak MM, Siddiqua A, Ward DT, Carter DH, Dallas SL, Nemeth EF & Riccardi D. (2004). Physiological changes in extracellular calcium concentration directly control osteoblast function in the absence of calciotropic hormones. *Proc Natl Acad Sci U S A* **101,** 5140-5145.

Eblaghie MC, Reedy M, Oliver T, Mishina Y & Hogan BLM. (2006). Evidence that autocrine signaling through Bmpr1a regulates the proliferation, survival and morphogenetic behavior of distal lung epithelial cells. *Dev Biol* **291,** 67-82.

Featherstone NC, Jesudason EC, Connell MG, Fernig DG, Wray S, Losty PD & Burdyga TV. (2005). Spontaneous propagating calcium waves underpin airway peristalsis in embryonic rat lung. *Am J Respir Cell Mol Biol* **33,** 153-160.

Ferry S, Traiffort E, Stinnakre J & Ruat M. (2000). Developmental and adult expression of rat calcium-sensing receptor transcripts in neurons and oligodendrocytes. *Eur J Neurosci* **12,** 872-884.

Fisher CE, Michael L, Barnett MW & Davies JA. (2001). Erk MAP kinase regulates branching morphogenesis in the developing mouse kidney. *Development* **128,** 4329-4338.

Fleury V. (2001). Sur une symétrie fondamentale entre la morphogenèse et le fonctionnement des organes arborisésA fundamental symmetry between

morphogenesis and function of branched organs. *Comptes Rendus de l'Académie des Sciences - Series III - Sciences de la Vie* **324,** 405-412.

Fleury V & Watanabe T. (2002). Morphogenesis of fingers and branched organs: how collagen and fibroblasts break the symmetry of growing biological tissue. *Comptes Rendus Biologies* **325,** 571-583.

Fox J, Lowe SH, Conklin RL, Petty BA & Nemeth EF. (1999a). Calcimimetic Compound NPS R-568 Stimulates Calcitonin Secretion But Selectively Targets Parathyroid Gland Ca2+ Receptor in Rats. *J Pharmacol Exp Ther* **290,** 480-486.

Fox J, Lowe SH, Petty BA & Nemeth EF. (1999b). NPS R-568: A Type II Calcimimetic Compound that Acts on Parathyroid Cell Calcium Receptor of Rats to Reduce Plasma Levels of Parathyroid Hormone and Calcium. *J Pharmacol Exp Ther* **290,** 473-479.

Fox L, Sadowsky J, Pringle KP, Kidd A, Murdoch J, Cole DEC & Wiltshire E. (2007). Neonatal Hyperparathyroidism and Pamidronate Therapy in an Extremely Premature Infant. *Pediatrics* **120,** e1350-1354.

Gama L, BaxendaleCox LM & Breitwieser GE. (1997). Ca2+-sensing receptors in intestinal epithelium. *American Journal of Physiology-Cell Physiology* **42,** C1168-C1175.

Garrett JE, Capuano IV, Hammerland LG, Hung BCP, Brown EM, Hebert SC, Nemeth EF & Fuller F. (1995a). Molecular Cloning and Functional Expression of Human Parathyroid Calcium Receptor cDNAs. *J Biol Chem* **270,** 12919-12925.

Garrett JE, Tamir H, Kifor O, Simin RT, Rogers KV, Mithal A, Gagel RF & Brown EM. (1995b). Calcitonin-Secreting Cells of the Thyroid Express an Extracellular Calcium Receptor Gene. *Endocrinology* **136,** 5202-5211.

Geibel J, Sritharan K, Geibel R, Geibel P, Persing JS, Seeger A, Roepke TK, Deichstetter M, Prinz C, Cheng SX, Martin D & Hebert SC. (2006). Calcium-sensing receptor abrogates secretagogue-induced increases in intestinal net fluid secretion by enhancing cyclic nucleotide destruction. *Proc Natl Acad Sci U S A* **103,** 9390-9397.

Hammerland LG, Garrett JE, Hung BCP, Levinthal C & Nemeth EF. (1998). Allosteric Activation of the Ca2+ Receptor Expressed in Xenopus laevis Oocytes by NPS 467 or NPS 568. *Mol Pharmacol* **53,** 1083-1088.

Hanrahan JP, Tager IB, Segal MR, Tosteson TD, Castile RG, Van Vunakis H, Weiss ST & Speizer FE. (1992). The effect of maternal smoking during pregnancy on early infant lung function. *Am Rev Respir Dis* **145,** 1129-1135.

Harding R & Hooper SB. (1996). Regulation of lung expansion and lung growth before birth. *J Appl Physiol* **81,** 209-224.

Healy AM, Morgenthau L, Zhu X, Farber HW & Cardoso WV. (2000). VEGF is deposited in the subepithelial matrix at the leading edge of branching airways and stimulates neovascularization in the murine embryonic lung. *Dev Dyn* **219,** 341-352.

Hirai Y, Nose A, Kobayashi S & Takeichi M. (1989). Expression and role of E- and P-cadherin adhesion molecules in embryonic histogenesis. I. Lung epithelial morphogenesis. *Development* **105,** 263-270.

Ho C, Conner DA, Pollak MR, Ladd DJ, Kifor O, Warren HB, Brown EM, Seidman JG & Seidman CE. (1995). A mouse model of human familial hypocalciuric hypercalcemia and neonatal severe hyperparathyroidism. *Nat Genet* **11,** 389-394.

Hobson SA, McNeil SE, Lee F & Rodland KD. (2000). Signal transduction mechanisms linking increased extracellular calcium to proliferation in ovarian surface epithelial cells. *Exp Cell Res* **258,** 1-11.

Hobson SA, Wright J, Lee F, McNeil SE, Bilderback T & Rodland KD. (2003). Activation of the MAP kinase cascade by exogenous calcium-sensing receptor. *Mol Cell Endocrinol* **200,** 189-198.

Hogan BL. (1999). Morphogenesis. *Cell* **96,** 225-233.

Hooper SB & Harding R. (1995). Fetal lung liquid: a major determinant of the growth and functional development of the fetal lung. *Clin Exp Pharmacol Physiol* **22,** 235-247.

Hough TA, Bogani D, Cheeseman MT, Favor J, Nesbit MA, Thakker RV & Lyon MF. (2004). Activating calcium-sensing receptor mutation in the mouse is associated with cataracts and ectopic calcification. *Proc Natl Acad Sci U S A* **101,** 13566-13571.

House MG, Kohlmeier L, Chattopadhyay N, Kifor O, Yamaguchi T, Leboff MS, Glowacki J & Brown EM. (1997). Expression of an extracellular calcium-sensing receptor in human and mouse bone marrow cells. *J Bone Miner Res* **12,** 1959-1970.

Hu JX, Reyes-Cruz G, Chen WZ, Jacobson KA & Spiegel AM. (2002). Identification of acidic residues in the extracellular loops of the seven-transmembrane domain of the human Ca2+ receptor critical for response to Ca2+ and a positive allosteric modulator. *J Biol Chem* **277,** 46622-46631.

Huang C & Miller RT. (2007). The calcium-sensing receptor and its interacting proteins. *J Cell Mol Med* **11,** 923-934.

Huang CF, Hujer KM, Wu ZZ & Miller RT. (2004). The Ca2+-sensing receptor couples to G alpha(12/13) to activate phospholipase D in Madin-Darby canine kidney cells. *American Journal of Physiology-Cell Physiology* **286,** C22-C30.

Huang Y & Breitwieser GE. (2007). Rescue of calcium-sensing receptor mutants by allosteric modulators reveals a conformational checkpoint in receptor biogenesis. *J Biol Chem* **282,** 9517-9525.

Janicic N, Pausova Z, Cole DE & Hendy GN. (1995). Insertion of an Alu sequence in the Ca(2+)-sensing receptor gene in familial hypocalciuric hypercalcemia and neonatal severe hyperparathyroidism. *Am J Hum Genet* **56,** 880-886.

Jaskoll TF, Johnson R, Don G & Slavkin HC. (1986). Embryonic mouse lung morphogenesis in serumless, chemically-defined medium in vitro. *Prog Clin Biol Res* **217A,** 381-384.

Jesudason EC. (2006). Small lungs and suspect smooth muscle: congenital diaphragmatic hernia and the smooth muscle hypothesis. *J Pediatr Surg* **41,** 431-435.

Jesudason EC, Smith NP, Connell MG, Spiller DG, White MRH, Fernig DG & Losty PD. (2005). Developing rat lung has a sided pacemaker region for morphogenesis-related airway peristalsis. *Am J Respir Cell Mol Biol* **32,** 118-127.

Jesudason EC, Smith NP, Connell MG, Spiller DG, White MRH, Fernig DG & Losty PD. (2006). Peristalsis of airway smooth muscle is developmentally regulated and uncoupled from hypoplastic lung growth. *American Journal of Physiology-Lung Cellular and Molecular Physiology* **291,** L559-L565.

Kaartinen V, Voncken JW, Shuler C, Warburton D, Bu D, Heisterkamp N & Groffen J. (1995). Abnormal lung development and cleft palate in mice lacking TGF-[beta]3 indicates defects of epithelial-mesenchymal interaction. *Nat Genet* **11,** 415-421.

Kallay E, Bajna E, Wrba F, Kriwanek S, Peterlik M & Cross HS. (2000). Dietary calcium and growth modulation of human colon cancer cells: Role of the extracellular calcium-sensing receptor. *Cancer Detect Prev* **24,** 127-136.

Kallay E, Bonner E, Wrba F, Thakker RV, Peterlik M & Cross HS. (2003). Molecular and functional characterization of the extracellular calcium-sensing receptor in human colon cancer cells. *Oncol Res* **13,** 551-559.

Kallay E, Kifor O, Chattopadhyay N, Brown EM, Bischof MG, Peterlik M & Cross HS. (1997). Calcium-dependent c-myc proto-oncogene expression and proliferation of

CACO-2 cells: A role for a luminal extracellular calcium-sensing receptor. *Biochem Biophys Res Commun* **232,** 80-83.

Katoh M, Hirai M, Sugimura T & Terada M. (1996). Cloning, expression and chromosomal localization of Wnt-13, a novel member of the Wnt gene family. *Oncogene* **13,** 873-876.

Kelly RG, Brown NA & Buckingham ME. (2001). The arterial pole of the mouse heart forms from Fgf10-expressing cells in pharyngeal mesoderm. *Dev Cell* **1,** 435-440.

Keyt BA, Berleau LT, Nguyen HV, Chen H, Heinsohn H, Vandlen R & Ferrara N. (1996). The Carboxyl-terminal Domain(111-165) of Vascular Endothelial Growth Factor Is Critical for Its Mitogenic Potency. *J Biol Chem* **271,** 7788-7795.

Kifor O, MacLeod RJ, Diaz R, Bai M, Yamaguchi T, Yao T, Kifor I & Brown EM. (2001). Regulation of MAP kinase by calcium-sensing receptor in bovine parathyroid and CaR-transfected HEK293 cells. *American Journal of Physiology-Renal Physiology* **280,** F291-F302.

Kling DE, Lorenzo HK, Trbovich AM, Kinane TB, Donahoe PK & Schnitzer JJ. (2002). Pre- and postnatal lung development, maturation, and plasticity - MEK-1/2 inhibition reduces branching morphogenesis and causes mesenchymal cell apoptosis in fetal rat lungs. *American Journal of Physiology-Lung Cellular and Molecular Physiology* **282,** L370-L378.

Kos CH, Karaplis AC, Peng JB, Hediger MA, Goltzman D, Mohammad KS, Guise TA & Pollak MR. (2003). The calcium-sensing receptor is required for normal calcium homeostasis independent of parathyroid hormone. *J Clin Invest* **111,** 1021-1028.

Kovacs CS, Ho-Pao CL, Hunzelman JL, Lanske B, Fox J, Seidman JG, Seidman CE & Kronenberg HM. (1998). Regulation of murine fetal-placental calcium metabolism by the calcium-sensing receptor. *J Clin Invest* **101,** 2812-2820.

Kovacs CS & Kronenberg HM. (1997). Maternal-Fetal Calcium and Bone Metabolism During Pregnancy, Puerperium, and Lactation. *Endocr Rev* **18,** 832-872.

Kwak JO, Kwak J, Kim HW, Oh KJ, Kim YT, Jung SM & Cha SH. (2005). The extracellular calcium sensing receptor is expressed in mouse mesangial cells and modulates cell proliferation. *Exp Mol Med* **37,** 457-465.

Lammerding-Koppel M, Greiner-Schroder A & Drews U. (1995). Muscarinic receptors in the prenatal mouse embryo. Comparison of M35-immunohistochemistry with [3H]quinuclidinyl benzylate autoradiography. *Histochem Cell Biol* **103,** 301-310.

Lebeche D, Malpel S & Cardoso WV. (1999). Fibroblast growth factor interactions in the developing lung. *Mech Dev* **86,** 125-136.

LeBoff MS, Shoback D, Brown EM, Thatcher J, Leombruno R, Beaudoin D, Henry M, Wilson R, Pallotta J, Marynick S & et al. (1985). Regulation of parathyroid hormone release and cytosolic calcium by extracellular calcium in dispersed and cultured bovine and pathological human parathyroid cells. *J Clin Invest* **75,** 49-57.

Lee YM, Jeong CH, Koo SY, Son MJ, Song HS, Bae SK, Raleigh JA, Chung HY, Yoo MA & Kim KW. (2001). Determination of hypoxic region by hypoxia marker in developing mouse embryos in vivo: a possible signal for vessel development. *Dev Dyn* **220,** 175-186.

Li C, Xiao J, Hormi K, Borok Z & Minoo P. (2002). Wnt5a participates in distal lung morphogenesis. *Dev Biol* **248,** 68-81.

Li CG, Hu LY, Xiao J, Chen HY, Li JT, Bellusci S, Delanghe S & Minoo P. (2005). Wnt5a regulates Shh and Fgf10 signaling during lung development. *Dev Biol* **287,** 86-97.

Lienhardt A, Bai M, Lagarde JP, Rigaud M, Zhang ZX, Jiang YF, Kottler ML, Brown EM & Garabedian M. (2001). Activating mutations of the calcium-sensing receptor: Management of hypocalcemia. *J Clin Endocrinol Metab* **86,** 5313-5323.

Lienhardt A, Garabedian M, Bai M, Sinding C, Zhang ZX, Lagarde JP, Boulesteix J, Rigaud M, Brown EM & Kottler ML. (2000). A large homozygous or heterozygous in-frame deletion within the calcium-sensing receptor's carboxylterminal cytoplasmic tail that causes autosomal dominant hypocalcemia. *J Clin Endocrinol Metab* **85,** 1695-1702.

Lin KI, Chattopadhyay N, Bai M, Alvarez R, Dang CV, Baraban JM, Brown EM & Ratan RR. (1998). Elevated extracellular calcium can prevent apoptosis via the calcium-sensing receptor. *Biochem Biophys Res Commun* **249,** 325-331.

Litingtung Y, Lei L, Westphal H & Chiang C. (1998). Sonic hedgehog is essential to foregut development. *Nat Genet* **20,** 58-61.

Liu Y, Martinez L, Ebine K & Abe MK. (2008). Role for mitogen-activated protein kinase p38[alpha] in lung epithelial branching morphogenesis. *Dev Biol* **314,** 224-235.

Loretz CA, Pollina C, Hyodo S, Takei Y, Chang W & Shoback D. (2004). cDNA Cloning and Functional Expression of a Ca2+-sensing Receptor with Truncated C-terminal Tail from the Mozambique Tilapia (Oreochromis mossambicus) 10.1074/jbc.M410098200. *J Biol Chem* **279,** 53288-53297.

Luck W, Nau H, Hansen R & Steldinger R. (1985). Extent of nicotine and cotinine transfer to the human fetus, placenta and amniotic fluid of smoking mothers. *Dev Pharmacol Ther* **8,** 384-395.

MacLeod RJ, Hayes M & Pacheco I. (2007). Wnt5a secretion stimulated by the extracellular calcium-sensing receptor inhibits defective Wnt signaling in colon cancer cells. *Am J Physiol Gastrointest Liver Physiol* **293,** G403-411.

Mailleux AA, Kelly R, Veltmaat JM, De Langhe SP, Zalfran S, Thiery JP & Bellusci S. (2005). Fgf10 expression identifies parabronchial smooth muscle cell progenitors and is required for their entry into the smooth muscle cell lineage. *Development* **132,** 2157-2166.

Maldonado-Perez D, Breitwieser GE, Gama L, Elliott AC, Ward DT & Riccardi D. (2003). Human calcium-sensing receptor can be suppressed by antisense sequences. *Biochem Biophys Res Commun* **311,** 610-617.

Mamillapalli R, VanHouten J, Zawalich W & Wysolmerski J. (2008). Switching of G-protein usage by the calcium sensing receptor reverses its effect on PTHrP secretion in normal versus malignant breast cells. *J Biol Chem,* M801738200.

Marchese C, Felici A, Visco V, Lucania G, Igarashi M, Picardo M, Frati L & Torrisi MR. (2001). Fibroblast Growth Factor 10 Induces Proliferation and Differentiation of Human Primary Cultured Keratinocytes. **116,** 623-628.

McAteer JA, Cavanagh TJ & Evan AP. (1983). Submersion culture of the intact fetal lung. *In Vitro* **19,** 210-218.

McGehee DS, Aldersberg M, Liu KP, Hsuing SC, Heath MJS & Tamir H. (1997). Mechanism of extracellular Ca2+ receptor-stimulated hormone release from sheep thyroid parafollicular cells. *Journal of Physiology-London* **502,** 31-44.

McLarnon SJ, Holden D, Ward DT, Jones MN, Elliott AC & Riccardi D. (2002). Aminoglycoside antibiotics induce pH-sensitive activation of the calcium-sensing receptor. *Biochem Biophys Res Commun* **297,** 71-77.

McLarnon SJ & Riccardi D. (2002). Physiological and pharmacological agonists of the extracellular Ca2+-sensing receptor. *Eur J Pharmacol* **447,** 271-278.

McNeil L, Hobson S, Nipper V & Rodland KD. (1998a). Functional calcium-sensing receptor expression in ovarian surface epithelial cells. *Am J Obstet Gynecol* **178,** 305-313.

McNeil SE, Hobson SA, Nipper V & Rodland KD. (1998b). Functional calcium-sensing receptors in rat fibroblasts are required for activation of SRC kinase and mitogen-

activated protein kinase in response to extracellular calcium. *J Biol Chem* **273,** 1114-1120.

Mentaverri R, Yano S, Chattopadhyay N, Petit L, Kifor O, Kamel S, Terwilliger EF, Brazier M & Brown EM. (2006). The calcium sensing receptor is directly involved in both osteoclast differentiation and apoptosis. *FASEB J* **20,** 2562-+.

Metzger DE, Xu Y & Shannon JM. (2007). Elf5 is an epithelium-specific, fibroblast growth factor-sensitive transcription factor in the embryonic lung. *Dev Dyn* **236,** 1175-1192.

Metzger RJ, Klein OD, Martin GR & Krasnow MA. (2008). The branching programme of mouse lung development. *Nature* **453,** 745-750.

Miettinen PJ, Warburton D, Bu D, Zhao JS, Berger JE, Minoo P, Koivisto T, Allen L, Dobbs L, Werb Z & Derynck R. (1997). Impaired lung branching morphogenesis in the absence of functional EGF receptor. *Dev Biol* **186,** 224-236.

Min HS, Danilenko DM, Scully SA, Bolon B, Ring BD, Tarpley JE, DeRose M & Simonet WS. (1998). Fgf-10 is required for both limb and lung development and exhibits striking functional similarity to Drosophila branchless. *Genes Dev* **12,** 3156-3161.

Minoo P, Su GS, Drum H, Bringas P & Kimura S. (1999). Defects in tracheoesophageal and lung morphogenesis in Nkx2.1(-/-) mouse embryos. *Dev Biol* **209,** 60-71.

Miquerol L, Gertsenstein M, Harpal K, Rossant J & Nagy A. (1999). Multiple Developmental Roles of VEGF Suggested by a LacZ-Tagged Allele. *Dev Biol* **212,** 307-322.

Mithal A, Kifor O, Kifor I, Vassilev P, Butters R, Krapcho K, Simin R, Fuller F, Hebert SC & Brown EM. (1995). The reduced responsiveness of cultured bovine parathyroid cells to extracellular Ca2+ is associated with marked reduction in the expression of extracellular Ca(2+)-sensing receptor messenger ribonucleic acid and protein. *Endocrinology* **136,** 3087-3092.

Mody N, Leitch J, Armstrong C, Dixon J & Cohen P. (2001). Effects of MAP kinase cascade inhibitors on the MKK5/ERK5 pathway. *FEBS Lett* **502,** 21-24.

Monkley SJ, Delaney SJ, Pennisi DJ, Christiansen JH & Wainwright BJ. (1996). Targeted disruption of the Wnt2 gene results in placentation defects. *Development* **122,** 3343-3353.

Mori K, Ikeda K, Hayashida S, Tokieda K, Ishimoto H, Fujii Y, Fukuzawa R & Kitano Y. (2001). Pulmonary epithelial cell maturation in hyperplastic lungs associated with fetal tracheal agenesis. *J Pediatr Surg* **36,** 1845-1848.

Nemeth EF. (2004). Calcimimetic and calcilytic drugs: just for parathyroid cells? *Cell Calcium* **35,** 283-289.

Nemeth EF & Scarpa A. (1987). Rapid mobilization of cellular Ca2+ in bovine parathyroid cells evoked by extracellular divalent cations. Evidence for a cell surface calcium receptor. *J Biol Chem* **262,** 5188-5196.

Nemeth EF, Steffey ME, Hammerland LG, Hung BCP, Van Wagenen BC, DelMar EG & Balandrin MF. (1998). Calcimimetics with potent and selective activity on the parathyroid calcium receptor. *Proceedings of the National Academy of Sciences* **95,** 4040-4045.

Nogawa H & Hasegawa Y. (2002). Sucrose stimulates branching morphogenesis of embryonic mouse lung in vitro: A problem of osmotic balance between lumen fluid and culture medium. *Dev Growth Differ* **44,** 383-390.

Oda Y, Tu CL, Chang WH, Crumrine D, Komuves L, Mauro T, Elias PM & Bikle DD. (2000). The calcium sensing receptor and its alternatively spliced form in murine epidermal differentiation. *J Biol Chem* **275,** 1183-1190.

Oda Y, Tu CL, Pillai S & Bikle DD. (1998). The calcium sensing receptor and its alternatively spliced form in keratinocyte differentiation. *J Biol Chem* **273,** 23344-23352.

Olver RE & Strang LB. (1974). Ion fluxes across the pulmonary epithelium and the secretion of lung liquid in the foetal lamb. *J Physiol* **241,** 327-357.

Orrenius S, Zhivotovsky B & Nicotera P. (2003). Regulation of cell death: the calcium-apoptosis link. *Nat Rev Mol Cell Biol* **4,** 552-565.

Pacheco I, Hayes M & Macleod RJ. (2007). Extracellular calcium-sensing receptor (CaSR) stimulates Wnt5a secretion which inhibits beta-catenin signaling of intestinal epithelial cells independent of the orphan receptor Ror2. *Gastroenterology* **132,** A302-A303.

Pacheco II & MacLeod RJ. (2008). Extracellular Calcium-Sensing Receptor (CaSR) stimulates secretion of Wnt5a from Colonic Myofibroblasts to stimulate CDX2 and sucrase-isomaltase using Ror2 on intestinal epithelia. *Am J Physiol Gastrointest Liver Physiol,* 00560.02007.

Park WY, Miranda B, Lebeche D, Hashimoto G & Cardoso WV. (1998). FGF-10 is a chemotactic factor for distal epithelial buds during lung development. *Dev Biol* **201,** 125-134.

Pearce SH, Trump D, Wooding C, Besser GM, Chew SL, Grant DB, Heath DA, Hughes IA, Paterson CR, Whyte MP & et al. (1995). Calcium-sensing receptor mutations in familial benign hypercalcemia and neonatal hyperparathyroidism. *J Clin Invest* **96,** 2683-2692.

Pearce SHS, Bai M, Quinn SJ, Kifor O, Brown EM & Thakker RV. (1996a). Functional characterization of calcium-sensing receptor mutations expressed in human embryonic kidney cells. *J Clin Invest* **98,** 1860-1866.

Pearce SHS, Williamson C, Kifor O, Bai M, Coulthard MG, Davies M, LewisBarned N, McCredie D, Powell H, KendallTaylor P, Brown EM & Thakker RV. (1996b). A familial syndrome of hypocalcemia with hypercalciuria due to mutations in the calcium-sensing receptor. *N Engl J Med* **335,** 1115-1122.

Pearce SHS, Wooding C, Davies M, Tollefsen SE, Whyte MP & Thakker RV. (1996c). Calcium-sensing receptor mutations in familial hypocalciuric hypercalcaemia with recurrent pancreatitis. *Clin Endocrinol (Oxf)* **45,** 675-680.

Pepicelli CV, Lewis PM & McMahon AP. (1998). Sonic hedgehog regulates branching morphogenesis in the mammalian lung. *Curr Biol* **8,** 1083-1086.

Peterlik M & Cross HS. (2005). Vitamin D and calcium deficits predispose for multiple chronic diseases. *Eur J Clin Invest* **35,** 290-304.

Peters K, Werner S, Liao X, Wert S, Whitsett J & Williams L. (1994). Targeted Expression of a Dominant-Negative Fgf Receptor Blocks Branching Morphogenesis and Epithelial Differentiation of the Mouse Lung. *EMBO J* **13,** 3296-3301.

Peters KG, Werner S, Chen G & Williams LT. (1992). Two FGF receptor genes are differentially expressed in epithelial and mesenchymal tissues during limb formation and organogenesis in the mouse. *Development* **114,** 233-243.

Petrel C, Kessler A, Dauban P, Dodd RH, Rognan D & Ruat M. (2004). Positive and negative allosteric modulators of the Ca2+-sensing receptor interact within overlapping but not identical binding sites in the transmembrane domain. *J Biol Chem* **279,** 18990-18997.

Pi M, Spurney RF, Tu QS, Hinson T & Quarles LD. (2002). Calcium-sensing receptor activation of Rho involves filamin and Rho-guanine nucleotide exchange factor. *Endocrinology* **143,** 3830-3838.

Pidasheva S, Canaff L, Simonds WF, Marx SJ & Hendy GN. (2005). Impaired cotranslational processing of the calcium-sensing receptor due to signal peptide missense mutations in familial hypocalciuric hypercalcemia. *Hum Mol Genet* **14,** 1679-1690.

Pidasheva S, Grant M, Canaff L, Ercan O, Kumar U & Hendy GN. (2006). Calcium-sensing receptor dimerizes in the endoplasmic reticulum: biochemical and biophysical characterization of CASR mutants retained intracellularly. *Hum Mol Genet* **15,** 2200-2209.

Pierce RA & Nguyen NM. (2002). Prenatal Nicotine Exposure and Abnormal Lung Function. *Am J Respir Cell Mol Biol* **26,** 10-13.

Pinkerton KE & Joad JP. (2000). The mammalian respiratory system and critical windows of exposure for children's health. *Environ Health Perspect* **108,** 457-462.

Pollak MR, Brown EM, Chou Y-HW, Hebert SC, Marx SJ, Stelnmann B, Levi T, Seidman CE & Seidman JG. (1993). Mutations in the human Ca2+-sensing receptor gene cause familial hypocalciuric hypercalcemia and neonatal severe hyperparathyroidism. *Cell* **75,** 1297-1303.

Pollak MR, Brown EM, Estep HL, McLaine PN, Kifor O, Park J, Hebert SC, Seidman CE & Seidman JG. (1994a). Autosomal dominant hypocalcaemia caused by a Ca(2+)-sensing receptor gene mutation. *Nat Genet* **8,** 303-307.

Pollak MR, Chou YH, Marx SJ, Steinmann B, Cole DE, Brandi ML, Papapoulos SE, Menko FH, Hendy GN, Brown EM & et al. (1994b). Familial hypocalciuric hypercalcemia and neonatal severe hyperparathyroidism. Effects of mutant gene dosage on phenotype. *J Clin Invest* **93,** 1108-1112.

Quinn SJ, Ye CP, Diaz R, Kifor O, Bai M, Vassilev P & Brown E. (1997). The Ca2+-sensing receptor: A target for polyamines. *American Journal of Physiology-Cell Physiology* **42,** C1315-C1323.

Quinn TM, Sylvester KG, Kitano Y, Kitano Y, Liechty KW, Jarrett BP, Adzick NS & Flake AW. (1999). TGF-beta 2 is increased after fetal tracheal occlusion. *J Pediatr Surg* **34,** 701-704.

Racz GZ, Kittel A, Riccardi D, Case RM, Elliott AC & Varga G. (2002). Extracellular calcium sensing receptor in human pancreatic cells. *Gut* **51,** 705-711.

Rehan VK, Wang Y, Sugano S, Santos J, Patel S, Sakurai R, Boros LW, Lee WP & Torday JS. (2007). In utero nicotine exposure alters fetal rat lung alveolar type II cell proliferation, differentiation, and metabolism. *Am J Physiol Lung Cell Mol Physiol* **292,** L323-333.

Riccardi D, Hall AE, Chattopadhyay N, Xu JZ, Brown EM & Hebert SC. (1998). Localization of the extracellular Ca2+ polyvalent cation-sensing protein in rat kidney. *American Journal of Physiology-Renal Physiology* **43,** F611-F622.

Riccardi D, Park J, Lee WS, Gamba G, Brown EM & Hebert SC. (1995). Cloning and functional expression of a rat kidney extracellular calcium/polyvalent cation-sensing receptor. *Proc Natl Acad Sci U S A* **92,** 131-135.

Ridgway EB, Gilkey JC & Jaffe LF. (1977). Free calcium increases explosively in activating medaka eggs. *Proc Natl Acad Sci U S A* **74,** 623-627.

Ringer S. (1883). A third contribution regarding the Influence of the Inorganic Constituents of the Blood on the Ventricular Contraction. *J Physiol* **4,** 222-225.

Ritchie G, Kerstan D, Dai L-J, Kang HS, Canaff L, Hendy GN & Quamme GA. (2001). 1,25(OH)2D3 stimulates Mg2+ uptake into MDCT cells: modulation by extracellular Ca2+ and Mg2+. *Am J Physiol Renal Physiol* **280,** F868-878.

Ritter CS, Slatopolsky E, Santoro S & Brown AJ. (2004). Parathyroid cells cultured in collagen matrix retain calcium responsiveness: Importance of three-dimensional tissue architecture. *J Bone Miner Res* **19,** 491-498.

Rodriguez L, Tu C, Cheng Z, Chen T-H, Bikle D, Shoback D & Chang W. (2005). Expression and Functional Assessment of an Alternatively Spliced Extracellular Ca2+-Sensing Receptor in Growth Plate Chondrocytes
10.1210/en.2005-0256. *Endocrinology* **146,** 5294-5303.

Roman J. (1995). Effects of Calcium-Channel Blockade on Mammalian Lung Branching Morphogenesis. *Exp Lung Res* **21,** 489-502.

Romoli R, Lania A, Mantovani G, Corbetta S, Persani L & Spada A. (1999). Expression of calcium-sensing receptor and characterization of intracellular signaling in human pituitary adenomas. *J Clin Endocrinol Metab* **84,** 2848-2853.

Rothenpieler UW & Dressler GR. (1993). Differential Distribution of Oligodeoxynucleotides in Developing Organs with Epithelial-Mesenchymal Interactions. *Nucleic Acids Res* **21,** 4961-4966.

Ruat M, Molliver ME, Snowman AM & Snyder SH. (1995). Calcium sensing receptor: molecular cloning in rat and localization to nerve terminals. *Proc Natl Acad Sci U S A* **92,** 3161-3165.

Sanford LP, Ormsby I, Gittenberger-de Groot AC, Sariola H, Friedman R, Boivin GP, Cardell EL & Doetschman T. (1997). TGFbeta2 knockout mice have multiple developmental defects that are non-overlapping with other TGFbeta knockout phenotypes. *Development* **124,** 2659-2670.

Schwartz TW & Holst B. (2006). Ago-allosteric modulation and other types of allostery in dimeric 7TM receptors. *J Recept Signal Transduct Res* **26,** 107-128.

Serra R, Pelton RW & Moses HL. (1994). Tgf-Beta-1 Inhibits Branching Morphogenesis and N-Myc Expression in Lung Bud Organ-Cultures. *Development* **120,** 2153-2161.

Seto ES & Bellen HJ. (2004). The ins and outs of Wingless signaling. *Trends Cell Biol* **14,** 45-53.

Shalaby F, Rossant J, Yamaguchi TP, Gertsenstein M, Wu XF, Breitman ML & Schuh AC. (1995). Failure of blood-island formation and vasculogenesis in Flk-1-deficient mice. *Nature* **376,** 62-66.

Shi W, Zhao JS, Anderson KD & Warburton D. (2001). Gremlin negatively modulates BMP-4 induction of embryonic mouse lung branching morphogenesis. *American Journal of Physiology-Lung Cellular and Molecular Physiology* **280,** L1030-L1039.

Shimizu T, Morishima S & Okada Y. (2000). Ca2+-sensing receptor-mediated regulation of volume-sensitive Cl- channels in human epithelial cells. *Journal of Physiology-London* **528,** 457-472.

Shoback D, Thatcher J, Leombruno R & Brown E. (1983). Effects of extracellular Ca++ and Mg++ on cytosolic Ca++ and PTH release in dispersed bovine parathyroid cells. *Endocrinology* **113,** 424-426.

Shoback DM, Thatcher J, Leombruno R & Brown EM. (1984). Relationship between Parathyroid Hormone Secretion and Cytosolic Calcium Concentration in Dispersed Bovine Parathyroid Cells. *Proceedings of the National Academy of Sciences* **81,** 3113-3117.

Shorte SL & Schofield JG. (1996). The effect of extracellular polyvalent cations on bovine anterior pituitary cells Evidence for a Ca2+-sensing receptor coupled to release of intracellular calcium stores. *Cell Calcium* **19,** 43-57.

Shu WG, Guttentag S, Wang ZS, Andl T, Ballard P, Lu MM, Piccolo S, Birchmeier W, Whitsett JA, Millar SE & Morrisey EE. (2005). Wnt/beta-catenin signaling acts upstream of N-myc, BMP4, and FGF signaling to regulate proximal-distal patterning in the lung. *Dev Biol* **283,** 226-239.

Shu WG, Jiang YQ, Lu MM & Morrisey EE. (2002). Wnt7b regulates mesehchymal proliferation and vascular development in the lung. *Development* **129,** 4831-4842.

Sickmann T, Klose A, Huth T & Alzheimer C. (2008). Unexpected suppression of neuronal G protein-activated, inwardly rectifying K+ current by common phospholipase C inhibitor. *Neurosci Lett* **436,** 102-106.

Smajilovic S, Sheykhzade M, Holmegard HN, Haunso S & Tfelt-Hansen J. (2007). Calcimimetic, AMG 073, induces relaxation on isolated rat aorta. *Vascular Pharmacology* **47,** 222-228.

Smith NP, Jesudason EC, Featherstone NC, Corbett HJ & Losty PD. (2005). Recent advances in congenital diaphragmatic hernia. *Arch Dis Child* **90,** 426-428.

Souza P, Obrodovich H & Post M. (1995). Lung Fluid Restriction Affects Growth but Not Airway Branching of Embryonic Rat Lung. *Int J Dev Biol* **39,** 629-637.

Steddon S & Cunningham J. (2005). Calcimimetics and calcilytics - fooling the calcium receptor. *Lancet* **365,** 2237-2239.

Steele MP, Speer MC, Loyd JE, Brown KK, Herron A, Slifer SH, Burch LH, Wahidi MM, Phillips JA, III, Sporn TA, McAdams HP, Schwarz MI & Schwartz DA. (2005). Clinical and Pathologic Features of Familial Interstitial Pneumonia. *Am J Respir Crit Care Med* **172,** 1146-1152.

Stege G, Fenton A & Jaffray B. (2003). Nihilism in the 1990s: the true mortality of congenital diaphragmatic hernia. *Pediatrics* **112,** 532-535.

Steinmann B, Gnehm HE, Rao VH, Kind HP & Prader A. (1984). Neonatal severe primary hyperparathyroidism and alkaptonuria in a boy born to related parents with familial hypocalciuric hypercalcemia. *Helv Paediatr Acta* **39,** 171-186.

Straub SG, Kornreich B, Oswald RE, Nemeth EF & Sharp GWG. (2000). The calcimimetic R-467 potentiates insulin secretion in pancreatic beta cells by activation of a nonspecific cation channel. *J Biol Chem* **275,** 18777-18784.

Sutherland D, Samakovlis C & Krasnow MA. (1996). Branchless encodes a Drosophila FGF homolog that controls tracheal cell migration and the pattern of branching. *Cell* **87,** 1091-1101.

Tefft D, Lee M, Smith S, Crowe DL, Bellusci S & Warburton D. (2002). mSprouty2 inhibits FGF10-activated MAP kinase by differentially binding to upstream target proteins. *American Journal of Physiology-Lung Cellular and Molecular Physiology* **283,** L700-L706.

Tfelt-Hansen J, Chattopadhyay N, Yano S, Kanuparthi D, Rooney P, Schwarz P & Brown EM. (2004). Calcium-Sensing Receptor Induces Proliferation through p38 Mitogen-Activated Protein Kinase and Phosphatidylinositol 3-Kinase But Not Extracellularly Regulated Kinase in a Model of Humoral Hypercalcemia of Malignancy. *Endocrinology* **145,** 1211-1217.

Tfelt-Hansen J, Hansen JL, Smajilovic S, Terwilliger EF, Haunso S & Sheikh SP. (2006). Calcium receptor is functionally expressed in rat neonatal ventricular cardiomyocytes. *Am J Physiol Heart Circ Physiol* **290,** H1165-1171.

Tfelt-Hansen J, MacLeod RJ, Chattopadhyay N, Yano S, Quinn S, Ren X, Terwilliger EF, Schwarz P & Brown EM. (2003). Calcium-sensing receptor stimulates PTHrP release by pathways dependent on PKC, p38 MAPK, JNK, and ERK1/2 in H-500 cells. *American Journal of Physiology-Endocrinology and Metabolism* **285,** E329-E337.

Topol L, Jiang X, Choi H, Garrett-Beal L, Carolan PJ & Yang Y. (2003). Wnt-5a inhibits the canonical Wnt pathway by promoting GSK-3-independent {beta}-catenin degradation. *J Cell Biol* **162,** 899-908.

Tu C-L, Chang W, Xie Z & Bikle DD. (2008). Inactivation of the Calcium Sensing Receptor Inhibits E-cadherin-mediated Cell-Cell Adhesion and Calcium-induced Differentiation in Human Epidermal Keratinocytes. *J Biol Chem* **283,** 3519-3528.

Tu CL, Chang WH & Bikle DD. (2001). The extracellular calcium-sensing receptor is required for calcium-induced differentiation in human keratinocytes. *J Biol Chem* **276,** 41079-41085.

Tu Q, Pi M, Karsenty G, Simpson L, Liu S & Quarles LD. (2003). Rescue of the skeletal phenotype in CasR-deficient mice by transfer onto the Gcm2 null background. *J Clin Invest* **111,** 1029-1037.

van Tuyl M, Liu J, Wang JX, Kuliszewski M, Tibboel D & Post M. (2005). Role of oxygen and vascular development in epithelial branching morphogenesis of the developing mouse lung. *American Journal of Physiology-Lung Cellular and Molecular Physiology* **288,** L167-L178.

VanHouten J, Dann P, McGeoch G, Brown EM, Krapcho K, Neville M & Wysolmerski JJ. (2004). The calcium-sensing receptor regulates mammary gland parathyroid hormone-related protein production and calcium transport. *J Clin Invest* **113,** 598-608.

VanHouten JN, Neville MC & Wysolmerski JJ. (2007). The Calcium-Sensing Receptor Regulates Plasma Membrane Calcium Adenosine Triphosphatase Isoform 2 Activity in Mammary Epithelial Cells: A Mechanism for Calcium-Regulated Calcium Transport into Milk. *Endocrinology* **148,** 5943-5954.

Vizard TN, O'Keeffe GW, Gutierrez H, Kos CH, Riccardi D & Davies AM. (2008). Regulation of axonal and dendritic growth by the extracellular calcium-sensing receptor. *Nat Neurosci* **11,** 285-291.

Wada M, Furuya Y, Sakiyama J, Kobayashi N, Miyata S, Ishii H & Nagano N. (1997). The calcimimetic compound NPS R-568 suppresses parathyroid cell proliferation in rats with renal insufficiency. Control of parathyroid cell growth via a calcium receptor. *J Clin Invest* **100,** 2977-2983.

Wang J, Ito T, Udaka N, Okudela K, Yazawa T & Kitamura H. (2005). P13K-AKT pathway mediates growth and survival signals during development of fetal mouse lung. *Tissue Cell* **37,** 25-35.

Wang R, Xu CQ, Zhao WM, Zhang J, Cao K, Yang BF & Wu LY. (2003). Calcium and polyamine regulated calcium-sensing receptors in cardiac tissues. *Eur J Biochem* **270,** 2680-2688.

Warburton D, Bellusci S, De Langhe S, Del Moral PM, Fleury V, Mailleux A, Tefft D, Unbekandt M, Wang K & Shi W. (2005). Molecular mechanisms of early lung specification and branching morphogenesis. *Pediatr Res* **57,** 26R-37R.

Warburton D, Gauldie J, Bellusci S & Shi W. (2006). Lung Development and Susceptibility to Chronic Obstructive Pulmonary Disease. *Proc Am Thorac Soc* **3,** 668-672.

Warburton D & Olver RE. (1997). Coordination of genetic, epigenetic, and environmental factors in lung development, injury, and repair. *Chest* **111,** S119-S122.

Ward DT. (2004). Calcium receptor-mediated intracellular signalling. *Cell Calcium* **35,** 217-228.

Ward DT, Brown EM & Harris HW. (1998). Disulfide Bonds in the Extracellular Calcium-Polyvalent Cation-sensing Receptor Correlate with Dimer Formation and Its Response to Divalent Cations in Vitro. *J Biol Chem* **273,** 14476-14483.

Ward DT, Maldonado-Perez D, Hollins L & Riccardi D. (2005). Aminoglycosides induce acute cell signaling and chronic cell death in renal cells that express the calcium-sensing receptor. *J Am Soc Nephrol* **16,** 1236-1244.

Ward DT, McLarnon SJ & Riccardi D. (2002). Aminoglycosides increase intracellular calcium levels and ERK activity in proximal tubular OK cells expressing the extracellular calcium-sensing receptor. *J Am Soc Nephrol* **13,** 1481-1489.

Ward DT & Riccardi D. (2002). Renal physiology of the extracellular calcium-sensing receptor. *Pflugers Archiv-European Journal of Physiology* **445,** 169-176.

Watanabe T, Bai M, Lane CR, Matsumoto S, Minamitani K, Minagawa M, Niimi H, Brown EM & Yasuda T. (1998). Familial hypoparathyroidism: Identification of a

novel gain of function mutation in transmembrane domain 5 of the calcium-sensing receptor. *J Clin Endocrinol Metab* **83,** 2497-2502.

Weaver M, Dunn NR & Hogan BLM. (2000). Bmp4 and Fgf10 play opposing roles during lung bud morphogenesis. *Development* **127,** 2695-2704.

Weaver M, Yingling JM, Dunn NR, Bellusci S & Hogan BLM. (1999). Bmp signaling regulates proximal-distal differentiation of endoderm in mouse lung development. *Development* **126,** 4005-4015.

Weber A, Herz R & Reiss I. (1964). Role of Calcium in Contraction and Relaxation of Muscle. *Fed Proc* **23,** 896-900.

Wettschureck N, Lee E, Libutti SK, Offermanns S, Robey PG & Spiegel AM. (2007). Parathyroid-Specific Double Knockout of Gq and G11 {alpha}-Subunits Leads to a Phenotype Resembling Germline Knockout of the Extracellular Ca2+-Sensing Receptor. *Mol Endocrinol* **21,** 274-280.

Whitsett JA, Wert SE & Trapnell BC. (2004). Genetic disorders influencing lung formation and function at birth. *Hum Mol Genet* **13,** R207-R215.

Wilborn AM, Evers LB & Canada AT. (1996). Oxygen toxicity to the developing lung of the mouse: Role of reactive oxygen species. *Pediatr Res* **40,** 225-232.

Wilson SM, Olver RE & Walters DV. (2007). Developmental regulation of lumenal lung fluid and electrolyte transport. *Respiratory Physiology & Neurobiology* **159,** 247-255.

Winnier G, Blessing M, Labosky PA & Hogan BL. (1995). Bone morphogenetic protein-4 is required for mesoderm formation and patterning in the mouse. *Genes Dev* **9,** 2105-2116.

Wongtrakool C & Roman J. (2008). APOPTOSIS OF MESENCHYMAL CELLS DURING THE PSEUDOGLANDULAR STAGE OF LUNG DEVELOPMENT AFFECTS BRANCHING MORPHOGENESIS. *Exp Lung Res* **34,** 481 - 499.

Woods NM, Cuthbertson KS & Cobbold PH. (1987). Agonist-induced oscillations in cytoplasmic free calcium concentration in single rat hepatocytes. *Cell Calcium* **8,** 79-100.

Wu S, Palese T, Mishra OP, Delivoria-Papadopoulos M & De Luca F. (2003). Effects of Ca2-sensing receptor activation in the growth plate
10.1096/fj.03-0294fje. *FASEB J,* 03-0294fje.

Wuenschell CW, Zhao JS, Tefft JD & Warburton D. (1998). Nicotine stimulates branching and expression of SP-A and SP-C mRNAs in embryonic mouse lung

culture. *American Journal of Physiology-Lung Cellular and Molecular Physiology* **18,** L165-L170.

Xie Z & Bikle DD. (2007). The Recruitment of Phosphatidylinositol 3-Kinase to the E-cadherin-Catenin Complex at the Plasma Membrane Is Required for Calcium-induced Phospholipase C-{gamma}1 Activation and Human Keratinocyte Differentiation. *J Biol Chem* **282,** 8695-8703.

Yamaguchi T, Chattopadhyay N, Kifor O, Butters RR, Sugimoto T & Brown EM. (1998). Mouse osteoblastic cell line (MC3T3-E1) expresses extracellular calcium (Ca-0(2+))-sensing receptor and its agonists stimulate chemotaxis and proliferation of MC3T3-E1 cells. *J Bone Miner Res* **13,** 1530-1538.

Yamaguchi T, Chattopadhyay N, Kifor O, Sanders JL & Brown EM. (2000). Activation of p42/44 and p38 mitogen-activated protein kinases by extracellular calcium-sensing receptor agonists induces mitogenic responses in the mouse osteoblastic MC3T3-E1 cell line. *Biochem Biophys Res Commun* **279,** 363-368.

Yamaguchi TP, Dumont DJ, Conlon RA, Breitman ML & Rossant J. (1993). flk-1, an flt-related receptor tyrosine kinase is an early marker for endothelial cell precursors. *Development* **118,** 489-498.

Yamamoto M, Igarashi T, Muramatsu M, Fukagawa M, Motokura T & Ogata E. (1989). Hypocalcemia increases and hypercalcemia decreases the steady-state level of parathyroid hormone messenger RNA in the rat. *J Clin Invest* **83,** 1053-1056.

Ye CP, Yano S, Tfelt-Hansen J, MacLeod RJ, Ren XH, Terwilliger E, Brown EM & Chattopadhyay N. (2004). Regulation of a Ca2+-activated K+ channel by calcium-sensing receptor involves p38 MAP kinase. *J Neurosci Res* **75,** 491-498.

Zhang W-h, Fu S-b, Lu F-h, Wu B, Gong D-m, Pan Z-w, Lv Y-j, Zhao Y-j, Li Q-f, Wang R, Yang B-f & Xu C-q. (2006). Involvement of calcium-sensing receptor in ischemia/reperfusion-induced apoptosis in rat cardiomyocytes. *Biochem Biophys Res Commun* **347,** 872-881.

Zhang Z, Jiang Y, Quinn SJ, Krapcho K, Nemeth EF & Bai M. (2002). L-Phenylalanine and NPS R-467 Synergistically Potentiate the Function of the Extracellular Calcium-sensing Receptor through Distinct Sites. *J Biol Chem* **277,** 33736-33741.

Zhou L, Dey CR, Wert SE & Whitsett JA. (1996). Arrested lung morphogenesis in transgenic mice bearing an SP-C-TGF-beta 1 chimeric gene. *Dev Biol* **175,** 227-238.

Ziegelstein RC, Xiong Y, He C & Hu Q. (2006). Expression of a functional extracellular calcium-sensing receptor in human aortic endothelial cells. *Biochem Biophys Res Commun* **342,** 153-163.